ULTRAVIOLET ASSISTED FENTON OXIDATION HYBRID PROCESS FOR TREATING RECALCITRANT TEXTILE WASTEWATER

ARCHINA BUTHIYAPPAN

FACULTY OF ENGINEERING
UNIVERSITY OF MALAYA
KUALA LUMPUR

2016

ULTRAVIOLET ASSISTED FENTON OXIDATION HYBRID PROCESS FOR TREATING RECALCITRANT TEXTILE WASTEWATER

ARCHINA BUTHIYAPPAN

THESIS SUBMITTED IN FULFILMENT OF THE REQUIREMENTS FOR THE DEGREE OF DOCTOR OF PHILOSOPHY

FACULTY OF ENGINEERING
UNIVERSITY OF MALAYA
KUALA LUMPUR

2016

UNIVERSITY OF MALAYA

ORIGINAL LITERARY WORK DECLARATION

Name of Candidate: Archina Buthiyappan

Registration/Matric No: KHA120051

Name of Degree: Doctor of Philosophy

Title of Thesis: Ultraviolet Assisted Fenton Oxidation Hybrid Process for Treating Recalcitrant Textile Wastewater

Field of Study: Health, Safety & Environment

I do solemnly and sincerely declare that:

(1) I am the sole author/writer of this Work;
(2) This Work is original;
(3) Any use of any work in which copyright exists was done by way of fair dealing and for permitted purposes and any excerpt or extract from, or reference to or reproduction of any copyright work has been disclosed expressly and sufficiently and the title of the Work and its authorship have been acknowledged in this Work;
(4) I do not have any actual knowledge nor do I ought reasonably to know that the making of this work constitutes an infringement of any copyright work;
(5) I hereby assign all and every rights in the copyright to this Work to the University of Malaya ("UM"), who henceforth shall be owner of the copyright in this Work and that any reproduction or use in any form or by any means whatsoever is prohibited without the written consent of UM having been first had and obtained;
(6) I am fully aware that if in the course of making this Work I have infringed any copyright whether intentionally or otherwise, I may be subject to legal action or any other action as may be determined by UM.

    Candidate's Signature   Date: 11/11/2016

Subscribed and solemnly declared before,

    Witness's Signature   Date:11/11/2016

Name:

Designation

ABSTRACT

It is estimated that about 17-20% of freshwater pollution worldwide occurs due to untreated textile wastewater discharges. Advanced oxidation processes (AOPs) are more suitable for treating textile wastewaters contaminated with recalcitrant organic compounds. In this regard, Batik Industry in Malaysia, which are commonly operated in a cottage set-up, are in dire need for stand alone, simple and cheaper treatment system based on AOPs. Among AOPs, the Fenton process is commonly used for degradation of organic pollutants. However operating cost due to high chemical consumption and excessive sludge production limits the large-scale application. In order to improve degradation performance and reagent utilization efficiency, as well as reduce treatment cost and sludge, ultraviolet radiated integrated Fenton oxidation hybrid process (UV-Fenton) was investigated for Batik wastewater treatment.

In this study, the treatment efficiencies of Fenton process and UV-Fenton hybrid process was evaluated using a laboratory sized experimental setup for batik industry wastewater equipped with a low-pressure UV lamp with or without irradiation. The operating parameters evaluated are initial pH of the wastewater, retention time, mass ratios of H_2O_2:COD and H_2O_2:Fe^{2+} and UV radiation intensity. Response surface methodology was used to design the experiment and optimize the operating parameters. The efficiency was evaluated based on COD, TOC and color removals. The kinetic model was also established in this study. Additionally, SEM/EDX and particle size analyses were conducted to characterize the generated sludge. The intermediate species formed during the reaction were observed through GC/MS, FTIR and HPLC analyses. Studies on the treatment efficiencies of direct photolysis, UV/H_2O_2, UV/Fe^{2+} coagulation and Fe^{2+} coagulation were also evaluated as a comparison.

Among the processes evaluated, the highest COD removal was achieved for UV -Fenton oxidation (91.2 %) , followed by Fenton process (81.4 %) , UV/H_2O_2 (68.0 %), UV- Fe^{2+} coagulation (55.0 %), Fe^{2+} coagulation (43.0 %) and UV photolysis (10.0 %). This study confirms that UV-Fenton exhibited higher COD, TOC and color removal efficiencies compared to other investigated AOPs. The maximum color removal (99.9%), COD removal (91.2 %) and TOC removal (78.5 %) were achieved at the optimum operating condition.

Compared to Fenton process, UV -Fenton resulted in about 10%, 20% and 24% in reagent consumption, sludge volume reduction and saving in cost respectively. The instrumental analyses (FTIR, GC/MS, and HPLC) of the treated samples revealed that the UV-Fenton could oxidize high-molecular-weight substances into small organic compounds. The kinetic study confirms that UV-Fenton treatment systems best fit the first-order kinetic reaction with higher rate of reaction compared to Fenton process. UV -Fenton confirms to be highly effective for degradation of textile wastewater with minimum electrical energy per order (EE/O) of 1.19 kWhr/m^3 compared to other photochemical AOPs. The study investigated the robustness of a statistical model developed for COD, TOC and color removals as a function of operating parameters for selected types of real wastewater, POME, leachate and wastewater from metal-finishing industry. In conclusion, this study proved that the UV-Fenton is suitable for enhancing the biodegradability of recalcitrant contaminants, and economically viable for cottage industries in Malaysia.

ABSTRAK

Adalah dianggarkan bahawa kira-kira 17-20 % daripada pencemaran air tawar di seluruh dunia berlaku akibat daripada pelepasan air sisa yang tidak diwarat. Proses-Proses Pengoksidaan Lanjutan (AOPs) boleh merawat air sisa yang tercemar oleh sebatian organik tahan panas. Industri batik, merupakan industri desa di Malaysia yang memerlukan sistem AOP yang cekap, berkesan dan kos yang rendah untuk memastikan pematuhan alam sekitar bagi efluen yang dilepaskan. Pengoksidaan Fenton menggunakan radikal hidroksil dengan oksidan elektro-kimia tinggi bagi pemineralan lengkap. Namun, kos pengoperasian yang tinggi yang berpunca daripada penggunaan bahan kimia dan penghasilan enapcemar yang berlebihan menghadkan penggunaan proses pengoksidaan Fenton berskala besar. Maka, penyelesaian yang mampan dan berpatutan adalah diperlukan. Kajian terkini menyelidik kebolehlaksanaan sistem berintegrasi fotolisis (UV)-pengoksidaan Fenton untuk mengatasi kekangan ini. Kesemua ujikaji bagi sistem Fenton dan sistem berintegrasi UV-Fenton telah dijalankan di dalam reaktor foto skala kelompok yang dilengkapi dengan lampu UV bertekanan rendah dengan atau tanpa sinaran. Parameter operasi utama merangkumi pH awal efluen, masa retensi, nisbah jisim H_2O_2:COD dan H_2O_2:Fe^{2+} dan keamatan sinaran UV. Parameter ini dinilai secara ujikaji dengan menggunakan beberapa set ujikaji yang direka oleh Metadologi Tindakbalas Permukaan. Kecekapan rawatan ditentukan oleh pengurangan COD, TOC dan warna. Tambahan, SEM/EDS dan analisa saiz zarahan telah digunakan untuk mencirikan enapcemar yang terhasil. Spesis pertengahan yang terbentuk semasa tindakbalas telah diperhatikan melalui GC/ MS dan analisa FTIR.

Antara proses-proses yang dikaji, degradasiCOD yang paling tinggi dicapai melalui proses UV- Fenton (91.2 %), diikuti dengan proses Fenton (81.4 %), UV/H_2O_2 (68.0 %), UV -Fe^{2+} (55.0 %), koagulasi Fe^{2+} (43.0 %) and UV fotolisis (10.0 %). Kajian ini

mengesahkan integrasi proses UV- Fenton menunjukan pengurangan COD, TOC dan warna yang paling tinggi, berbanding dengan lain-lain AOPs yang dikaji. Pengurangan maksimum warna (99.9%), COD (91.2 %) dan TOC (78.5 %) telah dicapai pada kondisi operasi yang optimum. Berbanding dengan proses Fenton, UV-Fenton menunjukkan lebih kurang 10%, 20% dan 24% penggurangan dalam penggunaan bahan kimia, dan isipadu enapcemar, dan penjimatan kos masing-masing.

Analisa instrument (FTIR, GC/MS, dan HPLC) membuktikan bahawa UV-pengoksidaan Fenton mampu degradasi sebatian organik. Kajian kinetik menunjukkan bahawa kedua-dua sistem rawatan Fenton dan UV-Fenton merupakan penyesuaian terbaik bagi tindakbalas kinetik peringkat pertama. UV- Fenton menunjukkan kecekapan yang tinggi untuk degradasi air sisa tekstil dengan 'electrical energy per order (EE/O) yang minimum iaitu 1.19 kWhr/m^3 berbanding dengan proses lain. Kajian ini menyelidik kemantapan model statistik yang dibangunkan bagi pengurangan COD, TOC dan warna sebagai fungsi parameter operasi bagi tiga jenis air sisa sebenar yang berbeza, air sisa kelapa sawit (POME), larut resap, dan air sisa daripada industri saduran logam. Nilai yang dimodelkan adalah sangat hampir dengan nilai ujikaji. Maka, kajian ini merumuskan bahawa proses berintegrasi UV-Fenton adalah sesuai bagi meningkatkan biodegradasi bahan cemar degil dan praktikal dalam aspek ekonomi bagi industri desa di Malaysia.

ACKNOWLEDGEMENTS

TABLE OF CONTENTS

LIST OF FIGURES

LIST OF TABLES

LIST OF ABBREVIATIONS

ARI   Approximate Relative Index

AOPs   :   Advanced Oxidation Processes

BOD   :   Biological Oxygen Demand

CCD   :   Central Composite Design

COD   :   Chemical Oxygen Demand (mg/l)

CR   :   Color Removal (ADMI)

Eq.   :   Equation

F-value :   Fisher's Value

H_2O_2 :   Hydrogen Peroxide

RBB   :   Remazol Brilliant Blue

RSM   :   Response Surface Methodology

RT   :   Retention Time (min)

pH   :   pH value

Sig.   :   Significant

TOC   :   Total Organic Carbon (mg/l)

TSS   :   Total Suspended Solids (mg/l)

FTIR   :   Fourier Transform Infrared Spectroscopy

GC/MS :   Gas Chromatography Mass Spectrometry

HPLC :   High-Performance Liquid Chromatography

SEM   :   Scanning Electron Microscopy

EDX   :   Energy Dispersive X-ray (SEM/EDX)

PSD   :   Particle Size Distribution

UV   :   Ultraviolet

LIST OF NOMENCLATURE AND SYMBOLS

hv   :   Photon

$HO^{\bullet}$:   Hydroxyl radical

Fe^{2+} :   Ferrous ion

k   :   Reaction rate constant Zero Order ($M\,s^{-1}$), First-order (s^{-1}), Second-order ($M\,s^{-1}$)

kWh   :   Kilowatt-hour

mM   :   Molar (mol/L)

min   :   minute

s   :   seconds

T   :   Temperature (^{0}C)

t   :   time (min)

W   :   Watt

w/w   :   weight/weight (mg/mg)

α   :   Sun altitude

β   :   Inclination of an inclined surface with respect to a horizontal plane

λ   :   Wavelength (nm)

CHAPTER 1: INTRODUCTION

1.1   Background

The textile industry is one of the multi-billion-dollar industries that play a pivotal role in the world economy in terms of employment (Asghar et al., 2015; Qiu et al., 2012; Zaharia et al., 2012). It can be classified into small, medium and large-scale industries (Sahoo, 1993; Sharma, 2006). Batik industry is an example of a traditional small-scale textile industry in Malaysia with an annual turnover of around RM 160 million and it contributes positively to the economic growth of Malaysia (Nair, 2014). Regardless of technology advancement, the effluents generated still contain high levels of dyes, lubricant, surfactant, heavy metals, oil and grease, sulfides, wax, suspended solids, soap and high pH values (Rashidi et al., 2016; Rashidi et al., 2012; Sathian et al., 2014). The local environmental law mandates the effluent to be treated before disposal, which is often a difficult task using conventional treatment methods.

Generally, wastewater from textile industry contains a high concentration of COD (150-10,000 mg/l), BOD (100- 4,000 mg/l), intense color (50- 2500 ADMI) and a variety of recalcitrant organic compounds (Grcic et al., 2011; Pera-Titus et al., 2004). Synthetic dyes are extensively used for dyeing and printing in textile industry. Commercially there are more than 10,000 types of dyes available in the market with the annual production exceed 7×10^5 metric tons worldwide (Engin et al., 2008; Inoue et al., 2006; McMullan et al., 2001). Approximately 10-20% of the dyestuffs are lost in the effluent during manufacturing processes (Ali et al., 2008; Ghodbane et al., 2009). It is estimated that 100 liters of wastewaters are produced for every kilogram of textile product, which is equivalent to about 3.7 million liters per day worldwide (Amaral et al., 2014). The release of this untreated effluent into environment affects the aesthetic properties of aquatic

environments, interferes with the growth of bacteria, and causes chronic health effects to living organisms due to their toxicity and mutagenicity processes (Allegre et al., 2006; Cardoso et al., 2011; Gunukula et al., 2001; Martins et al., 2011).

Conventional techniques based on physicochemical, chemical and microbiological methods such as adsorption (Yeh et al., 2002), coagulation/flocculation (Alinsafi et al., 2005), activated sludge system (Germirli Babuna et al., 1998), membrane separation (Metivier et al., 2003; Xu et al., 1999), ion exchange and reverse osmosis (Jager et al., 2014) have been used for the treatment of textile wastewaters (Akan et al., 2009; Faryal et al., 2005; Savin et al., 2008). However, most of these methods are only efficient for color removal (Blanco et al., 2012) but concurrently transferring the pollutant from aqueous to a solid phase, generate a rich, and concentrated stream, foul membrane surface, and generate solid waste (Rauf et al., 2009). Due to the increasing complexity of textile wastewater, conventional wastewater treatment technologies often fail to meet the minimum national standards for treated wastewater (Dias et al., 2016). Considerable efforts are being made to identify and develop a simple and economically feasible wastewater treatment system with high efficiency to remove the recalcitrant compounds, especially in cottage industries, which often limited by footprint.

Among the treatment techniques that have been investigated, Advanced Oxidation Processes (AOPs) have received the most attention (Balcıoğlu et al., 2003; Marcinowski et al., 2014). AOPs are based on the destruction of organic compounds by the generation of highly reactive oxidants such as hydroxyl radical ($HO\bullet$) with electrochemical oxidant potential of 2.8 eV (Soon et al., 2011). AOPs are widely used in wastewater treatment for overall organic content reduction, specific pollutant destruction, sludge treatment, color and odor reduction (Gunukula et al., 2001; Kavitha et al., 2004; Lucas et al., 2006). The most commonly used AOPs include heterogeneous photocatalytic oxidation (Bauer et al.,

1993), ozonation (Meric et al., 2005), UV/H_2O_2, and Fenton oxidation (Borba et al., 2012; Chergui et al., 2010; Oturan et al., 2011)

In particular, Fenton oxidation process based on the generation of $HO \bullet$ radical by the catalytic decomposition of hydrogen peroxide with ferrous ion is proven to be very effective (Karthikeyan et al., 2011; Mantzavinos et al., 2004; Meric et al., 2004). It is a simple, relatively cheap and easily operatable systems, with a high oxidation potential, and fast oxidation kinetics (Alaton et al., 2007; Xu et al., 2004; Yu et al., 2016; Gotvajn et al., 2011). Therefore, it could be a suitable candidate for a stand-alone and small wastewater treatment system. However, there are few limitations that need to be addressed in order to increase the acceptance level of the method by the industries to treat their respective effluents. The factors include: (i) high chemical consumption (up to 50–80 ppm of Fe^{2+}/Fe^{3+} in solution) (ii) pH dependence (effective in the range of pH 2–4), (iii) high cost of H_2O_2 (iv) generation of sludge (v) necessity of post-treatment (v) required for neutralization of the treated sample before disposal, and (vi) decomposition of H_2O_2 (Iurascu et al. 2009; Babuponnusami et al., 2012, Ali et al. 2013). Limitations of Fenton process can be overcome by integrating with energy dissipating agents such as ozone, US, UV, solar light, microwave as suggested by a number of researchers (Bagal et al., 2014; Eren, 2012; Gogate, 2008; S.-T. Liu et al., 2013; Mahamuni et al., 2010; Pang et al., 2011; Soares et al., 2015). Fenton integrated with energy dissipating components offers several advantages such as an increase in the rate of reaction, less fouling of solid catalyst, lower reaction time, lesser sludge formation, and elimination of mass transfer limitation.

Among the energy dissipating agents, Fenton hybrid system, integrated with UV radiation has received the most attention among the researchers working in wastewater treatment as the contaminants can be destructed by direct oxidation, UV-photolysis and synergistic action of UV with oxidants and catalyst (Banat et al., 2005; Y. J. Jung et al., 2012; P. Liu

et al., 2013). UV radiation has been proven useful for environmental applications such as, drinking water treatment (Wenhai et al., 2016), decolorization of dyes, (Chang3 et al., 2010) oxidation of organic compounds, pesticides removal (Chelme-Ayala et al., 2010), leachate treatment (Hu et al., 2011), pharmaceutical compounds degradation, and palm oil refinery effluents degradation (Leong et al., 2012) and degradation of recalcitrant organic pollutants (Azimi et al., 2012; Matafonova et al., 2012; Zoschke et al., 2014). However, based on the literature study conducted, the potential applications of Fenton process or UV integrated with Fenton oxidation process is not well explored for the treatment of real wastewater especially textile wastewaters. In this regard, it is imperative to evaluate the suitability of using UV integrated Fenton oxidation process for degrading real textile wastewater, especially from small scale industries to develop a small, simple and stand-alone treatment system.

1.2   Problem Statement

The conventional wastewater treatment processes for the textile industry are not capable of degrading many of the recalcitrant pollutants present in industrial wastewater. Among AOPs, Fenton process which is a simple and stand-alone treatment system is considered to be an efficient way to remove recalcitrant organics in wastewater. Nevertheless, the large volume of sludge generation and consumption of a high amount of Fenton's reagent have been identified as few limitations that influence the applicability of conventional Fenton process for industrial wastewater.   Therefore to overcome the drawback, the practical treatment system which integrated Fenton with UV was investigated in this study to degrade the wastewater from cottage industries. But it's important to conduct detailed studies to evaluate the suitability of the suggested method since to-date no study is available on using batik wastewater for UV integrated Fenton oxidation. In Malaysia, there are approximately 1,500 Batik textile factories operate as cottage industries. The Batik industry has expanded beyond traditional domain and has gone international. Batik

making process consumes a large amount of water and produces wastewater high in color, especially reactive dyes, resin, grease, surfactants (sodium silicate), wax, and suspended solids. According to the report by Department of Environment of the state of Kelantan, the compliant rate of Batik industry is relatively low compared to other cottage industries (DOE Kelantan Report, 2011) due to mainly unavailability of a proper treatment system. Therefore, Batik industry require the development of wastewater treatment system which is highly efficient, stand-alone, simple , small and economically viable to reduce the recalcitrant contaminants to meet the minimum wastewater discharge standard fixed by Department of Environment Malaysia.

In the UV integrated Fenton oxidation, pollutants removal is highly depends on the initial pH of wastewater, dosages of H_2O_2 and Fe^{2+}, retention time and UV radiation intensity. Therefore, all the above-stated parameters need to be evaluated and optimized for maximum removal efficiency. Most of the available studies only focus on the color removal efficiency, not the TOC or COD removal efficiencies to represent the effectiveness of the process. Color removal indicates the removal of the color imparting functional group from the dyestuff, and not necessarily mineralization of the dyestuff. Therefore, COD and TOC are required as these parameters indicate the reduction in the organic contaminants concentration in the wastewater. In addition, the characterization of sludge is also needed since it is the main limitation of the practical application of the Fenton process and UV integrated Fenton oxidation processes. Analytical methods such as GC/MS, FTIR, and HPLC are further used to study the superiority of the process by evaluating the intermediate products.

To understand the mechanism of mineralization and degradation various analytical analysis were also conducted to determine the organic contaminants present in the effluent before and after the treatment using analytical methods such as GC/MS, FTIR and HPLC. Besides, to complete the understanding of the degradation process, kinetic

studies were also conducted besides conducting comparative studies with other photochemical and non-photochemical processes.

1.3   Aim and Objectives of the Study

The aim of this study is to develop a simple, stand-alone, small and highly efficient treatment system by integrating Fenton oxidation with UV radiation for small scale industries. To achieve this aim, three main objectives are identified and the activities conducted to achieve the objectives are listed as follows:

1. To evaluate the pollutant removal efficiency of Fenton process and UV integrated Fenton process in term of COD, TOC and color removal efficiencies.

    i.   To determine the effects of operating parameters namely; mass ratios of H_2O_2:COD and H_2O_2:Fe^{2+}, the initial pH value of the wastewater, UV-radiation intensity and retention time.

    ii.   To identify the optimum reaction conditions to degrade the Batik wastewater by using the model developed through response surface methodology.

    iii. To evaluate the organic pollutant removal efficiency of both Fenton and UV integrated Fenton oxidation processes through FTIR and GCMS, HPLC analyses.

    iv.   To conduct the sludge characterization study to analyze the composition of sludge produced from Fenton and UV integrated Fenton oxidation processes.

    v.   To compare the treatment efficiencies of UV integrated Fenton oxidation process with UV combined with H_2O_2, UV photolysis, UV-Fe^{2+} coagulation, Fe^{2+} coagulation and Fenton process in terms of COD removal.

    vi.   To determine the effects of Fe^{2+} coagulation on Fenton process and UV integrated Fenton oxidation process.

2. To conduct an economical and environmental feasibility study for the developed system. The activities conducted to achieve this objective are as follows:

    i.   Comparative studies of cost estimation of Fenton process and UV –Fenton oxidation process

    ii.   Develop a cost efficient treatment system for cottage industry in Malaysia.

    iii.   Treatment system with non-toxic by-products.

3. To validate the model developed for Batik wastewater with other industrial wastewater containing high strength contaminates. For this reason model developed for Batik wastewater is tested for the applications of industrial wastewaters collected from palm oil mills, leachate industry and metal finishing industry.

1.4   Novelty

The novelty of the work is in providing a clear strategy and know-how for developing a simple, cheaper, stand-alone and efficient treatment system suitable for small-scale industries with recalcitrant wastewater generation.

1.5   Scope of the Study

The scope of this study is limited to the development of Fenton hybrid system by integrating with UV radiation to increases the applicability of AOPs for the small scale industries, in particular, Batik industry wastewater. Amongst various cottage industries, Batik industry is chosen as a wastewater since the Batik wastewater discharged after conventional treatment has the lowest level of compliance with the department's law and regulations. The Batik wastewater used in this study was collected from a local Batik manufacturing company (Institut Kraf Negara, Rawang, Malaysia) with COD ranged between 1600- 1900 mg/l. And the wastewater was filtered through a filter paper to remove the wax prior to experimental studies. The preliminary study was conducted using simulated reactive dye wastewater containing 'Remazol Brilliant Blue' as this is one of

the common types of dye used in Batik industry to evaluate the treatment efficiency of Fenton oxidation. With the aim to increase the efficiency and overcome the limitation caused by this process, low-pressure UV-C lamp was integrated with Fenton process as it is energy efficient and optimum organic pollutant removal occurs in UV range between 245 and 285 nm. In addition, the model developed for Batik wastewater was tested for suitability through using various industrial wastewaters with high, medium and low COD values to get the foundation for future industrial system application.

1.6   Thesis Outline

This thesis starts with an abstract followed by five chapters dealing with different aspects of the current study and ending with references and appendixes.

Chapter 1: Introduction

This introduction chapter provides brief background knowledge of the textile wastewater and advanced oxidation processes, particularly Fenton process. It also includes the drawbacks of Fenton oxidation with highlighting the importance of developing a simple and economical integrated Fenton process for the treatment of recalcitrant wastewater from small scale industries. Justification of choosing UV integrated Fenton oxidation process based on literature study also briefly discussed. Based on the problem statement, the aim and objectives of the study are defined. The outline of the thesis is also included in this chapter.

Chapter 2: Literature Review

This chapter establishes the literature review covering characteristics of textile wastewaters, Batik industry and the manufacturing processes involved, limitation of conventional wastewater treatment methods, the mechanism, and concept of various advanced oxidation methods and their advantages over the conventional methods. This

chapter also discussed advantages of Fenton´s oxidation among other AOPs, Fenton´s reaction mechanisms, different applications of Fenton oxidation for the treatment of a variety of wastewaters, operations conditions and various enhancement techniques of Fenton oxidation to overcome its limitation for industrial application. Fenton integrating with UV radiation found to be the simple and cheap method for degrading recalcitrant contaminants and literature about this method was also reviewed. The justification for the selected method was given in this section as well.

Chapter 3: Methodology

An overview of the methodology of the research activities is described in this chapter. The characteristics of synthetic dye wastewater (Remazol brilliant Blue) and Batik wastewater, chemicals and materials used, description of photo–reactor, and the procedures of the experiments and method of analyses are presented in this chapter. In addition, methods for the determination of degradation efficiency of wastewater using COD, TOC and color removal apart from GC/MS, FTIR, HPLC, SEM/EDX, and particle size distribution are also described. The detailed information on the response surface methodology, a statistical used in this work also briefly explained.

Chapter 4: Experimental Results and Discussion

Chapter 4 contains the results and discussion on the degradation efficiency of Fenton process, and UV integrated Fenton process, in a batch scale experiment for the treatment of batik industry. The chapter also discussed the preliminary results obtained using Fenton process for simulated dye wastewater. The detailed information of the effects of the operating parameters was also presented. The kinetic study was successfully conducted and presented in this chapter. In addition, analyses conducted to identify the organic contaminants in the treated and untreated wastewater are also presented in this chapter.

The comparison of Fenton oxidation and UV integrated Fenton oxidation in terms of degradation efficiency, economical analysis and environmental implication are presented, which provided the motivation to develop this integration work. Furthermore, the performance of UV/H_2O_2, Fe^{2+} coagulation and UV/Fe^{2+} coagulation processes in terms of COD, TOC and color removal are also discussed in details to further validate the efficiency of UV integrated Fenton process.

Chapter 5: Conclusion

Chapter 5 includes the summary of this study and concluding remarks of the main findings. The future direction is also provided in this chapter.

CHAPTER 2: LITERATURE REVIEW

2.1   Textile Industry

The textile industry is steadily increasing in ASIA, due to the growth of world population and gross domestic product (GDP). The textile industry is a very diverse and a broad sector that contributes significantly to the economic and social development. This industry is unique in the global economy because its provide employment for women, has low entry barriers, does not require huge capital, low skills, and the most protected among all the manufacturing industries in the global (Economic et al., 2007). Therefore, this industry is considered as a highly competitive industry. However, the production of textiles is considered as one of the biggest consumers of high water quality and chemicals.

Textile effluents are graded as one of the most polluting of all industry wastewater, in terms of volumes of discharged and composition. For every kilogram of textile product produced, approximately 100 liters of water are consumed; which translate into approximately 3.7 million liters of wastewater released, each day worldwide (Amaral et al., 2014). Thus, the wastewater released from textile sector estimated to exceed 4-8 million cubic meters per year, by considering 40 million tons of textile fibers per year (Wang et al., 2004).

2.1.1   General Textile Processes

Textile processing involves many different processes and the composition of wastewater depends greatly on the processes and chemicals used. Generally, processes involved in the textile industry are divided into two: i) dry process and ii) wet process. The drying process consists of an opening, blending, mixing, carding, combing, spinning, weaving, and knitting. The quantity of water used in these processes is negligible. On the other

hand, the wet process consists of sizing and resizing, scouring, bleaching, dyeing and finishing, require large amounts of water at each stage and also generates a significant amount of wastewater which varies in composition. (Vilar et al., 2011). Figure 2.1 exemplifies some of the potentials contaminants generated from each textile processing step (Patel et al., 2015). Figure 2.1 confirms that this industry produces wastewater rich in color (dyes), resin, grease, surfactants (sodium silicate), wax, suspended solids and other recalcitrant contaminants. The next section discusses in detail the steps involved in each manufacturing activity.

1. Sizing
• Sizing Metals, and Cleaning waste

2. Desizing
• Water soluble sizes, Enzymes, Starch, Waxes, Ammonia, and Lubricants

3. Scouring
• NaOH, surfactants, soaps, waxes, oils, solvents, enzymes, and disinfectants residues

4. Bleaching
• H_2O_2, AOX, sodium silicate or organic stabalizer, and high pH wastewater

5. Mercerizing
• High pH wastewater and NaOH

6. Dyeing
• Colors, salts, surfactants, sulphide, metals, acidity/alkalinity, spent solvents, formaldehyde, high BOD and COD wastewater

7. Printing
• Suspended solids, urea, solvents, colored wastewater and metals, heat, and Foam

8. Rinsing
• Resins, waxes, cholorinated compounds, acetate, stearate, softeners, solvents and suspened solids

Figure 2.1: Potentially contaminants from textile processing steps

2.1.1.1 Sizing and Desizing

In sizing process, the starch or starch derivatives, or synthetic sizing agents such as polyvinyl alcohol (PVA), polyacrylates and carboxymethyl cellulose, are applied on the cloth to gain the strength and minimize the breaking of the fibers. Sizing produces small amount, but concentrated wastewater with high levels of COD, BOD and suspended solids (Hassan et al., 2009). After the weaving, the sizes removed from the fabric as the presence of sizing agents hinders dyeing, printing and finishing process by acting as a barrier to dyes and other chemicals. Generally, this process contributes 50 % of the BOD.

2.1.1.2 Dyeing Process

The dyeing process consumes large quantities of water, chemicals and dyes, generating a large amount of wastewater (Dantas et al., 2006). The treatment of wastewater after the dyeing process involves the removal of unfixed dyestuff and organic compounds. Approximately, about 40 % of the dyes remain unused and generally present in the effluents from the dye-bath and first rinsing step. Dyeing also contributes to the almost all the salts and color present in the textile effluents. Textiles were primary dyed with natural dyes (Ingamells et al., 1993). Natural dyes gives several inherent disadvantages such as non-reproducible and poor color fastness (Vankar, 2007).

Synthetic dyes can provide a viable alternative to the natural dyes in an industrial context. In the 21st century, synthetic dyes are widely produced and used as a colorant in textile, leather, painting and printing industry due to their unique properties such as high wet fastness profile, brilliant shades, lower cost and simple synthesis methods. It is estimated that over 100,000 commercial dyes with an annual production of 7×10^5 tons are available and most of them are synthetic and soluble compounds. Synthetic dyes are categorized as acidic, reactive, disperse, vat, metal complex, mordant, direct, basic and sulfur dyes based on their application (Engineers, 2005; Reife et al., 1996; Youssef et al., 2016).

Synthetic dyes used in the textile industry contains complex aromatic amide groups with alkyl, halogen, nitro, hydroxyl, sulfonic acid, substituent(s) and inorganic sodium salts. Table 2.1 shows the classification of different types of dyes based on their applications. From the table, it can be concluded that the main types of dyes used in the textile industry can be grouped into seven categories such as reactive dyes, acid dyes, basic dyes, direct dyes, disperse dyes, sulfur dyes and vat dyes.

Among others, reactive dyes are commonly used in Malaysia Batik industry. Reactive dyes were commercially introduced in 1956 by Imperial Chemical Industries, ICI (Leube, 2004). Reactive dyes are the most important dyes for cellulosic materials. Currently, one-third of the dyes used for cellulose fibers are reactive dyes. More than 80,000 tons of reactive dyes are produced and consumed each year. The better wet fastness, brilliant shades, bright colors, easy applicability and reproducibility than other dyes have attracted the manufacturers to choose reactive dyes for textile dyeing (Choudhury, 2006). Besides, reactive dyes also chemically react with textile fibers by forming covalent bonding. Covalent bond is formed between a carbon atom of the dye and oxygen, nitrogen or sulfur of a hydroxyl, amino or thiol group from the polymer of fibers under the influence of pH and temperature (Christie, 2014). Reactive dyes are able to react with fibers only in alkaline conditions, whereas under neutral conditions they adsorb and diffuse inside the fiber. Approximately, 70 to 150 liters water and 30 to 60 g of dyestuff are needed for dyeing per kilogram of cotton with reactive dyes (Allègre et al., 2006). Industrial dyes are generally toxic, carcinogenic and stable as they contain also, anthraquinone, sulfur, triphenyl methyl and phthalocyanine groups in their structure (Al-Amrani et al., 2014). Therefore, dye effluents contain a high concentration of recalcitrant compounds, toxic substances, detergents and soaps, oil and grease, sulfides, soda, and alkaline rich wastes. The pollutants that are present in textile wastewater in a large quantity are unfixed dyes, or dispersing agents that are organic and highly colored which are washed out during the

dyeing process. It is estimated that about 12- 15% of the dyes are lost and discharged in the effluent during the wet processing activities (Al-Amrani et al., 2014) because dyes are not completely fixed to the fibers during the dyeing process. Figure 2.2 gives the percentage of unfixed dyes for various dyes together with their applications. It's very clear from the figure that, reactive dyes have the poorest fixation compared to other types of dyes. The dyeing process contributes 15- 20 % of the total wastewater and it is strongly colored.

2.1.1.3 Printing

Printing paste consists of water, dyes, urea, and thickeners. Wastewater from printing process is small in quantity but more concentrated compared to the dyeing process and contain high level of COD and solid waste derived from the print pastes.

Table 2.1: Classification of dyes based on the application

Dyes	Application	Chemicals
Reactive	Wool, cotton, silk and nylon.	Anthraquinone, formazan, phthalocyanine, azo noxazine and basic.
Acid	Wool, nylon, silk	Anthraquinone, xanthene, azo, nitro, and triphenylmethane.
Basic	Nylon, and polyester	Hemicyanine, azo, cyanine, diazahemicyanine, azine diphenylmethane, xanthene, triarylmethane, acridine, anthraquinone and oxazine.
Direct	Nylon, rayon, and cotton.	Phthalocyanine, azo, oxazine, and stilbene.
Disperse	Polyamide,acrylic polyester,	Benzodifuranone, azo, anthraquinone, nitro, and styryl.
Sulfur	Rayon and cotton.	Indeterminate structures
Vat	Wool and cotton.	Indigoids and anthraquinone.
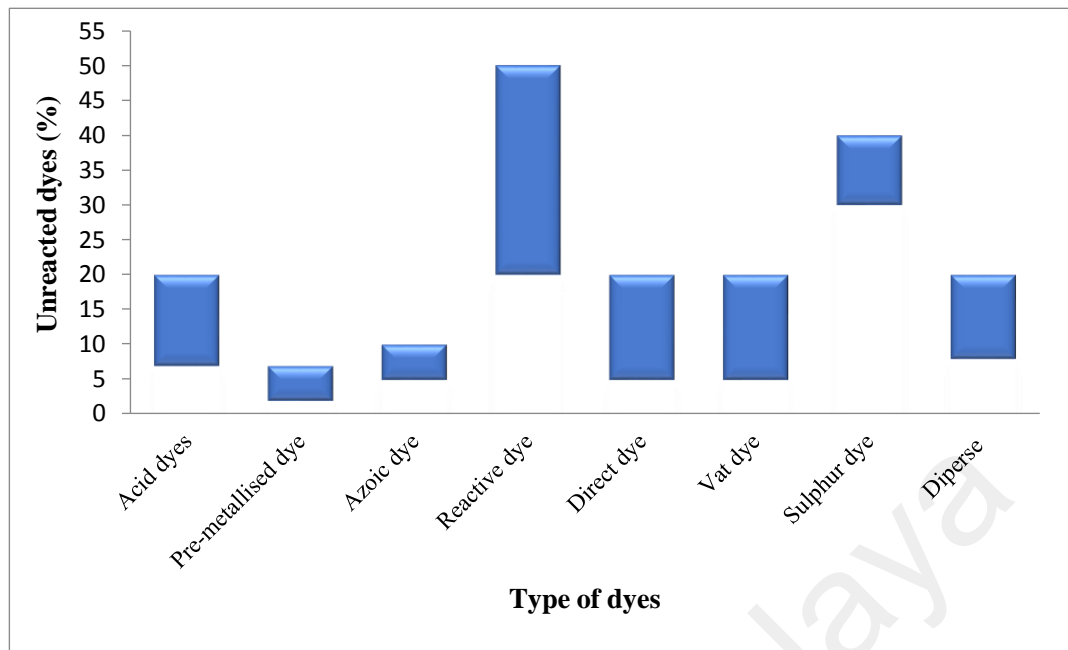
Figure 2.2: Percentage of unreacted dyes from industrial process based on the type of dyes

2.1.1.4 Rinsing

Depending on the dyeing processes applied, the rinsing process consumes approximately 50- 80% of the total water consumption. Rinsing is needed to remove the unfixed dyestuffs from the cloth. The wastewater generated from rinsing has a high salt concentration, heavy colors, soaps, gums, minerals, and organic substances (Cervantes et al., 2006). This process contains a major source of wastewater.

In summary, most of the textile processes consume a large amount of water and generates significant quantities of wastewater, which varies in composition. The most important sources of pollution among various process steps are sizing, desizing, dyeing, printing and finishing of the textile materials. Effluents discharged from various processes contribute to rising in organic load and the highly colored water causes reduction of sunlight and affect the photosynthetic activity and aquatic organism. Besides, the colored

wastewater also affects the microorganisms and fish species as most of the dyes are toxic and carcinogenic.

2.2   Batik Industry in Malaysia

Batik industry is one of the oldest textile industries in Malaysia which has been in existence since 1921 and its commercial production started in the 1960s. In Malaysia, this artistic industry has developed into a profitable cottage industry from a small scale operation (Nordin et al., 2012). This industry creates jobs and business opportunities in the rural areas besides contributing to the economy of the nation (Nair, 2014). Batik industry also has benefited the tourism industry of Malaysia as Batik production in Malaysia has its own design niche which is up-to-date, fresh and stylish.

Batik manufacturing needs high skills coupled with the right equipment to produce high-quality batiks. Batik involved the resist techniques which can be explored by the artist, art lover and Batik artisan. The artist's creativity determines the type of depth, color, dimension and style that she wants to express. Traditionally, the process of making a batik industry is illustrated in Figure 2.3. There are two main types batik in Malaysia i) hand painted and ii) block printed. And both types are often combined and this way gives the textiles more colors and open patterns. The canting process is filled with wax and used to trace the outline of the pattern on the cloth. The wax is normally made up of bee's wax, paraffin wax, resin, fat and a synthetic wax mixed in varying quantities. Wax helps dye penetration and creates a marbled look and the resin makes the wax cling to the textile. Nowadays, in batik industry, synthetic dyes, and mostly reactive dye is used as the coloring substance because of their brilliant colors and ability to attach easily to the cloth. And the colors are fixed by using sodium silicate.

Batik industry consumes large amount of high quality water and also generates large volume of high strength wastewater due to the usage of various chemicals. Batik wastewater contains dyes, waxes and chemicals such as ludigol (brighter and vibrant color), natrium or sodium silicate, sodium carbonate, sodium alginate (thicken dye), and potassium aluminum sulfate (pre-treatment process) which results in higher levels of COD and total suspended solids (TSS) value. The boiling process of painted fabrics also generates wastewater that contains surfactants, suspended solids, unfixed dyes and waxes from canting process. Normally, these wastewaters are recalcitrant in nature due to the presence of a variety of chemicals. Some of the most difficult pertinent problems in the textile industry are reduction of water usage, color and salt removal from waste water besides COD removal. This makes Batik effluent is difficult to be treated using conventional method.

1 Preparation of Cloth

o Wash in hot water
o Soaked in solution of castor oil or coconut oil
o Oil boiled away
o Placed in starch solution
o Dried in sun
o Cloth pounded and beaten with wooden hammer

2 Coating &Wax Application

o Design drawn on the cloth
o Canting tools - used to apply wax to outlines and lines motifs
o Tool with a flat, wide spout, used for filling in larger sections
o Cap - a hand stamp, allowing the motif to be printed on the cloth (wax always applied to both sides of the cloth)

[Low]

[High]

Batik Wastewater

5 Rinsing & Drying

o Washed with water
o Dried in the sunshine

[Medium]

[High]

[High]

4 Soaking, Rinsing & Boiling

o Soaking with Sodium silicates- to make color fastness on the cloth
o Then cloth is washed
o After that, cloth is immerse into the boiling water to remove the molten wax and excess dye

3 Dyeing

o Immerse the cloth into the dye bath until the correct shade is obtained
o Fabric rinsed and dried overnight
o Wax scratched away from Batik
o Cloth rinsed

Figure 2.3: Processes and level of wastewater generated in Batik Industry

2.3   Characteristics of Textile Wastewater

Characteristics of the wastewater generated in the textile industry are dependent on the type of process, fabric, dyes and chemicals used. Recalcitrant textile wastewater generally contains high concentrations of organic compounds (expressed as high COD), colors associated with residual dyes, a wide range of pH, low biodegradability and high salt content (Balcioglu et al., 1997; Blanco et al., 2012; Hammami et al., 2012; Hassan et al., 2009; Lahkimi et al., 2006; Punzi et al., 2012; Rodrigues et al., 2009; Schrank et al., 2007). Some general values could be given, although the wastewater characteristics vary within the same process. The typical characteristics of textile wastewater are depicted in Table 2.2 (Adapted from (Al-Kdadi et al., 2004). It shows that, large amount recalcitrant contaminants is released from textile and dyeing industry. On average, 58-81% of water is discharged from the textile industry, with average water consumption of 73%.

Table 2.2: Typical textile industrial wastewater characteristics

Parameters	Range
COD	150 to 12000 mg/L
Total suspended solids	2900 and 3100 mg/L
Total nitrogen	70 to 80 mg/L
BOD	80 to 6000 mg/L
BOD/COD	0.25

The water environment can be adversely affected by just a small amount of dyes and therefore removal of organic contaminants from wastewater has become an environmental concern. It is more complicated to treat colored industrial effluents because they are highly inconsistent in both the hues and concentrations of color. The toxic effect of dyestuff, and another organic contaminants being released into the environment is well understood by the public and the increasing concern about the environmental impact has led to the closure of several small-scale industries worldwide. Textile wastewater can cause severe impacts on the environment by obstructing sunlight

penetration into the aquatic environment, reducing reoxygenation, affecting the aesthetic value of water resources and interfering with aquatic biological processes which eventually affect the eco balance (Torrades et al., 2004). Recalcitrant textile effluents also potentially hazardous for a human being by affecting the inhalation process, body tissues, inflammation or irritation of tissues, and causing allergic reactions. Besides, the acidic waste generated from the textile mill processes are also may corrode the metal and concrete structure.

2.4 Limitations of Conventional Textile Wastewater Treatment

Conventional techniques based on physicochemical, chemical and microbiological methods such as coagulation, adsorption, ion exchange and ultra-filtration are traditionally used for degrading persistent organic pollutants that commonly discovered in the textile wastewater. Conventional wastewater treatment plants are not able to ensure that the treated effluent meets the discharge criteria of wastewater in terms of COD. Conventional methods are ineffective due to the high generation of solid wastes and sludge, which require secondary treatment (Babuponnusami et al., 2013; Punzi et al., 2012; C. -H. Wu et al., 2008). The adsorbent regeneration, intermediate products generation and rapid fouling of the used membranes are some of the other disadvantages of conventional treatment processes. The characteristics of persistent organic pollutants such as high stability to sunlight irradiation, resistance to microbial attack and temperature impair their removal efficiency of conventional wastewater treatment.

It has been frequently quoted that conventional treatment methods such as biological and simple physical-chemical treatments are not efficient for complete mineralization as most of the pollutants are highly recalcitrant (Bandala et al., 2008; Karthikeyan et al., 2011). Table 2.3 summarizes the limitation of conventional methods for the treatment of textile wastewater. New environmental concerns and regulations are urging the textile industry

to reduce pollutants and recycle the process water as textile effluent rarely meets the discharge standards (Karthikeyan et al., 2011). Based on the review conducted on the limitations of the methods, it is necessary to conduct an intensive research to identify more effective wastewater treatment systems. The treatment should also focus on the removal of biodegradable components of wastewater, followed by degradation of recalcitrant contaminants. Alternative treatment technologies capable of mineralizing refractory molecules effectively such as pesticides, surfactants, coloring matter and endocrine disrupting chemicals must be optimally developed. Therefore, developing a practical and efficient water treatment system has been of global interest over the past decades.

2.5   Chemical Oxidation

The chemical oxidation process is one of the alternatives to conventional wastewater treatment to treat highly recalcitrant textile wastewater (Tunay et al., 2010). Chemical oxidation is capable of degrading organic contaminates partially or completely. And complete degradation reduces the organic compounds into water and carbon dioxide. It can be divided into two classes: i) classical chemical treatments and ii) AOPs (Comninellis et al., 2008; Marco S. Lucas, Dias, et al., 2007). In recent years, chemical oxidation has been used widely used to remove organic pollutants that cannot be degraded completely by conventional biological methods (Tekin et al., 2006; Donglei Wu et al., 2012). Section 2.5 1 discusses briefly the type of oxidants used in the wastewater treatment.

Table 2.3: Limitation of conventional methods for treating textile wastewaters

Conventional methods	Advantages	Limitation
1. Biodegradation 2. Coagulation /flocculation 3. Activated carbon adsorption 4. Reverse osmosis 5. Ozone treatment 6. Ultra- filtration 7. Nano-filtration	- Elimination of insoluble dyes - High degradation of biodegradable substances - Higher color removal - Removal of mineral salts - Suspended solids and organic substance removal	- Low biodegradability of soluble reactive dyestuff - Non-destructive - Transfer the dye from liquid to solid wastes - Generate large amounts of sludge - Low efficiency - Low reaction rate of the treatment - Regeneration of adsorbents - A complex organic chemical that is resistant to biological degradation - Contains various non-biodegradable organics, inorganic and color materials. - Produce toxic intermediates, - Limit their applicability in highly contaminated pollutants. - High cost - Low reduction of COD - Iron hydroxide sludge

2.5.1   Type of Chemical Oxidants

Chlorine, chlorine dioxide, ozone, hydrogen peroxide, peracetic acid and permanganate are the most commonly used chemical oxidants. These oxidants have been employed based on the targeted pollutants, types and properties of the effluents. Chemical oxidants are also known to react preferentially with the electron-rich organic functional groups such as aromatic compounds (phenol, aniline, and polycyclic aromatic, for example), organosulfur compounds, and deprotonated amines (Glaze, 2000).

2.5.1.1 Chlorine and Chlorine Dioxide

Chlorine and chlorine dioxide are the most commonly used disinfectant for drinking water and wastewater for many years due to their strong bactericide properties, easily applied, measured and controlled, fairly persistent and relatively cheap (Y. Wang et al., 2015). Besides, helping to disinfect the water, chlorine also able to destroy the hydrogen sulfide, remove color and odor in the wastewater, and oxidize iron and manganese (Hey et al., 2012; A. Zhang et al., 2014). Although, chlorination proven to be effective for killing bacteria and virus, it has some drawbacks such as formation of toxic and carcinogenic by-products (Gao et al., 2014).

2.5.1.2 Ozone

Ozonation has been used as the oxidation technology for textile wastewater because of its strong oxidizing properties. Ozonation always involves these two species: ozone (O_3) and $HO\bullet$ radical. Ozone attacks the organic contaminants in wastewater through direct reaction (as molecular O_3) or by forming free radical ($HO\bullet$) via a complex decomposition the reaction according to the reaction (2.1) - (2.6). (Legube et al., 1985; J. L. Wang et al., 2012)

$$O_3 + OH^- \rightarrow O_2^- \cdot + HO_2 \cdot \qquad (2.1)$$

$$HO_2 \cdot \rightarrow O_2^- \cdot + H^+ \qquad (2.2)$$

$$O_3 + O_2^- \cdot \rightarrow O_3^- \cdot + O_2 \qquad (2.3)$$

$$O_3 \cdot^- + H^+ \rightarrow HO_3^- \cdot \qquad (2.4)$$

$$HO_3 \cdot \rightarrow HO \cdot + O_2 \qquad (2.5)$$

$$HO \cdot + M \rightarrow R \cdot \qquad (2.6)$$
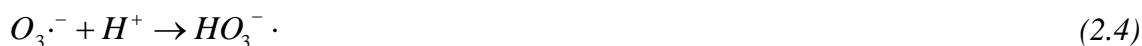
* M (organic compounds) that has alkyl group (R)

At low pH, molecular ozone is predominant where organic compounds are subjected to electrophilic attraction and decomposition. In contrary, at higher pH, ozone molecules decompose into free radicals ($O_2 \cdot$ and $HO_2 \cdot$) and subsequently to $HO \bullet$ radical. These radicals are free to react with organic pollutant at rapid rates (rate constant = 10^8 to 10^{10} $M^{-1}s^{-1}$) (Cooper et al., 1999). But the direct reaction with ozone and organic compound take place very slowly with kinetic constant in the range of 0.01 to $10^4 M^{-1}s^{-1}$. Many researchers have reported the efficiency of ozonation for disinfection, decolorization, dewatering, degradation of toxic synthetic organic compound traces, removal of persistent organic pollutants, odor, sludge and foam (Amat et al., 2005; Biń et al., 2012; Bustos et al., 2010; Ding et al., 2014; Gong et al., 2008; J. Wu et al., 2008; Zhao et al., 2013). Conditions that contribute to the formation of ozone and $HO \bullet$ radical vary with characteristics of pollutants, water quality, and concentration of the targeted compound, temperature, pH and level of ozonation.

On the contrary, there are several disadvantages associated with ozonation, which limit its application in larger and industrial scale textile wastewater treatment. The main disadvantage of ozonation is due to the higher consumption of electrical energy. Besides, O_3 also unstable and selective to unsaturated aromatic and aliphatic compounds. It requires complex mixing techniques that are associated with the high equipment and maintenance cost. In addition, there is also a potential of bromate formation. However, researchers have discovered that the limitations of ozonation can be overcome by combining it with other oxidants such as H_2O_2, ultraviolet radiation and ultrasound (Amat et al., 2005; Gogate et al., 2004b; Gong et al., 2008; Zhao et al., 2013). This hybrid process is termed as an Advanced Oxidation Process (AOP).

2.5.1.3 Hydrogen Peroxide

Oxidation by H_2O_2 is a well-established method for the destruction of recalcitrant organic contaminants. H_2O_2 is one of the most powerful oxidants and it is stronger than chlorine, chlorine oxide, and permanganate (Asghar et al., 2015; Moyer et al., 2004; Neyens et al., 2003). Hydrogen peroxide is an easy and efficient method to remove organic pollutants from wastewater. It was first used to remove odors from wastewater and later it has been used widely to treat various organic and inorganic pollutants to reduce BOD and COD (Y. J. Jung et al., 2012). Hydrogen peroxide can be converted into $HO \bullet$ radical which has the second highest reactivity to fluorine and twice as reactive as chlorine through catalysis. H_2O_2 is an attractive alternative to the industrial oxidants because it's highly active and non-selective oxidant (Cheremisinoff, 2002; Samanta, 2008). The catalytic oxidation of hydrogen peroxide is highly influenced by retention time of reaction, amount of H_2O_2, and temperature of the reaction. H_2O_2 has not been used often as an oxidant because of its slow rate of reaction. The oxidation rate of H_2O_2 can be enhanced by

integrating with other oxidants such as ozone, ultraviolet radiation (UV), ultrasound (US), persulphate or metal salts.

Chemical oxidation has been investigated in both pilot and full-scale for water disinfection and organic pollutant degradation. However, the cost of wastewater treatment through chemical oxidation is normally more expensive than through conventional physical and biological methods. Owing to their high operation cost their full-scale application is limited.

Advanced oxidation processes (AOPs), based on the in-situ generation of powerful oxidizing agents such as hydroxyl radical have been studied by many researchers in the last two decades. AOP is a complete, irreversible degradation process that does not produce toxic and unstable products (Ikehata et al., 2004; Prousek et al., 2007; Tony et al., 2012).

2.6   Advanced Oxidation Processes

Over the past 30 years, many studies have been conducted to investigate the efficiency of advanced oxidation processes (AOPs) in treating different recalcitrant wastewaters that contain refractory and toxic pollutants (Balcıoğlu et al., 2003). Most of the AOPs uses a combination of strong oxidants such as hydrogen peroxide, ozone with catalysts such as iron salts, transition metals, UV, US, microwave irradiation (Gogate et al., 2004a). AOPs are based on the generation of highly reactive oxygen-containing intermediates such as $HO\bullet$ radical, which has a high electrochemical oxidant potential (Gaya et al., 2008; Nezamzadeh-Ejhieh, & Amiri, 2013; Nezamzadeh-Ejhieh et al., 2014; Nezamzadeh-Ejhieh, & Shirvani, 2013; Soon et al., 2011). Having the strong oxidizing potential, and readily attack or degrade almost all recalcitrant organic compounds to carbon dioxide, water and inorganic ions via hydroxylation or dehydrogenation. AOPs are widely used

in wastewater treatment for overall organic content reduction, specific pollutant destruction, sludge treatment, color and odor reduction (Gunukula et al., 2001; Kavitha et al., 2004; M. Lucas et al., 2006; Nezamzadeh-Ejhieh, & Banan, 2013). The feasibility of AOPs for wastewater treatment is further enhanced by their ability to produce $HO\bullet$ radical through different means.

A thorough search of the literature indicate that Advanced Oxidation Processes (AOPs) are technologies with significant importance to reduce or fully treat many types of wastewaters. The concept of AOPs was first established by Glaze and others (1987). There have been a steady increase in interest of the research related with AOPs, which is evident on the rise in the annual number of research papers that have been published. This technology has gained popularity as an imperative technology for oxidation and destruction of refractory compounds in wastewater treatment areas (Tony et al., 2012). To compensate for the limited biodegradability contaminants, AOPs have been considered as an alternative. AOPs are a set of processes involving the instantaneous use of more than one oxidation process and rapid production of the highly reactive and non-selective $HO\bullet$ radical, and other reactive oxygen species.

The $HO\bullet$ radical is the second strongest oxidizing species with a relative oxidation power of 2.8 EV as can be seen in Table 2.4. This non-selective primary oxidant instantly reacts with pollutant and oxidized organic contaminants to water, carbon dioxide and inorganic ions (Vujević et al., 2010). $HO\bullet$ radical attack organic molecules through three possible means: i) dehydrogenation of a hydrogen atom to form water; ii) hydroxylation of a non-saturated bond; and iii) redox reaction. Figure 2.4 illustrates some special characteristics of $HO\bullet$ radical which make AOPs a powerful method for organic contaminant degradation. Feasibility of AOPs for wastewater treatment is enhanced by the fact that they offer multiple means for generation of highly potent free radicals.

Table 2.4: Relative oxidation power of some relevant oxidants. (Ullmann's 1991)

Oxidant	Symbol	E^0 (V)
Fluorine	F	3.03
Hydroxyl radical	$HO \cdot$	2.80
Single oxygen	O_2	2.42
Ozone	O_3	2.42
Hydrogen peroxide	H_2O_2	1.78
Perhydroxyl radical	$HO_2 \cdot$	1.70
Permanganate	$KMnO_4$	1.68
Chlorine dioxide	ClO_2	1.57
Hypochloric acid	$HClO$	1.45
Chlorine	Cl	1.36
Bromine	Br	1.09
Iodine	I	0.54
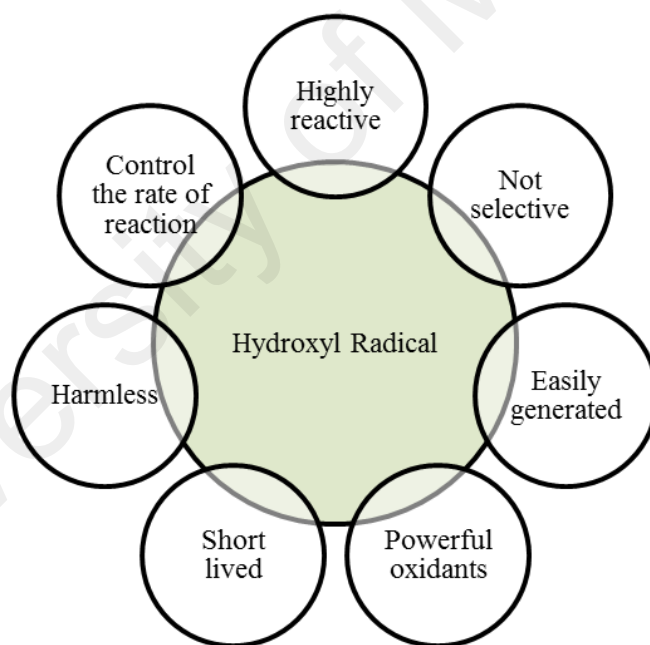
Figure 2.4: Features of hydroxyl radical

Advanced Oxidation Processes (AOPs) such as Fenton oxidation, photocatalytic oxidation, photo-Fenton process, H_2O_2 photolysis, ozonation, electro-Fenton oxidation and electrochemical oxidation processes have been proposed as potentially useful environmental remediation technologies (Archina et al., 2015; Ayodele et al., 2012; Blanco et al., 2012; Buthiyappan et al., 2015; Cañizares et al., 2009; J. Chen et al., 2007; Silva et al., 2009; Tehrani-Bagha et al., 2010).

Various AOPs such as heterogeneous photocatalytic oxidation (Bauer.R et al., 1993), ozone-based processes (Meric et al., 2005), Fenton oxidation @ Fenton process, photo-Fenton reaction (Borba et al., 2012; Bouafia-Chergui et al., 2010; Oturan et al., 2011), Electro-Fenton reaction and electrochemical processes have been proposed as potentially useful environmental remediation technologies (Archina et al., 2015; Ayodele et al., 2012; Blanco et al., 2012; Buthiyappan et al., 2015; Cañizares et al., 2009; J. Chen et al., 2007; Silva et al., 2009; Tehrani-Bagha et al., 2010). Table 2.5 illustrates the classification of AOPs based on their mechanism.

Table 2.5: AOPs classification based on the mechanism

Reaction	Mechanism	AOPs
Homogeneous	Chemical	O_3
		O_3/H_2O_2
		Fenton oxidation
	Electrochemical	Electro-Fenton
		ElectroPhoto Fenton
	Photochemical	O_3/UV
		$O_3/H_2O_2/UV$
		H_2O_2/UV
		Photo-Fenton
Heterogeneous	Photochemical	$TiO_2/O_2/UV$

Based on the literature review, combinations of different AOPs have been found to be more efficient compared to individual oxidation process due to the generation of more radicals and high rate of reaction. Gogate and others (2004b) also reviewed that, the AOPs are not cost effective and energy efficient if used individually. Furthermore, they also concluded that, the efficiency of the process is highly dependent on the reactor configuration as it plays a crucial role to achieve maximum utilization of free radicals generated in the system and to create better contact between the catalyst and oxidants.

Hybrid AOPs with integrating oxidant, catalyst and energy dissipating components such as H_2O_2, ozone, US, UV, solar light, microwave offers better treatment efficiency compared to single systems (Autin et al., 2012; Babuponnusami et al., 2014; Biń et al., 2012; Antonio Zuorro et al., 2013). AOPs combined with energy dissipating components provide some advantages, including an increase in the rate of reaction, amount of $HO \bullet$ radical, less fouling of solid catalyst, enhanced pollutant removal efficiency, lower reaction time, lesser sludge formation, and elimination of mass transfer limitation (Mahamuni et al., 2010; Vujević et al., 2010; X. -R. Xu et al., 2009). Among others, UV integrated with AOPs has received great attention among the researchers working in wastewater treatment (X. -R. Xu et al., 2009; Zhao et al., 2013; A. Zuorro et al., 2013). UV oxidation is a destruction process that mineralized or oxidizes a variety of organic contaminants found in wastewater by the addition of oxidants, catalyst and irradiated with UV light. In the UV-AOPs system, the contaminants are destructed by direct oxidation, UV-photolysis and synergistic action of UV with oxidants and catalyst. As per reported in the literature, UV is attaining greater attention for drinking water treatment, microbial disinfection and degradation of the organic compound through direct or indirect photolysis (Alkan et al., 2007; Biń et al., 2012). The efficiency of UV light absorption proven to be improvised by the addition of oxidants or photosensitizing agents (Banat et al., 2005; Y. J. Jung et al., 2012; P. Liu et al., 2013). The available literature shows that

radiation has been useful for environmental applications such as, drinking water treatment, wastewater treatment, decolorization of dyes, (Chang, Chung, et al., 2010) oxidation of organic compounds, pesticide removal (Chelme-Ayala et al., 2010), leachate treatment (Hu et al., 2011), pharmaceutical compound degradation, and palm oil refinery effluents degradation (Leong et al., 2012). There is growing research focus on the application of UV for the degradation of recalcitrant organic pollutants (Azimi et al., 2012; Matafonova et al., 2012; Zoschke et al., 2014). As a conclusion, selection of oxidant, catalyst and energy dissipating agents are playing very important role in AOPS to enhance the degradation and mineralization efficiency of recalcitrant contaminants.

2.7   Advantages and Limitations of Conventional AOPs

In the past 30 years, the efficiency of AOPs in treating different recalcitrant wastewaters containing refractory and toxic pollutants has been studied (Balcıoglu et al., 2003). AOPs and various combinations of AOPs are known to generate strong $HO\bullet$ radical. These processes, increase the efficiency of the decomposition of impurities present in textile wastewater and reduce the cost of the process. Previous researches have proven that AOPs are effective for wastewater treatment. AOPs offer several advantages such as the effective removal of organic compounds and the complete mineralization of organic compounds into H_2O and CO_2. They have low selectivity, which helps solve many pollution problems. Besides, AOPs can generate $HO\bullet$ radical through various methods and can be used as a pretreatment method to fully or partially degrade non-biodegradable pollutants before conventional biological treatments to reduce the overall treatment cost. AOPs are more frequently used to degrade contaminants that are resistant to conventional treatment. However, AOPs are ineffective due to the high consumption of reagents, especially H_2O_2. Besides, homogeneous Fenton-based AOPs also has some limitation generate contaminated intermediate products and sludge, which require secondary

treatment. The limitation of Fenton oxidation can be overcome by integrating with oxidant or catalyst. Table 2.6 summarizes the advantages and limitations of the most commonly applied AOPs for wastewater treatment.

2.8   Industrial-Scale Applications of AOPs

Although AOPs are highly efficient at laboratory scale, more studies are needed to evaluate their applicability at industrial scale. Economic viability and efficiency of AOPs are major factors that limit their industrial application. Among AOPs, ozonation and UV/H_2O_2 have been used widely in industrial scale for drinking H_2O treatment. Table 2.7 summarizes the existing AOP treatment systems at industrial scale and it is clear that AOPs are widely used for drinking and groundwater treatment but rarely used in wastewater treatment. It should be noted that the industrial application of AOPs, especially Fenton-based processes for wastewater treatment, has not been much explored. Most of the previous studies have been conducted to evaluate the degradation performance using simulated wastewater. Limited research has been conducted on the effectiveness of AOPs for real industrial effluent treatment. The degradation mechanisms vary with contaminants. Therefore, the comparison between AOPs should be made in terms of removal efficiency, operation safety, manageability, applicability, and technical effectiveness of real wastewater, the necessity of post-treatment, secondary pollution prevention, toxicity reduction, and economic viability. There are limited studies on the cost estimation of different AOPs. The cost of different AOPs includes capital, operating, and maintenance costs. An overall kinetic model is required to design AOPs and determine the most efficient or economic operating regions. Along with the full-scale kinetic models, such cost is dependent on the operating parameters, such as H_2O_2 concentration, initial pollutant content, irradiation of light, and catalyst concentration.

Table 2.6: Advantages and limitations of conventional advanced oxidation processes

AOP	Advantages	Limitation	References
O_3	Strong oxidation power, Easily performed, Short reaction time No sludge remains, All residual of ozone easily decomposed	Higher operation cost, Energy consuming process, Needs pre-treatment	(Abu Amr & Aziz, 2012; Fanchiang & Tseng, 2009; Ikehata & El-Din, 2004)
O_3/UV	Higher efficiency, More efficiency at generating hydroxyl radicals, More effective than O_3 alone or UV alone	Not cost effective, Energy intensive, Mass transfer limitation, Sludge production, Turbidity can interfere with the penetration of light	(Guittonneau et al., 1990; Marco S. Lucas et al., 2010; Popiel et al., 2008; Rao & Chu, 2010; Ruppert et al., 1994)
H_2O_2/UV	Disinfectant, Simple process	Turbidity can interfere with the penetration of light, Less efficient in generating hydroxyl radical	(Elmorsi et al., 2010; Hu et al., 2011; Karci et al., 2012)
O_3/H_2O_2	More efficient than O_3 or H_2O_2 alone Effective for water treatment	Bromote formation, Excess usage of H_2O_2, Not cost effective, Energy intensive	(Ikehata et al., 2006; Lanao et al., 2008; Latifoglu & Gurol, 2003)
O_3/H_2O_2/UV	Non-selectively with all species in solution, Degradation of aromatic and polyphenols was found to be significantly faster	Expensive, COD removal not complete, Sludge production	(Marco S. Lucas et al., 2010; Monteagudo et al., 2005)
Fenton based Process	Rapid reaction rates, Small footprint Cost and energy effective, Generate strong hydroxyl radicals, Degrade a wide range of recalcitrant components, No mass transfer, Recycling of ferrous catalysts by reduction of Fe^{3+}	Not full scale application exists, Small of Sludge production, Acidic environment	(Catrinescu et al., 2012; Giroto et al., 2008; J. H. Park et al., 2006; Pignatello et al., 2006; H. Zhang et al., 2005)

Table 2.7: Application of AOPs in industrial scale (Audenaert et al., 2011; Sarathy et al., 2010)

Treatment system	Company	Pollutant
Ozonation	Cadillac motor car division of general motors corporation, detroit, michigan (usa).	Cyanides removal
Ozonation	Bell telephone laboratories in 1973,	Control of bacteria,
Ozone/UV	Tinker Air Force Base (Oklahoma, USA) to	Metal complexed cyanides and refractory organics.
Ozone/GAC	ARCO Products Company, Richmond, CA (USA)	Petroleum industry
UV/ H_2O_2	Milan Army Ammunition Plant (Milan, TN, USA)	To treat holding ponds contaminated with explosive compounds
UV/ H_2O	Air Force & EPA DemoEdwards AFB, CA	Organic contaminants
UV/ H_2O	U.S. Navy Site, NJ	Groundwater (organic contaminants)
UV/ H_2O	Winthrop Superfund Site, ME	Ground water (pre-treatment for iron)
UV/O_3/H_2O_2	Bofors nobel superfund site, located near muskegon, mi (USA)	Decomposition of hazardous wastewaters containing benzene, Toluene, chlorobenzene, tetrachloroethane, benzidine
UV/H_2O_2	Trojan Technologies, Cornwall, ON, Canada	Drinking water (to treat taste and odour compounds)
UV /H_2O_2	San Jose, CA	Ground water (Halogenated hydrocarbons, VOCs, pesticides)
UV /H_2O_2/O_3	Kansas City Plant, MO	VOCs
Fenton	Chemical factory in South Poland	Removal of color, mineralization (COD), Toxicity removal.
Fenton	Specialty Chemical Manufacturer, Louisiana	Phenols compounds
Fenton	Refinery, Southeast US	Pre-treatment
Fenton	Wood Treating Facility in Western US	Phenols, napthols and cresols
Fenton	Aircraft Painting Stripping and Maintenance Facility, Midwest US	Reduce Toxic organics prior to discharge to the municipal wastewater collection system.
Fenton	Chemical Plant, Alabama	Phenol

2.9   Fenton Oxidation Process

In this study, emphasis has been placed on the application of Fenton and UV integrated Fenton oxidation processes as a promising alternative technology for the Batik wastewater treatment at room temperature and pressure (Babuponnusami et al., 2014; Qiu et al., 2012; Torrades et al., 2014). Amongst all AOPs, the Fenton oxidation process or Fenton process is considered an efficient, low-cost and environmental friendly treatment method to treat highly recalcitrant wastewater (Babuponnusami et al., 2013; M. Lucas et al., 2006; X. R. Xu et al., 2004). Fenton system is effective in degrading various recalcitrant compounds at rapid oxidation kinetics with a cheap and easily maintained operating system (Hartmann et al., 2010; H. Li et al., 2015). It should be noted that very limited studies have been conducted on the Fenton process using real wastewaters. Most of the researchers studied model wastewaters, and lack of detail studies on detail kinetics, optimization, and reactor design and modelling had made it difficult to be considered for large-scale application.

The Fenton's reagent was discovered by Fenton in 1894 (Fenton, 1894). Fenton's oxidation accommodate the advantages of both oxidation and coagulation processes. The mechanistic study of the Fenton oxidation process indicates that the interaction between Fe^{2+} and H_2O_2 under acidic medium results in the production of highly oxidative free radicals such as $HO\bullet$ radical. Characterized by high oxidizing potential (2.78eV) and non-selective nature, the Fenton oxidation process does not only minerals recalcitrant pollutants, but increase the biodegradability of the treated effluent (Gogate et al., 2004a). Generally Fenton's oxidation process consists of four important steps: i) pH adjustment ii) oxidation iii) neutralization and iv) coagulation. So, the organic substances are removed in two stages of the oxidation and the coagulation.

Ferrous ions initiate and catalyze H_2O_2 oxidation process to generate highly reactive, short lived $HO \bullet$ radical (Marco S. Lucas, & Peres, 2007), as depicted in Eq. (2.7) and (2.8) (Buxton et al., 1988; Neyens et al., 2003; Rigg et al., 1954; Cheves Walling, 1975). The generation of the radicals involves a complex reaction sequence in an aqueous solution.

$$Fe^{2+} + H_2O_2 \rightarrow Fe^{3+} + HO \cdot + OH^- \qquad (2.7)$$

$$Fe^{2+} + HO \cdot \rightarrow Fe^{3+} + OH^- \qquad (2.8)$$

Furthermore, the ferric ions formed can react with hydrogen peroxide, causing it to regenerate ferrous ions and form and hydroperoxyl radical during the process. The reactions are shown in Eq. (2.9 to 2.10) (Garrido-Ramírez et al., 2010; Haber et al., 1934; Y. S. Jung et al., 2009; Pignatello et al., 2006; C. Walling et al., 1973).

$$Fe^{3+} + H_2O_2 \rightarrow Fe - OOH^{2+} + H^+ \qquad (2.9)$$

$$Fe - OOH^{2+} \rightarrow Fe^{2+} + HO_2 \cdot \qquad (2.10)$$

The reaction of hydrogen peroxide with ferric ions is referred to as a Fenton-like reaction and shown in reactions (2.11) and (2.13) (Bielski et al., 1985; C. Walling et al., 1973).

$$Fe^{2+} + HO_2 \cdot \rightarrow Fe^{3+} + HO_2^- \qquad (2.11)$$

$$Fe^{3+} + HO_2 \cdot \rightarrow Fe^{2+} + O_2 + H^+ \qquad (2.12)$$

$$HO \cdot + H_2O_2 \rightarrow HO_2^- + H_2O \qquad (2.13)$$
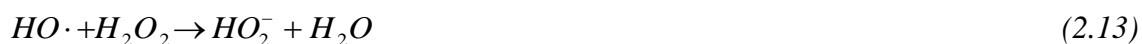
Based on the reaction (2.13), H_2O_2 can act as a scavenger as well as an initiator (reaction (2.7)). H_2O_2 can oxidize organics (RH) by abstraction of protons producing organic radicals $R \cdot$ which are highly reactive and can be further oxidized (C. Walling et al., 1971).

$$RH + OH\cdot \rightarrow H_2O + R\cdot \rightarrow \quad \textit{Further oxidation} \qquad\qquad (2.14)$$

Fenton process has many advantages including high treatment efficiency, the simple system operated at room temperature and atmospheric pressure, safe and cheap oxidants and catalyst and non-toxic end products as break down to the water and carbon dioxide. Fenton process appears to have the capability to completely decolorize and mineralize wastewater from many sources such as leachate, textile dyeing, pharmaceutical, petroleum, olive oil processing, paper mill and tannery industry within a short period of time (Liu et al., 2007; Lopez et al., 2004; M. Lucas et al., 2006; M. S. Lucas et al., 2009; Shemer et al., 2006). It is able to completely destroy the chromophoric structure of azo dyes and the degradation competency depends on the structure and nature of auxiliary groups attached to the aromatic nuclei of the dyes (Singh et al., 2013). High COD removal was observed because $HO\bullet$ radical generated in Fenton process could effectively transform low-molecular-weight biodegradable organic matter into the more biodegradable matter that can be subsequently treated using biological processes. But in literature very limited studies have been found regarding the application of the Fenton reaction to real textile wastewater treatment.

Torrades and Garcia-Montano (2014) are among the few researchers who have conducted such studies. They investigated the use of Fenton reagent and UV- irradiation for the treatment of real dye wastewater from a Spanish textile manufacturer in one of their studies at laboratory scale and reported that 120 min of treatment resulted in a 62.9% and 76.3% reduction in the chemical oxygen demand after Fenton and photo-Fenton treatments respectively under optimum conditions. Table 2.8 summarizes the previous experimental works and operating parameters involved in Fenton oxidation for the treatment of various textile wastewaters. Based on the literature, it can be concluded that homogenous systems are highly affected by the concentration and type of catalysts, the

pH of the treatment system, light intensity, type of pollutant, concentration of oxidants, presence of ion species, and type of intermediates.

However, although the Fenton process has been studied widely and has performed in textile wastewater treatment and many other wastewaters, it still has some disadvantages the limiting the applicability in full scale industrial wastewater system include high chemical consumption (up to 50–80 ppm of Fe ions in solution), pH dependence (effective in the range of pH 2–4), high cost of hydrogen peroxide, generation of iron sludge, necessity of post treatment, necessity of neutralization of the treated sample before disposal and decomposition of hydrogen peroxide (M. E. M. Ali et al., 2013; Babuponnusami et al., 2012; Iurascu et al., 2009). Besides, treatment of Fe ions-containing sludge as the last wastewater treatment step is expensive and it requires a huge amount of chemicals and manpower. The practicality of Fenton process is severely restricted by all the above stated limitations.

In order to overcome the limitations, there is a need to modify the conventional Fenton process to improve the oxidation efficiency and reduce the operating cost by reducing the reagent usage. There has been continuous research on exploring the alternatives to modify the classical Fenton process. Various homogeneous and heterogeneous catalysts have been developed and investigated (Balcioglu et al., 2001; Mahamuni et al., 2010). Besides that, physical fields such as photo field, electro field, cavitation effect, and microwave field also has been used in the conventional Fenton process (Al-Kdadi et al., 2004). Typical physical fields are UV radiated Fenton, electro-Fenton, and microwave-Fenton.

Table 2.8: Previous researches in Fenton process for the treatment of textile wastewaters

Effluents	Experimental Conditions	Treatment Efficiency (%)	Ref.
Reactive Black , Reactive Orange 16 and Reactive Blue 2	[Dye]: 0.1 mM, [H_2O_2] : 0.16 g/L 74.07 g carrier/L, pH: 3	X_{CR}: 96- 99% X_{COD}: 34- 49 % (100 min)	(Su et al., 2011a)
Real naphthalene dye	COD:7300 mg/L, [H_2O_2]: 4.9 g/L, Fe^{2+}/H_2O_2: 1/20, pH: 2.5	X_{COD}: 93% X_{TOC}: 62%	(Gu et al., 2012)
Dyeing and finishing mill	[COD]: 314–404 mg/L, [COD]:[Fe^{2+}]:[H_2O_2] = 1:0.95:3.17, pH: 3, SiO_2 :74.07 g/L	X_{CR}: 92% X_{COD}: 87% (60 min)	(Su et al., 2011b)
Everdirect supra turquoise blue	[COD]: 500 mg/L, [H_2O_2] :5.2, [Fe^{2+}]: 3.6, pH: 2.45	X_{TOC}:93.06 % (15 min)	(Karthikeyan et al., 2011)
Reactive black 5	[Dye]:500 mg/L, [H_2O_2]:1 mM, [Fe^{2+}]: 0.1 mM, pH: 5, T: 20 °C	X_{CR}: 91% (60 min)	(Marco S. Lucas, Dias, et al., 2007)
Peach red azo dye	[Dye]:0.2 mM, [H_2O_2]:30 mM, pH:3, [Fe^{2+}]:0.6 mM	k:1.8×10^8 M^{-1} s^{-1}	(Chang, & Chern, 2010)
C.I. Acid Yellow	[Dye]:40 mg/L [H_2O_2]: 17 mM, [Fe^{2+}]: 0.05 mM, pH: 3	X_{Dye}: < 60 % (25 min)	(Modirshahla et al., 2007)
Real textile wastewater	[COD]:8100 mg/L, [H_2O_2]:0.882 mM, Fe^{2+}:40 mg/L, pH:3	X_{CR}: 71.5% X_{COD}: 45%	(Papadopoulos et al., 2007)
Reactive Black 5, Reactive Blue 13, and Acid Orange	[Dye]:50 mg/L, [Fe^{2+}]:0.27 mM, [H_2O_2]:1.47 mM , pH:3	X_{CR}: >95% X_{COD}: 41- 91 %	(Lodha et al., 2007)
Reactive Black 5	[H_2O_2]$_0$/[RB5]$_0$:4.9:1, [H_2O_2]$_0$/[Fe^{2+}]$_0$: 9.6:1 and pH :3.0	X_{CR}: 97.5% X_{TOC}: 21.6% (30min)	(M. Lucas et al., 2006)

Amongst others, in this study, UV integrated Fenton process is chosen as a cost effective process to overcome the shortcoming of Fenton process and it can also work in a wide range of initial pH. Besides, it also improves the hydroxyl radical generation, yields high reaction rate, reduces the consumption of catalyst and oxidant, and generates very little iron sludge.

2.9.1   Typical Fenton Oxidation Operational System

A batch Fenton reactor consists of stirring reactor with a metering pump for the addition of acid, base, ferrous salt catalyst and hydrogen peroxide. Since the Fenton reaction is aggressive, it is necessary to coat the reactor with anti-corrode material to minimize the corrosion effect. The ideal pH for most of the organic pollutants in the acidic range between 3- 4. It is well known that, pH is one of the most important operating parameters to optimize the formation of $HO \bullet$ radicals. The Fenton process is started with adjustment of pH by using dilute sulfuric acid (acidic conditions) or sodium hydroxide (base conditions) followed by catalyst addition. Lastly, the addition of hydrogen peroxide and it is indicating the start-up of the Fenton process. Alkaline solution will be added in the neutralizing tank to quench the reaction followed by flocculation tank and solid-liquid separation tank before it's discharged as treated wastewater. Figure 2.5 shows the descriptive schematic diagram of the Fenton process.
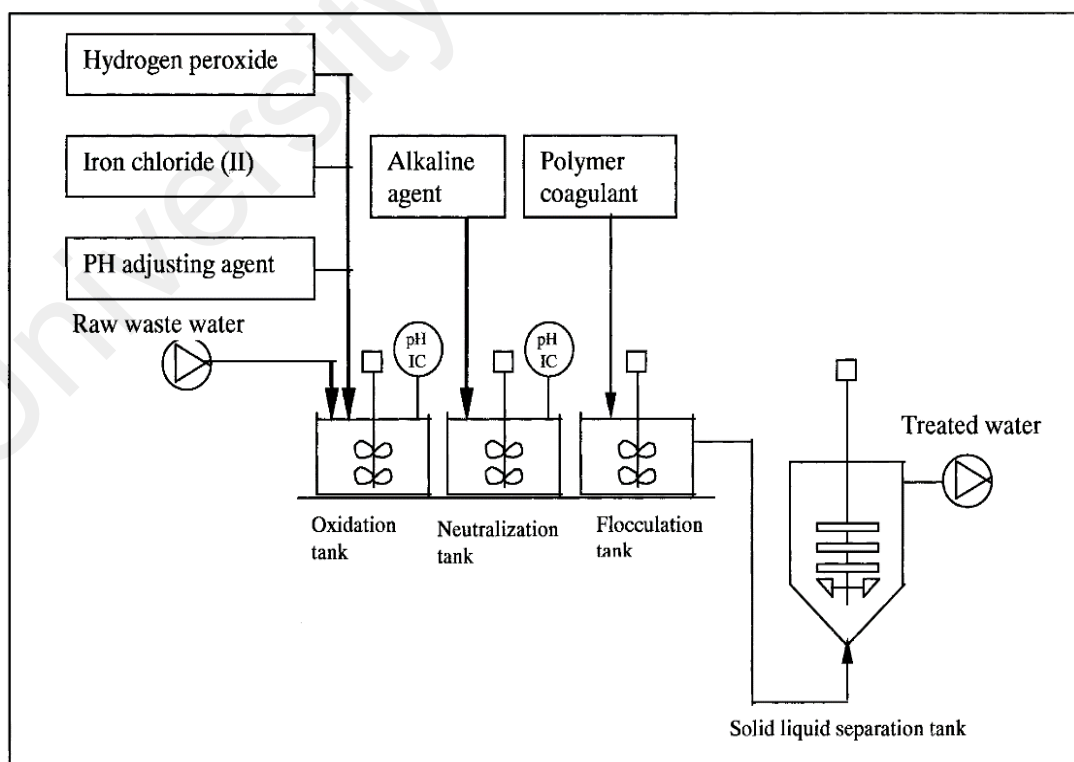
Figure 2.5: Schematic diagram of the Fenton process (Gogate et al., 2004a)

2.10   UV Integrated Fenton Oxidation Process

UV radiation provides energy to enhance the production of $HO \bullet$ radical, reduce the dosage of catalyst and enhance the catalytic capacity of the catalyst when integrated with Fenton process. Complete mineralization of numerous organic compounds in aqueous solutions can be achieved through the application of UV irradiation. UV radiation occurs as electromagnetic waves at a wavelength between 100 and 400 nm. It is classified into four subgroups: UV-A (315-400 nm), UV-B (280 – 315 nm), and UV-C (200-280 nm) and vacuum UV (100-200 nm). The optimum germicidal effects occur in UV range between 245 and 285 nm (USEPA, 1999) and its primary in the UV-C range. Application of low-pressure UV lamp is always preferred for wastewater treatment as they are energy efficient. It is estimated that about 40 % electrical input power converted into UV-C light output at wavelength 254 nm. The medium pressure lamp produces greater UV-C light intensity, thus it's achieve given UV light dosage within a short irradiation time although it is not electrically efficient.

The effectiveness of the process involved UV radiation depends on hydraulic properties of the reactor, UV light intensity, retention time and characteristics of wastewaters. Turbidity is playing an important role in UV system as the success of the system is related to the amount of total suspended solids (TSS) present in the wastewater. If the quality of the wastewater is poor, the effectiveness of the process will be decreased as radiation couldn't penetrate solid presence. UV disinfection with low pressure lamp is not suitable for effluents with high TSS (above 30 mg/l). The UV system also should be built to have a uniform flow to maximize the UV radiation as well as to avoid the dead zone, which can result in inefficient use of power and reduce the contact time. Table 2.9 outlines some of the critical factors that affect the efficiency of the UV treatment system.

The efficiency of UV irradiation in Fenton oxidation is attributed to photo-reduction of Fe^{3+} to Fe^{2+} ions, which produces new $HO\bullet$ radical with H_2O_2 (Navarro et al., 2010). In many studies, UV-Fenton has been reported to be more efficient for degradation and decolorization of organic contaminants compared to Fenton treatment (Qiu et al., 2010). The investigated organic contaminants include polymers, pesticide, reactive dyes, EDTA, landfill leachate, sulfonylurea herbicide, oil refinery wastewater, penicillin, ibuprofen, 2-chlorophenol, livestock wastewater, acetaminophen, malathion pesticide, polyphenols, tea manufacturing wastewater, palm oil refinery effluent, simulated industrial wastewater, phthalic anhydride and naval derusting wastewater (Giroto et al., 2008; H. Kusic et al., 2006; Zarora et al., 2010; Y. Zhang et al., 2010).

Table 2.9: Critical factors affect the UV- treatment system

Factors	Remarks
Hydraulic properties of reactor	Design: - Uniform flow - Avoided dead zone - Eliminate short circuiting
UV light intensity	Effected by: - Age of lamps - Lamp fouling - Configuration of placement of lamp in the reactor
Characteristics of wastewaters	Effected by: - Flow rate - Total suspended solids (turbidity) - Intensity of microorganism presence in the effluents - Other physical and chemical properties

In photo irradiated Fenton reaction, two extra reactions can occur compared to the conventional Fenton process. Under acidic conditions Fe^{3+} ions, which exists in the form of $Fe(OH)^{2+}$, will be reduced to Fe^{2+} ions under UV radiation (Eq. (2.15)). Additionally, generated Fe^{2+} produces more $HO\bullet$ radical to react with H_2O_2 and increase the emoval efficiency of treatment system. Hydrogen peroxide could generate two $HO\bullet$ radicals by the photolysis process under shorter wavelength radiation (Eq. (2.16)).

$$Fe(OH)^{2+} + hv \rightarrow Fe^{2+} + HO\cdot \quad (\lambda < 580 \text{ nm}) \qquad (2.15)$$

$$H_2O_2 + hv \rightarrow 2HO\cdot \quad (\lambda < 310 \text{nm}) \qquad (2.16)$$
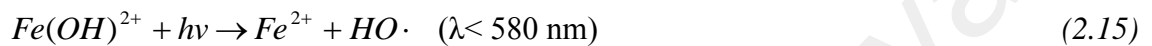
In addition, ferric ion complexes, $[Fe^{3+}(OH)^-]^+$ and $[Fe^{3+}(RCO_2)^-]^{2+}$ are the main light-absorbing compounds in the system which produce additional Fe^{2+} through photo-induced, ligand-to-metal charge-transfer reactions .

Table 2.10 summarizes the previous experimental works and operating parameters involved in UV integrated Fenton oxidation for the treatment of various textile wastewaters. Recent research has proven that the UV integrated Fenton process has a better performance that the Fenton process in terms of removal percentage of organic pollutants (Romero et al., 2016). Punzi and others (2012) evaluated the treatment efficiency of both homogeneous and heterogeneous photo-Fenton oxidation processes to treat synthetic wastewater. The highest chemical oxygen demand (COD) removal was achieved through homogenous Fenton oxidation with complete decolorization and COD reduction of 96 %. Tony and others (2012) investigated the application of the photo-Fenton process for the treatment of wastewater contaminated with hydrocarbon oil and achieved approximately 50% COD removal and the removal percentage increased to

approximately 75% at the optimized conditions when preceded by physicochemical treatment.

UV-Fenton degradation of livestock wastewater was carried out by Park and others (2006). The results obtained showed that the photo-Fenton process showed higher COD (79 %) and fecal coliform (99.4%) removal efficiencies at the optimal condition. This process also produced less sludge compared to the Fenton process. However, it had a lower color removal (70 %) efficiency compared to the Fenton process. Marcinowskia and others (2014) applied the Fenton, photo-Fenton and H_2O_2/UV processes to treat cosmetic wastewaters that were previously coagulated by $FeCl_3$. The photo-Fenton process at pH 3.0 was the most effective with 74.0% COD removal compared to all other investigated AOPs. Ginni and others (2014) studied the feasibility of the solar photo-Fenton process for the treatment of a pulp and paper mill's wastewater. Complete color and 93 % COD removals were obtained under the optimal conditions. Their study also showed that the degradation rate of the solar photo-Fenton process was faster than the Fenton process.

The literature review confirms that coupling the Fenton process with UV radiation enhances pollutant removal, reduces the treatment cost and chemical consumption. UV-Fenton enhances the reaction rate through the generation of high-valence Fe intermediates that directly attack the organic compounds (Giroto et al., 2008; Lopez-Alvarez et al., 2012). High-valence Fe-based oxidants were formed through the absorption of visible light by the complex formed between Fe^{3+} and H_2O_2. Degradation efficiency of UV-Fenton is strongly affected by the pH of the solution, initial H_2O_2 and Fe^{2+} concentration, UV dosage, scavengers, temperature and contact duration.

Table 2.10: Previous research in UV integrated Fenton oxidation for the treatment of textile wastewaters

Effluents	Experimental Conditions	Treat. Eff. (%)	Ref.
Real dye wastewater	pH=3, $[H_2O_2]$=73.5 mM, $[Fe(II)]$ = 1.79 mM.	COD: 76.3	(Torrades & García-Montaño, 2014)
Reactive red 241	[Dye]: 0.050 g/L $[Fe^{2+}]$: 5.0 x 10^{-4} M, $[H_2O_2]$: 2mL/L	CR : 100 TOC: 18.6	(Patel et al., 2013)
Simulated dye house wastewater	$[Fe^{2+}]$: 0.97×10^{-3} mol L^{-1} $[H_2O_2]$: 0.03 mol/L	TOC: 61	Grcic et al. (2011)
Mordant Red 73 azo dye	[Fe^{2+}]: 0.11 g/L [Pollutant]: 5×10^{-2} mM $[H_2O_2]$: 2.5×10^{-3} M pH: 3	COD: 85 CR : 99	Elmorsi et al. (2010)
C.I. Acid Blue 9	$[H_2O_2]/[Fe^{2+}]$: 2.0 to 3.5 $[H_2O_2]/[Dye]$: 7.0	CR: 98	Qiu and Huang (2010)
Reactive Dye	[Dye]: 100 mg/L $[Fe^{2+}]$: 0.5mM $[H_2O_2]$: 2.5mM pH : 3	CR: 100 TOC: 73.8	Vujevic et al. (2010)
Reactive Black 39	$[Fe^{3+}]$: 1.5 mM $[H_2O_2]$: 35 mM	CR: 100 COD: 84 TOC: 53	Arslan-Alaton et al. (2009)
Reactive Black B	$[H_2O_2]$: 22,000 mg/L UV irradiation: 45 W $[Fe^{2+}]$: 200 mg/L pH : 3	TOC: 98	Huang et al. (2008)
C.I. Acid Yellow 23	$[H_2O_2]$: 700 mg /L $[Fe^{2+}]$: 0.1 mM [Dye]: 40 mg/L pH value : 3	COD: 90 CR : 100	Modirshahla et al. (2007)
Reactive Black B	$[H_2O_2]$: 22,000 mg/L $[Fe^{2+}]$: 200 mg/L pH : 3	TOC: 98	Huang et al. (2008)
Azo Dye C.I. Acid Red 14	[Pollutant]: 50 mg/L [Fe^{2+}]: 0.2 mmol/L $[H_2O_2]$: 10 mmol/L	CR : 100	Daneshvar and Khataee (2006)
Everdirect supra turquoise blue	$H_2O_2:Fe^{2+}$: 1.63 -15.25 pH: 3	TOC: 95	Liu et al. (2007)

2.11   Ultraviolet Radiation Combined H$_2$O$_2$ System

Photolysis of hydrogen peroxide (H$_2$O$_2$) using ultraviolet (UV) light remains the most often investigated advanced oxidation method for water and wastewater treatment. UV/H$_2$O$_2$ is still a promising technique because no sludge is produced at the end of the reaction with easier handling and shorter reaction time to degrade contaminants compared to other AOPs (Aleboyeh et al., 2005; Autin et al., 2012). Besides, UV/H$_2$O$_2$ system is appropriate AOP technology for removing toxic organic since hydrogen peroxide is cheaper, simpler and requires fewer safety precautions.

Oxidation in UV/H$_2$O$_2$ system may occur via one of three general pathways such as hydrogen abstraction, electron transfer and radical addition. The reaction between UV light and hydrogen peroxide generates powerful $HO\bullet$ radical (H. Xu et al., 2011; Antonio Zuorro et al., 2013). Radiation with a wavelength lesser than 400 nm is suitable to photolyze H$_2$O$_2$ molecule into $HO\bullet$ radical with a quantum yield of two $HO\bullet$ radicals per quantum of radiation absorbed (Eq. 2.16). Other reactions can also happen depending on the process conditions as shown in Eqs. (2.17) to (2.20)). The photolysis reaction of H$_2$O$_2$ is dependent on the conditions of the system, including temperature, the initial concentration of H$_2$O$_2$, pollutant and pH (Banat et al., 2005; W. Li et al., 2011; Malik, 2004; Shu et al., 2006; Yonar et al., 2006).

Hydroxyl-radical propagation and termination steps (eqs.):

$$HO\cdot + H_2O_2 \rightarrow HO_2\cdot + H_2O \tag{2.17}$$

$$HO\cdot + HO_2^- \rightarrow O_2^- + OH^- + H^+ \tag{2.18}$$

$$H_2O_2 + HO_2\cdot \rightarrow HO\cdot + H_2O_2 + O_2 \tag{2.19}$$

$$HO\cdot + organic\ compound \rightarrow products \tag{2.20}$$

As reported in the previous studies, low mercury vapor lamps (254 nm) are the most common UV source used in the UV/H$_2$O$_2$ system. The limitation of UV/H$_2$O$_2$ is a high concentration of H_2O_2 is needed to generate sufficient amount of $HO\bullet$ radical and this excessive amount of H_2O_2 causes the scavenging of radicals and makes the treatment system less effective.

In addition, the degradation rate of UV/H$_2$O$_2$ strongly depends on the pH (Muruganandham et al., 2006; Shu et al., 2005a). At high pH value, hydrogen peroxide deprotonates and generates H$_2$O$_2$/HO$_2$$^-$ equilibrium (Aleboyeh et al., 2005). As shown in reaction (2.21), a non-dissociated molecule of H_2O_2 reacts with HO_2^- species and breaks down to oxygen and water instead of $HO\bullet$ radical (Schrank et al., 2007).

$$HO_2^- + H_2O_2 \rightarrow H_2O + O_2 + OH^- \tag{2.21}$$

Decomposition of H$_2$O$_2$ decreases the amount of $HO\bullet$ radical available and eventually decreases degradation rate. Besides, hydrogen peroxide shows a very high self-decomposition rate at higher pH (Schrank et al., 2007; Shu et al., 2005b).

As a summary, raising pH results in reducing dye degradation rate since H$_2$O$_2$ dissociates into water and oxygen rather than $HO\bullet$ radical in alkaline condition. So it is necessary to determine the optimum value of pH for each treatment system investigated. Besides that, a dose of hydrogen peroxide also controls the efficiency of mineralization and decolorization of pollutants found in wastewaters. Removal efficiency increases as the dose of H$_2$O$_2$ is increased up to a certain critical value at which hydrogen peroxide inhibit the degradation

2.12   The Main Operating Parameters Affecting AOPs

The performance efficiency of AOPs is greatly dependent on the generation of $HO\bullet$ radical. Various operating parameters which significantly affect the generation of $HO\bullet$ radical have been described by many researchers. Based on the literature review, the parameters that highly affect advanced oxidation processes include pH of the treatment system, type and initial concentration of catalyst and oxidant, temperature, presence of catalyst, retention time, agitation speed, partial pressure of ozone, light intensity, initial concentration of pollutant, matrix of pollutant, type of buffer used for pH adjustment, radiant flux, wavelength of the irradiation, aeration, presence of ions species, reactor design and concentration of gas fed to the photoreactor (Alvárez' et al., 2009; Ramirez et al., 2007). The effects of all the above parameters on the efficiency of AOP systems have been widely investigated by many researchers (Alaton et al., 2007; Bagal et al., 2014; Gogate et al., 2004a; J.-j. Lin et al., 2008). Figure 2.6 summarized the effects of main operating parameters on treatment efficiency of Fenton process, UV integrated Fenton, photolysis, UV combined H_2O_2 and coagulation.

2.13   Concentration of Pollutants

Many studies have reported that the initial concentration of pollutants has a significant effect on the degradation efficiency of the AOPs treatment system (Babuponnusami et al., 2013; Pignatello et al., 2006; J. L. Wang et al., 2012) As indicated by many researchers, the degradation rate of pollutant decreases as the concentration increases regardless of the type of pollutant. More organic contaminants are available in the treatment system when the targeted concentration of pollutant increases, which subsequently increases the requirement of free radicals for oxidation purpose. However, a number of radical species ($HO\bullet$ radical and O_2) on the catalyst surface remains constant for a given light intensity, catalyst amount and irradiation time. An inadequate amount of

$HO \bullet$ radical species to treat highly concentrated wastewater, reducing the degradation efficiency. Besides, dye degradation rate decreases with increasing dye concentration due to interference from the intermediates formed upon degradation of the parental dye molecules. UV based AOPs are inefficient in treating wastewater with high pollutant concentration due to insufficient penetration of UV radiation.

Initial pollutant concentration plays a significant role in the efficiency of Fenton also UV-Fenton process. It has been observed that degradation potential of UV decreases with increase in pollutant concentration (Y. Zhang et al., 2010). This is because light penetration decreases with increase in turbidity. It does not only result in decreases in the photo-degradation rates of targeted contaminant but also significantly reduce the photo-reduction of ferric ions (reaction 6) and H_2O_2 to $HO \bullet$ radical (reaction 9). Tokumura and others (2013) evaluated the efficiency of photo-Fenton process for simultaneous color wastewater treatment. The initial Orange II concentration varied from 22 to 78 ppm to determine the effects of initial Orange II concentration. All the other operating parameters were kept constant with the initial hydrogen peroxide concentration of 297 ppm; initial total iron ion concentration of 10 ppm, a solution pH of 2.5, and a total UV-A light intensity of 94.7 W/m^2. It was reported that k decreased with increasing initial Orange II concentration from 22 ppm (k= 0.445 min^{-1}) to 78 ppm (k=0.334 min^{-1}).

Figure 2.6: Effects of operating parameters on treatment efficiency AOPs

From the above studies, it can be concluded that the UV - Fenton process becomes inefficient at higher concentration of pollutant. In this situation, more $HO\bullet$ radicals are required for efficient degradation which can only be possible through utilizing high concentrations of iron salt and hydrogen peroxide.

2.13.1   Amount of Oxidant

The amount of hydrogen peroxide contributes to the degradation efficiency of the targeted pollutants in the photo-Fenton process. H_2O_2 can generate powerful $HO\cdot$ radicals by

acting as an electron acceptor as in Eq. (2.22) (Alkan et al., 2007; Elmorsi et al., 2010). The absorbance of UV light by hydrogen peroxide can generate two $HO\bullet$ radicals as shown in Eq. (2.17).

$$H_2O_2 + e^- \rightarrow HO\cdot + OH^- \qquad (2.22)$$

Based on the observed result, degradation efficiency, increased with the amount of hydrogen peroxide. However, the concentration of hydrogen peroxide should be selected carefully to avoid excessive hydrogen peroxide as it can decrease the degradation efficiency or does not improve the degradation. This might be due to auto decomposition of hydrogen peroxide to oxygen and water together with recombination of $HO\bullet$ radical which result in scavenging effect as shown in (2.23) to (2.24).

$$2H_2O_2 \rightarrow 2H_2O + O_2 \qquad (2.23)$$

$$H_2O_2 + HO\cdot \rightarrow H_2O + HO_2\cdot \qquad (2.24)$$

$$HO_2\cdot + HO\cdot \rightarrow H_2O + O_2 \qquad (2.25)$$

$$HO\cdot + HO\cdot \rightarrow H_2O_2 \qquad (2.26)$$
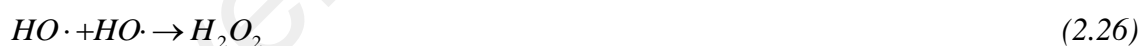
Besides, the dosage of hydrogen peroxide highly depends on the type of organic contaminants, so it is very important to optimize the value based on the treatment. Papic and others (2009) evaluated the degradation of three different reactive dyes using homogeneous photo-Fenton process. The optimum H_2O_2 concentration was found to be 20mM for C.I. Reactive Yellow 3 (RY3), 2.5mM for C.I. Reactive Blue 2 (RB2) and 50mM for C.I. Reactive Violet 2 (RV2) and increasing the dosage more than the optimum value, decreases the degradation efficiency of all the investigated dyes. Duran and others (2011) evaluated the photo-Fenton mineralization of synthetic municipal wastewater

effluent containing acetaminophen in a pilot plant. The results showed that the degradation rate continuously increased with the peroxide flow rate, as more $HO\bullet$ radicals are generated. Further analysis was conducted to understand the effects of hydrogen peroxide by analyzing the remaining and consumed H_2O_2 in the solution. The increase in H_2O_2 flow rates was not proportional to the increase in degradation rate. This is due to the formation of oxonium ion ($H_3O_2^+$) and intermediate product through H_2O_2 reaction with organic pollutants. H_2O_2 contributes to $HO\bullet$ radicals scavenging capacity at higher H_2O_2 dosages. Therefore, optimal H_2O_2 should be determined to achieve the most efficient degradation.

2.13.2   Amount of Catalyst

The amount of ferrous ions is one of the main factors that influence the process due to its action as a catalyst to decompose hydrogen peroxide to generate $HO\bullet$ radical. According to the previous studies, the minimum ferrous ion concentration required for the reaction is between 3 and 15 mg/L. As reported by Vujevicet and others (2010) and Tony and the others (2012) degradation rate increased with an increase in the concentration of ferrous ion till certain concentration and it became inefficient above that value.

Increasing ferrous ion above the optimal value has adverse impacts on reaction, where it may act as a $HO\bullet$ radical scavenger (Vujevic et al., 2010). Excessive Fe^{2+} can result in a great self-consumption of free radicals, which can inhibit the oxidation reaction. Besides, the enormous increase of ferrous ion leads to the formation of sludge which requires post treatment and this is not economically viable (Tony et al., 2012). Vujevic and others (2010) conducted a study on decolorization and mineralization of reactive dye by the UV / Fenton process. The effects of Fe^{2+} concentration on dye degradation efficiency were investigated within the range from 0.05 to 1.0 mM in this study. The results indicated that mineralization increased from 35% to 73.8% with an increase in the initial Fe^{2+}

concentration from 0.05 to 0.5 mM. Therefore, it can be concluded from the results that the degradation rate decreased when the iron concentration is above 0.5mM.The degradation of terephthalic acid (TPA), isophthalic acid (IPA) and benzoic acid (BA) from terephthalic acid wastewater by advanced oxidation processes was evaluated by Thiruvenkatachari and others (2006). The authors have reported enhancement in the removal efficiency was observed for all three targets organic species in the Photo-Fenton process compared to UV/H_2O_2 system were due to more $HO\bullet$ radicals in UV assisted Fenton. Besides, it was found that the removal efficiency, increased with increase in Fe concentration. The rate of organic destruction is faster in the early stage of the reaction than in the later stage. It is because ferrous ion catalyzes H_2O_2 quickly in the first stage of reaction to form $HO\bullet$ radical, so more degradation of organic compounds occur in the early stage of the reaction. In this study, the selectivity of $HO\bullet$ radical for certain specific organic materials was observed. Complete removal of BA was observed within a short period of reaction time when only about 60% of TPA and IPA were degraded. The amount of ferrous ion is one of the main parameters that influence the efficiency of photo-Fenton process. On the other hand, ferrous ion concentration depends on the type of organic contaminants present in the wastewater and therefore should be optimized for each particular treatment system.

2.13.3 Operating pH

Each AOP only works efficiently and economically within a range of pH (Beltrán et al., 2012; T. Y. Chen et al., 2009; Ikehata et al., 2004; Loeb et al., 2012; Vogna et al., 2004). The $HO\bullet$ radical generation by Fenton and UV-Fenton processes are strongly dependent on the initial pH of the solution since the pH value has a significant effect on the oxidation potential of $HO\bullet$ radical. This is due to the inverse relation between the oxidation potential and pH value ($E_o = 2.8$ V and $E_{14} = 1.95$ V) (Lide, 2004). At acidic conditions,

the efficiency of the process improves regardless of types of pollutant to be degraded (Philippopoulos et al., 2003). This is due to the acidic conditions that favor the formation of $HO\bullet$ radical whereas, H_2O_2 is decomposed into O_2 at higher pH values and it loses its oxidation ability. However, high acidic conditions are also not suitable for the efficient OH radical generation since. Hydrogen peroxide gets solvated and becomes more stable at pH below 2, reducing its reactivity with a ferrous ion to generate hydroxyl radical (Duran et al., 2011). Axonium ion $(H_3O_2)^+$ is formed at a higher concentration of H^+ making hydrogen peroxide more stable and preventing it from reacting with ferrous ion (Feng et al., 2006). Therefore, the pH value needs to be optimized for efficient production of $HO\bullet$ radical to improve the overall degradation efficiency.

Besides $HO\bullet$ radical, availability of ferrous iron in the reaction medium is also influenced by pH value. Different forms of iron species in relation to pH values are summarized in Table 2.11. It is clear from the table that at very low pH, iron is present in the form of ferric iron complex, which acts slowly with hydrogen peroxide to form $HO\bullet$ radical (M. Lucas et al., 2006). Most of the ferrous iron precipitates as Fe $(OH)_3$ and forms amorphous oxyhydrides $(Fe_2O_3 \cdot nH_2O)$ at higher pH (Ghiselli et al., 2004). The presence of iron precipitates does not only decrease the light absorption, but also increase the cost of the post treatment process.

Most of the studies related to Fenton and UV integrated Fenton processes have suggested pH 3 as the optimum pH value. For instance, Lucas and others (2006) studied the decolorization of azo dye Reactive Black 5 by photo-Fenton oxidation within the pH range of 1-3. The color removal efficiencies of 32.6 %, 61 % and 98.6% were obtained at pH 1, 2 and 3 respectively. The result showed that maximum color removal was obtained at pH 3. Lower degradation at pH 1 and 2 was caused by the hydrogen scavenging effect due to excessive H^+ as mentioned earlier. In contrast, Park and others (2006) have

discovered pH=5 as the optimum pH value for degradation of livestock wastewater through Photo-Fenton process. The authors commented that hydrogen peroxide was the most stable in the range of pH 3–4, but the decomposition rate increased rapidly at pH 5 and decreased above pH=5. In addition, Dopar and others (2011) highlighted the effect of UV type on pH for the treatment of simulated industrial wastewater. It was observed that optimum pH value varied with UV type used. The highest degradation rate was obtained at pH of 3.88 ($[Fe^{2+}] = 5.01$ mM and $[H_2O_2] = 30$ mM) for UV-C irradiation while a pH of 1.9 ($[Fe^{2+}] = 8.39$ mM and $[H_2O_2] = 30$ mM) was observed at optimum pH for UV-A light.

Table 2.11: Iron species generated in photo-Fenton as a function of pH value (Neamtu et al., 2003)

Fe^{3+} species	pH range
$Fe(H_2O)_6^{3+}$	1–2
$Fe(OH)(H_2O)_5^{2+}$	2–3
$Fe(OH)_2(H_2O)_4^{+}$	3–4

In addition, the degradation rate of UV/H_2O_2 is also strongly dependent on the pH values (Muruganandham et al., 2006; Shu et al., 2005a). At high pH value, hydrogen peroxide deprotonates and generates a H_2O_2/HO_2^- equilibrium (Aleboyeh et al., 2005). Non-dissociated molecule of H_2O_2 reacts with HO_2^- species and is broken down to oxygen and water instead of $HO\bullet$ radical (Schrank et al., 2007). Decomposition of H_2O_2 decreases the amount of $HO\bullet$ radical available and eventually decreases the degradation rate. Besides, hydrogen peroxide shows a very high self-decomposition rate at higher pH (Schrank et al., 2007; Shu et al., 2005b). As a summary, raising pH results in reducing dye degradation rates since H_2O_2 dissociates into water and oxygen rather than $HO\bullet$ radical in alkaline condition. So it is necessary to determine the optimum value of pH for each treatment system investigated. And UV-Fenton oxidation and Fenton process also

has to be optimized for each type of UV system and target pollutant, as evident from the results obtained by Dopar and others (2011).

2.13.4 Intensity of Radiation

UV irradiation can significantly influence the direct formation of $HO \bullet$ radical as well as the photo-reduction rate of Fe^{3+} to Fe^{2+} (Papic et al., 2009). The reaction rate is directly proportional to the intensity of radiation, but the reaction rate decreases beyond a certain magnitude of intensity. Use of radiation in AOPs helps increase decolorization and mineralization efficiency. The decolorization efficiency of the system also depends on both the reactivity and photosensitivity of the dye. Since most of the dyes are light resistant, it is necessary that UV radiation is combined with a powerful oxidant such as H_2O_2 to enhance the photolysis process (Eq. 2.16) (Dükkancı et al., 2014). Besides, irradiation wavelength is important in an irradiated system. It should be noted that shorter wavelengths are recommended for better removal efficiency.

2.14 Summary of Literature Review

The textile industry is one of the industries that consume a large amount of water, fuel and chemicals. Effluent from the textile industry is characterized by high color content, COD, BOD, TSS, TDS and recalcitrant contaminants. The characteristics of textile wastewater depend on the raw materials used, processes involved and other factors. Synthetic dyes are extensively used for dyeing and printing in the textile industry. In Malaysia, batik industry is classified under the small-scale textile industry that contributes significantly to the economy, but the industry has poor environmental management.

In view of the harmful impacts of wastewater on the environment and society, the Malaysian government has imposed stringent limits on the quality of the discharged wastewater. The conventional wastewater treatment processes for the textile industry are

less capable of degrading many of the dyes present in industrial effluents. Therefore, considerable efforts are being made to find an effective, simple, stand-alone, small, economically feasible and energy efficient wastewater treatment system. Among the treatment techniques that have been investigated to reduce organic contaminants to a safe and acceptable state, Advanced Oxidation Processes (AOPs) have the potential to treat wastewater contaminated with toxic and biorefractory organic compounds.

Based on the review conducted, it can be concluded that amongst the AOPs, Fenton process is effective in degrading various recalcitrant compounds by using highly oxidative $HO\bullet$ radical and rapid oxidation kinetics with a cheap and easily maintained operating system. However, AOPS are associated with some problems such as large chemical consumption, sludge generation and narrow pH requirement in the media that have limited its application at larger scales. In order to overcome the limitations, there is a need to modify the conventional Fenton oxidation process to improve the oxidation efficiency and reduce the operating cost by reducing the reagent usage.

There has been continuous research on exploring alternatives to modify the conventional Fenton process. Various homogenous and heterogeneous catalysts have been developed and investigated. Besides, various physical fields such as photo field, electro field, cavitation effect and microwave field have also been used in the conventional Fenton process. The Fenton process can possibly be enhanced by ultraviolet radiation (UV). This hybrid system could improve $HO\bullet$ radical generation, yield high reaction rate, reduce the consumption of catalyst and oxidant and generate very little iron sludge. Based on the literature study, the major factors that affect the efficiency of AOPS are initial pH of the solution, light intensity, the initial concentration of oxidant, catalyst and pollutant. Additionally, literature also confirms that very limited studies have been conducted on the Fenton process and UV integrated Fenton process using real wastewater, particularly

textile wastewater. In addition, most of the available studies only focus on the decolourization efficiency, not the mineralization or degradation efficiencies to represent the effectiveness of both the processes. Therefore, distinct studies are required to establish the application of the Fenton process by integrating it with UV to treat the real textile wastewater.

Therefore, this study aims at developing a simple, stand-alone, small and highly efficient treatment system by integrating Fenton process with UV radiation for small-scale industries. To achieve this aim, the efficiency of the Fenton and UV integrated Fenton oxidation system is evaluated in terms of COD, TOC and color removals. The effects of various operating parameters such as initial pH of the wastewater, mass ratios of H_2O_2:COD and H_2O_2:Fe^{2+}, retention time and UV radiation intensity on the degradation efficiency were analyzed. Each operating parameter was evaluated by using Central Composite Design (CCD), a form of Response Surface Methodology (RSM). The kinetic model was established in this study as this is useful for designing a scale-up system. The characteristics of the sludge were also evaluated. Besides, the intermediate study was conducted before and after the treatment by using FTIR, GC/MS and HPLC. Then, the model developed for the textile wastewater was further validated using the other types of real wastewater with low, medium and high COD values. This study also compared whether the integrated process was better than the Fenton and other AOPs including direct photolysis, UV/H_2O_2 and Fe^{2+} and UV/Fe^{2+} coagulations.

CHAPTER 3: METHODOLOGY

3.1   Introduction

In this chapter, the materials and methods used to conduct the experiments and analyses are presented. Response surface methodology is used to design the experiments. Operating parameters such as initial pH, retention time, UV intensity, mass ratios of H_2O_2:COD and H_2O_2:Fe^{2+} were used to determine the degradation efficiencies in terms of COD, TOC and color removals. The degradation efficiencies of Fenton and UV integrated Fenton processes were further evaluated on the basis of intermediate and final products formed. For this purpose, GC/MS, FTIR and HPLC analyses are performed. Furthermore, the sludge is characterized using SEM/EDX and PSD. The overall methodology used is illustrated in Figure 3.1.

3.2   Materials and Chemicals

All chemicals used in the present study were of analytical grade and used without further purification. Sodium Hydroxide (NaOH), Hydrogen Peroxide (H_2O_2, 30%, w/v), Ferrous Sulfate Heptahydrate ($Fe_2SO_4.7H_2O$), and Sulphuric Acid (H_2SO_4) were purchased from Merck & Co and Sigma- Aldrich. Distilled water was used to prepare all solutions. UVC low pressure lamps emitting monochromatic light around 254 nm and power output of 10-75 W was used. UV-C lights were purchased from Philips Lighting.
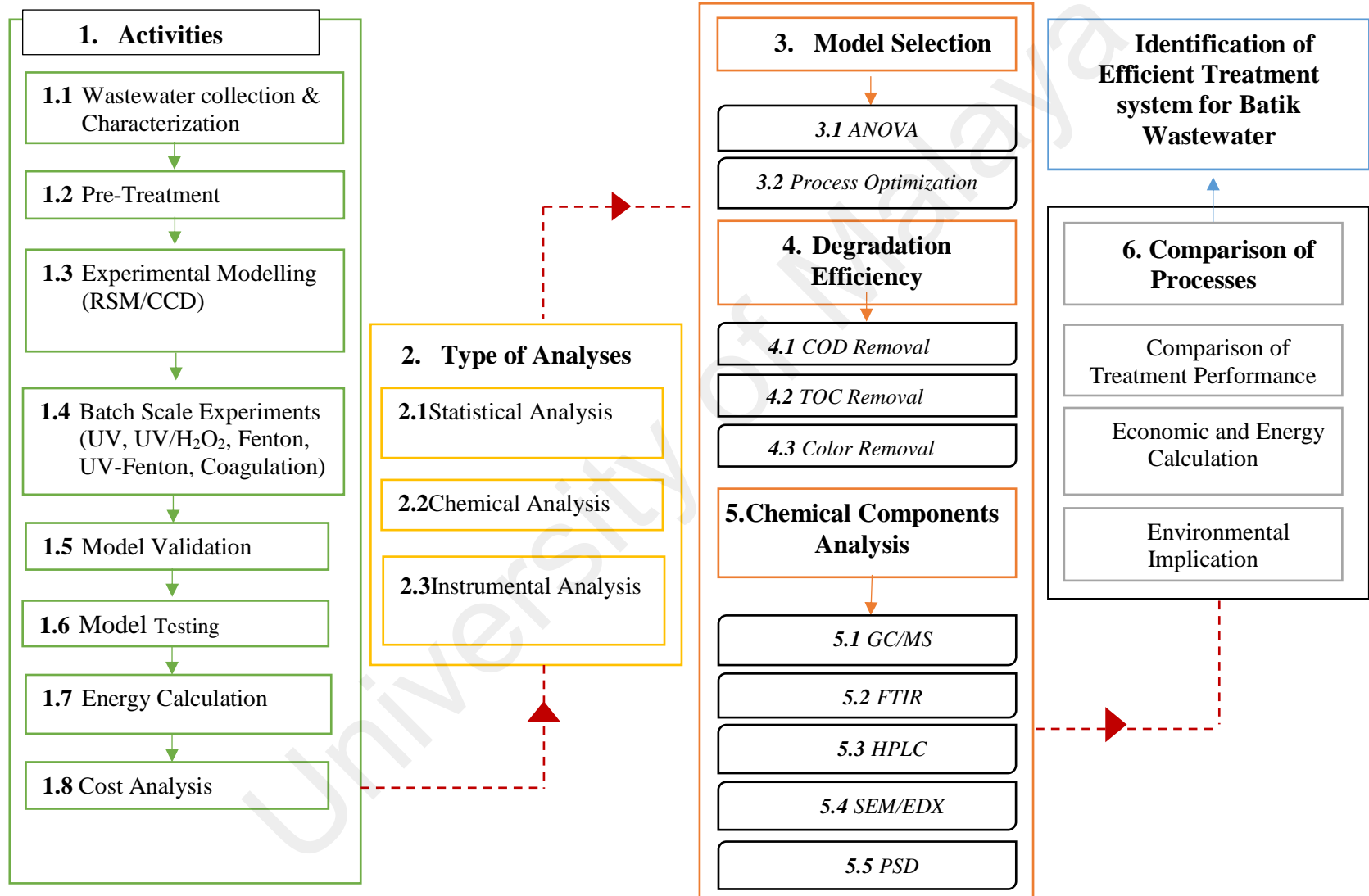
Figure 3.1: Experimental methodology

3.3 Wastewater Sampling and Characterization

Remazol Brilliant Blue solution (synthetic wastewater) was chosen as a prototype organic pollutant because it is a synthetic dye widely used as a coloring agent in textile industry. The real textile wastewater sample was collected from a local Batik manufacturing company (Institut Kraf Negara, Rawang, Malaysia). Sampling bottles were rinsed with samples before the collection was done. The samples were collected in a 30 liters-plastic container and immediately refrigerated at 4^0C in accordance with the standard method. The pH value, COD, TOC, and color (ADMI unit) of the wastewater sample were determined and presented in Table 3.1. It shows that the batik wastewater was a dark-color wastewater with a high content of organic compounds.

Table 3.1: Characteristics of batik wastewater

Parameters	Mean value± standard deviation	Standard Method
COD (mg/l)	1600- 1900 ±15	EPA 410.4, US Standard Methods 5220 D, and ISO 15705
TOC (mg/l)	170 ± 15	5310 B
Color (ADMI)	1500 ± 50	ADMI
pH	12.5 ± 2	-
Appearance	Dark Blue	-

3.4 UV-Based Experimental Setup

All the UV based experiments were carried out in a laboratory scale UV-reactor system setup as shown in Figure 3.2. A low pressure Philips UV lamp, which emits light at 253.7 nanometers (nm) wavelength were used as the UV source. UV lamps are positioned on the top of the stainless box which was centered at a distance of 5 cm from the reactor vessel. All the UV based processes were conducted in an Erlenmeyer flask of 500 ml of capacity. Since UV system has different power outputs and to ensure the same irradiance

at the reactor surface, the distance between the UV lamp and the reactor was fixed at 5 cm. The experiments were carried out at room temperature.
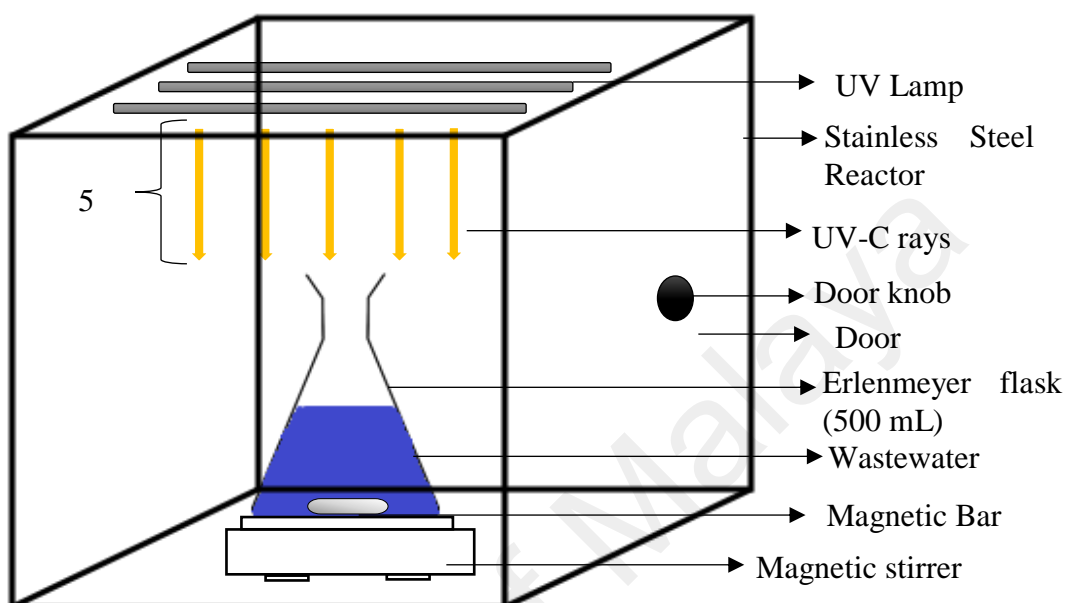
Figure 3.2: Sketch of batch scale UV-reactor

3.5   Experimental Procedures

3.5.1   Fenton and UV integrated Fenton Oxidation Processes

The Fenton process was carried out in a 500 ml-Erlenmeyer flask containing 100 ml of real textile wastewater equipped with a magnetic stirrer. The initial pH of the wastewater was adjusted to the desired level by using 1M NaOH or 0.5M H_2SO_4 solution. A specific quantity of Fe^{2+} catalyst was added in the form of $FeSO_4.7H_2O$ into the pH-adjusted samples and the samples were stirred continuously at 250 rpm. The Fenton reaction was initiated by adding a specific amount of H_2O_2 based on the mass ratios of H_2O_2: COD and H_2O_2: Fe^{2+}. The UV light was switched on immediately when hydrogen peroxide was added in the UV integrated Fenton process.

After the preset reaction time is reached, the pH of the solution was measured and an appropriate amount of 1M NaOH solution was added to adjust the pH level to 12 to stop the reaction. This is because Fe^{2+} precipitates as Fe^{3+} and H_2O_2 decompose to H_2O and oxygen at higher pH values, which results in the quenching of the reaction. In the Fenton based processes, the addition of NaOH is important because it prevents the interference of H_2O_2 in the COD measurement. After a settling time of half an hour, samples were taken and filtered through 0.45 mm filter papers (Millipore, USA) to remove the sludge (ferric hydroxide precipitation). All the experiments were performed at room temperatures and atmospheric pressures. For the development of the Fenton oxidation process, batch experiments were performed using hydrogen peroxide as the oxidant and ferrous iron as the catalyst. All experiments were duplicated to ensure the data quality and reproducibility. The procedures are illustrated in Figure 3.3.

3.5.2 H_2O_2/UV Process

UV/H_2O_2 experiment was carried out in a batch-scale UV-reactor equipped with a low-pressure UV lamp. A magnetic stirrer was attached to the Erlenmeyer flask to ensure sufficient mixing of the solution. The reactor was fed with batik wastewater and the initial pH of the wastewater was adjusted. A defined quantity of H_2O_2 was added and the sample was stirred continuously at 200 rpm. The UV light was switched on immediately when hydrogen peroxide was added. Upon completion of required irradiation time, the pH of the solution is adjusted around twelve to stop the reaction. All experiments were duplicated to ensure the data quality and reproducibility.
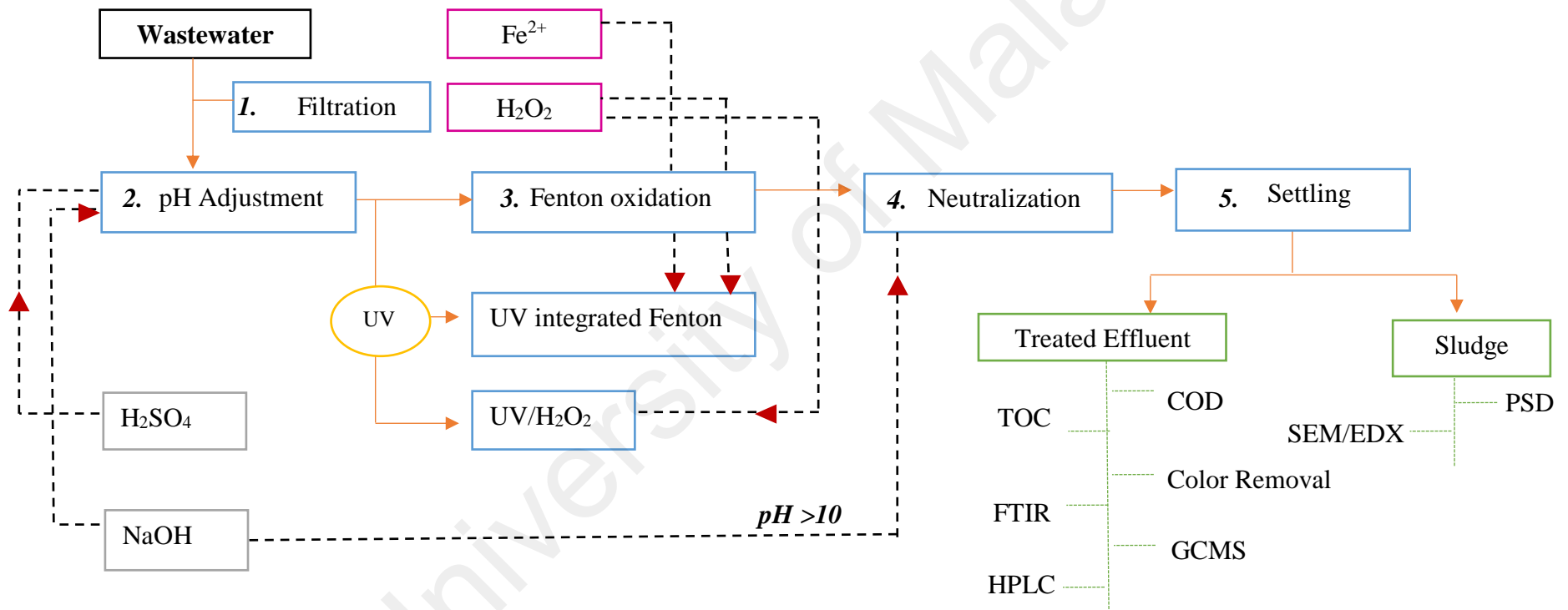
Figure 3.3: Experimental steps for the Fenton, UV integrated Fenton and UV/H_2O_2

3.5.3 Fe^{2+} and UV/ Fe^{2+} Coagulations

Fe^{2+} and UV/Fe^{2+} chemical coagulation experiments were conducted in beakers with magnetic stirring at ambient temperature with and without UV radiation. The operating parameters were the dosage of Fe^{2+}, initial pH of wastewater and UV- intensity. Every beaker was first filled with 100 ml of wastewater sample and the pH was adjusted. The specific amount of Fe^{2+} was added and the coagulation experiments proceeded by rapid mixing of wastewater sample at 200 rpm for preset retention time based. Then all the experiments proceeded with slow mixing at 50 rpm for 150 min and then left for settling for 30 min. The solutions were filtered through filter paper and the supernatant was withdrawn for COD analysis. Figure 3.4 illustrates the experimental procedures for the Fe^{2+} coagulation and UV/Fe^{2+} coagulation.

3.6   Experimental Design, Data Analysis and Process Optimization

Conventional approaches such as one-factor-at-time (OFAT) studies the effects of one variable at one time while the other variables are constant. OFAT is time-consuming, challenging and not economically viable with no capability to detail the interaction between the studied parameters (Bingöl et al., 2012). The design of Experiments (DOE) is an optimization tool that involves a minimal number of experiments to achieve a regression model, by combining the individual effects of different variables and their interactions. Design Expert software version 8.0 (Stat-Ease, Inc., USA) was used in this study for the experimental design and statistical analysis. Design experts establish a number of experimental runs needed, and ANOVA is also established the statistical significance of operating parameters. Besides, based on the predicted models, the best values for each of the factors can be determined using a numerical optimizer. The optimization feature can be used to calculate the optimum operating parameters for a

process. It also offers rotatable 3D plots and interactive 2D graphs to easily view response surfaces

```
┌─────────────────────────────┐
│      Filtered Wastewater    │
└─────────────────────────────┘
  H₂SO₄ &  - - - ▶
  NaOH          │
                ▼
┌─────────────────────────────┐
│         pH Adjustment       │
└─────────────────────────────┘
  Fe²    - - - ▶
                │
                ▼
┌─────────────────────────────┐
│     Addition of Coagulant   │
└─────────────────────────────┘
                │
                ▼
┌─────────────────────────────┐
│       High Speed mixing     │
└─────────────────────────────┘
                │
                ▼
┌─────────────────────────────┐
│       Low Speed Mixing      │
└─────────────────────────────┘
                │
                ▼
┌─────────────────────────────┐
│          Settlement         │
└─────────────────────────────┘
                │
                ▼
┌─────────────────────────────┐
│          Filtration         │
└─────────────────────────────┘
                │
                ▼
┌─────────────────────────────┐
│    Analysis & Measurement   │
└─────────────────────────────┘
```
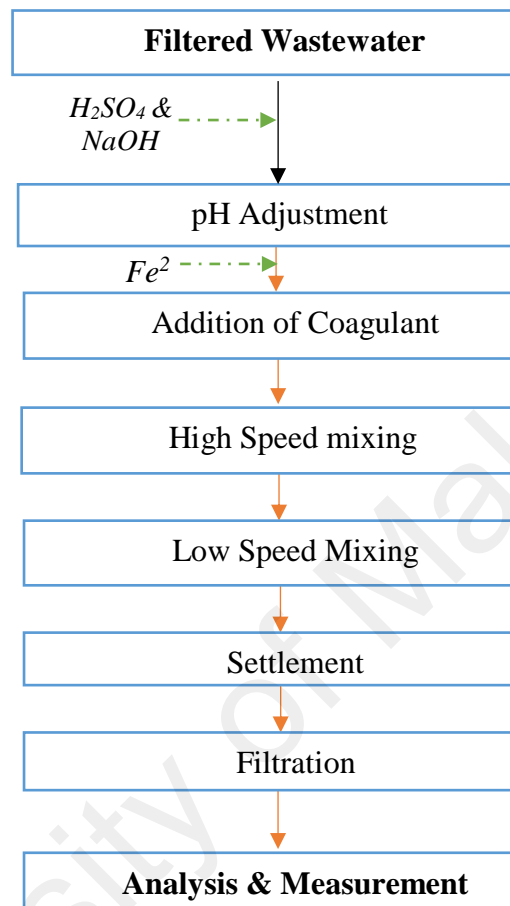
Figure 3.4: Experimental steps for the Fe^{2+} and UV/ Fe^{2+} Coagulations

3.6.1   Response Surface Methodology

Response Surface Methodology (RSM) is a multivariate statistical tool for modeling, analysis and optimization of research problems. Response surface methodology (RSM) has been used to study the effects of several independent variables on COD removal efficiency (Asghar et al., 2014; Benatti et al., 2006; M. A. Bezerra et al., 2008; Diya'uddeen Basheer Hasan et al., 2012; Módenes et al., 2012; Saldaña-Robles et al., 2014; A. Zuorro et al., 2013). It usually employs lower-order polynomials to define the relationship between response functions and independent variables. This technique is

capable of studying the interaction of variables with a reasonable number of experiments to identify the subsequent responses (Colombo et al., 2013; Diya'uddeen Basheer Hasan et al., 2012; Shojaeimehr et al., 2014). Moreover, it determines optimal conditions by defining the experimental range of each factor and provides optimized values based on the desirability factor.

In this context, Central Composite Design (CCD) was employed to design and optimize the experiments for Fenton oxidation. CCD is a response surface design which provides information on direct effects, pair-wise interaction effects, and curvilinear variable effects and is widely used for formulation and process optimization. Mass ratios of H_2O_2:COD and H_2O_2:Fe^{2+}, initial pH and retention time were chosen as the independent variables while COD, TOC, color removal percentages were the response variables. All the response variables are represented by a second-order polynomial equation that correlates response surfaces for evaluating the experimental results. The second-order polynomial equation (quadratic equation) is as follows:

$$\gamma = \beta_0 + \sum\nolimits_{j=1}^{k}\beta_j x_j + \sum\nolimits_{j=1}^{k}\beta_{jj} x_j^2 + \sum\nolimits_{j=1}^{k}\sum\nolimits_{i=1}^{i<j}\beta_{jj} x_i x_j + \varepsilon \qquad (3.1)$$

Where, Y is the response value, Xi is the coded value of factor, β_0 is constant, β_i is the linear coefficient, β_{ii} is the quadratic coefficient and β_{ij} is the interaction coefficient. Multiple linear regression analysis was conducted to estimate the coefficient parameters while 3D and 2D contour plots of the response models were used to study the interaction of the variables. **Figure 3.5** shows the strategy used to design the experiment using RSM.

3.7 Analytical Methods

All the analyses were performed according to the procedures described in the Standard Methods (ALPHA). All measurements of the physicochemical parameters were made for each treated and untreated wastewater sample.

3.7.1 Chemical Analysis

All the analyses were performed according to the procedures described in the standard method (ALPHA). All physicochemical parameters were measured for each treated and untreated wastewater sample.

3.7.1.1 Chemical Oxygen Demand

Chemical Oxygen Demand (COD) was measured according to the standard method (APHA 5220 D). The required amount of the samples was filled into the COD test cells supplied by Merck and heated in a thermo reactor (Spectroquant TR 420) for 2 hours at 140 ^{0}C followed by subsequent measurement by a UV-spectrophotometer according to the Standard Method. The COD removal efficiency was calculated using Eq. (3.2).

$$COD\ Removal\ (\%) = \left(1 - \frac{COD_f}{COD_o}\right) x\ 100 \qquad (3.2)$$

Where, COD_f and COD_o represent initial and final COD values obtained.

3.7.1.2 Total Organic Carbon

Total Organic Carbon (TOC) analyzer (Shimadzu, Japan) was used to measure the TOC concentration in the solutions. The 680 °C combustion catalytic oxidation method was used to achieve total combustion of samples in an oxygen-rich environment inside TC combustion tubes filled with a platinum catalyst. The analysis was conducted to assess

69

the extent the organic components were decomposed into CO_2. The mineralization of the samples was analyzed using a combustion/non dispersive infrared gas analysis method. TOC is measured by subtracting the measured inorganic carbon (IC) from the measured total carbon (TC), which is the sum of organic carbon and inorganic carbon. The TOC removal efficiency is calculated using Eq. (3.3).

$$TOC\ Removal\ (\%) = \left(1 - \frac{TOC_f}{TOC_o}\right) x\ 100 \hspace{2cm} (3.3)$$

Where, TOC_f and TOC_o represent initial and final TOC values obtained.
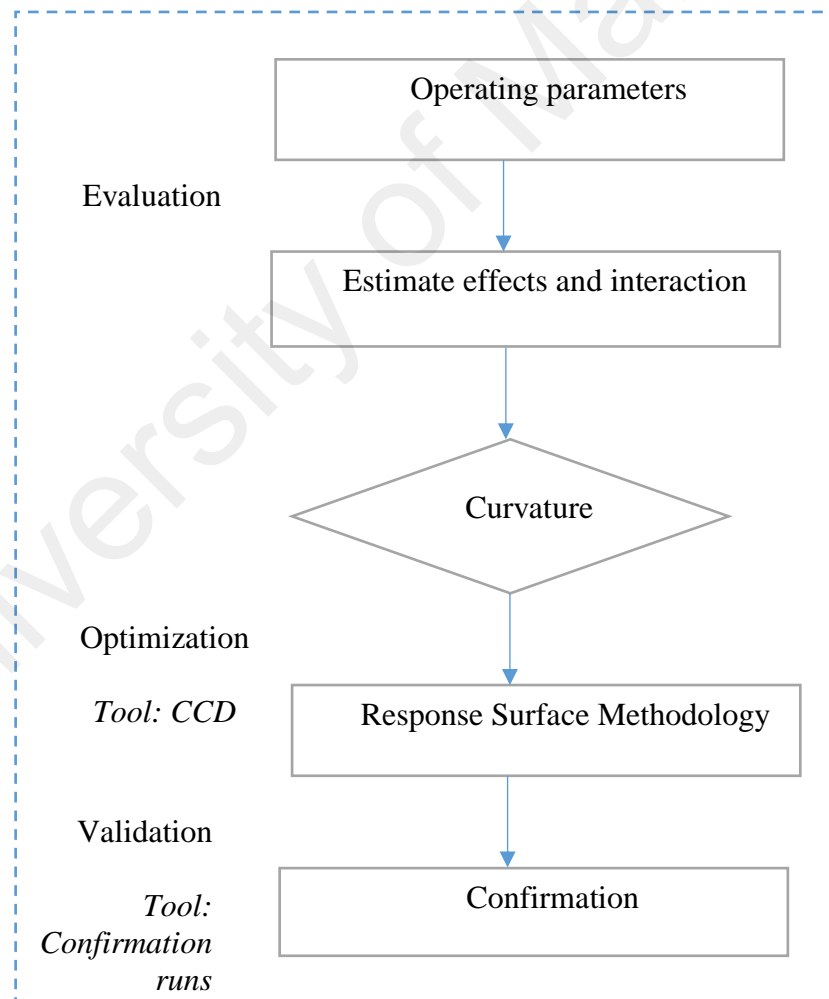
Figure 3.5: Strategy of RSM experimentation

3.7.1.3 Color Removal

An ADMI unit was used for the color measurement and determined using a UV-Spectrophotometer (Spectroquant Pharo 300, Merck, Germany) after filtration. The decolorization efficiency of the treated sample was calculated using Eq. (3.4).

$$Color\ Removal\ (\%) = \left(1 - \frac{ADMI_f}{ADMI_o} \right) x\ 100 \tag{3.4}$$

Where, $ADMI_f$ and $ADMI_o$ represent initial and final ADMI values obtained.

3.7.1.4 pH Measurement

The pH value of each sample was determined by using a digital pH meter (Metrhorm). The pH meter is calibrated prior to analysis using buffer solutions at pH 4.0, 7.0 and 10.0.

3.7.2   Instrumental Analysis

3.7.2.1 Gas Chromatography/Mass Spectrometry Analysis

The gas chromatography/mass spectrometry (GC/MS) analyses were performed using an Agilent Technologies 6890 gas chromatograph, equipped with an HP-5MS column (30 m x 0.25 mm i.d. x 0.25 mm), coupled to an MSD 5973 selective mass detector (Agilent Technologies). A split–less injector was used under the following conditions: an injection volume of 5 uL and an injector temperature of 250 ^{0}C. The temperature program was 4 min at 105^{0}C, 25^{0}C/min to 180^{0}C, 5 ^{0}C/min to 230^{0}C, and 30^{0}C/min to 260^{0}C. The analyses were performed using the electron impact ionization (EI) mode at 70 eV. The spectrometer detector was run in a full-scan mode from 50 to 500 amu. The temperature of the MS interface and the ionization source was fixed at 280^{0}C and 250^{0}C, respectively.

3.7.2.2 High Performance Liquid Chromatography

The decomposition of intermediates was determined by high performance liquid chromatography (HPLC) using Agilent Technology 1200 series. C18 column (4.6 mm x 250 mm x 5 um) at 20^0C was used as the separation column. The effluent used to be 60% acetonitrile / 40% water (v/v); the injection volumes were 10 mL, and the effluent flow rate was 1 mL/min. The detection wavelength was set at 254 nm.

3.7.2.3 Fourier Transform Infrared (FT-IR) Spectroscopy

The unique characteristics of the treated and untreated samples were presented by the Fourier transform infrared (FTIR) spectrum of the solution and recorded using FTIR (Perkin Elmer Spectrum One FTIR Spectrometer). In the present study, the attenuated total reflection (ATR) technique in the mid infrared region (MIR) of 4000–400 cm^{-1} wavelength was used for the characterization and assessment.

3.7.2.4 Scanning Electron Microscopy with Energy Dispersive X-Ray Spectroscopy

Scanning electron microscopy with energy dispersive X-ray spectroscopy (SEM/EDX) is a surface analytical technique. In this work, surface morphology and composition of the sludge were analyzed using the 122 Phenom ProX SEM. The surface area method was used to calculate the percentage composition of the sludge generated and characterized by EDX for the purpose of quantification of the constituents' atomic/ weight percentages.

3.7.2.5 Particle Size Distribution

Particle size distribution (PSD) of the treated effluent with sludge (non-filtered sample) was measured by Malvern Mastersizer 2000, which works on the principle of laser detection. Malvern Mastersizer can measure particles in the size range of 0.02 µm to

2000 µm. The process was fully automated and the results were based on the standardized operating procedures provided by the manufacturer to eliminate user-to-user variability.

3.7.3 Electrical Energy per Order Evaluation

The electric energy supplied to the AOPs is strongly related to the cost of the operating system. Figures of merit such as electrical energy per order are frequently used to measure the process effectiveness. Electrical energy per order (EE/O) of the processes was calculated using the Eq. (3.5). EE/O can be defined as the number of kWh (kilo Watt hour) of electrical energy required to reduce the concentration of a pollutant by 1 order of magnitude in $1m^3$ of contaminated water. The EE/O ($kWhm^{-3}$ $order^{-1}$) calculated using the following equation:

$$\frac{EE}{O} = \frac{P_{el} \times t \times 1000}{V \times 60 \times \log\left(\frac{c_i}{c_f}\right)} \tag{3.5}$$

Where, P_{el} is the electrical power input (kW), t is the irradiation time (min), V is the volume of effluent used (L), C_i and C_f is the initial and final effluent concentration (ppm).

3.8 Safety Precautions and Waste Disposable

The hazardous information of the chemicals used in this study was collected and provided in Table 3.2. Table 3.2 shows that most of the chemicals used in this study categorized as a dangerous and proper precaution were taken while handling them. Appropriate chemical safety goggles, gloves, and lab coat were used while conducting experiments. Ultraviolet absorbing protective safety glasses were used while working with ultraviolet light to protect skin from potential burns. The standard safety procedure of preparing the chemical solution was adhered in this work, which also includes the use of a fume cupboard.

Additionally, waste generated, excess chemicals and unused collected real wastewaters are stored in a proper container prior to disposal.

Table 3.2: Safety Data Sheets of Chemicals Used In This Study

Chemical	Hazard class	Hazards Information	Precautionary Statements
H_2O_2	Danger	- Causes severe skin burns and eye damage - Harmful if swallowed - Harmful if inhaled - May cause respiratory irritation - May intensify fire	- Use only outdoors or in a well-ventilated area - Do not breathe mist, vapors or spray. - Wash thoroughly after handling. - Remove contaminated clothing and wash before reuse. - Wear protective gloves/ protective clothing/ eye protection/ face protection - Keep away from heat, sparks, and flame - Do not store near combustible materials. - Keep container closed when not in use. - Take any precaution to avoid mixing with flammables
$FeSO_4.7H_2O$	Warning	- Harmful if swallowed. - May cause central nervous system effects. - Irritating to eyes and skin. - May cause irritation of respiratory tract.	

Table 3.2: Continued
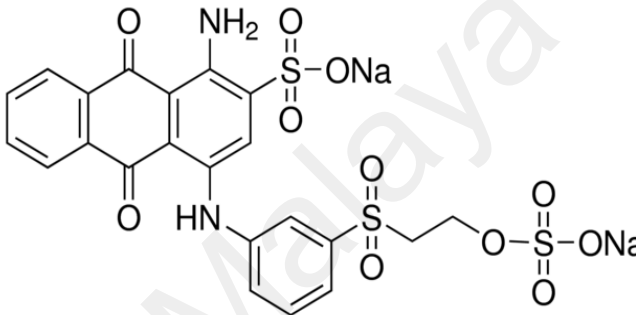
Chemical	Hazard class	Hazards Information	Precautionary Statements
H_2SO_4	Danger	- High chemical reactivity - Reactive and dangerous explosion hazard - Strong oxidizer that enhances the combustion of other substances - Causes severe skin burns and eye damage. - Exposure can cause headache, nausea and vomiting - May irritate lung causing coughing or shortness of breath	
NaOH	Danger	- May be corrosive to metals. - Causes severe skin burns and eye damage - May cause severe irritation to gastrointestinal tract if swallowed	

4.1 Treatment of Synthetic Textile Dye Solution by Fenton Oxidation Process

Reactive dyes are widely used in the textile industries due to their bright color, superior colorfastness, high solubility and photolytic stability (Balcioglu et al., 2001; Pelosi et al., 2014). Therefore, for the preliminary study, Remazol Brilliant Blue (RBB), one of the reactive dyes, was chosen as a model pollutant. Experiments were performed to investigate the potential of Fenton process to degrade synthetic dye containing solution prior to its application to real textile wastewater. The process efficiency was evaluated in terms of COD and color removal efficiencies. Table 4.1 presents the chemical and structural properties of RBB dye. It consists of substituted aromatic and heterocyclic groups, which are non-biodegradable, carcinogenic, toxic at very low concentration and recalcitrant organo-pollutants. RBB have a tendency to bind itself with water molecules and results in the hydrolysis of dye. It makes the effluent more complex as 10-50% of the unfixed dyes are discharged through dyeing and rinsing operation (Ahmad et al., 2014). Discharge of unfixed dyes contributes to an increase in COD and color intensity of the wastewater. It may affect the efficiency of Fenton process. Therefore, a systematic approach is required to identify and select the suitable ranges for operating parameters, responsible for affecting the efficiency of Fenton process. Thus, the design of experiments is used and efficiency of Fenton process is evaluated for RBB dye prior to real textile wastewater application.

Table 4.1: Properties of Remazol Brilliant Blue

Properties	Description
Molecular formula	$C_{22}H_{16}N_2Na_2O_{11}S_3$
Composition	~50% dye content
Molecular Weight (g/mol)	626.54
Color Index Number	61200
Max Absorption Peak	595 nm
Appearance (Color)	Dark Blue to Black
Appearance (Form)	Powder
Structure	

4.1.1 Experimental Design Using RSM-CCD

In this preliminary study, the experimental design was designed using RSM in the Design Expert Software. CCD model was used to assess the relationship between the responses and independent variables (Marcos Almeida Bezerra et al., 2008). All the experiments were conducted at room temperature (298 K). Since mixing speed affects the solubility of iron salt and reaction rate, preliminary experiments were conducted to identify the best mixing speed within the range of 50–300 rpm (for 100 ml of wastewater in 500 ml of Erlenmeyer flask using 45 mm magnetic bar). The COD removal efficiency was observed to increase the mixing speed to 250 rpm, and no significant changes were observed at 300 rpm. Therefore, 250 rpm was selected as the optimized mixing speed and made constant during the course of the treatment process.

Three operating parameters were selected as the control factors to study the efficiency of Fenton process: mass ratios of H_2O_2: COD and H_2O_2: Fe^{2+}, and initial pH of the solution. The selected range of the operating parameters and level of the independent variables are given in Table 4.2. The values of the independent variable and the variation range were selected based on the published work (Hasan et al., 2011) and reconfirmed with several set of preliminary experiments.

Table 4.2: Experimental design of RB-19 degradation by Fenton process

Independent variable	Symbol	Factor level			Unit
		-1	0	+1	
H_2O_2:COD	A	1	6.5	12	mg/mg
H_2O_2:Fe^{2+}	B	2	8.5	15	mg:mg
Initial pH	C	2	3.5	5	

A total of twenty experiments were carried out in accordance with the model suggested by RSM-CCD. Values of each factor are coded to standard values that vary from (-1) that correspond to minimum level up to (+1) that suit to the maximum level in the selected range of parameters. The COD, TOC and color removal efficiencies were chosen as the response variables because they could provide necessary information for evaluating the analytical performance. The responses based on the experimental runs on color, COD and TOC removal efficiencies proposed by RSM-CCD are given in Table 4.3. The results presented in the table are the duplicates of the experimental results at each operating condition proposed by CCD.

Table 4.3: Observed and predicted results corresponding to RSM design

Run	Designed Parameters			COD Removal (%)		Color Removal (%)	
	H_2O_2:COD	H_2O_2:Fe^{2+}	pH	Pred.	Exp.	Pred.	Exp.
1	1.0	2.0	5.0	38.5	40.1	86.2	82.2
2	12.0	2.0	2.0	62.2	63.1	88.1	85.1
3	12.0	8.5	3.5	66.4	65.0	89.5	86.4
4	12.0	15.0	5.0	48.7	50.5	79.0	70.2
5	1.0	8.5	3.5	50.0	49.0	88.1	84.3
6	1.0	15.0	5.0	28.4	27.3	79.0	72.8
7	12.0	15.0	2.0	58.0	58.0	89.3	87.1
8	6.5	15.0	3.5	54.7	54.1	97.0	92.2
9	6.5	2.0	3.5	61.8	60.4	96.2	95.0
10	1.0	15.0	2.0	45.6	46.2	87.5	78.3
11	6.5	8.5	3.5	67.0	68.0	98.0	98.5
12	6.5	8.5	5.0	62.5	62.2	85.0	85.3
13	6.5	8.5	2.0	72.9	72.4	88.6	88.0
14	6.5	8.5	3.5	67.7	68.0	96.0	96.2
15	1.0	2.0	2.0	49.8	50.2	86.0	80.4
16	6.5	8.5	3.5	67.5	70.3	99.0	97.2
17	6.5	8.5	3.5	67.4	69.0	99.2	95.0
18	12.0	2.0	5.0	58.7	58.4	89.8	86.6
19	6.5	8.5	3.5	67.2	67.0	98.1	93.7
20	6.5	8.5	3.5	67.7	68.5	97.9	93.6

COD values of initial dye solution: 230 mg/l, Exp.: Experimental values, Pred.: Predicted Values

4.1.2 Response Surface Model

In this study, responses have been fitted to a second order polynomial model which is often used to determine the critical points (maximum, or minimum,). Based on the experimental results, the final quadratic equations of responses in terms of coded factors are presented as Eq. (4.1 and 4.2) as shown in Table 4.4. These equations can be used to predict the percentage of COD and color removal efficiencies with reasonably good accuracy. Negative and positive values of the coefficients represent, respectively, the antagonistic and synergistic effect of each model term on the responses (Fard Masoumi

et al., 2013). The positive effect means that the COD and color removal efficiencies increase with factors and negative effect represents response is decreased when the factor level increases. From the equation, it is clear that, mass ratio of $H_2O_2:Fe^{2+}$ (B), initial pH of the wastewater (C), interaction between of $H_2O_2:Fe^{2+}$(B) and initial pH (C), the quadratic effect of H_2O_2: COD (A) and quadratic effect of $H_2O_2:Fe^{2+}$ (B^2) had a negative effect on the COD removal. However, the mass ratio of H_2O_2: COD (A) and interaction between H_2O_2: COD (A) and initial pH (C) had a significant positive effect within the range investigated. For color removal, the mass ratio of H_2O_2:COD (C) , and interaction between the quadratic effect of $H_2O_2:Fe^{2+}$ (A) had a significant positive effect within the investigated range of COD removal. Negative effect was observed for the mass ratio of $H_2O_2:Fe^{2+}$, initial pH (C), interaction between of H_2O_2:COD (A) and $H_2O_2:Fe^{2+}$ (B), of H_2O_2:COD (A) and initial pH (C), $H_2O_2:Fe^{2+}$(B) and initial pH (C), quadratic effect of H_2O_2:COD (A^2), $H_2O_2:Fe^{2+}$ (B^2) and initial pH of solution (C^2). Consequently, Eq. (4.1 and 4.2) provides a good visualization of the interactions and effects of the factors on the response.

Table 4.4: Quadratic polynomial models for the COD and color removal of RBB

Res. (%)	Proposed Quadratic model	Eq.
COD removal	$67.70 + 8.17\,(H_2O_2:COD) - 3.56\,(H_2O_2:Fe^{2+})$ - $5.17\,(pH)$ $+ 1.96\,(H_2O_2:COD \times pH) - 1.46\,(H_2O_2:Fe^{2+} \times pH) - 9.51$ $(H_2O_2:COD)^2 - 9.46\,(H_2O_2:Fe^{2+})^2$	4.1
Color removal	$94.51 + 1.8\,(H_2O_2:COD) - 2.90\,(H_2O_2:Fe^{2+}) - 2.30\,(pH)$ $- 0.25\,(H_2O_2:COD \times H_2O_2:Fe^{2+}) - 1.50\,(H_2O_2:COD \times pH)$ $- 3.25\,(H_2O_2:Fe^{2+} \times pH) - 8.27\,(H_2O_2:COD)^2 + 0.23$ $(H_2O_2:Fe^{2+})^2 - 6.77\,(pH)^2$	4.2

In this study, approximate relative index (ARI) is used to indicate the effects of operating parameters on the COD and color removal efficiencies. This analysis is conducted to determine the significance of operating parameters for both COD and color removal efficiencies based on the quadratic models proposed by RSM-CCD. The effects of

operating parameters and its interaction are summarized using Approximate Relative Index (ARI) as shown in Figure 4.1. The graph shows that, the mass ratio of H_2O_2: COD has the most significant effect on COD removal efficiency followed by, initial pH of the dye solution and mass ratio of H_2O_2: Fe^{2+}. Color removal is much effected by the interaction between mass ratios of H_2O_2: Fe^{2+} and initial pH of the dye solution. The interaction between mass ratios of H_2O_2:COD and initial pH of the dye solution is found to be the least significant factor that affects the COD removal and interaction between mass ratios of H_2O_2:COD and H_2O_2:Fe^{2+} for color removal.
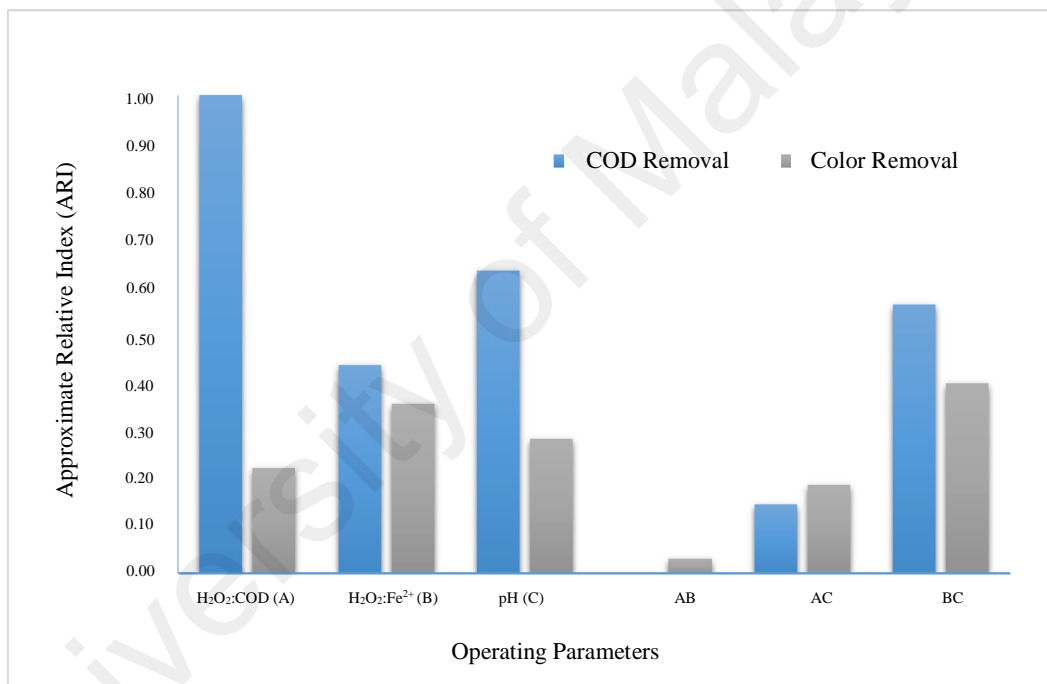
Figure 4.1: Approximate relative index based on quadratic equations for COD and color removals

4.1.3   Model Analysis

The mathematical equation developed using RSM/CCD has its limitation as it only identifies the important operating parameters and it is unable to describe the domain of the model adequately. Therefore, Analysis of Variance (ANOVA) is added to the analysis to confirm the statistical consistency (95% confidence level) of the developed quadratic

model in this study. The fit of the model was evaluated by means of ANOVA revealing the effects of the model that were statistically significant for a confidence level of 95% (p-value <0.05). F test analysis of variance (ANOVA) is presented in Table 4.5 to check the statistical significance of the quadratic model for a percentage of COD removal. The p-value represents the probability that F occurred due to noise; the smaller the value of p, the more significant is the corresponding parameter in the model. Values of, '*Prob > F*' is lesser than 0.0500 (α= 0.05, 95% confidence level), indicates that the present quadratic models are statistically significant. .

The ANOVA analyses showed that both models for COD and color removal efficiencies had a P value less than 0.0001. This confirms that the model is highly significant to describe the color and COD removal efficiencies of RBB. In this case, mass ratios of H_2O_2:COD, and H_2O_2:Fe^{2+} and initial pH of the solution are significant model terms for both COD and color removals. Therefore, it confirms that all the three investigated operating parameters in this study have a substantial force on the percentage of COD and color removal efficiencies. Moreover, the validity of models was determined by values of lack of fit. The lack of fit for both models was insignificantly relevant to the pure error because p-value (0.1971 (COD) and 0.3024 (color)) was higher than 0.050, revealing that the models were adequate for the prediction of the percentage of COD and color removals.

Table 4.5: ANOVA results for response surface quadratic model using Fenton process for (a) COD and (b) color removals

Variation source	Sum of Squares	df	Mean Square	F value	P-value	Prob>F
COD Removal						
Model	2547.75	7	363.96	198.64	<0.0001	Highly Sig.
A-H_2O_2:COD	667.49	1	667.49	364.29	<0.0001	Highly Sig.
B-H_2O :Fe^{2+}	126.74	1	126.74	69.17	<0.0001	Highly Sig.
C-pH	267.29	1	267.29	145.88	<0.0001	Highly Sig.
AC	30.81	1	30.81	16.82	0.0015	Sig.
BC	17.11	1	17.11	9.34	0.0099	Sig.
A^2	289.18	1	289.18	157.83	<0.0001	Highly Sig.
B^2	286.15	1	286.15	156.17	<0.0001	Highly Sig.
Residual	21.99	12	1.83	-	-	-
Lack of Fit	16.65	7	2.38	2.23	0.1971	Not Sig.
Pure Error	5.33	3	0.62	-	-	-
Cor Total	2569.73	29	-	-	-	-
Adeq Precision	51.93	-	-	-	-	-
R^2	0.9914	-	-	-	-	-
Adj R^2	0.9865	-	-	-	-	-
Pred R^2	0.9656	-	-	-	-	-
Color Removal						
Model	1159.86	9	128.87	23.04	< 0.0001	Highly Sig.
A-H_2O_2:COD	32.40	1	32.40	5.79	0.0400	Sig.
B-H_2O_2:FE	84.10	1	84.10	15.03	0.0031	Highly Sig.
C-pH	52.90	1	52.90	9.46	0.0100	Highly Sig.
AB	0.50	1	0.50	0.09	0.7700	Not Sig.
AC	18.00	1	18.00	3.22	0.1000	Sig.
BC	84.50	1	84.50	15.10	0.0030	Highly Sig.
A^2	188.20	1	188.20	33.64	0.0002	Sig.
B^2	0.14	1	0.14	0.03	0.8766	Not Sig.
C^2	126.14	1	126.14	22.55	0.0008	Sig.
Residual	55.95	10	5.59	-	-	-
Lack of Fit	34.61	5	6.92	1.62	0.3042	Not Significant
Pure Error	21.33	5	4.27	-	-	-
Cor Total	1215.80	19	-	-	-	-
Adeq Precision	15.81	-	-	-	-	-
R^2	0.9540	-	-	-	-	-
Adj R^2	0.9126	-	-	-	-	-
Pred R^2	0.6372	-	-	-	-	-

Besides, the model *F-values* of 198.64 and 23.04 more than the *F*-distribution implies that the model fitted well and important for the COD and color removal efficiencies. There is just a 0.01% chance that an *F*-value this large could occur due to interference. And the F- values also prove that the model developed for COD removal is more accurate compared to color removal.

In addition, "Adeq Precision" measures the signal to noise ratio. A ratio greater than 4 is desirable. The adequate precision ratios of 51.93 and 15.81 derived from COD and color removal % indicated that there were adequate signals for all the response variables. This model can be used to navigate the design space.

In addition, the quality of the developed model can also be expressed as a correlation coefficient represented by R^2 value. The models were found to be adequate to fit all the experimental data with R^2, adjusted R^2, and predicted R^2 of 99.1%, 98.7%, and 96.6% for COD removal, and 95.4%, 91.2%, 63.7% for color removal, respectively. The R^2 value of the response variables for the COD removal is higher compared to color removal. This indicates the good predictability of the model for COD removal. The model for color removal did not fit real data well because color removal occurred within minutes and thus it was difficult to model color removal using the same retention time for COD removal. Also, the predicted values of COD and color removals obtained using the model equations were plotted versus experimental data which are shown in Figure 4.2 a and b. As it can be seen from the figure, the data points are distributed relatively close to the 45^0 line. This indicates an adequate agreement between experimental and predicted values for COD and color reduction is obtained.

Moreover, Figure 4.3 (a and b) are a perturbation plots, which illustrates the effect of all the factors at the center point in the design space. The plot was obtained for initial pH of 3.5, H_2O_2: COD= 6.5, H_2O_2: Fe^{2+}=8.5 and RT of 60 min. A steep plot indicates the

sensitivity of the response to the factors. As can be seen from the plot, COD removal efficiency is very sensitive to the mass ratio of H_2O_2: COD (A), followed by initial pH of the solution (C) and the mass ratio of H_2O_2:Fe^{2+} (B) for COD removal. But for color removal, H_2O_2:Fe^{2+} (B) is the most impactful followed by H_2O_2: COD (A), and initial pH of the solution (C). This observation is in agreement with Eq. (4.2 (a) and (b)).

4.1.4   Effect of Operating Parameters on Color Removal

The color content of the dye is linked to the chromophore groups present in the dye structure (Choi et al.; Turhan et al., 2012). These groups are active and can be easily broken down by the attack of highly oxidative $HO\bullet$ radical which results in color removal within few minutes. Nevertheless, color removal does not necessarily translate into complete mineralization (Turhan et al., 2012). It can also been seen from Table 4.4 that Fenton process is efficient for decolorization and rapid decolorization was obtained immediately after the addition of Fe^{2+} salt and H_2O_2 solution (Gomathi Devi et al., 2009). Maximum 98% decolorization efficiency was obtained. The dark-blue color was turned into pale yellow during this process and after filtration colorless solution was obtained. The color removal efficiency of RBB dye is further evaluated through three dimensional surface response plots attained from RSM-CCD. The surface response plots of Figure 4.4 to 4.6 shows the effects of mass ratios of H_2O_2:COD and H_2O_2:Fe^{2+} and initial pH of the dye solution on the color removal efficiency.
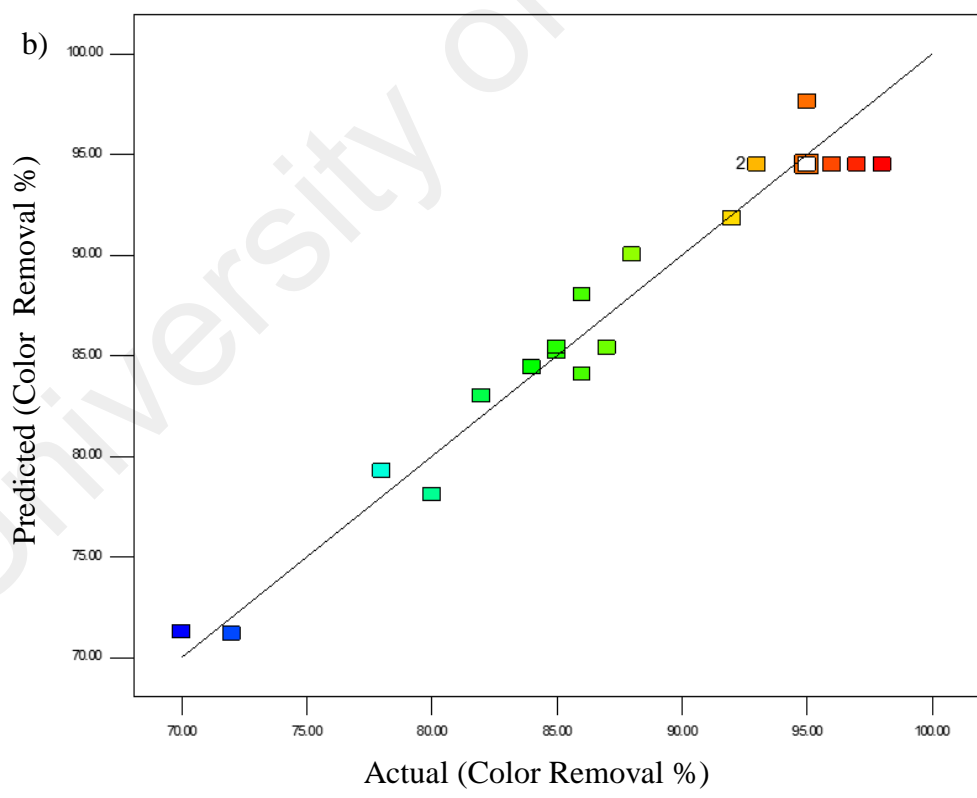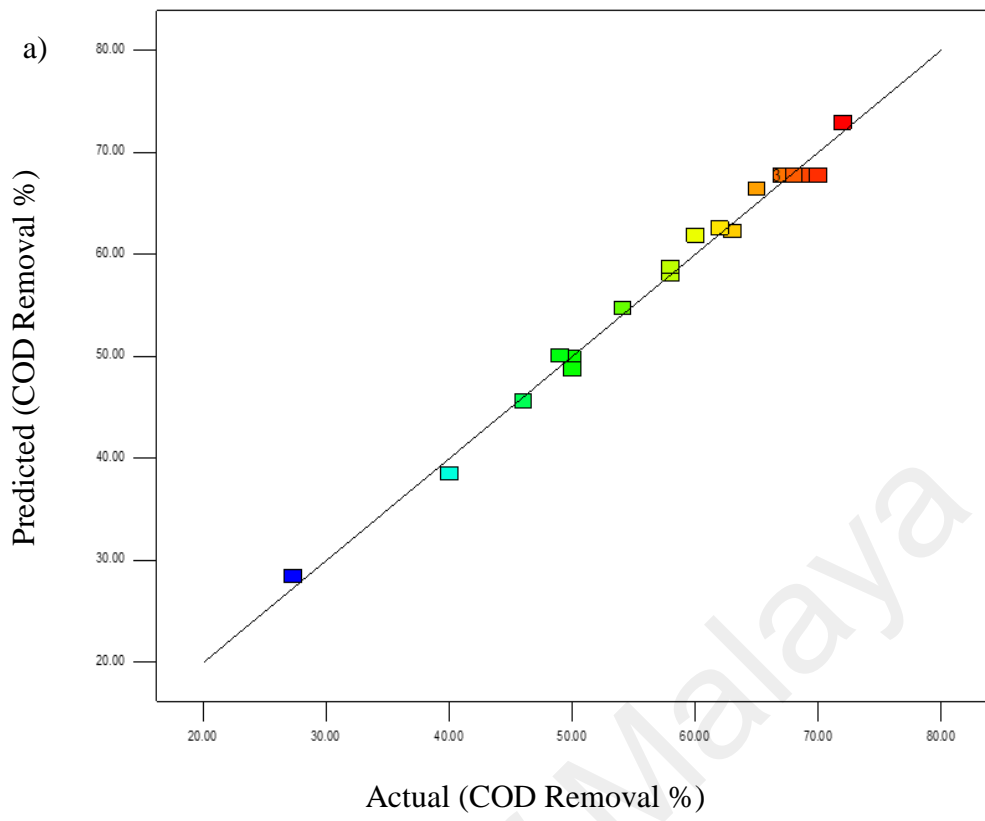
Figure 4.2: Regression plot of measured data versus predicted values from the quadratic model for the percent of (a) COD removal and (b) Color removal
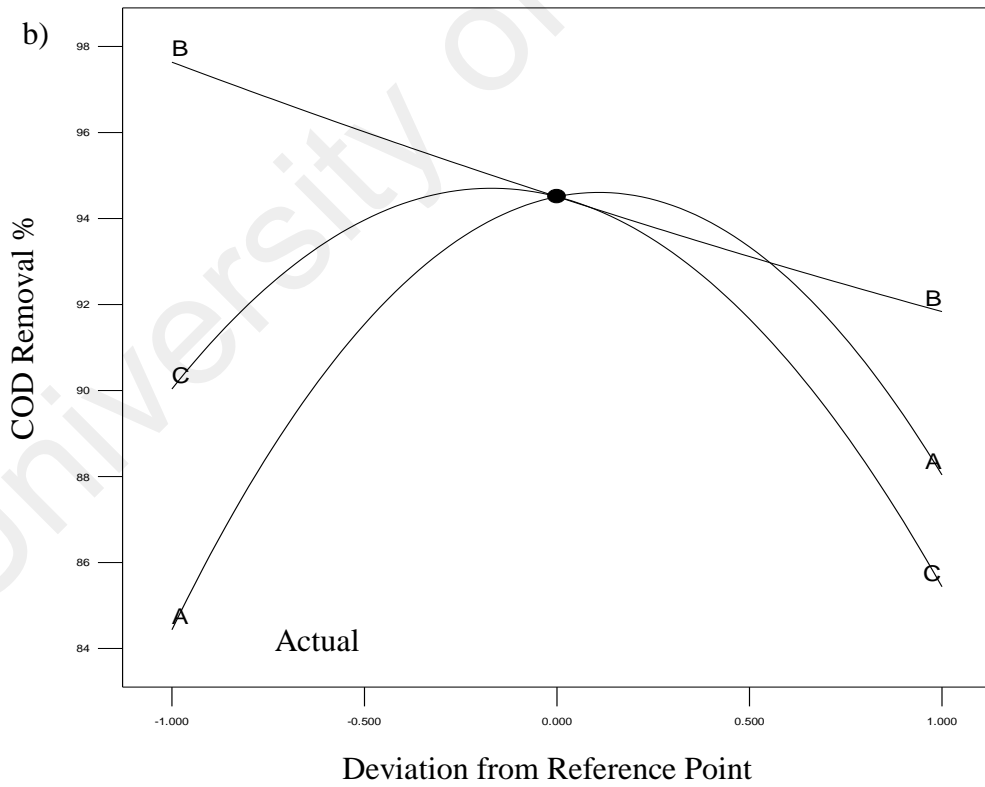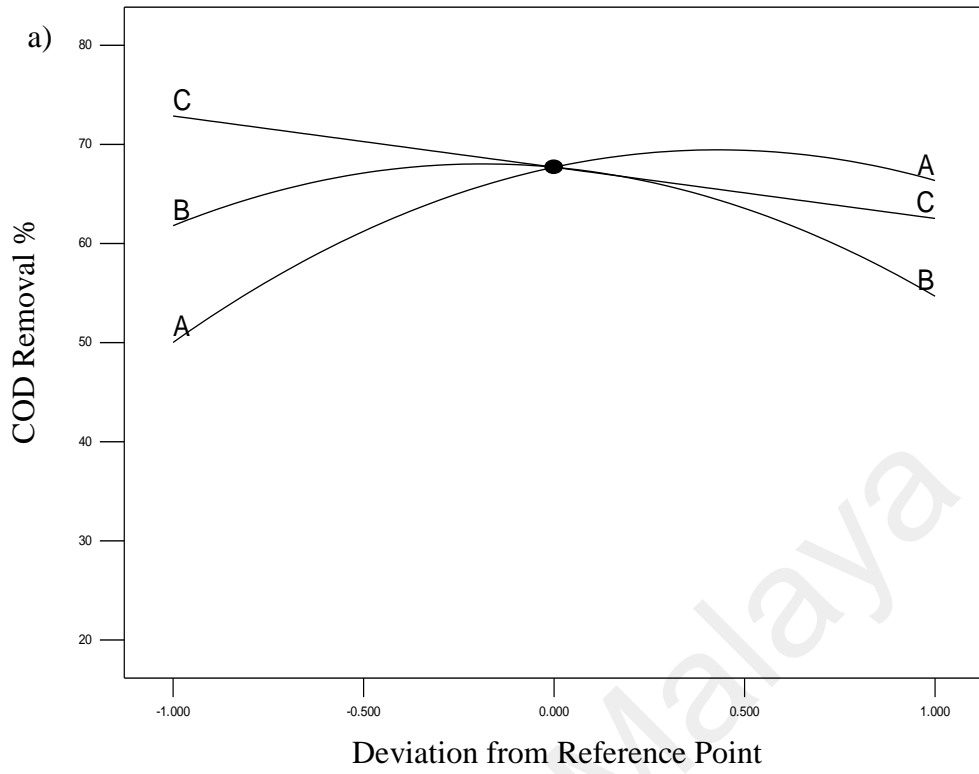
Figure 4.3: Perturbation plot for (a) COD removal and (b) Color removal

Fenton's reagent is the most significant parameter, which determines the chemical cost and affects the treatment efficiency by controlling the generation of $HO\bullet$ radical. The effect of mass ratios of H_2O_2:COD and H_2O_2:Fe^{2+} on color removal was investigated at constant COD of dye solution of 230 mg/l at the initial pH 3.5. As can be seen from Figure 4.4, color removal efficiency reached a maximum of 97.3%, with increasing the mass ratio of H_2O_2:COD from 1 to 8.5. However, a further rise in the mass ratio of H_2O_2:COD decreased the treatment efficiency caused by excessive amount of H_2O_2. When the amount of H_2O_2 exceeded, H_2O_2 acted as a scavenger of $HO\cdot$ which indicates the insufficient of $HO\bullet$ radical to oxidize the dyeing wastewater and give an influence on the color removal significantly (J. L. Wang et al., 2012). In addition, unreacted H_2O_2 in the solution increases COD of the wastewater (Buthiyappan et al., 2015).

Initial pH of the solution is also an important parameter that affects the color removal efficiency. The real textile wastewater has a wide pH range, therefore, the effect of pH on RBB color removal was assessed at different initial pH values varied from 2 to 5. Figure 4.5 and 4.6 shows that initial pH of the solution was remarkably influenced the color removal efficiency of RBB. When the pH value is 3.0, the color removal was 96.6 %. In homogenous systems pH 3 is known to be the optimal value for organic pollutant degradation. This result is supported by the work published by Ertugaya and Acar (2013) (Ertugay et al., 2013). However, color removal of RBB decreased from 96.6 % to 86.0% at pH 5. This is due to the formation of ferric hydroxo complex which limits the amount of Fe^{2+} to react with H_2O_2 to form $HO\bullet$ radical at higher pH values (Žgajnar Gotvajn et al., 2011). The higher pH with excessive amount of $HO\bullet$ radicals also did not improve and even reduce the color removal efficiency because of a scavenging effect on $HO\cdot$ by high concentration of H_2O_2 (Bouasla et al., 2010).

a)

b)
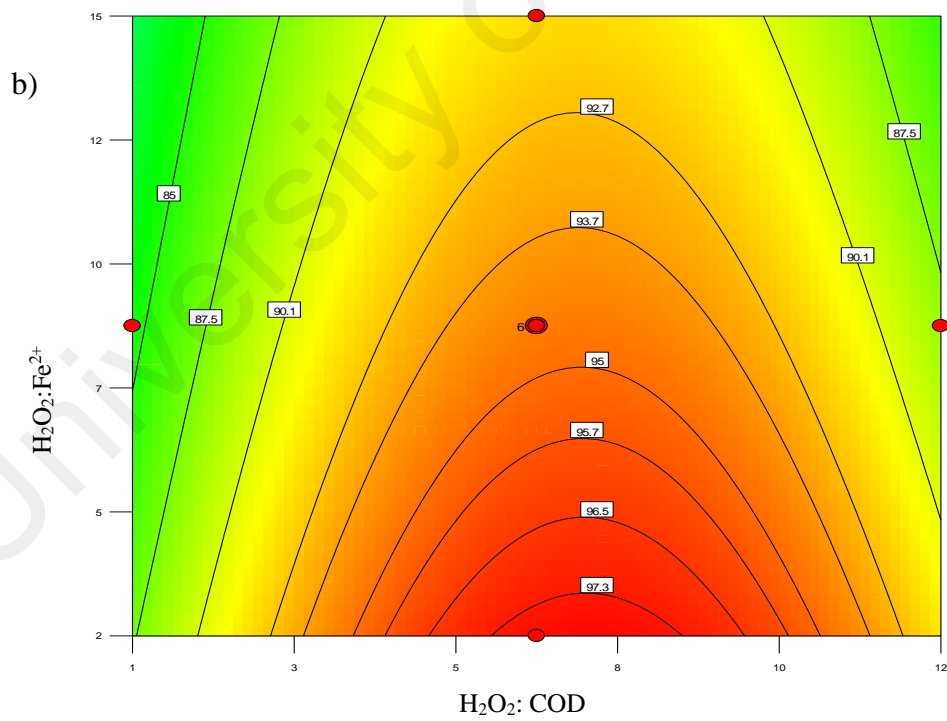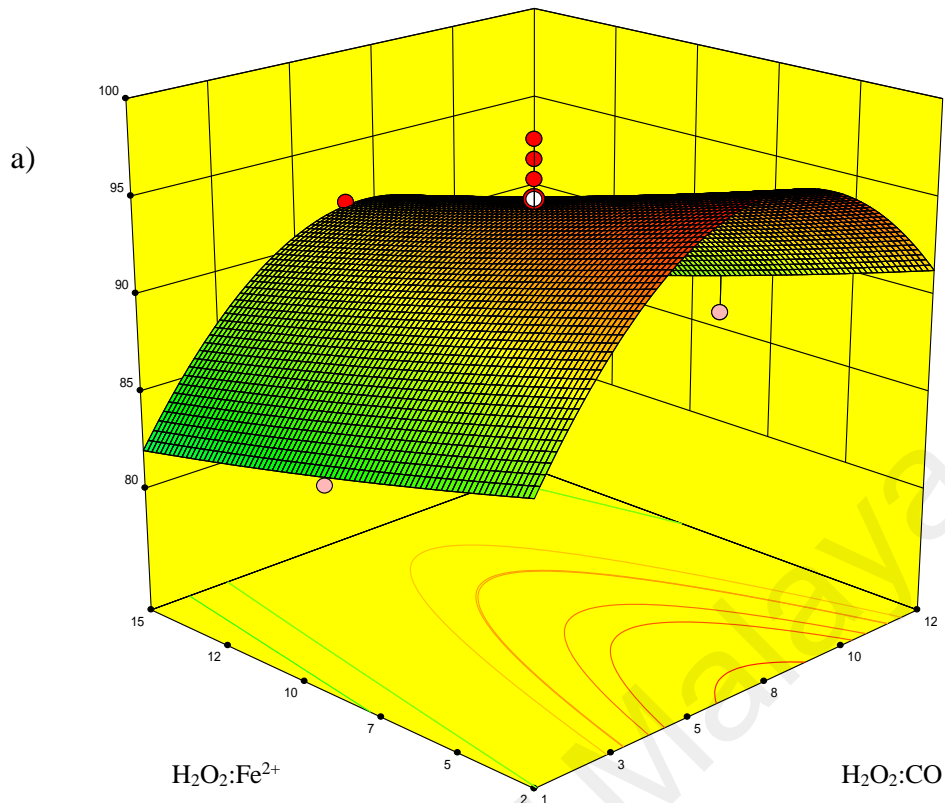
Figure 4.4: Effect of mass ratios of H_2O_2: COD and H_2O_2:Fe^{2+} on color removal
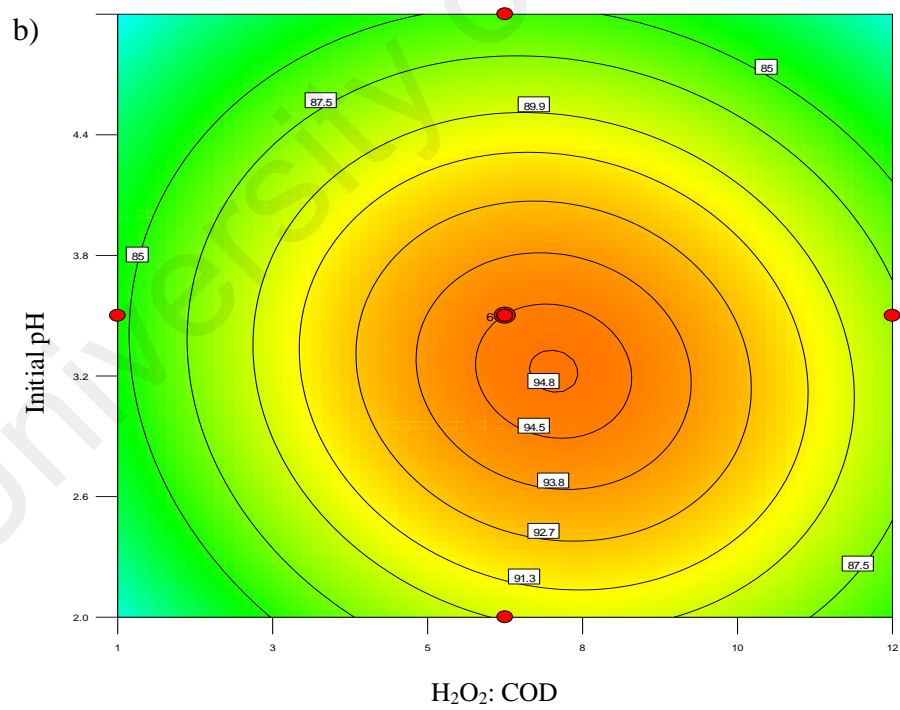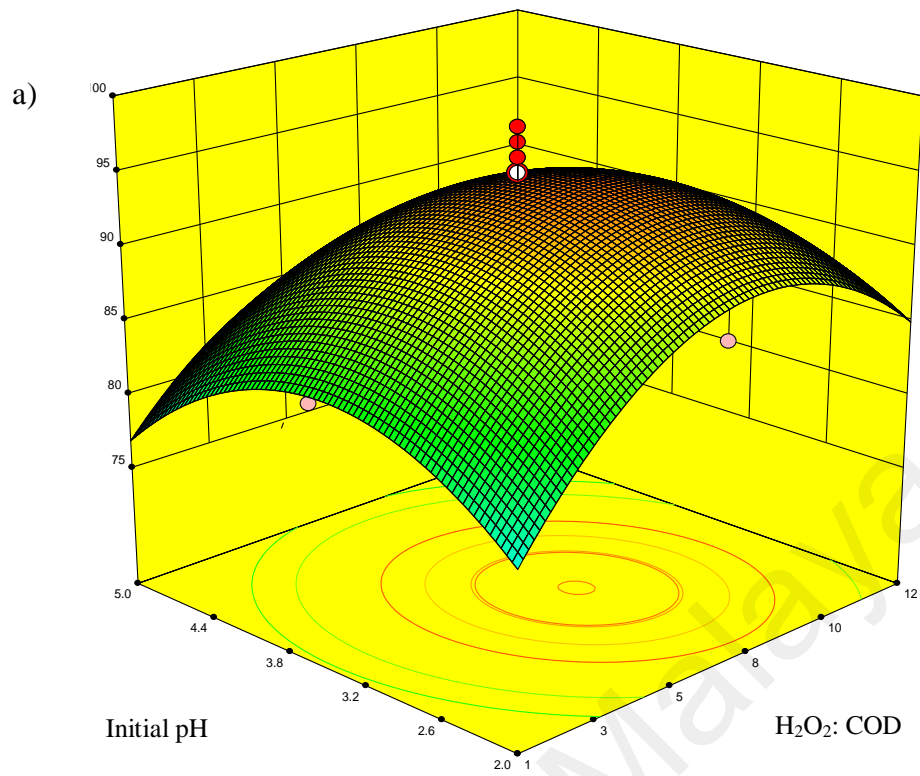
Figure 4.5: Effect of mass ratio of H_2O_2: COD and initial pH^+ on color removal

a)

b)
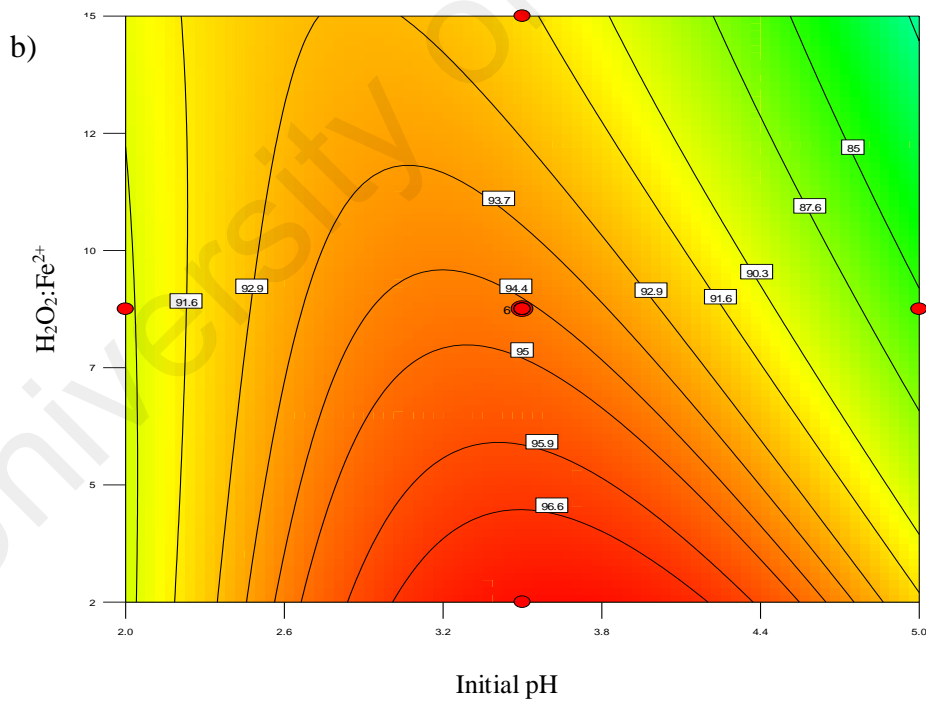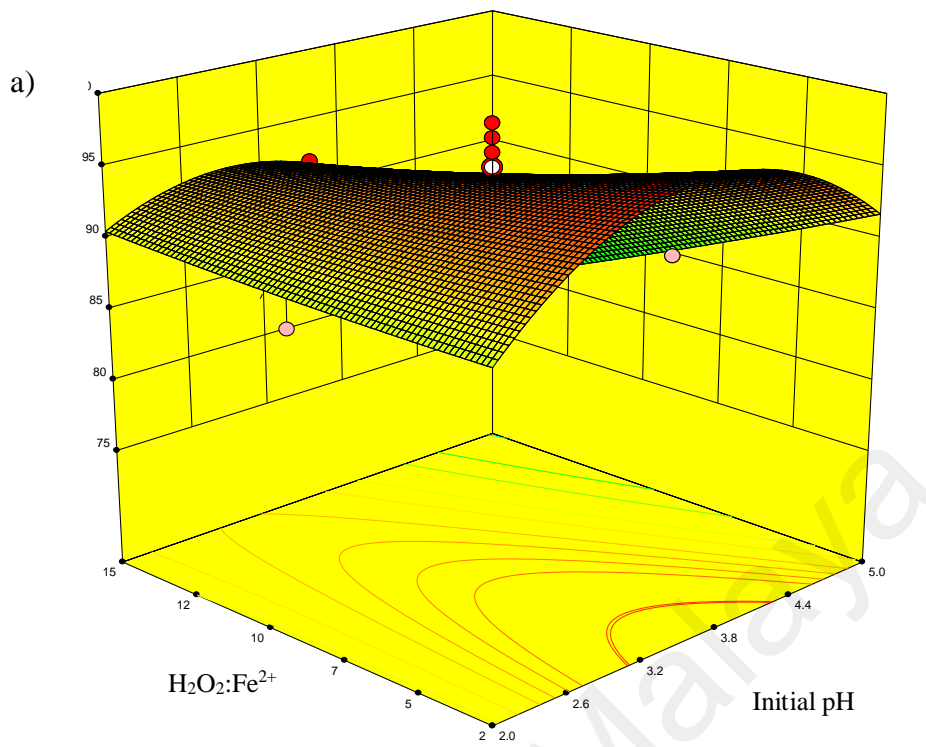
Figure 4.6: Effect of mass ratios of $H_2O_2:Fe^{2+}$ and initial pH on color removal

In summary, Fenton process could be effectively used for color removal of reactive dyes especially having anthraquinone chromophores. Operating parameters such as initial COD value, mass ratios of H_2O_2:COD, and H_2O_2:Fe^{2+} and initial pH of wastewater have a significant influence on the decolorization process. Complete color removal is important for a safety discharge of colored wastewater. However, maximum COD and TOC removal efficiencies are even more important. Discharging high amount recalcitrant organic contaminants into water bodies can alter the endocrine systems of a living organism and its being subject of huge concern nowadays.

4.1.5 Effect of Significant Factors on COD Removal Efficiency

Figures 4.7-4.9 depict the response surface modeling in two-dimensional and three-dimensional contours to reflect the effects of initial pH, mass ratios of H_2O_2: COD and H_2O_2: Fe^{2+} on the RBB removal efficiency at the center point in the design space. These figures are the graphical depictions of the regression analysis. The response function of two factors while all others were kept constant is presented in the plots. The illustrations show that the three operating factors investigated had a good effect on the COD removal efficiency.

4.1.5.1 Effect of Mass Ratio of H_2O_2:COD on COD removal

Based on the second-order polynomial equation (Eq. 4.1 (a)), the most influential operating parameter on COD removal was the mass ratio of H_2O_2: COD (A). The amount of H_2O_2 played an important role in the oxidation of RBB. The results revealed that increasing the dosage of H_2O_2 substantially improved the COD removal of the RBB dye wastewater. As observed in Figure 4.7, lower COD removal, which was around 50% was achieved at an initial pH of 3.5 and very low concentration of H_2O_2 (H_2O_2: COD = 1-4). Increasing the mass ratio of H_2O_2: COD to 9.4 improved the COD removal

efficiency and the highest COD removal of 69.5 % was obtained at pH 3.5. This is because the high concentration of oxidizers caused the formation of $HO\bullet$ radical which are responsible for attacking the organic contaminants in wastewater (Torrades et al., 2014).

But, as can be seen in Figure 4.7, increasing the mass ratio of H_2O_2: COD and H_2O_2: Fe^{2+} above the optimal point, which were approximately 9.4 and 7.2, caused a decrease in the removal efficiency (54 %). This confirmed the dependency of the Fenton process on the dosage of H_2O_2 and Fe^{2+} salts. Based on the previous studies, the degradation rate of organic compounds increased as the H_2O_2 concentration increased until a critical H_2O_2 concentration is achieved (Bouasla et al., 2010). Increasing the dosage above the optimal point did not improve the degradation efficiency significantly. This is due to the fact that $HO\cdot$ is non-selective and when $HO\cdot$ is present in excess, it oxidize species that are not supposed to be oxidized. This can cause the formation of intermediates, which can increase the COD of the wastewater. Besides, self-scavenging of $HO\cdot$ can also be caused by excessive H_2O_2 (Eq. 4.3) (M. Lucas et al., 2006; X. R. Xu et al., 2004).

$$H_2O_2 + \cdot OH \rightarrow HO_2\cdot + H_2O \tag{4.3}$$

It is suggested that the mass ratio of H_2O_2: COD should be less than 11 as a lower concentration of H_2O_2 is an attractive option from the economic point of view. The amount of H_2O_2 required for efficient RBB degradation also depends on the COD value or concentration of the treated pollutant. The concentration of H_2O_2 required to complete the degradation varies with the type of pollutants and it is necessary to optimize the parameters for each pollutant.
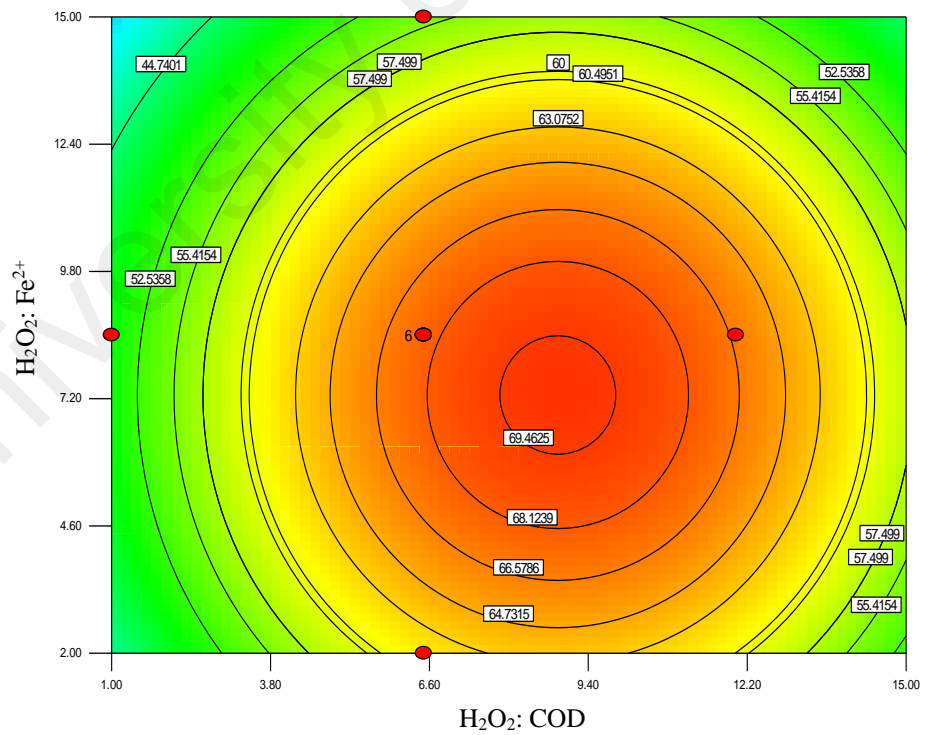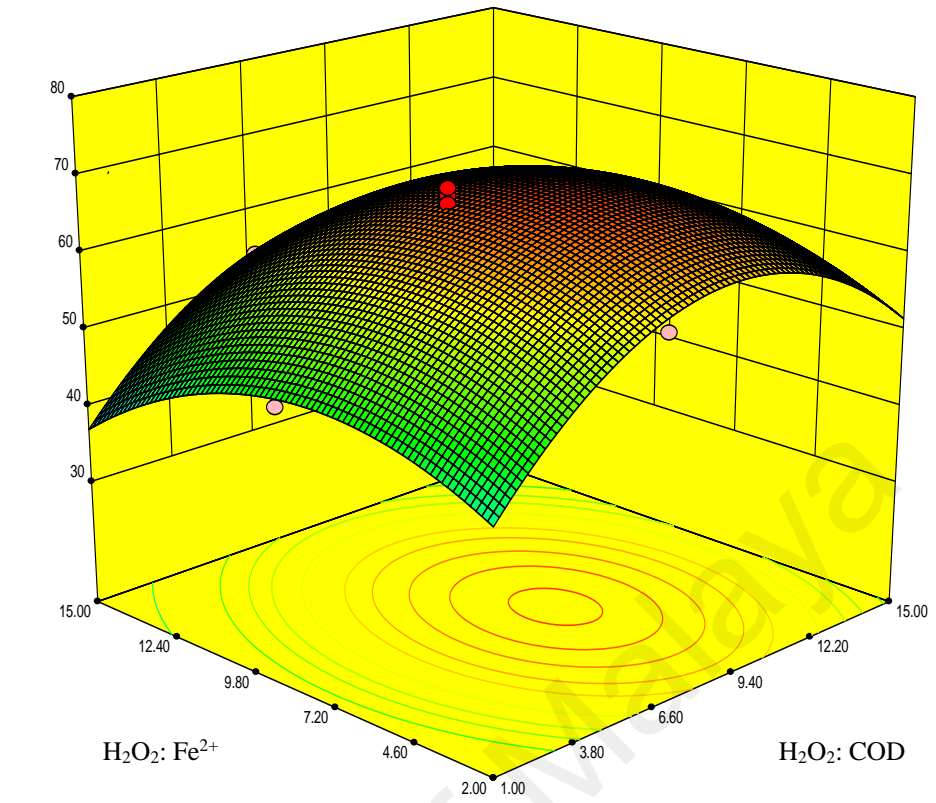
Figure 4.7 : Effect of mass ratios of $H_2O_2:Fe^{2+}$ and $H_2O_2:$ COD on COD removal

4.1.5.2 Effect of Mass Ratio of H_2O_2:Fe^{2+} on COD removal

The mass ratio of H_2O_2:Fe^{2+} was varied from 2 to 15 and other conditions were fixed at a central point (initial COD of dye of 230 mg/L, the initial pH value of 3.5 and a retention time of 60 min) to investigate the effect of Fe^{2+} concentration on COD removal efficiency. As observed in Figure 4.7, COD removal efficiency significantly increased with the mass ratios of H_2O_2:COD and H_2O_2:Fe^{2+}. The maximum COD removal (69.5 %) was achieved at mass ratios of H_2O_2:Fe^{2+} =7 and H_2O_2: COD =9.2 and a decrease in COD removal were observed when the mass ratio of H_2O_2:Fe^{2+} increased larger than 7. The increase in the COD removal efficiency at a higher concentration of Fe^{2+} could be attributed to the higher amount of Fe^{2+}, which actively reacts with H_2O_2 for the generation of $HO\bullet$ radical according to the Fenton reaction (Bielski et al., 1985; C. Walling et al., 1973). On the contrary, negative effects were observed at a higher dosage of Fe^{2+} (larger than H_2O_2:Fe^{2+}=7) due to a competitive reaction occurring between the generated $HO\bullet$ radical and Fe^{2+} in excess.

At a constant mass ratio of H_2O_2:COD, the increase in H_2O_2:Fe^{2+} does not cause changes to the amount of H_2O_2 but reduce the amount of Fe^{2+}. Therefore, the oxidation process becomes catalyst deficient, decreasing the COD removal efficiency. The direct relation between the mass ratio of H_2O_2:COD and COD removal efficiency while an inverse trend was observed with H_2O_2: Fe^{2+}. The increases in the COD removal efficiency was observed with the increase in the H_2O_2:COD ratio where the H_2O_2 available in the reaction medium increased, hence increasing the efficiency of the Fenton process. Figure 4.7 shows that the removal efficiency was the lowest in the range of 1-3 and increase the ratio of H_2O_2: COD up to 9 significantly improve the removal efficiency. Therefore, the mass ratio of H_2O_2:Fe^{2+} = 7.4 was employed as the optimum ratio for the rest of the experiments in this study in order to achieve the maximum COD removal.

4.1.5.3 Effect of Initial pH on COD Removal

An important characteristic of the Fenton process is, it promotes oxidation in acidic conditions. The optimum initial pH reported in the previous study for the conventional Fenton process ranges between 2.0 and 4.5 (Karthikeyan et al., 2011). Therefore, the initial pH was varied from 2 to 5 in this preliminary study to determine its effect on COD removal efficiency.

As can be seen in Figure 4.8, the maximum COD removal efficiency of about 72.3 % was achieved at the mass ratio of H_2O_2: COD of around 9.8 and initial pH of 2. A decrease in the COD removal (44.7 %) was observed with the increase of pH value from 2 to 5, as seen in Figure 4. Moreover, increasing the ratio of H_2O_2: COD above 9 and initial pH from 2 to 5 at H_2O_2:Fe^{2+}= 10 caused a steady decrease in the COD removal efficiency as depicted in Figure 4.9. It was proven that the dosage of H_2O_2 and Fe^{2+} had a strong interaction with the initial pH of the solution.

In summary, the optimum initial pH value was found to be in the very acidic range, which is between 2 to 2.6. This observation agrees with the values in literature (Bautista et al., 2007; Kim et al., 2001; M. Lucas et al., 2006; Modirshahla et al., 2007; Papadopoulos et al., 2007). As observed in Figures 4.9, when the initial pH continuously increased, a decrease in the COD removal efficiency was observed because of the formation of $Fe(OH)_3$, which had a lower catalytic activity for H_2O_2 decomposition compared to Fe^{2+} (Bouasla et al., 2010). In the light of this findings, it was deduced that the acidic pH was favored for degradation of RBB.
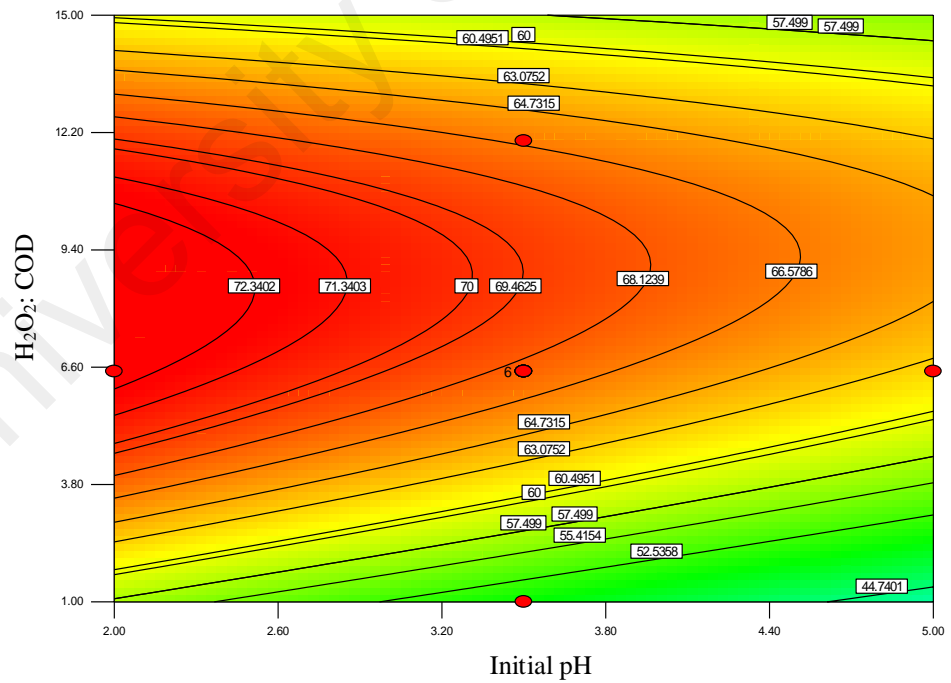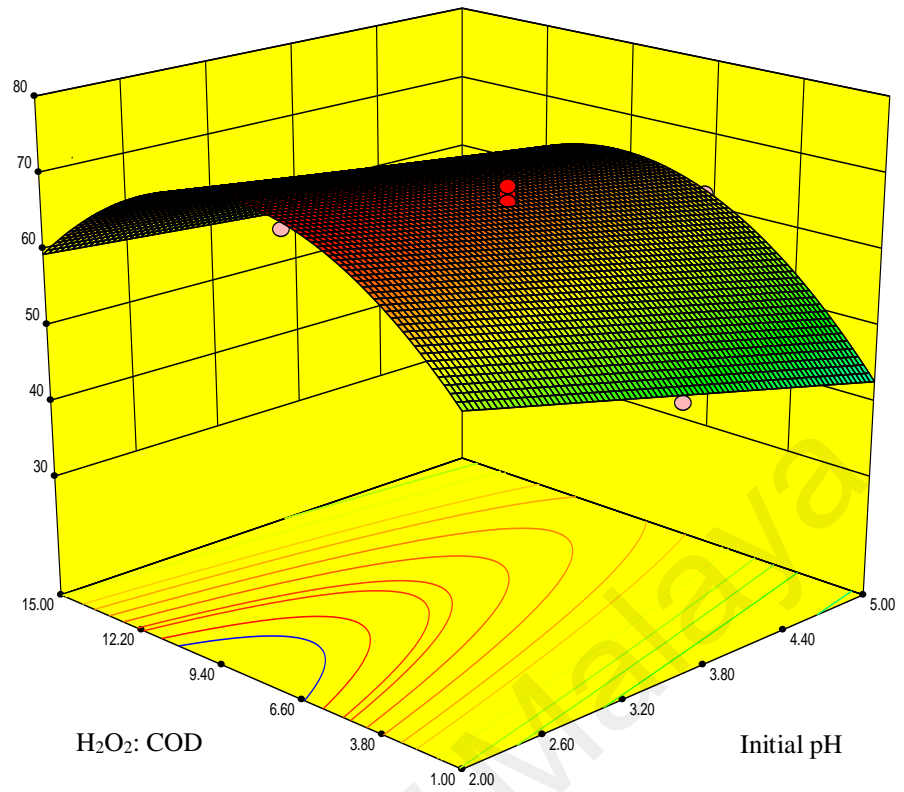
Figure 4. 8: Effect of mass ratios of H_2O_2: COD and initial pH on COD removal
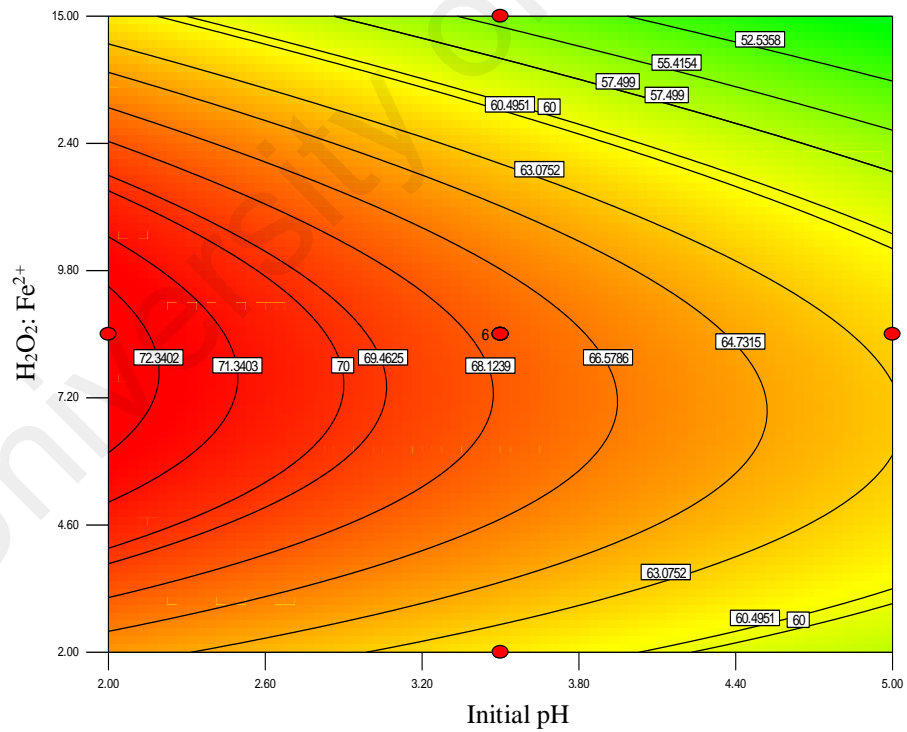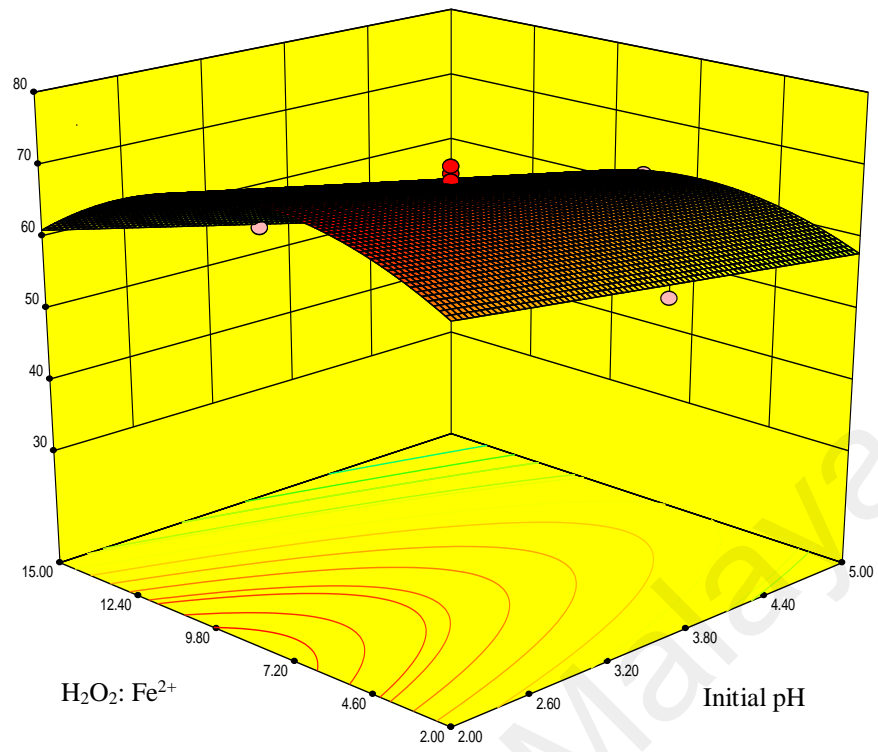
Figure 4.9: Effect of mass ratios of $H_2O_2:Fe^{2+}$ and initial pH on COD removal

4.1.6 Optimization by Response Surface Methodology and Model Validation

The redox reaction between highly active $HO\cdot$ and excess Fe^{2+} salts could aggravate the self-scavenging effect of $HO\cdot$, which reduces the degradation efficiency of pollutants. From the commercial point of view, it is necessary to identify an optimal amount of H_2O_2 and Fe^{2+} salts to minimize the sludge production that requires post treatment, which increases the cost of treatment.

The objective of the optimization process is to identify the optimum mass ratios of H_2O_2: COD, and H_2O_2:Fe^{2+} and initial pH of the solution to achieve the highest treatment performance. The combination of the operating parameters was selected based on the desired values. The high desirability (100%) was used to determine the optimum process parameters for maximum COD removal efficiency. Optimization process was carried out using the Design Expert 8.0 Software along with CCD. Design experts gives five options: none, maximum, minimum, target and within range for choosing the desirable goal for each variable and response. The favorable option for each operational condition was chosen as follows: "within the range" for the mass ratio of H_2O_2:COD and H_2O_2:Fe^{2+} and initial pH of the solution while "maximum" was chosen for the response (COD and color removal efficiency) to achieve the highest performance.

As per experimental design, Table 4.6 shows the optimum conditions proposed by the software and the result of the verification experiments at the optimum conditions together with the simulated values by Eq. (4.1 and 4.2). In this study, the initial pH was fixed at 3. At the optimum condition of H_2O_2:COD $=8.7$ and H_2O_2:$Fe^{2+}=7.4$, almost complete decolorization and the final COD removal efficiency reached the maximum value of 75 %, which was 57.8 mg/L. 1,736 mg of H_2O_2 amount and 233.3 mg of Fe^{2+} were consumed to reduce the COD of wastewater from 230 mg/L to 55.2 mg/L (75 %). The experimental

values were in good agreement with the predicted value of 71.1 % for COD removal and 96.0 % for color removal.

In summary, this study demonstrated that RSM-CCD able to determine the most significant operating parameters and optimum ratios of pollutant:oxidant:catalyst. The low deviation between the experimental and the predicted values confirmed that RSM is a simple, rapid and accurate tool for optimizing COD and color removal efficiencies in the Fenton process. The result obtained from this preliminary study also confirms the applicability of Fenton process for dye containing solution and the investigation of actual textile wastewater treatment could be designed using the data obtained from this preliminary study.

Table 4.6 : Optimum value of the process parameters for constraint conditions and experimental values

COD (mg/L)	H_2O_2:COD (wt/wt)	H_2O_2:Fe^{2+} (wt/wt)	pH	COD %		Color %	
				Pred.	Exp.	Pred.	Exp.
230.0	8.7	7.4	3.0	71.1	76.0	96.0	99.0

4.2   Application of Fenton Process for the Treatment of Batik Wastewater

With the preliminary results obtained as a basis, Fenton process is conducted using actual textile wastewater. This work is focused on the COD, TOC and color removal efficiencies. All these parameters representing degradation, mineralization and decolorization aspects of the AOPs were explored in this study. Furthermore, FTIR, GC/MS and HPLC analyses also conducted to identify the organic compounds before and after treatment. To add the completeness of the process evaluation, an elemental analysis was conducted to study the characteristic of sludge. Besides, the model developed for the textile wastewater using RSM-CCD was also further validated using selected types of industrial wastewaters with low, medium and high COD values. Duplicates were performed to control both accuracy and repeatability.

4.2.1   Fitting the Response Surfaces and Statistical Analysis

The performance of the Fenton process depends on various factors including initial pH of the solution, amount of H_2O_2 and Fe^{2+}, retention time, temperature, mixing speed and initial value of COD or concentration of wastewater as reported in literature (Archina et al., 2015; Babuponnusami et al., 2014; M. Lucas et al., 2006; Pignatello et al., 2006). As this study deals with actual wastewater which comprises of a wide range of unknown contaminants, it is important to consider all the above-stated parameters. Therefore, several preliminary experiments were conducted to identify the range of the variables in order to develop the experimental design using RSM-CCD.

Initial pH of the reaction is highly dependent on the characteristics of the pollutants and Fenton reagent (Žgajnar Gotvajn et al., 2011). Since this research focuses on the application of real textile effluents that comprise various components, the pH of the solution was varied from very acidic to basic conditions (initial pH values of 2 to 9). All

102

the experiments were conducted at room temperature (298 K) and pressure. Oxidation and coagulation can take place simultaneously in the Fenton process and this is the major advantage of this technique (Santos et al., 2015). 250 rpm was selected as the optimized mixing speed and made constant during the course of the treatment process based on preliminary experiments. Since real textile effluent was used, initial chemical oxygen demand ([COD]i) was selected instead of concentrations. The value of [COD]i was varied between 1600- 1900 mg/l and dependent on the samples collected from the Batik industry.

A total of thirty experiments was carried out in this analysis in accordance with the model proposed by the RSM-CCD. The selected range of the operating parameters and level of the independent variables are given in Table 4.7. The selected design required experiments outside the experimental range to allow the prediction of the response functions outside the selected range. The COD, TOC and color removal efficiencies were chosen as the response variables because they could provide necessary information for evaluating the analytical performance of Fenton process.

The responses based on the experimental runs on color, COD and TOC removal efficiencies proposed by RSM-CCD are given in Table 4.8. The results presented in the table are the duplicates of the experimental results at each operating condition. Based on the results obtained from the experimental runs, the second-order polynomial equation was used to correlate the experimental results with the response functions. Based on the experimental results, the final quadratic equation of the response in term of coded factors is presented in Eq. (4.6), (4.7) and (4.8), as shown in Table 4.9. The equations correlate the response variables, as a function of the operating factors and a bad equation will result in poor lack-of-fit and violation of the ANOVA assumptions.

Table 4.7: RSM-CCD experimental design

Independent variable		Units	Coded levels				
			-2	-1	0	+1	+2
			Actual levels				
H_2O_2:COD	A	w/w	4.5	1.0	6.5	12.0	17.5
H_2O_2:Fe^{2+}	B	w/w	4.5	2.0	8.5	15.0	21.5
pH	C	-	1.5	2.0	5.5	9.0	12.5
Retention time	D	min	0.0	30.0	60.0	90.0	120.0

The ANOVA results of the quadratic polynomial models for the Fenton process for the color, COD and TOC models are shown in Table 4.10. The equation clearly shows that all the four operating parameters had positive effects on the COD, TOC and color removal efficiencies within the investigated range. Based on the AR1 developed in this study, initial pH of the solution has the most effect, for COD, TOC and color removal efficiencies compared to other investigated parameters as can be seen in Figure 4.10. It also clear from the figure that besides independent effect, the interaction between mass ratios of H_2O_2:COD and H_2O_2:Fe^{2+} also affect the treatment efficiency in term of COD, TOC and color removals. Consequently, all the three polynomial equations gave a good visualization of the effects of the significant factors and their effects on the response.

Table 4.8: Observed results corresponding to RSM-CCD design by Fenton process for Batik wastewater

Run	Independent variable				Responses (%)		
	H_2O_2:COD	H_2O_2:Fe^{2+}	pH	Retention time	COD	TOC	Color
1	12.0	2.0	9.0	90.0	71.5	53.5	98.1
2	1.0	2.0	9.0	30.0	57.2	49.2	78.2
3	1.0	2.0	2.0	90.0	52.7	50.3	77.0
4	6.5	8.5	5.5	60.0	76.1	64.1	96.0
5	6.5	8.5	5.5	60.0	75.4	65.8	96.2
6	12.0	15.0	2.0	90.0	50.4	35.8	85.5
7	1.0	15.0	9.0	90.0	60.1	45.1	84.2
8	1.0	15.0	2.0	30.0	62.4	52.4	86.0
9	12.0	15.0	9.0	30.0	52.7	36.2	88.3
10	12.0	2.0	2.0	30.0	74.2	61.0	90.0
11	12.0	2.0	9.0	30.0	70.8	55.8	96.2
12	1.0	15.0	9.0	30.0	60.4	52.0	83.0
13	12.0	2.0	2.0	90.0	73.2	62.1	83.3
14	1.0	15.0	2.0	90.0	62.3	50.1	90.1
15	1.0	2.0	9.0	90.0	61.6	48.2	79.4
16	1.0	2.0	2.0	30.0	56.3	48.4	75.2
17	12.0	15.0	9.0	90.0	49.5	28.7	90.1
18	6.5	8.5	5.5	60.0	76.4	63.9	97.6
19	12.0	15.0	2.0	30.0	54.5	37.1	87.2
20	6.5	8.5	5.5	60.0	74.3	65.2	98.3
21	6.5	8.5	5.5	120.0	62.2	38.2	95.2
22	6.5	8.5	12.5	60.0	35.3	22.3	80.0
23	17.5	8.5	5.5	60.0	76.8	60.3	95.3
24	6.5	21.5	5.5	60.0	62.6	48.3	88.0
25	6.5	-4.5	5.5	60.0	78.3	68.2	85.4
26	6.5	8.5	5.5	60.0	74.6	61.9	96.0
27	6.5	8.5	1.5	60.0	41.5	33.1	73.2
28	4.5	8.5	5.5	60.0	70.2	62.8	86.0
29	6.5	8.5	5.5	00.0	56.2	39.2	95.3
30	6.5	8.5	5.5	60.0	74.3	62.9	96.2

Responses	Proposed quadratic model	Eq.
COD Removal	28.07 + 1.92 (H_2O_2:COD) + 0.88 (H_2O_2:Fe^{2+}) + 8.14 (pH) + 0.56 (RT) - 0.17 (H_2O_2:COD X H_2O_2:Fe^{2+}) - 0.04 (H_2O_2:COD X pH)- 0.04 (H_2O_2:Fe^{2+})^2 - 0.74 (pH)^2- 0.01(RT)^2	(4.6)
TOC Removal	11.80 + 1.50 (H_2O_2:COD) + 1.081 (H_2O_2:Fe^{2+}) + 8.23 (pH) + 0.88 (RT) - 0.17 (H_2O_2:COD X H_2O_2:Fe^{2+}) - 0.05(H_2O_2:COD X pH) - 0.01 (H_2O_2:Fe^{2+} X RT) - 0.01 (pH X RT) - 0.03 (H_2O_2:Fe^{2+})^2 - 0.72(pH)^2 - 0.01 (RT)	(4.7)
Color Removal	63.30 + 1.55 (H_2O_2:COD) + 2.24 (H_2O_2:Fe^{2+}) + 5.11 (pH) - 0.09 (H_2O_2:COD X H_2O_2:Fe^{2+}) + 0.10 (H_2O_2:COD * pH) - 0.08 (H_2O_2:Fe^{2+} X pH) - 0.06 (H_2O_2:COD)^2 - 0.06 (H_2O_2:Fe^{2+})^2 - 0.42 (pH)^2	(4.8)

The fit of the model was evaluated by ANOVA. Values of Prob>F less than 0.05 indicate that the model is significant and values greater than 0.01 imply that the model is insignificant. The results of the ANOVA analysis, showed that all the models had a P value less than 0.0001, indicating that the models were significant to describe the color, COD and TOC removal efficiencies. Furthermore, the validity of the models was determined by the values of lack-of-fit. The 'lack –of-fit' for both models was not significant relative to the pure error and this confirmed the good predictability of the model. However, the "Lack-of-Fit F-value" of 29.41 implied that the Lack-of-Fit was significant and the model was not fit for color removal %. This is because the color abatement occurred within 2- 5 minutes under all experimental conditions. Therefore, it was quite difficult to model color removal using the same time interval for COD, TOC and color on removals because near-complete decolorization could be achieved at this reaction time

Table 4.10: ANOVA result for response models for COD, TOC, color removals

Variation source	Sum of Squares	df	Mean Square	F value	P-value	Prob>F
COD Removal						
Model	3661.00	14	261.50	55.22	< 0.0001	Highly Sig.
A-H_2O_2:COD	41.61	1	41.61	20.25	0.0006	Sig
B-H_2O :Fe^{2+}	433.50	1	433.50	210.99	<0.0001	Highly Sig.
C-pH	16.67	1	16.67	8.11	0.0137	Sig.
D-RT	1.31	1	1.31	0.64	0.4395	Not. Sig.
AB	607.62	1	607.62	295.74	<0.0001	Sig.
AC	9.00	1	9.00	4.38	0.0565	Not. Sig.
AD	5.52	1	5.52	2.69	0.1251	Not. Sig.
BC	6.50	1	6.50	3.16	0.0986	Not. Sig.
BD	5.76	1	5.76	2.80	0.1179	Not. Sig.
CD	5.06	1	5.06	2.46	0.1405	Not. Sig.
A^2	2.82	1	2.82	1.37	0.2621	Not. Sig.
B^2	32.19	1	32.19	15.67	0.0016	Sig.
C^2	2269.28	1	2269.28	1104.09	<0.0001	Highly Sig.
D^2	480.01	1	480.01	233.63	<0.0001	Highly Sig.
Residual	61.56	13	4.74	-	-	-
Lack of Fit	59.07	10	5.91	7.10	0.0668	Not. Sig
Pure Error	2.50	3	0.83	-	-	-
Cor Total	3725.81	29	-	-	-	-
Adeq. Precision	25.22	-	-	-	-	-
R^2	0.9835	-	-	-	-	-
Adj R^2	0.9657	-	-	-	-	-
Pred R^2	0.8724	-	-	-	-	-
TOC Removal						
Model	4398.83	14	314.20	143.02	< 0.0001	Highly Sig.
A-H_2O_2:COD	38.76	1	38.76	17.64	< 0.0001	Highly Sig.
B-H_2O :Fe^{2+}	713.95	1	713.95	324.98	<0.0001	Highly Sig.
C-pH	104.54	1	104.58	47.60	<0.0001	Highly Sig.
D-RT	17.17	1	17.17	7.82	0.0152	Sig.
AB	601.48	1	601.48	273.79	<0.0001	Sig.
AC	14.25	1	14.25	6.49	0.0243	Sig.
AD	0.18	1	0.18	0.08	0.7788	Not. Sig.
BC	0.18	1	0.18	0.08	0.7788	Not. Sig.
BD	19.58	1	19.58	8.91	0.0105	Sig.
CD	18.28	1	18.27	8.32	0.0128	Sig.
A^2	4.05	1	4.05	1.84	0.1975	Not. Sig.
B^2	40.12	1	40.12	18.26	0.0009	Sig.

Table 4.10: Continued

Variation source	Sum of Squares	df	Mean Square	F value	P-value	Prob>F
TOC Removal						
C^2	2146.76	1	2146.76	977.18	<0.0001	Highly Sig.
D^2	1019.52	1	1019.57	464.10	<0.0001	Highly Sig.
'Residual	28.56	13	2.20	-	-	-
Lack of Fit	25.77	10	2.58	2.77	0.2173	Not Sig.
Pure Error	2.79	3	0.93	-	-	-
Cor Total	4443.07	29	-	-	-	-
Adeq Precision	40.90	-	-	-	-	-
R^2	0.9936	-	-	-	-	-
Adj R^2	0.9866	-	-	-	-	-
Pred R^2	0.9528	-	-	-	-	-
Color Removal						
Model	1554.58	14	111.04	29.15	< 0.0001	Highly Sig.
A-H_2O_2:COD	287.04	1	287.04	75.36	< 0.0001	Highly Sig.
B-H_2O :Fe^{2+}	22.04	1	22.04	5.79	0.0318	Sig.
C-pH	57.04	1	57.04	14.98	0.0019	Sig.
D-RT	0.38	1	0.38	0.10	0.3750	Not Sig.
AB	162.56	1	162.56	42.68	< 0.0001	Highly Sig.
AC	60.06	1	60.06	15.77	0.0016	Sig.
AD	10.56	1	10.56	2.77	0.1198	Not. Sig.
BC	52.56	1	52.56	13.80	0.0026	Sig.
BD	3.06	1	3.06	0.80	0.3862	Not. Sig.
CD	5.06	1	5.06	1.33	0.2697	Not. Sig.
A^2	85.00	1	85.00	22.32	0.0004	Sig.
B^2	209.00	1	209.00	54.87	<0.0001	Sig.
C^2	759.00	1	759.00	199.27	<0.0001	Highly Sig.
D^2	11.07	1	11.07	2.91	0.1119	Not. Sig.
Residual	49.52	13	3.81	-	-	-
Lack of Fit	49.02	10	4.90	29.41	0.0089	Sig.
Pure Error	0.50	3	0.17	-	-	-
Cor Total	1612.17	29	-	-	-	-
Adeq Precision	16.44	-	-	-	-	-
R^2	0.9691	-	-	-	-	-
Adj R^2	0.9359	-	-	-	-	-
Pred R^2	0.7775	-	-	-	-	-
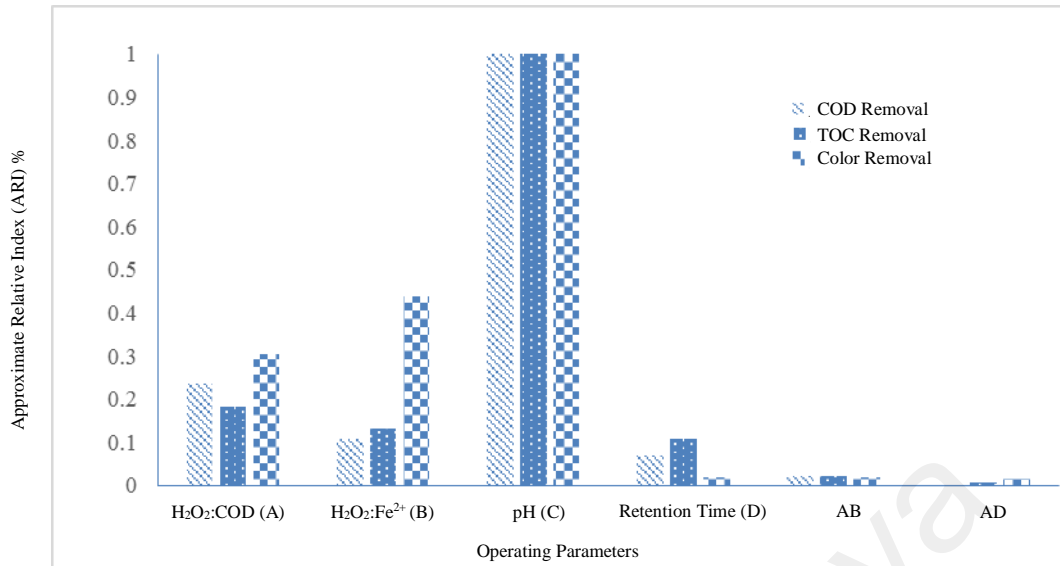
Figure 4.10: Effects of Operating Parameters based on Approximate Relative Index

ANOVA analysis showed that the *F* values for the COD, TOC and color removal models were 55.2.3, 143.0 and 29.2 respectively, indicating that the models were highly significant. There were only 0.015 chances that the 'model F value' could occur due to noise. In addition, the quality of fit of the polynomial models was expressed by the value of correlation coefficient (R^2). The models were found to be adequate to fit all the experimental data with R^2, adjusted R^2, and predicted R^2 of 98.3, 96.6, and 87.2% for COD removal; 99.3, 98.7, 95.3% for TOC removal; and 96.9, 93.6 and 77.7% for color removal. The R^2 value of the response variables, in descending order were TOC>COD>color removal. All the obtained predicted R^2 values were in reasonable agreement with the adjusted R^2, except for the color removal. This indicated the good predictability of the models for both COD and TOC removal %. The good agreement between the experimental and predicted values for COD, TOC and color removal %, as illustrated in Figure 4.11 revealed the accuracy of the model.

a)

b)
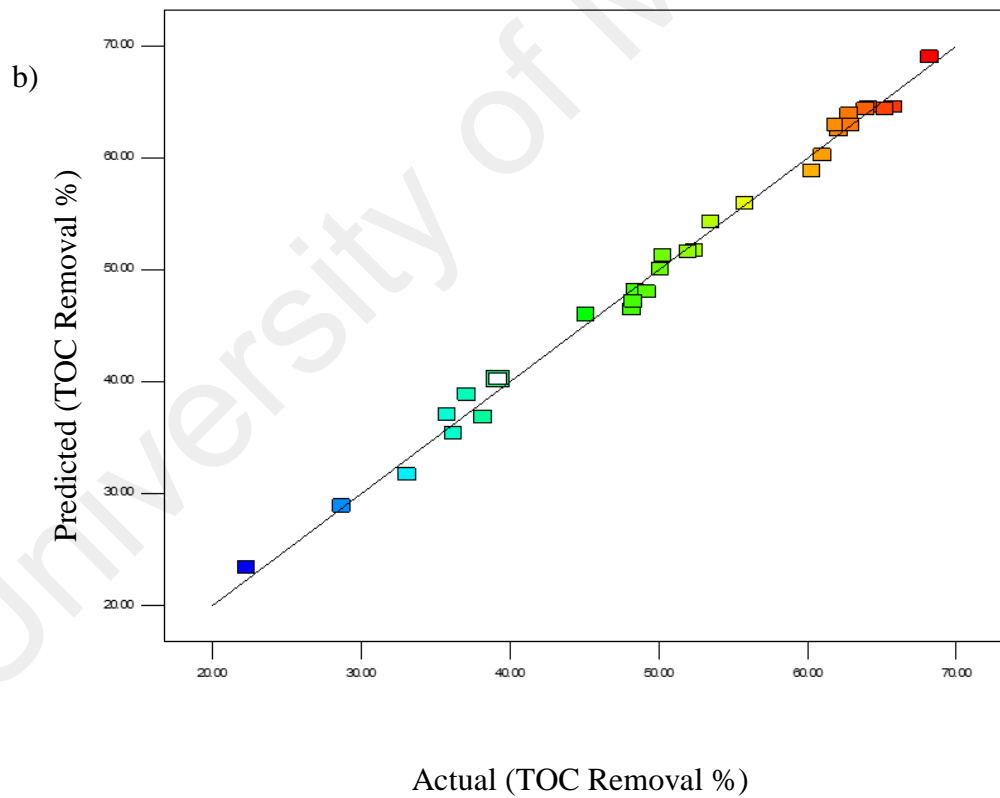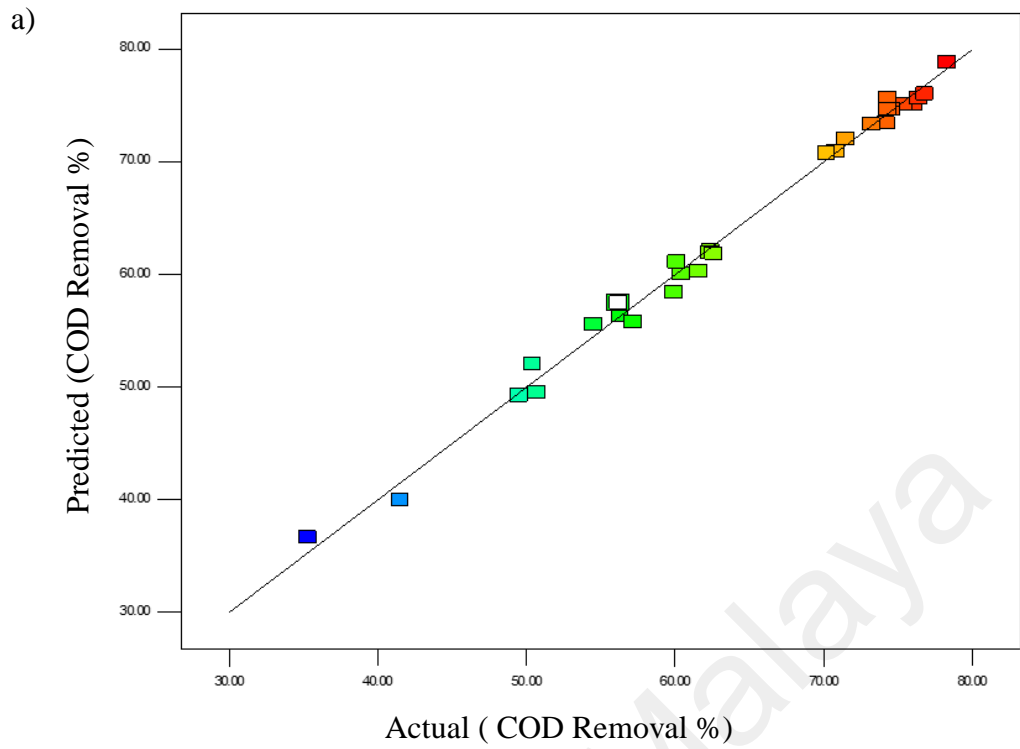
Figure 4.11: Experimental results plotted against the predicted values derived from the model of a) COD, b) TOC and c) Color removals

c)
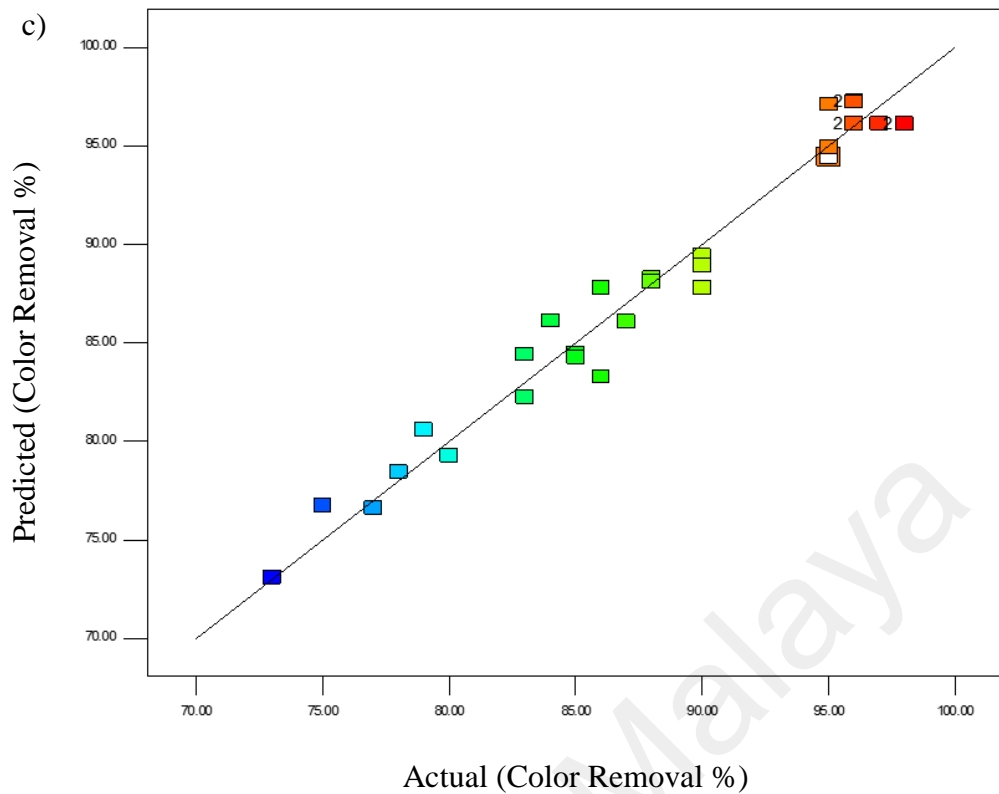
Figure 4.11: Continued

Besides, the adequate precision ratios of 25. 2, 40.9 and 16.4 derived from the COD, TOC and color removal efficiencies indicated that there were adequate signals for all response variables. The perturbation graph obtained based on the experimental result could be used to explain that all the four investigated operating factors had an effect on the treatment efficiency. Figure 4.12 (a, b and c) shows the perturbation graph of COD, TOC and color removals. The plot was obtained for initial pH 5.5, mass ratios of H_2O_2:COD= 6.5, H_2O_2:Fe^{2+}= 8.5 and retention time of 60 min. The steepness of the plot indicates the sensitivity of the response to the factors. The plot depicted that the COD, TOC and color removal efficiencies were very sensitive to the mass ratio of H_2O_2: COD, followed by initial pH, the mass ratio of H_2O_2:Fe^{2+} and retention time. In conclusion, based on the ANOVA analysis, the model was well explained and it could be used to navigate the design space in terms of COD and TOC removal efficiencies.
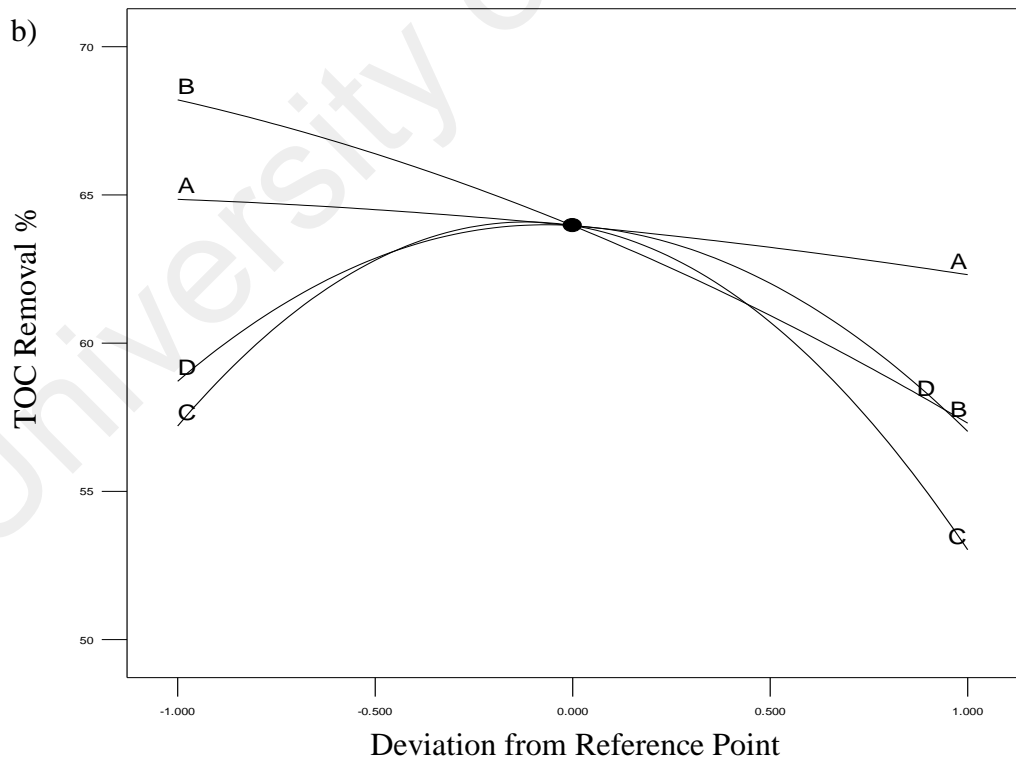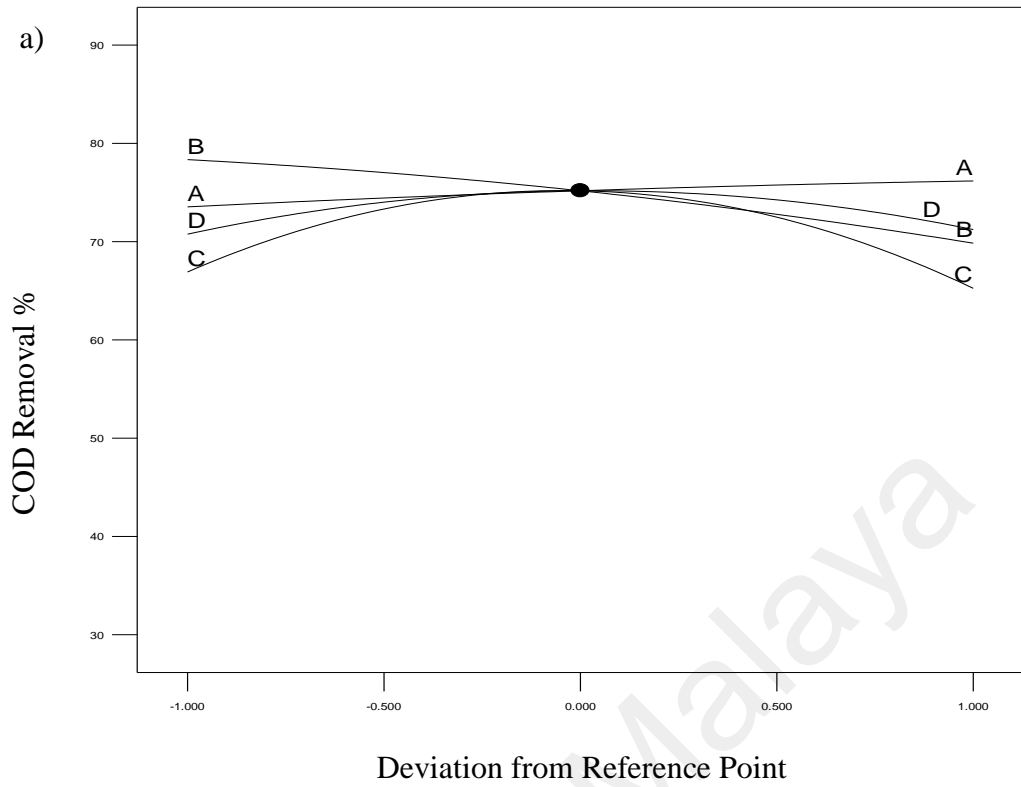
Figure 4.12: Perturbation plot of percentage of (a) COD (b) TOC and (c) Color removals (A-H_2O_2:COD, B-H_2O :Fe^{2+}, C-pH and D-RT)

c)
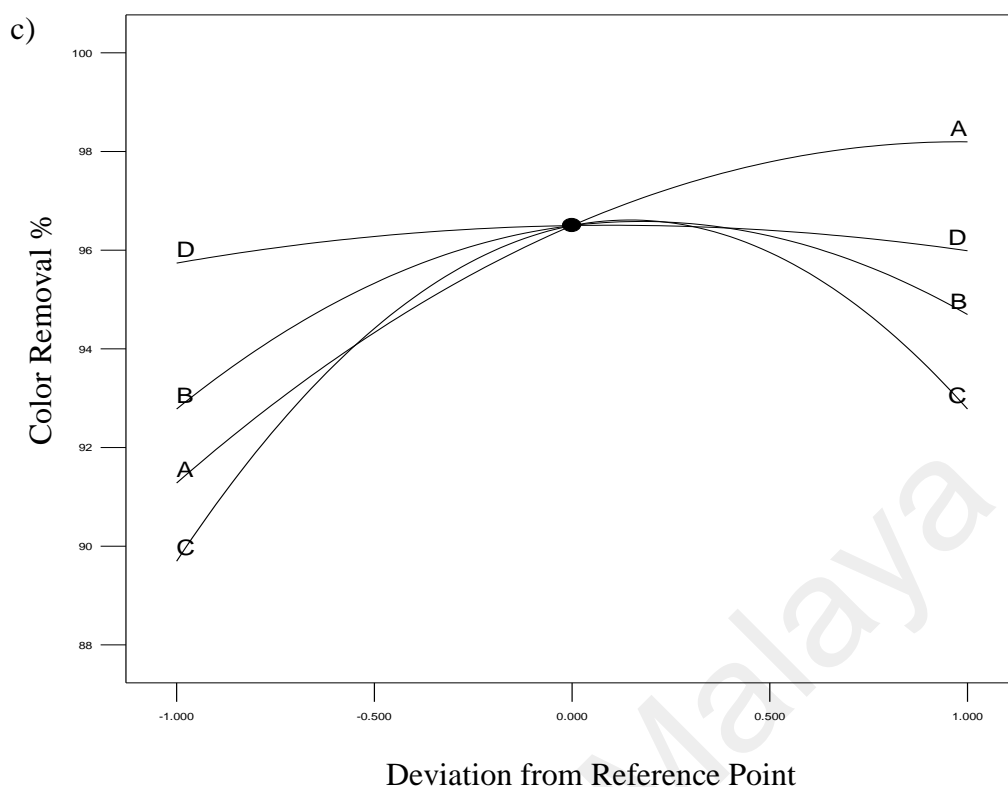
Figure 4.12: Continued

4.2.2 Effects of Operating Parameters on Color Removal Efficiency

ADMI Color (American Dye Manufacturer's Institute) metric is used to quantify the residual color of the batik wastewater in this study. It was observed that decolorization was very efficient through the Fenton process in real wastewater with the removal efficiency between 73% and 98% which is in accordance with reported values (Asghar et al., 2014; Youssef et al., 2016) and preliminary investigation conducted using RBB dyes in this study. Rapid decolorization (within 5 minutes) was observed in most of the experimental runs right after the Fenton reagent was added to the wastewater. The dark blue wastewater turned pale yellow and colorless after the filtration process. The pale yellow color was caused by the intermediates that destroyed the chromophore, which is responsible for the color of wastewater. Color removal during the Fenton process results from destruction of dyestuffs by $HO \bullet$ radical formed during the Fenton reaction or from

coagulation by Fe^{3+}(Balcioglu et al., 2001). Although almost a complete color removal was observed, the low COD and TOC removal percentages showed that it was difficult to destroy aromatic compounds or other functional groups contributing to the recalcitrant nature of the wastewater. Additionally chemical analyses such as GC/MS, FTIR, HPLC were carried out to investigate the organic contaminants in the wastewater.

Figure 4.13, 4.15 and 4.16 shows the 3D and 2D response surface plots representing the color removal efficiencies as a function of the ratio of H_2O_2:COD and H_2O_2:Fe^{2+}, H_2O_2:COD and pH, and H_2O_2:Fe^{2+} and initial pH of the wastewater. Figure 4.13 shows that color removal increased from 86.0to 98.4 % with an increased ratio of H_2O_2:COD from 1 to 12 at a minimum mass ratio of H_2O_2:Fe^{2+}. However, a further increase in the ratio of H_2O_2:COD and H_2O_2:Fe^{2+} beyond the optimum region resulted in insignificant changes in color removal efficiency as can be seen result presented in Table 4.8. Since excessive $HO\bullet$ radical in the system will be converted to hydroxyl ions and cause the precipitation of Fe^{3+} ions, the amount of Fe^{2+} was reduced, leading to decreased color removal (Karthikeyan et al., 2011). This result is supported by Bennatti and others (2006) (Benatti et al., 2006) who reported that the color removal efficiency of chemical laboratory wastewater was inversely proportional to the ratio of H_2O_2:Fe^{2+}.

Moreover, at constant retention time and ratio of H_2O_2:COD, an increase in color removal was observed with an increased ratio of H_2O_2:Fe^{2+} and initial pH of the solution. Figure 4.14 shows that the optimum pH for color removal (96.3 %) was approximately at pH 5.5 and the mass ratio of H_2O_2:Fe^{2+}= 7.2, beyond which, there was decreased decolorization. The wastewater pH is very important as it's determined the level of $HO\cdot$generation and concentration of Fe^{2+} salts. The results supported the fact that decomposition of H_2O_2 rapidly increases at pH above 6.5. The results showed that the color removal efficiency was significantly higher in weak acidic conditions compared to weak alkaline solutions.

The oxidation rate of the Fenton process is decreased at pH higher than 6, which is due to the precipitation of Fe^{3+} to ferric hydro complexes (Asghar et al., 2014). These findings are consistent with the results reported by other researchers (Bautista et al., 2007; Deng et al., 2006; Ghaly et al., 2001; Y. S. Jung et al., 2009)

Besides, increasing the ratio of $H_2O_2:Fe^{2+}$ from 2.0 to 7.2, and initial pH from 2 to 6, at a constant ratio of $H_2O_2:COD$ increased the color removal efficiency (Figure 4.16). However, a decrease in the efficiency was observed above the optimal value for both the $H_2O_2:Fe^{2+}$ and initial pH. This is because at constant $H_2O_2:COD$ ratio, increase in the ratio of $H_2O_2:Fe^{2+}$ contributed to the reduction in the concentration of Fe^{2+}. The color removal rate is declined because there was insufficient Fe^{2+} to react with H_2O_2 to generate $HO\bullet$ radical in the system. The observation was made where an immediate color change of the wastewater samples and formation of small flocs at pH higher than 5 with the addition of ferrous salt occurred. This clearly proved that coagulation has taken place. In conclusion, the favorable result obtained in this study proved the efficiency of Fenton process to decolorize synthetic dye solution as well as real textile wastewater.
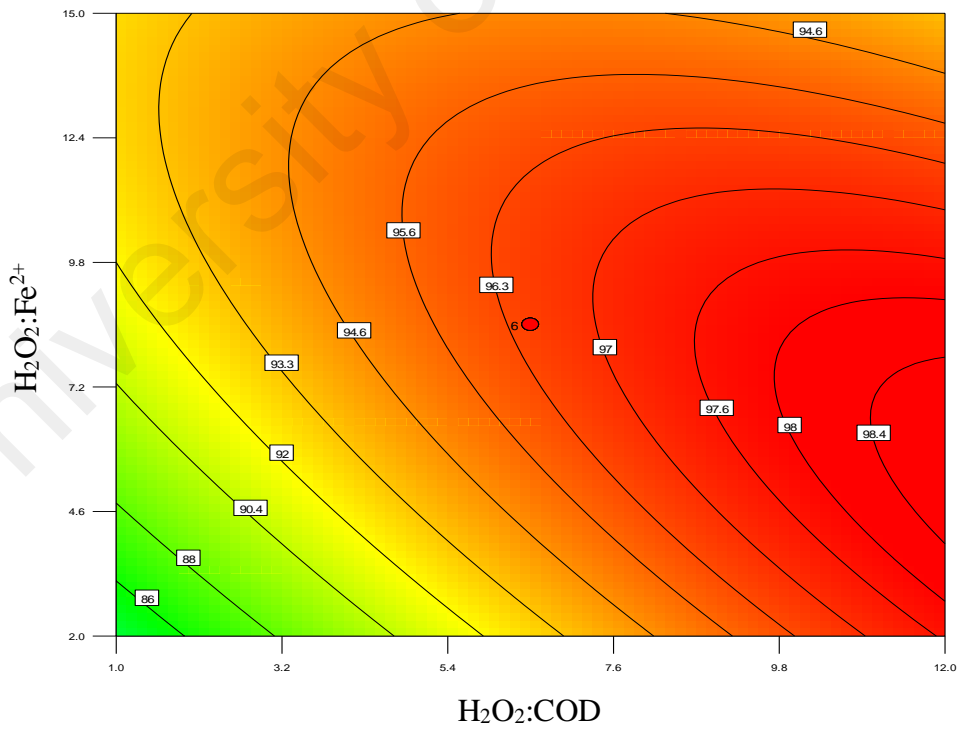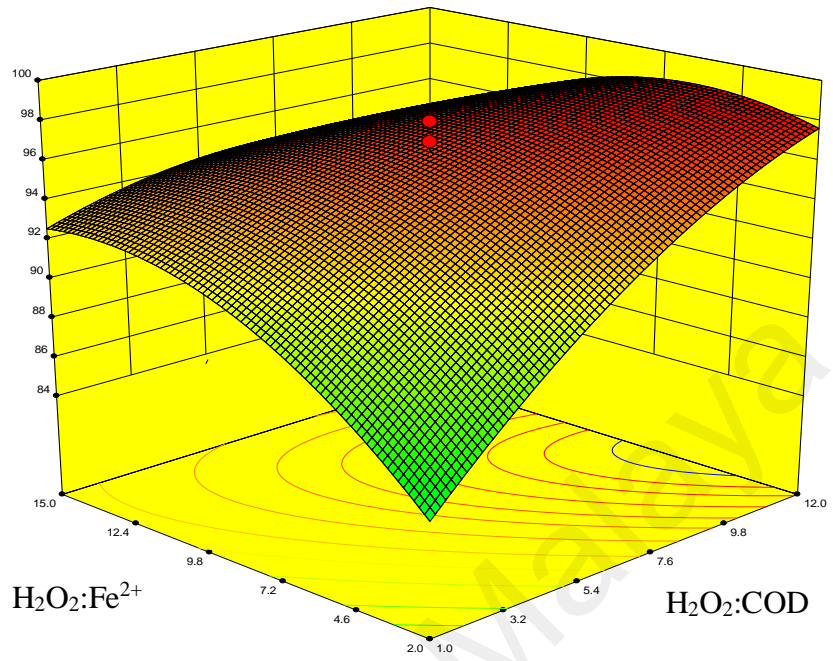
Figure 4.13: Response surface and contour for color removal percentage as a function of $H_2O_2:Fe^2$ and $H_2O_2:COD$ (Initial pH= 5.5, Retention time= 60 min)
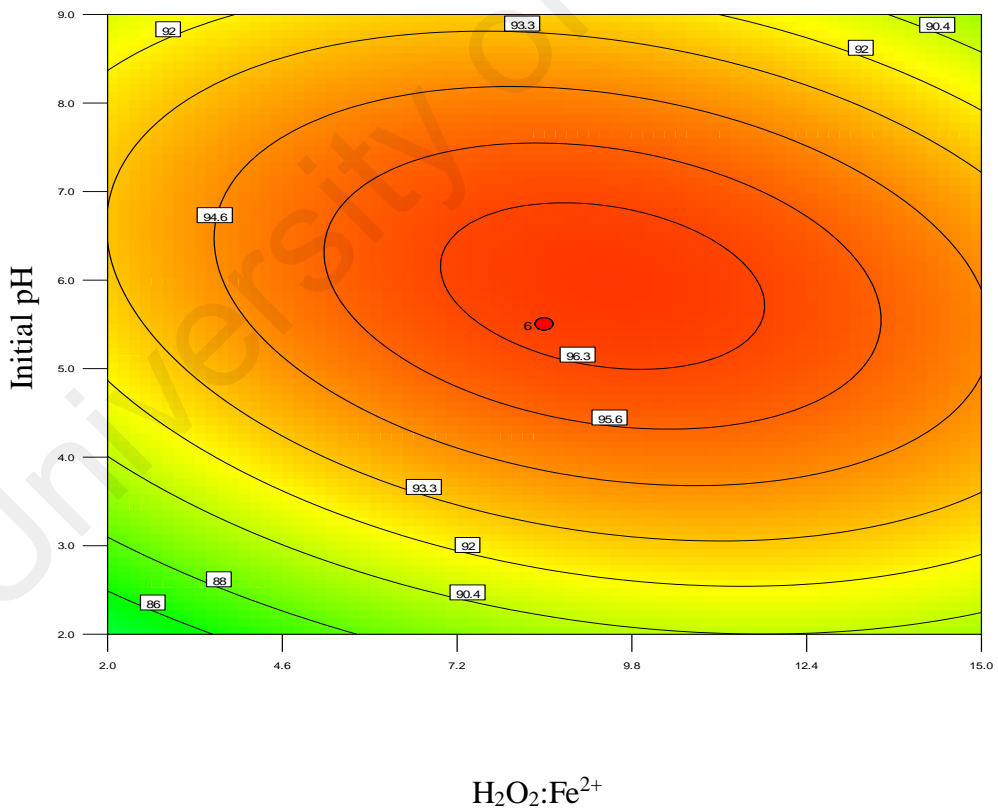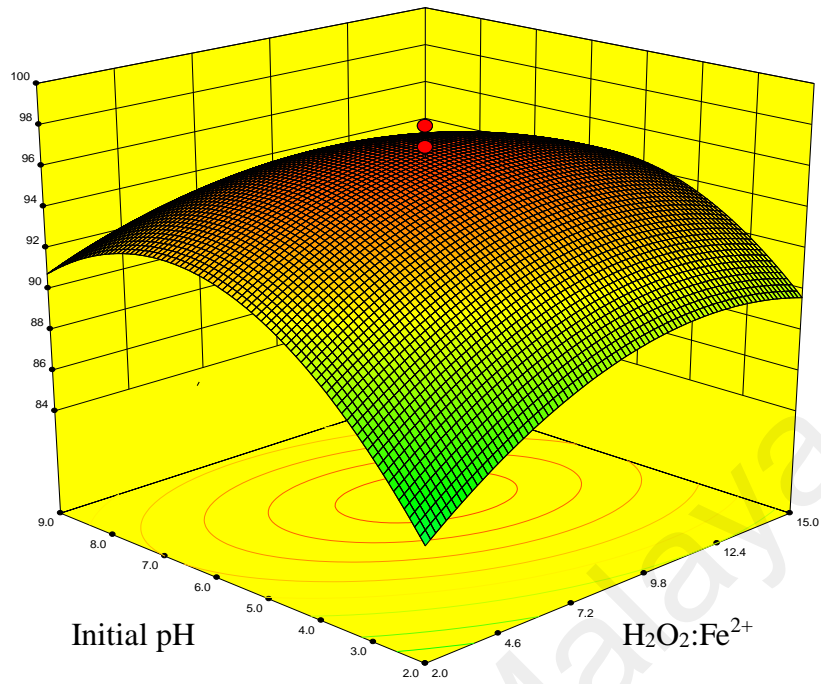
Figure 4.14: Response surface and contour for color removal percentage as a function of $H_2O_2:Fe^{2+}$ and initial pH ($H_2O_2:COD = 6.5$, Retention time= 60 min)
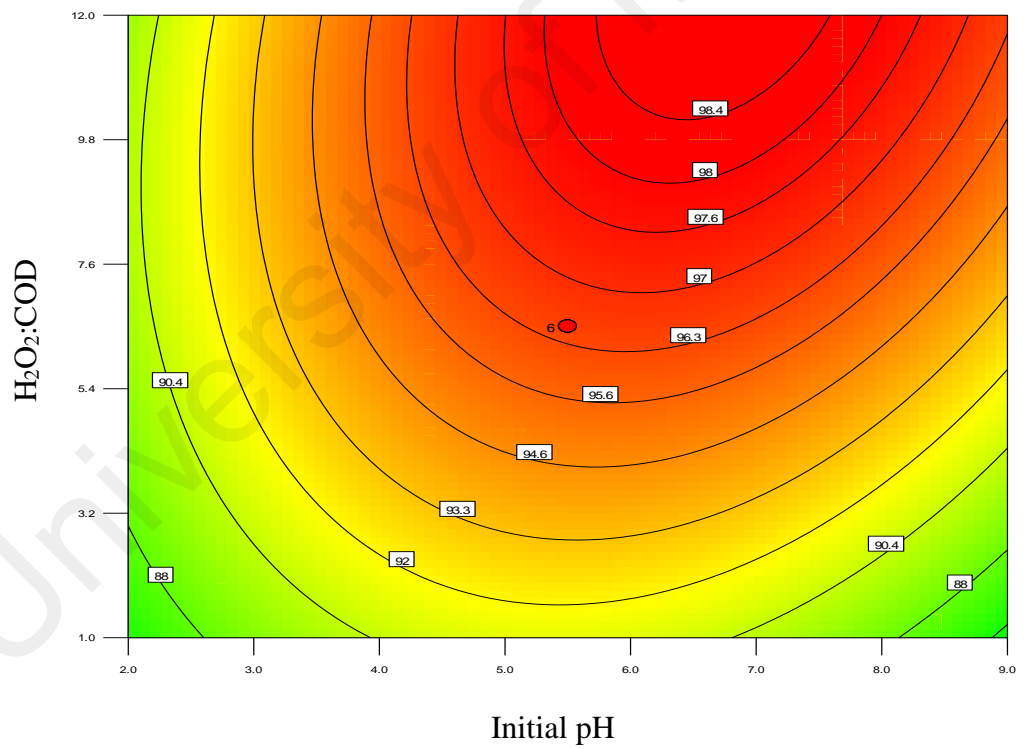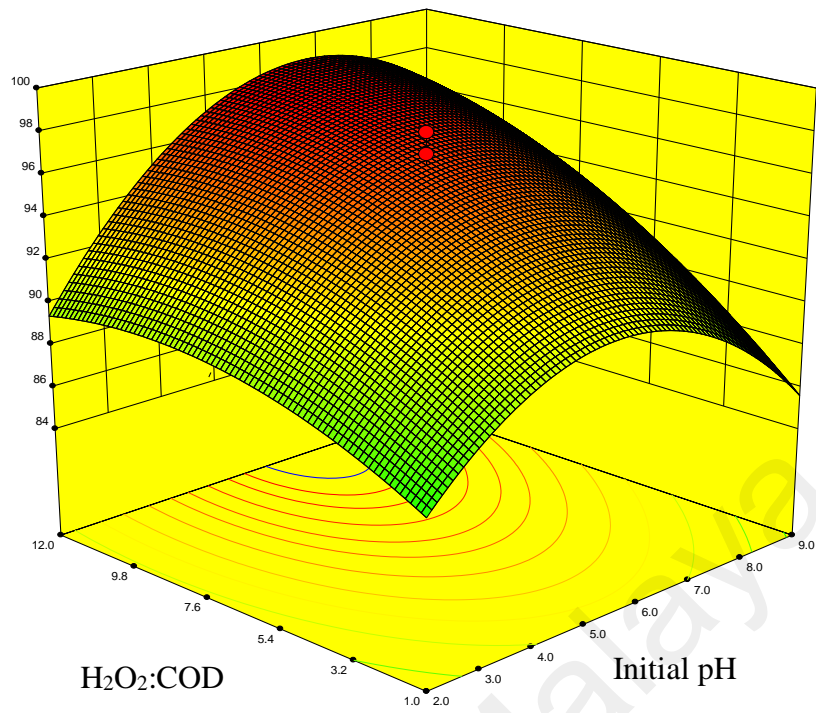
Figure 4.15: Response surface and contour for color removal percentage as a function of H_2O_2:COD and initial pH (H_2O_2:Fe^{2+} = 8.5, Retention time = 60 min)

4.2.3   Effect of Operating Parameters on COD and TOC removal Efficiencies

Since the removal percentage of COD and TOC follow the similar trend, the effects of the mass ratio of H_2O_2: COD and H_2O_2: Fe^{2+}, initial pH of the solution, retention time on COD and TOC removal efficiencies were discussed the following section.

4.2.3.1 Effects of Mass Ratios of H_2O_2:COD on COD and TOC Removals

In this context, the minimum and maximum ratios of H_2O_2:COD were chosen based on the previous studies reported in the literature   and preliminary experiments were also conducted to identify the suitable range to avoid excessive usage of oxidants. Raw textile wastewater with initial $[COD]_i$ of 1610– 1900 mg/l was used and it was kept constant throughout the Fenton oxidation process. Based on the second-order polynomial equation, it could be concluded that the key factor that contributed to the reduction of COD and TOC was the initial ratio of H_2O_2: COD. According to Karthikeyan and others (2011), the concentration of H_2O_2 played an influential in enhancing the degradation efficiency, but may cause scavenging or recombination of $HO\bullet$ radicals when present excessively as stated earlier (Pignatello et al., 2006; C. Walling et al., 1973). Therefore, it is important to optimize the dosage of H_2O_2 to generate a sufficient amount of $HO\bullet$ radicals in each operating system as the concentration of H_2O_2 required to complete the degradation varied with the initial COD of the samples.

Figure 4.16 shows the response surface analysis and contour between the mass ratios of H_2O_2: COD and H_2O_2: Fe^{2+} on the COD and TOC removal efficiencies. Removal of COD increased with an increase in the mass ratio of H_2O_2:COD. At the fixed COD value of 1610 mg/l and the mass ratio of H_2O_2:Fe^{2+} of 2, the final COD removal efficiency increased from 71.7 % to 85.0% at a retention time of 60 min when the mass ratio of H_2O_2:COD increased from 1 to 15. The increase in the removal efficiency was due to the increase in the $HO\bullet$ radical concentration as a result of the addition of H_2O_2 (Ting et al.,

2009). However, at a constant mass ratio of H_2O_2: COD, an increase in the mass ratio of H_2O_2: Fe^{2+} from 2 to 18 reduced the COD removal efficiency from 85% to 57.6%. It was because there was an insufficient amount of ferrous salts that was available in the system. Increasing the mass ratio of H_2O_2: Fe^{2+} at fixed COD and H_2O_2 dosage reduced the amount of Fe^{2+} to be catalyzed by hydrogen peroxide to produce $HO\bullet$ radical (Eq. (14)). This result was similar to the findings presented by Gulkaya and others (2006) (Gulkaya et al., 2006). This was agreeable since the developed polynomial model also showed that both ratios exhibited a negative interaction.

The highest COD reduction of 85 % was obtained at H_2O_2:COD=11 and H_2O_2:Fe^{2+}=2 at a center value of initial pH 5.5 and retention time of 60 min. But, decreases in the efficiency was observed when the ratio of H_2O_2:Fe^{2+} was less than 2 and H_2O_2:COD was above 12 (refer to Table 4.8). Moreover, the unfavourable effect in the COD removal was observed when a higher concentration of H_2O_2 was used. Self-scavenging of $HO\bullet$ radical caused by excessive amount of H_2O_2 contributed to this condition (M. Lucas et al., 2006; X. R. Xu et al., 2004). This means that insufficient or excess H_2O_2 and Fe^{2+} reduced the efficiency of $HO\bullet$ radical to oxidize the contaminants. Zhang and others (2007) also reported that the removal efficiency of organic materials in the leachate wastewater decreased with increased Fenton reagent dosage beyond an optimal value (H. Zhang et al., 2007). Therefore, based on the result obtained in this study it is suggested to keep the ratio lower than 11 and lower H_2O_2 concentration is also more economically viable compared to higher H_2O_2 concentration. The TOC removal percentage showed the similar trend as the COD removal efficiency with the highest mineralization of 70% observed at H_2O_2:COD =10. Besides, the TOC removal efficiency was found to decrease when the ratio increased above 12, as shown in Figure 4.16.

a) COD Removal %
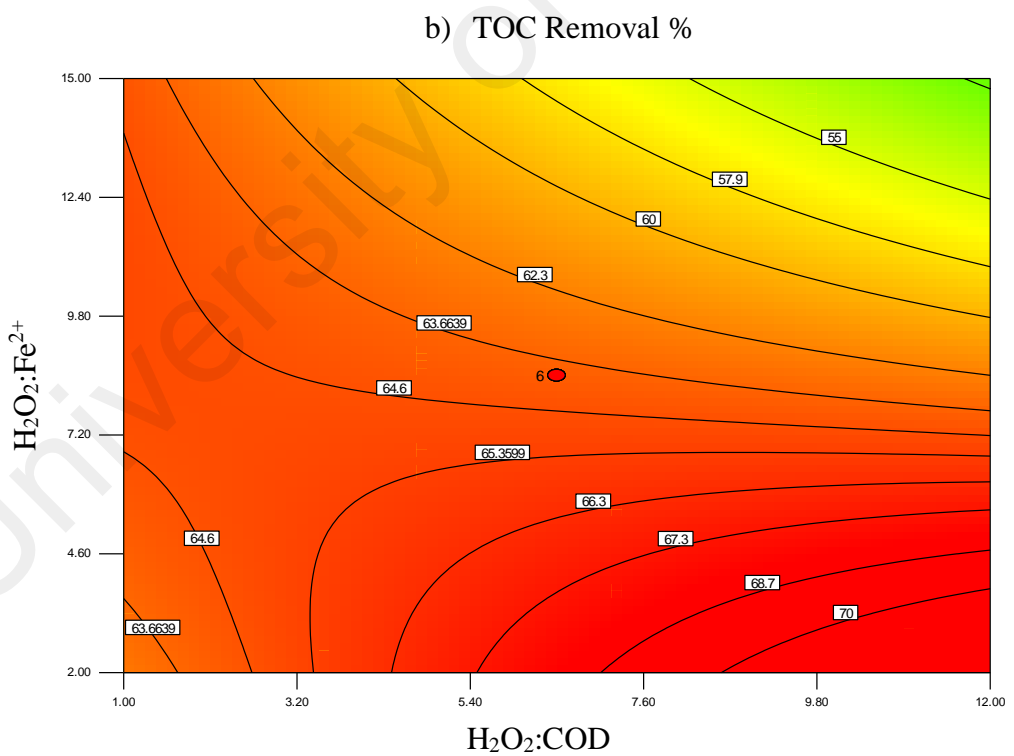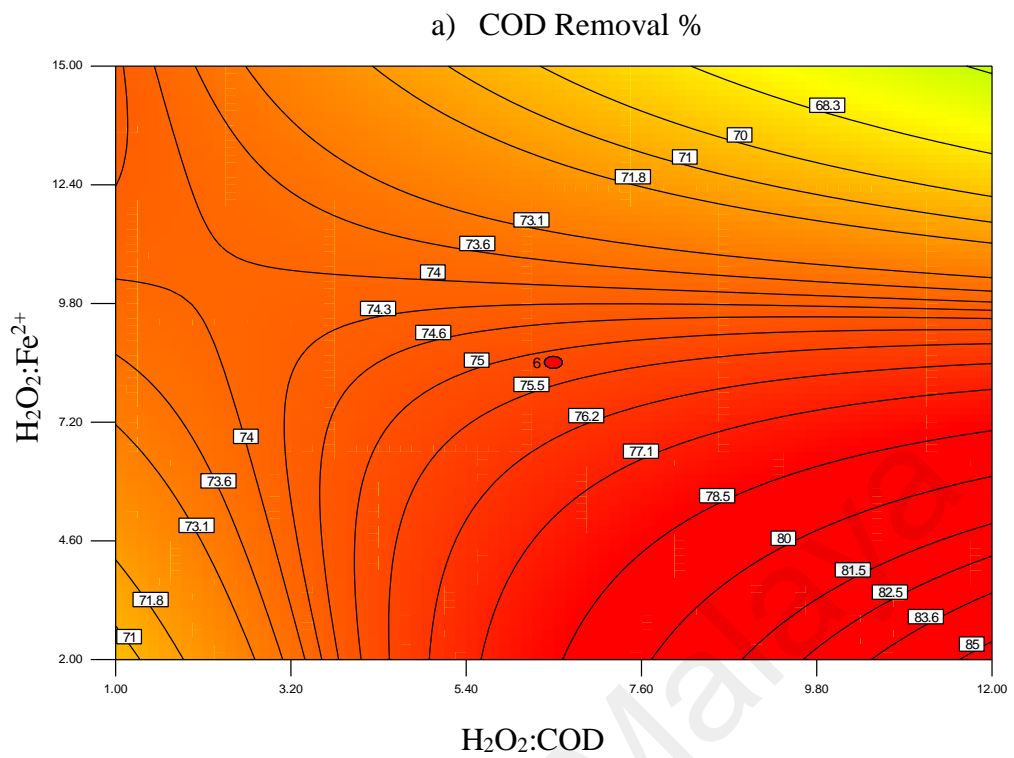
b) TOC Removal %

Figure 4.16: Contour for percent COD and TOC removals as a function of mass ratios of $H_2O_2:COD$ and $H_2O_2:Fe^{2+}$ at pH of 5.5 and retention time of 60 min

4.2.3.2 Effects of Mass Ratio of H_2O_2:Fe^{2+} on COD and TOC Removals

In this study, the mass ratio of H_2O_2: Fe^{2+} was varied from 2-15 to investigate the effect of Fe^{2+} concentration on COD removal efficiency. The results showed that the COD removal efficiency significantly increased with increased mass ratio of H_2O_2:Fe^{2+} from 2 to 11.6 and then decreased when the ratio was above 12. At a fixed H_2O_2:COD value, an increase in H_2O_2:Fe^{2+} did not affect H_2O_2 but reduced the amount of Fe^{2+}. Therefore, the oxidation process became catalyst deficient, which reduced the removal efficiency. On the other hand, there was a direct relation between the H_2O_2:COD ratio and COD removal efficiency whilst an inverse trend was observed between the H_2O_2: Fe^{2+} and COD removal An improvement in the COD removal efficiency was observed with an increase in the H_2O_2:COD ratio whereby the amount of oxidant (H_2O_2) available in the reaction medium was increased, hence, increasing the efficiency of the Fenton process.

Figure 4.16 (a) shows that the COD removal efficiency was the lowest (71- 74%) in the ratio range of 1-3 and an increase in the ratio of H_2O_2: COD significantly improved the removal efficiency. The COD removal percentage markedly increased from 71% to 85% by externally adding Fe^{2+} and H_2O_2 at the fixed initial pH of 5.5. Figure 4.16 shows that the COD removal efficiency increased dramatically when the mass ratio of H_2O_2:Fe^{2+} increased from 2- 11. However, based on the initial rates, the scavenging of $HO\bullet$ radical was present when the initial mass ratio of H_2O_2:Fe^{2+} increased above 11.6. This is due to limited Fe^{2+} in the system to catalyze excessive $HO\bullet$ radicals that were present. It contributed to the scavenging effects, as reported by (Bouafia-Chergui et al., 2010). The results prove that higher concentration of Fe^{2+} or H_2O_2 did not increase the efficiency of the Fenton process. The similar trends were observed for TOC removals can be seen in Figure 4.16 (b).

Moreover, the interaction effect between the initial pH and mass ratio of H_2O_2:COD and H_2O_2:Fe^{2+} at a fixed retention time of 60 min was also evaluated in this study. It was observed that there were significant changes in the removal efficiency when we used different initial pH values (2, 5.5, 9 and 12). Figure 4.17 shows that the removal efficiency decreased from 85 % to 76.1% and 53.1 % when the initial pH was changed to 9 and 12, respectively from 5.5 (which is a central point used to study the effect of H_2O_2:COD and H_2O_2:Fe^{2+}). A further reduction in the removal efficiency (79.1 %) was observed when the initial pH of 2 was used in the system. This showed that there was a strong interaction between the dosage of the Fenton reagent and the initial pH of the pollutant. The following section discusses the effects of initial pH and mass ratios of H_2O_2:COD and H_2O_2:Fe^{2+} on COD and TOC removal efficiencies.
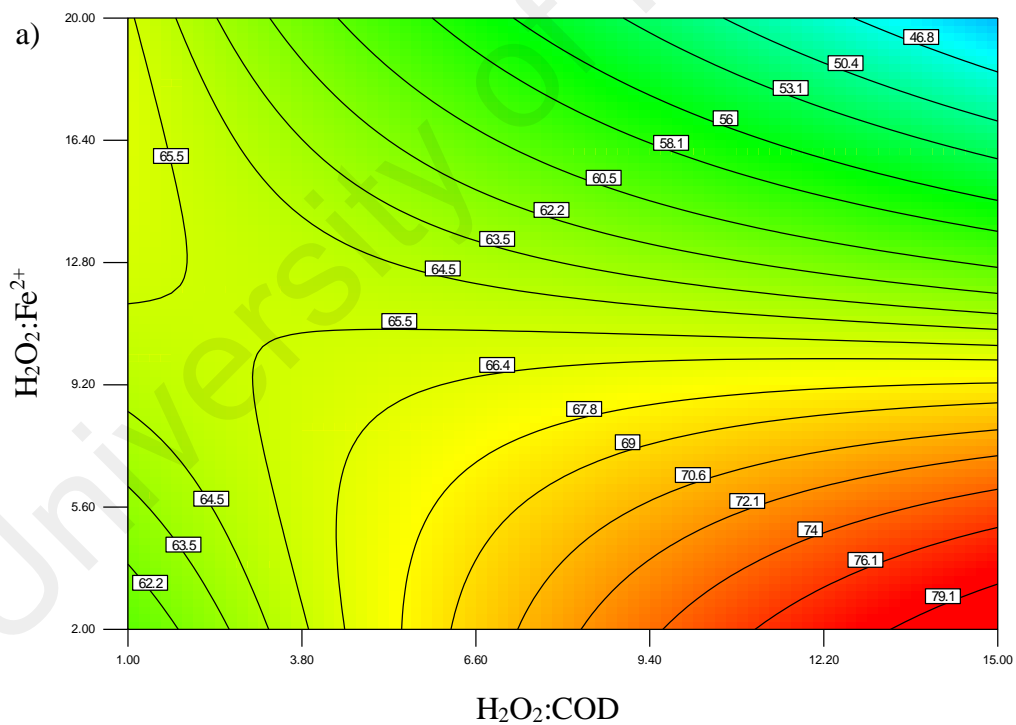
Figure 4.17: Contour graph for the COD removal percentage as a function of H_2O_2:COD and H_2O_2:Fe^{2+} at different initial pH (a) pH=2, (b) pH=9 (c) pH=12

b)

c)
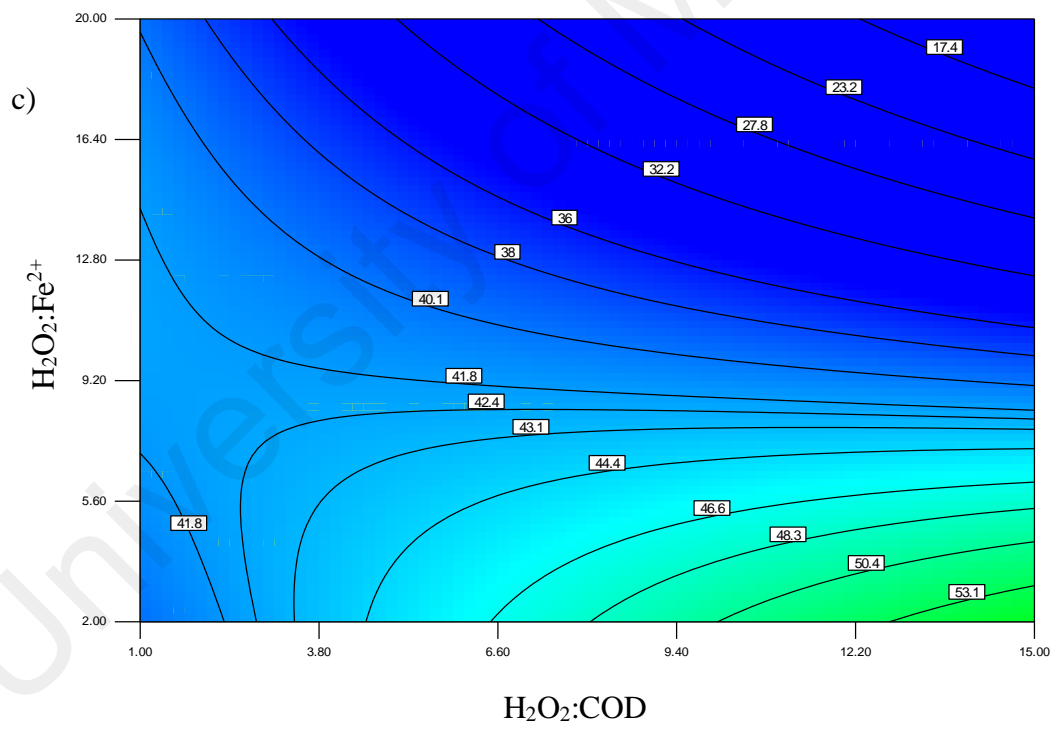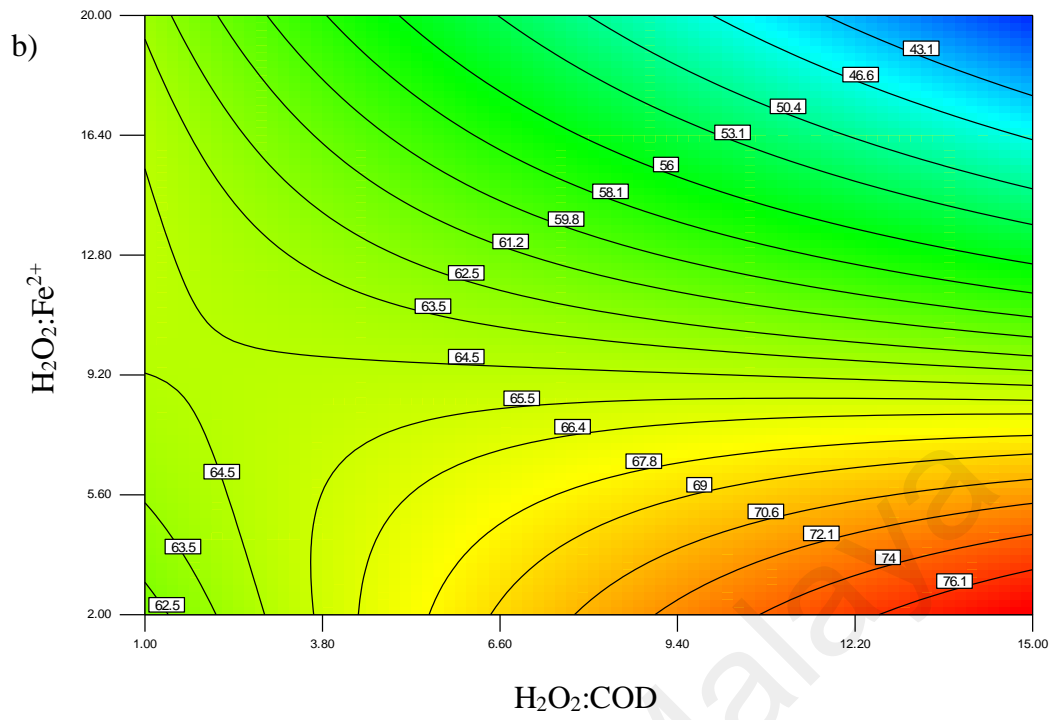
Figure 4.17: Continued

4.2.3.3 Effects of Initial pH on COD and TOC removals

The initial pH of the reaction medium is one of the variables that crucially affect the treatment efficiency of the Fenton process. Most of the studies have reported that the optimum pH for the Fenton reaction is around 3 (Bagal et al., 2014; Hrvoje Kusic et al., 2006). At higher pH, ferric ions form $Fe(OH)_3$, which reacts slowly with hydrogen peroxide (Babuponnusami et al., 2013). This process may reduce the efficiency of a Fenton process, as a less ferric ion is present to react with hydrogen peroxide to generate $HO \bullet$ radical. Moreover, auto-decomposition of hydrogen peroxide accelerates at higher pH. At very low pH, iron complex, $[Fe(H_2O)_6]^{2+}$ is present and it reacts with hydrogen peroxide in the solution. This reduces the amount of ferrous ion present in the solution (Navarro et al., 2010). In addition, at very low pH, H_2O_2 forms stable oxonium ions $[H_3O_2]^+$ that are stable and less reactive compared to $HO \bullet$ radical, reducing its efficiency in oxidizing the pollutants (Gogate et al., 2004a). In this study, the initial pH was varied from 2–9 to study the effects of initial pH of the solution on the degradation efficiency of real textile wastewater.

Figure 4.18 shows the semi-spherical response surface that explains the effects of initial pH of the solution on the COD and TOC removal efficiencies. The plot shows that the COD and TOC removal efficiencies increased with the initial pH of the solution from 2-5 but the efficiency decreased slightly above pH 6. The maximum COD and TOC removals were determined to be 76.0 % and 64.6 %, respectively. The removal efficiency was reportedly decreased to 67.1 % and 55.0 % when the pH was increased above 7 at a mass ratio of H_2O_2:Fe^{2+} =8.5, as illustrated in Figure 4.18. At the optimum condition, H_2O_2 was converted rapidly to hydroxyl free radicals that could non-selectively decompose these pollutants in the Batik wastewater.

Moreover, an increase in the ratio of H_2O_2:Fe^{2+} from 2- 15 at the lowest initial pH of 2 and fixed mass ratios of H_2O_2:COD= 6.5 caused a steady reduction in the removal efficiency of COD from 77.3 % to 63.9 %, as shown in Figure 4.18. This may be due to the scavenging of hydroxyl caused by ferrous ion (Eq. (8)) (Chakma et al.). Moreover, increasing the mass ratios of H_2O_2:Fe^{2+} above 15 caused a drastic change in the removal efficiency, whereby only 56.0% and 42.8% removals were achieved at the mass ratio of H_2O_2:Fe^{2+} of 20 and 30, respectively as can be seen in Figure 4.19 (a, b and c). It was proven that the dosage of Fe^{2+} and H_2O_2 had a strong interaction with the initial pH of the solution. I n conclusion, the result showed that the oxidation was more active in acidic conditions while alkaline conditions favored the coagulation process.
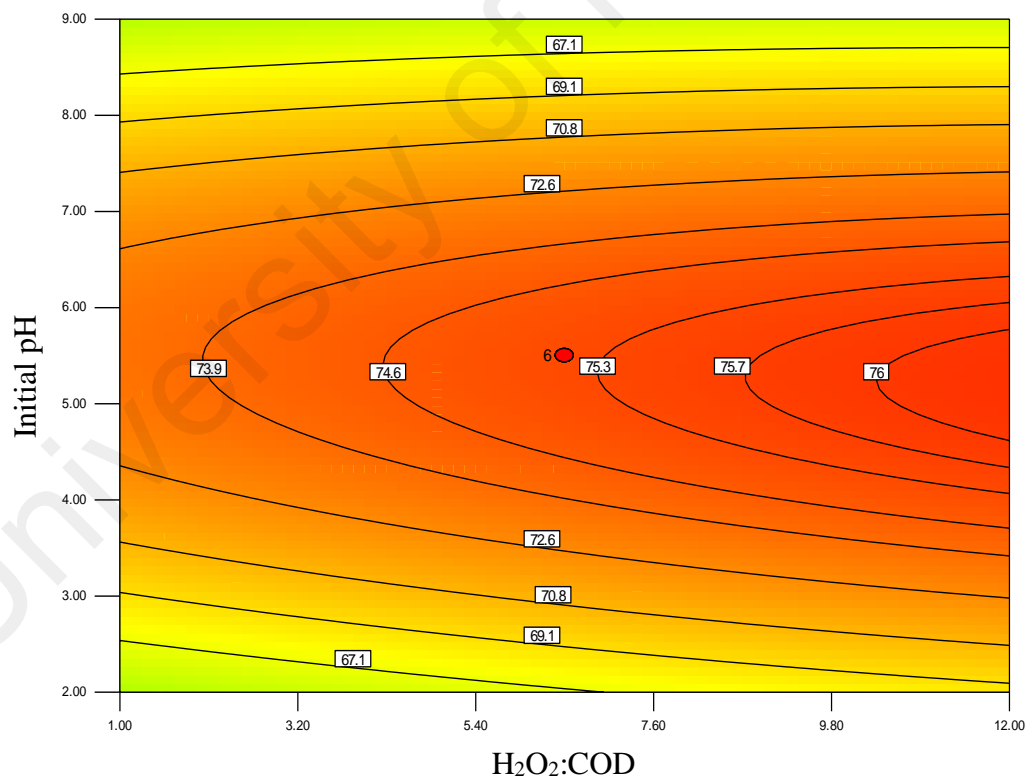
Figure 4. 18: a) Response surface contour for COD removal as a function of H_2O_2:COD and initial pH
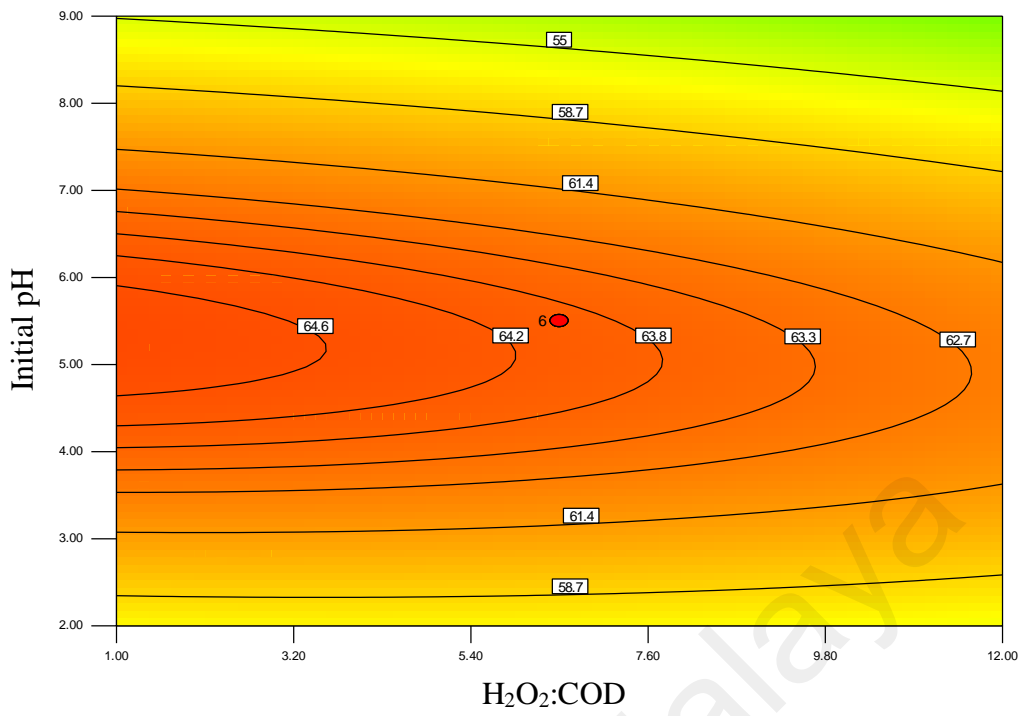
Figure 4.18: b) Response surface contour for TOC removal as a function of H_2O_2:COD and initial pH
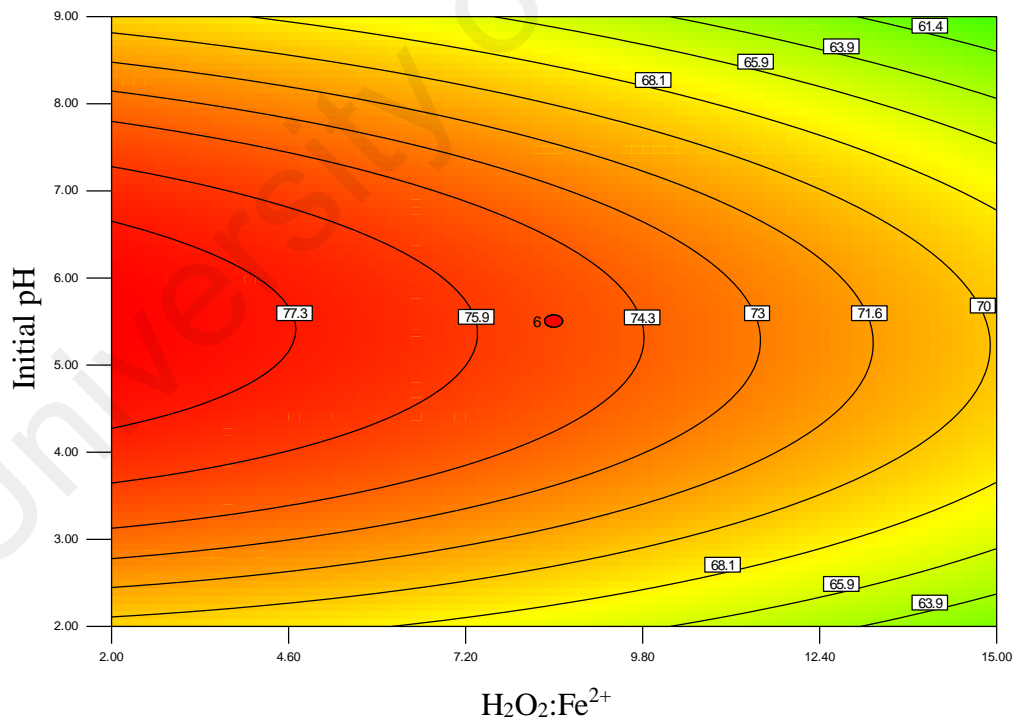
Figure 4.19: Response surface contour for COD removal as a function of H_2O_2:Fe^{2+} and initial pH of the solution (Retention Time: 60 Min)
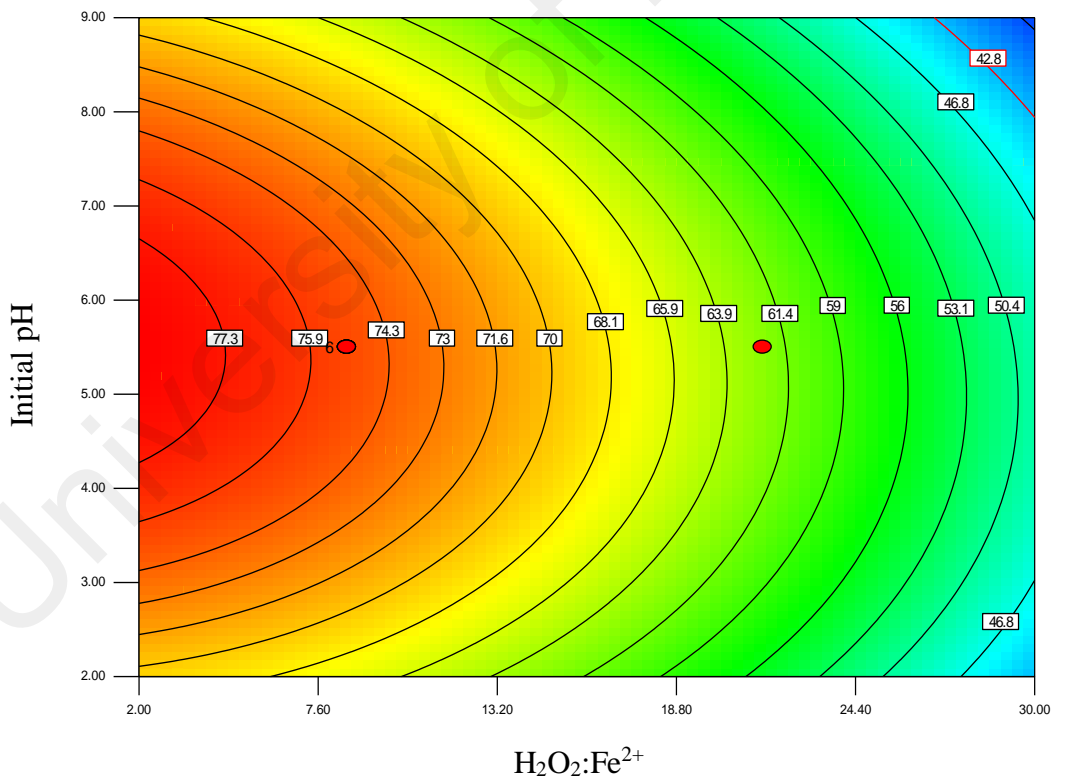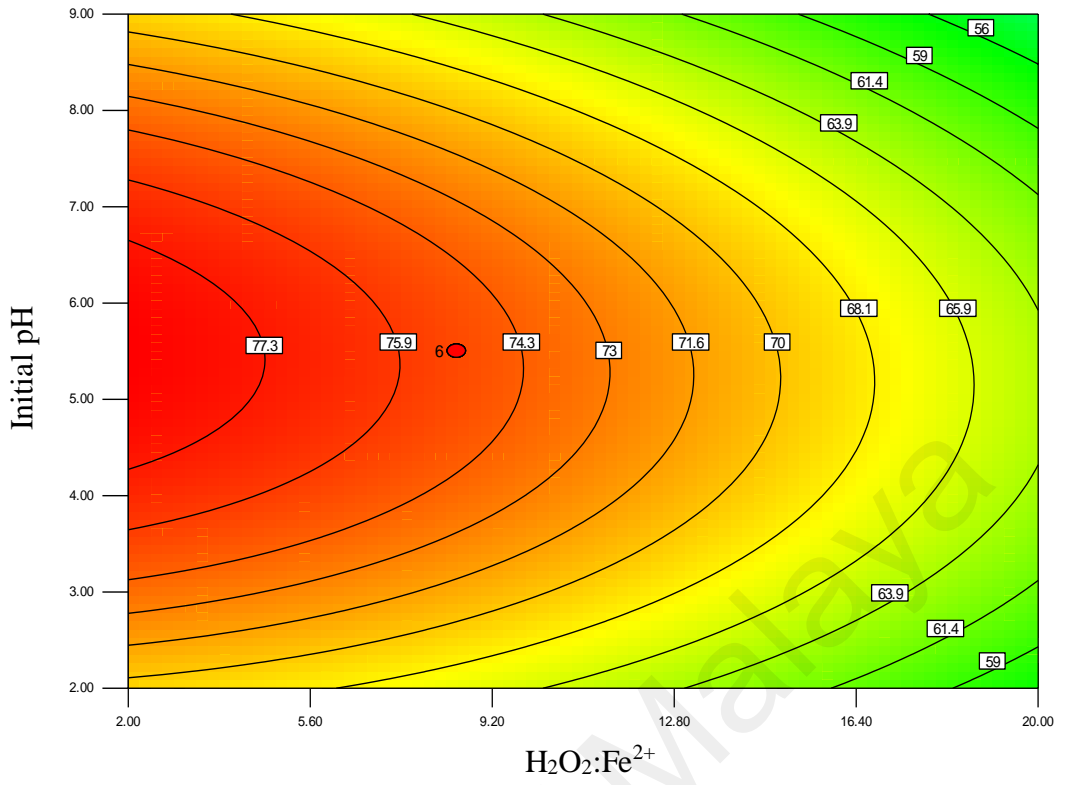
Figure 4.19: Continued

4.2.3.4 Effects of Retention Time on COD and TOC removals

Retention time is another parameter that affects the rate of organic contaminant removal in the Fenton process. The organic matters in wastewater cannot react with the Fenton's reagents completely when the retention time is too short. But, if the retention time is beyond the optimal point, organic pollutants tend to form more toxic intermediates, which will reduce the treatment efficiency. In addition, longer retention time also requires a larger reactor and increases the cost of the process. Therefore, it is important to ascertain the appropriate retention time to increase the treatment efficiency. Therefore, experiments were carried out at different retention times to obtain the appropriate oxidation time of the Fenton process for the batik wastewater.

Figure 4.20 shows the interaction between the mass ratio of H_2O_2:Fe^{2+} and retention time for the COD and TOC removals at the fixed mass ratios of H_2O_2:COD= 6.5 and initial pH of 5.5. It was observed that the COD removal efficiency increased with retention time. The maximum COD (77.9%) and TOC (67.3 %) removals were achieved at pH 5.5, mass ratio of H_2O_2:COD= 6.5, H_2O_2:Fe^{2+} = 2 at around 52 minutes. When the retention time increased beyond the optimal point, the COD and TOC removals were reduced to 67.1% and 52.5% respectively. A drop in the removal efficiency might be caused by longer treatment time that contributed to the formation of toxic intermediates or scavenging caused by excessive $HO\bullet$ radicals and iron salts. The result indicated that there should be an optimized oxidation time.

In addition, the interactions between the retention time and mass ratios of H_2O_2:Fe^{2+} and H_2O_2:COD were also evaluated in this study. When the H_2O_2:COD mass ratio was increased from 12 to 24 and 36, a significant decrease in the COD removal (to 61.4 %) was observed, as shown in Figure 4.21. This indicated that longer retention time and

excessive hydroxyl in the system might cause the formation of intermediates, which increased the toxicity level of the wastewater.
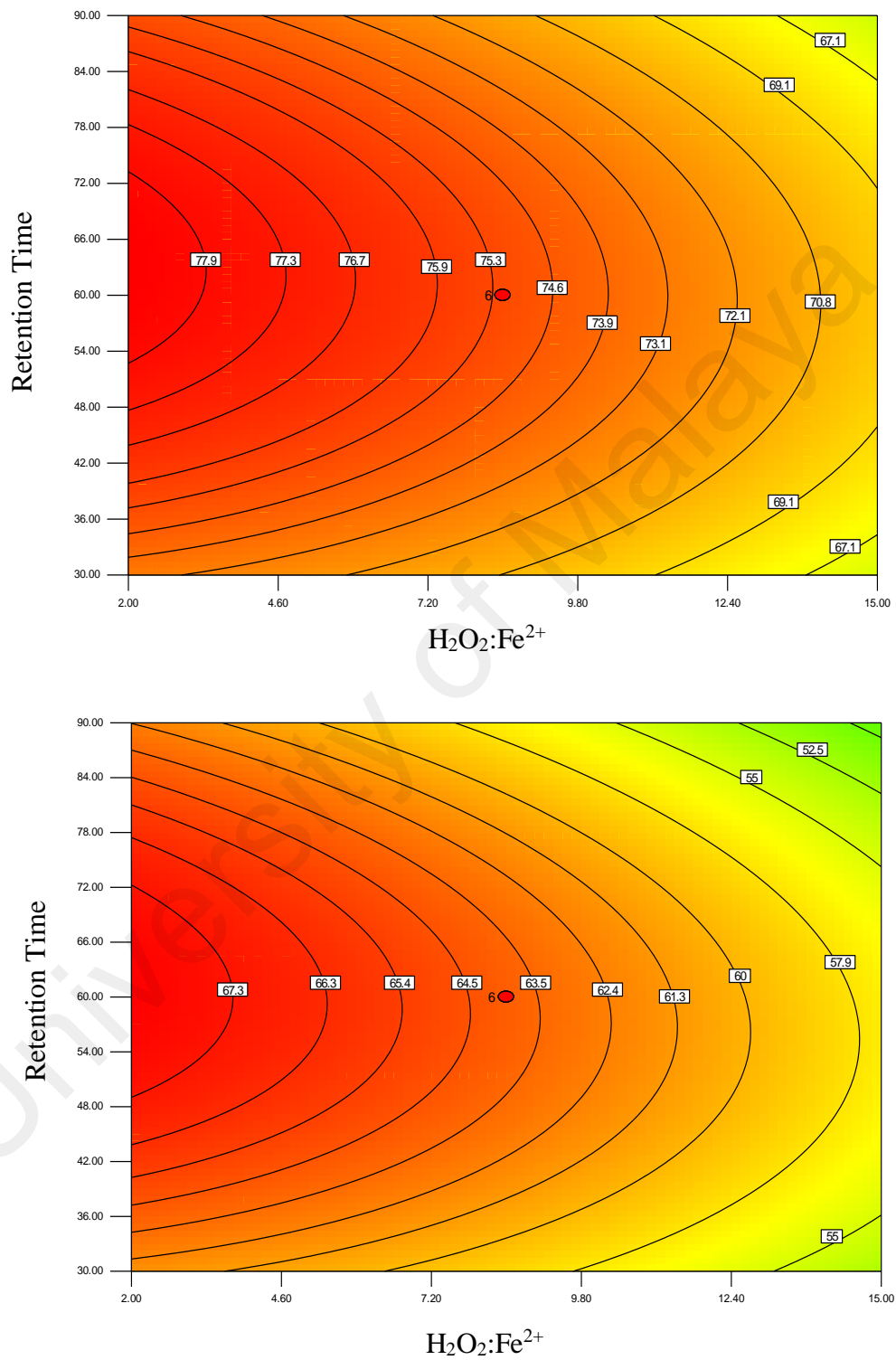
Figure 4.20: Response surface contour for percent COD and TOC removal as a function of $H_2O_2:Fe^{2+}$ and Retention time
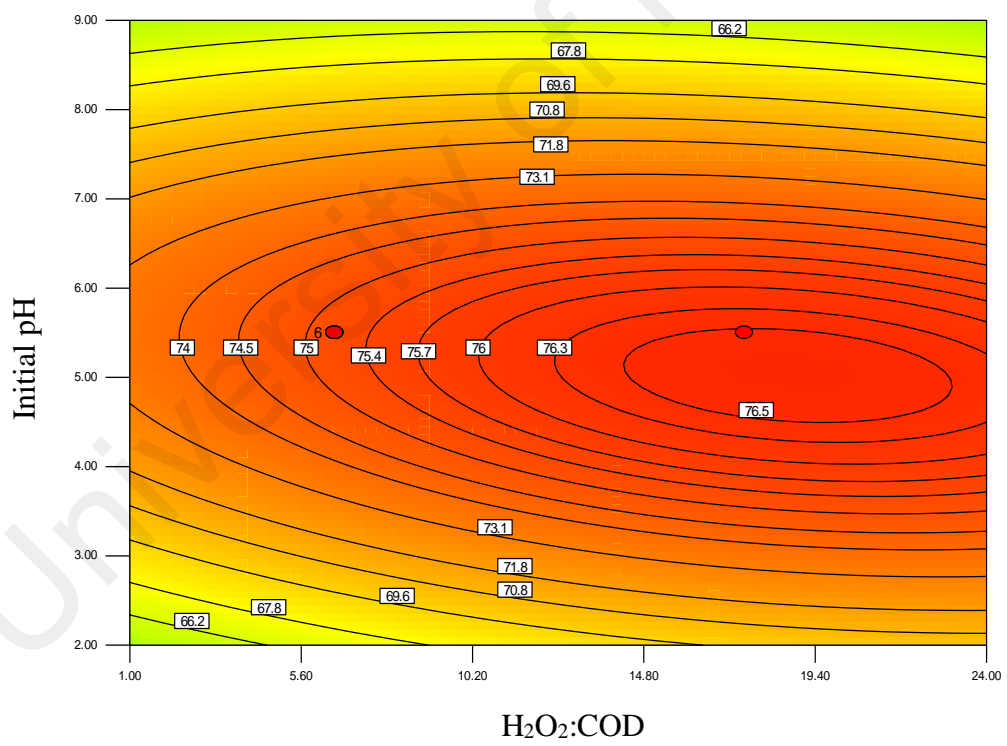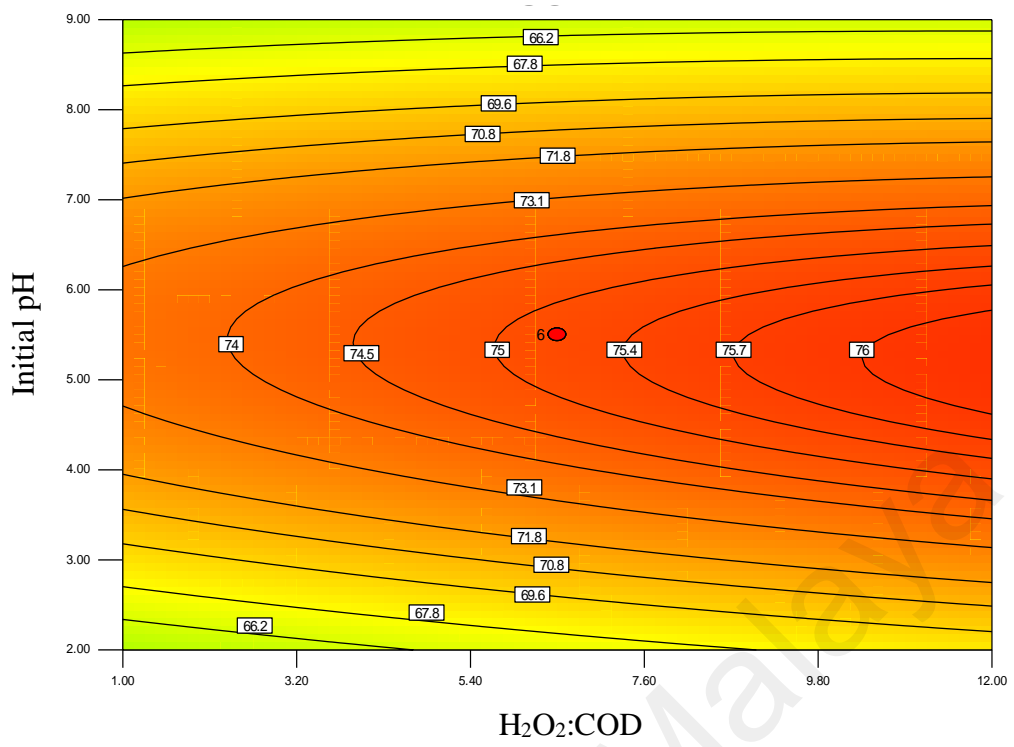
Figure 4.21: Response surface contour for percent of COD removal as a function of H$_2$O$_2$:COD and Retention time
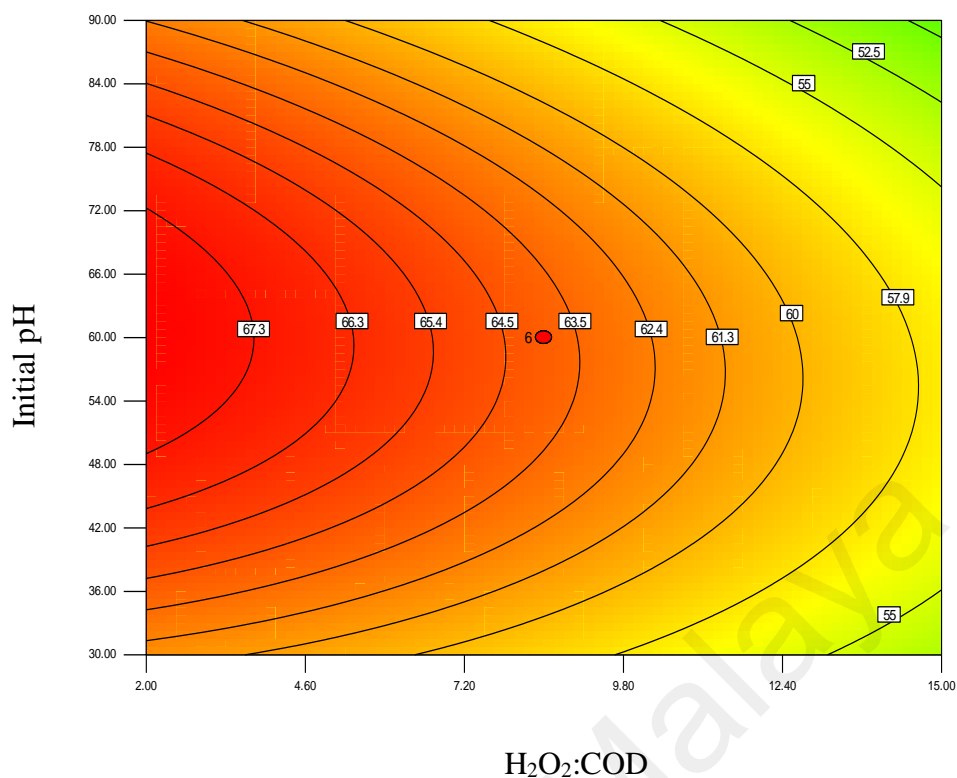
Figure 4.21: Continued

4.2.4 Model Validation and Confirmation of Optimized Conditions

It is possible to decide specific working conditions such as maximizing the responses or keeping them in the desired range by using RSM if multiple responses are applied. In the present study, the desired goals in terms of color, COD and TOC removal efficiencies were defined as "maximize" to achieve the highest removal efficiency. However, the operating parameters, mass ratio of H_2O_2:COD and H_2O_2:Fe^{2+}, initial pH of the wastewater, and retention time were selected to be "in the range" without considering the operating (chemicals and electrical energy) costs. Accordingly, the optimum working conditions and the respective removal efficiencies were established for constant initial COD (mg/l). The results are presented in Table 4.11. A verification experiment was carried out using the optimum conditions to confirm the adequacy of the predicted model. The average maximum degradation, mineralization and color removals were obtained from three replicate experiments, shown in Table 4.11. For an initial wastewater's COD

of 1610 mg/L, the model predicted 96.6 % of color, 80.1 % of COD and 68.2% of TOC removals under the optimized working conditions. The good agreement between the predicted value and the experimental value confirmed the validity of the model for the Fenton process of the batik wastewater. The result obtained revealed that it was possible to save considerable time and effort for estimating the optimum working conditions to achieve the highest treatment efficiencies by using RSM-based CCD.

Table 4.11 Optimum value of the process parameters for constraint conditions and experimental values

Res. (Removal %)	COD (mg/l)	H_2O_2:COD	H_2O_2:Fe^{2+}	pH	RT	Pred.	Exp.
Color	1610	10.2	4.7	4.8	63.4	96.6	99.6
COD	1610	10.2	4.7	4.8	63.4	80.1	81.4
TOC	1610	10.2	4.7	4.8	63.4	68.2	70.5

* Desirability=1, CR= Color removal

4.2.5 Kinetic Study of the Treatment

The kinetic study is considered as an organic matter index for the COD value because of the complexity of the wastewater. In the present study, zero-, first- and second-order reaction kinetics were tested to investigate the degradation efficiency (COD removal) of the Batik wastewater by the Fenton oxidation process. The individual expression is presented below (Eq. (4.9 – 4.11)):

Zero order reaction as shown in Eq. 4.9:

$$\frac{d_c}{d_t} = -k_0 \qquad (4.9)$$

First order reaction as shown in Eq. 4.10:

$$\frac{d_c}{d_t} = -k_2 C \qquad\qquad\qquad (4.10)$$

Second order reaction as shown in Eq. 4.11:

$$\frac{d_C}{d_t} = -k_2 C^2 \qquad\qquad\qquad (4.11)$$

Where C is the COD of wastewater; k_0, k_1 and k_2 represent the apparent kinetic rate constants of zero, first and second-order reaction kinetics, respectively; and t is the reaction time. By integrating Equation (4.9)–(4.11), the following equations can be obtained (Eq. (4.12)–(4.14)):

$$c_t = c_0 - k_0 \, t \qquad\qquad\qquad (4.12)$$

$$c_t = c_0 e^{-k1t} \qquad\qquad\qquad (4.13)$$

$$\frac{1}{c_t} = \frac{1}{c_0} + k_2 \, t \qquad\qquad\qquad (4.14)$$

Where C_t is COD of wastewater at reaction time t.

The regression analysis based on the zero-, first- and second-order reaction kinetics for the COD removal from the Batik wastewater using the Fenton oxidation process, which was conducted at the optimized conditions. The results are shown in Figure 4.22. It was found that that the regression coefficients, R^2 of the second-order reaction kinetics (Figure 10 (C)) was 0.9748, which was obviously much higher than that based on the zero-order ($R^2 = 0.8583$) and the first-order ($R^2 = 0.9601$) reaction kinetics. Comparing the regression coefficients obtained by the graphical representation, we concluded that the first-order reaction kinetics fit the reaction best. The first-order rate constant $k_1 = 0.0252s^{-1}$ was

calculated from the slope. The result obtained from this study was consistent with the

work from Nitoi and others (2013). (Nitoi et al., 2013).
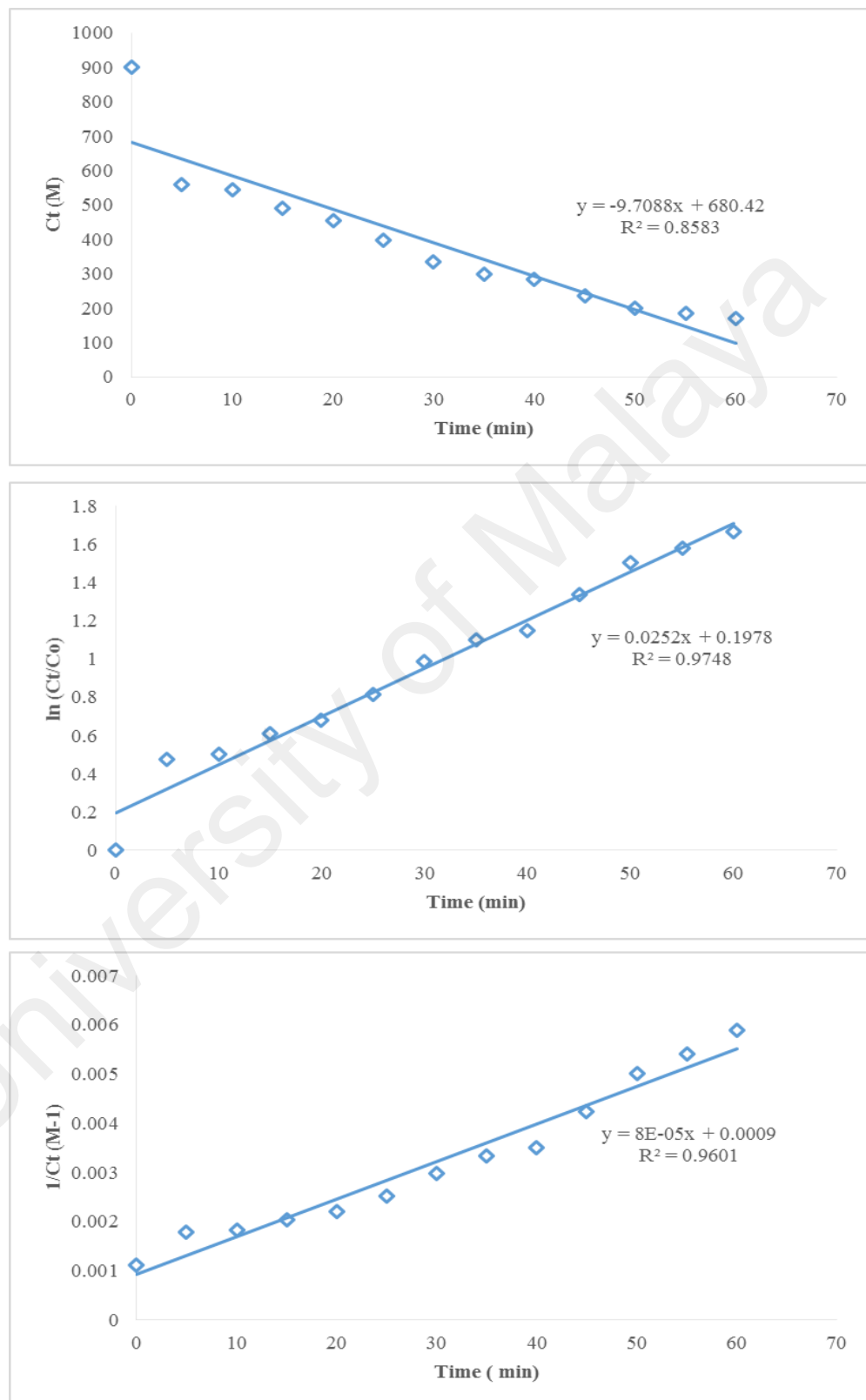
Figure 4.22: (a) Zero-order, (b) First-order and (c) Second-order
reaction kinetics for the COD removal by Fenton Process

4.2.6 Functional Group Analysis

FT-IR spectroscopy has been proven as a powerful tool for comprehensive characterization of organic contaminants. The unique characteristics of the material presented by the spectrum indicate the material properties, behavior and specific components represented by the functional groups. Infrared spectroscopy is based on the interactions of infrared radiation with matters. Infrared light causes functional groups to vibrate. The absorption bands in the spectrum indicate the uptake of energy. The intensity of the measured band depends on the content of the substances and the individual interaction of the functional groups with the infrared radiation at a distinct energy level. The near-infrared (NIR) region from $14,000 \text{ cm}^{-1} - 4000 \text{ cm}^{-1}$ and the mid-infrared (MIR) region from $4000 \text{ cm-1} - 400 \text{ cm}^{-1}$ are commonly applied for processes and product controls in many industrial fields (Smith, 2011; Deli Wu et al., 2016). The spectral pattern of the substances reveals the inherent features and thus the identity of the substances.

An understanding of the surface chemistry can be acquired through conducting FTIR analysis. FTIR spectroscopy is widely used to characterize and analyze the general functional groups present in wastewater. In the present study, the comparison of the FTIR spectrum of the untreated and treated batik wastewater clearly indicated the mineralization of wastewater by the Fenton oxidation process. Figure 4.23 shows the FTIR spectrum of the untreated batik wastewater and treated wastewater by the Fenton process at the optimized experimental conditions as followed: mass ratio of H_2O_2:COD=10.2, and H_2O_2:Fe^{2+}=4.7, initial pH 4.8 and retention time= 63.4 min. A decrease in the number of peaks shows that Fenton process successfully mineralized most of the organic compounds present in the batik wastewater. It was clear from the FTIR spectrum that the peaks at the wavelengths of 3317 cm^{-1} and 1637cm^{-1} were observed with a reduction in their intensity in the spectrum of the Fenton treated wastewater. A

strong and broad peak located at 3317 cm^{-1} can be associated with the presence of hydroxyl groups. It was believed that the band that occurred at 1637 cm^{-1} was caused by the aromatic C=C bonds, which were polarized by the oxygen atoms bond near one of the C atoms. This might be due to the incorporation of oxygen groups into the carbonaceous phase caused by the attacks by $HO \bullet$ radical.
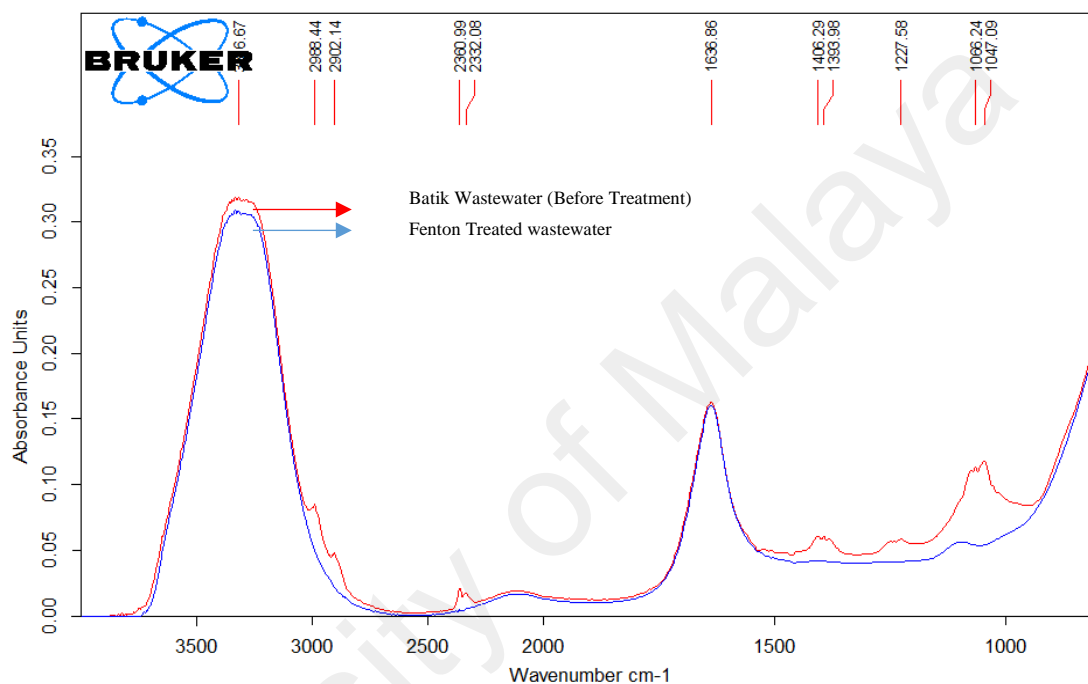
Figure 4.23: FTIR spectrum of Batik wastewater and Fenton treated wastewater

4.2.7   Sludge Characterization

Fenton process has been extensively studied and successfully used to treat highly toxic, recalcitrant, and colored wastewaters, which cannot be biologically treated. However, industrial application of the Fenton process is limited mainly because of the generation of iron oxyhydroxide during the neutralization process after oxidation (Buthiyappan, Abdul Aziz, et al., 2016; Karthikeyan et al., 2011). The solid waste generated in Fenton process is potentially hazardous because of the adsorbed organics from the treated wastewater. This is one of the main obstacles preventing full-scale Fenton process for

137

industrial wastewater treatment. The experimental study showed that the variation in the sludge amount was mainly due to the difference in the amount of the Fenton reagent used in the system for each run when the initial COD value of the wastewater was fixed. Besides, the volume of the sludge was also related to the extent of mineralization. Therefore, it is important to optimize the amount of Fenton reagents and other operating parameters as they affect the sludge properties. Although many studies have been conducted to investigate the feasibility of the Fenton process, very limited work has reported the characteristics of the sludge generated from the oxidation process. There have not been any comprehensive reports on the particle size and surface studies of the generated sludge. In this work, the sludge formed from the optimized conditions was characterized using SEM/EDX and the particle size study was performed.

4.2.7.1 SEM and Elemental Analysis of Sludge

Scanning Electron Microscopy (SEM) combined with Energy Dispersive Spectrometry (EDX) was also conducted to elucidate the morphology and the elements of the sludge generated through the Fenton process. The sludge conditioned by the Fenton's reagent showed a discontinuous and porous structure with a diameter of around 80 µm (Figure 4.24). The elemental analysis of the sample using EDX, as shown in Figure 4.25 indicated that O, Na, Fe, C, N and S were present in the sludge. Table 4.8 shows the percentage of the elements. Oxygen was the most abundant element followed by sodium. The presence of iron may cause particle destabilization and oxidation. Nevertheless, treating the Fenton treated samples with sodium hydroxide can reduce the of iron ions required. Based on the elemental analysis of the sludge produced in the Fenton process, it was proven that Fenton oxidation generates harmless end products.

Table 4.12: Elemental analysis for the Fenton treated sludge sample of the batik wastewater

Element Number	Element Symbol	Element Name	Weight (%)
8	O	Oxygen	56.3
11	Na	Sodium	25.8
26	Fe	Iron	3.9
6	C	Carbon	8.0
7	N	Nitrogen	5.4
16	S	Sulfur	0.6

4.2.7.2 Particle Size Distribution of Sludge

Particle size is one of the factors that affects the dewatering characteristics of sludge apart from pH, grease content, porosity, particle charge, solid concentration, nitrogen content and others. For this purpose, sludge samples were collected from a treated sample that was obtained as a result of the Fenton oxidation process under the optimized conditions. The particle size distribution analysis was performed by using Mastersizer 2000 and the particle size range was defined. The results presented above indicated that laser diffraction using Malvern Mastersizer 2000® was capable of providing rapid and reproducible results on the particle size distribution of the sludge. The particle size distribution of the sludge is illustrated in Figure 4.24, which shows the particles size between 0.02 to 2000 μm. As illustrated in the plot, the sludge formed in the Fenton oxidation process had a particle size of 10.24 to 50.78 microns. According to Neyens et al. (2003), particle size can be modified by the presence of acids. Repulsive electrostatic interactions created by the surface charge of the sludge particles are minimized within the pH range of 2.6–3.6, leading to the proximity of small particles. On the other hand, Fenton oxidation is a complex chain of reactions in which the generated ferrous ions react with hydroxide ions to form ferric hydroxide and ferric hydroxo complexes. These compounds possess a high capacity of coagulation and flocculation. Therefore, it is suggested that Fenton oxidation caused small sludge particles to flocculate to form larger particles.
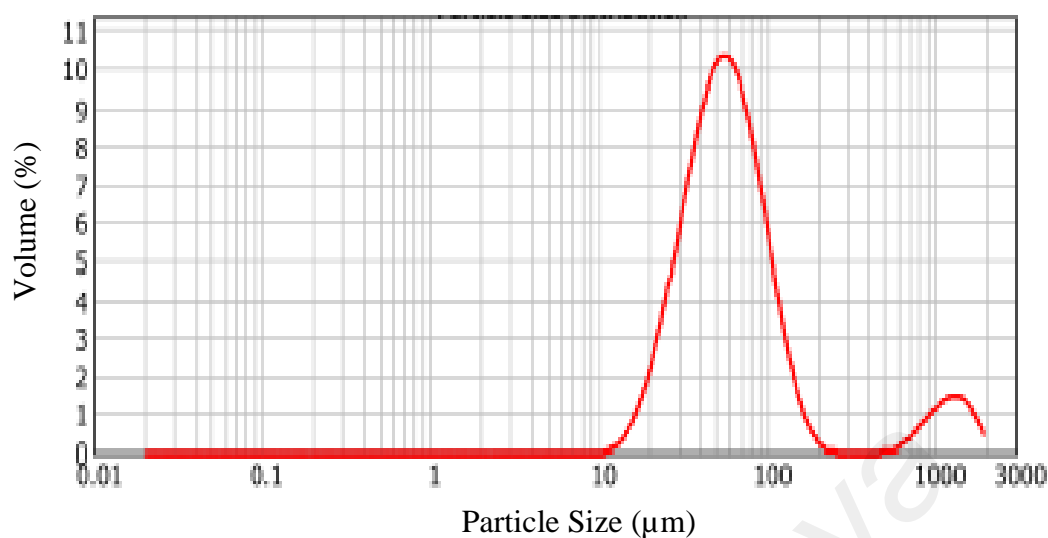
Figure 4.24: Particle size distribution of sludge generated in the Fenton process

4.2.8 Post and Pre-Treatment Analysis of Organic Contaminants in the Batik Wastewater

In order to further investigate the organic contaminant removal from the batik wastewater by the Fenton oxidation process, the effluent was analyzed by GC-MS before and after the treatment. Figure 4.25 shows that the concentration of organic contaminants in the batik wastewater reduced significantly after the Fenton oxidation process. The chromatogram illustrated that around 30 types of organic components were present in the influent. The organic compounds found in the batik effluent included seventeen siloxanes derived compounds, nine alkanes, two carboxylic acids, one ester and one aromatic hydrocarbon alkane. Among them, the semi-inorganic polymers, siloxanes or silicone derivatives were found in high proportion, which was around 57%. These nonionic surfactants could have been reduced from the sodium silicate that is used to fix the colors/dyes on the cloth. Sodium silicates are inorganic substances composed primarily of silicon oxide (SiO_2) and sodium oxide (Na_2O). The polysiloxanes found in the real wastewater included cyclohexasiloxane, silane, cyclodecasilaxne, cyclononasiloxane, heptasiloxane, heptasiloxan, octasiloxane, hexasiloxane, and cyclotrisiloxane. Siloxanes

based on polymerized siloxanes consist of chains made of alternating silicone and oxygen atoms. Besides, the wax used in the batik making process may cause the amount of hydrocarbons detected by GC/MS. Wax helps dye penetrate into textiles and creates a marbled look. About seventeen organic pollutants were completely removed by the Fenton oxidation process since they were not detected on the chromatogram of the effluent. After the Fenton oxidation process, about 71% of siloxanes were successfully removed from the wastewater. It was concluded that the Fenton oxidation process could oxidize high-molecular-weight substances into small organic compounds, which could then be readily detected by GC–MS. Additionally, the HPLC analysis showed that the treated effluent contained a small amount of carboxylic acids and sodium ions, which was in accordance with the GC/MS analysis (Figure 4.26).

4.2.9   Model Verification Using Different Types of Industrial Wastewaters

The ideal mass ratios of H_2O_2:COD and H_2O_2:Fe^{2+}, initial pH and retention time for the maximum pollutant removal efficiency differ with the types of wastewater. Further studies were conducted in order to determine if the model developed for the batik wastewater could be used for other types of industrial wastewater that required smaller treatment system. The validity of the RSM-predicted model for the optimum efficiency could be verified by applying the empirical model with varied initial COD values. The predicted and experimentally obtained treatment efficiencies of different types of real wastewater using the optimized values of the batik wastewater are presented in Table 4.13. In summary, the results obtained using the optimal conditions for COD, TOC and color removals showed that the RSM model attained for the batik wastewater could be used to treat different types of wastewater with higher removal efficiency.
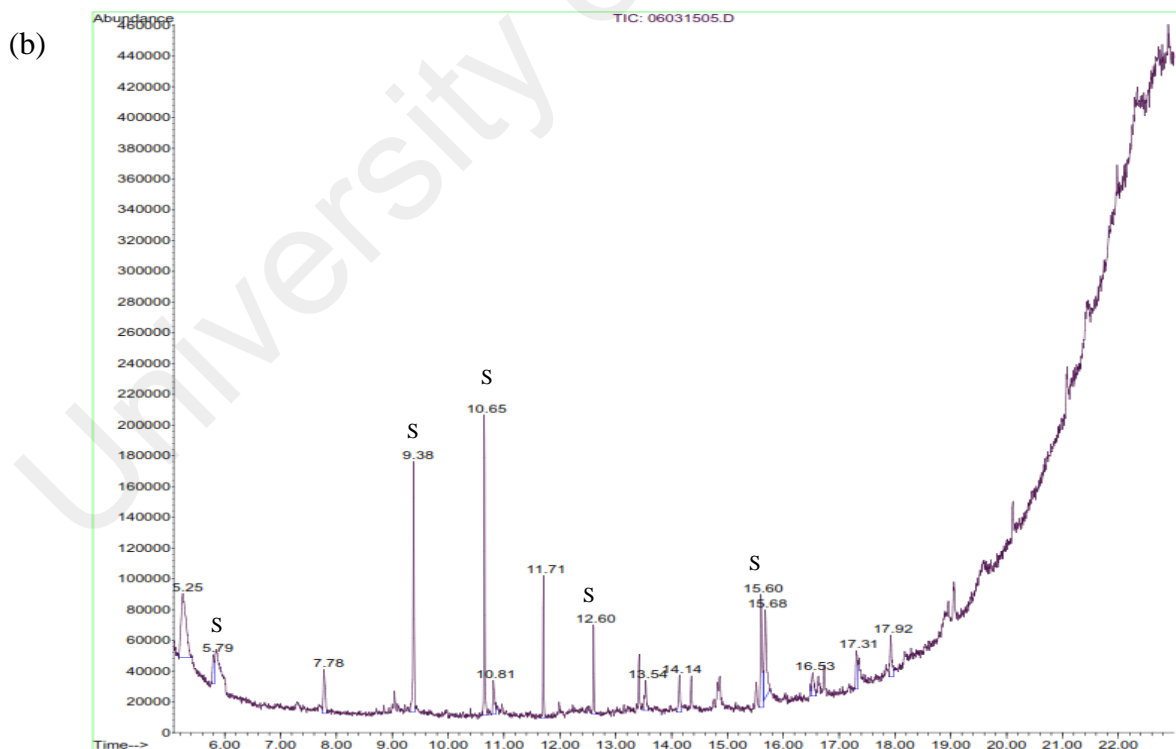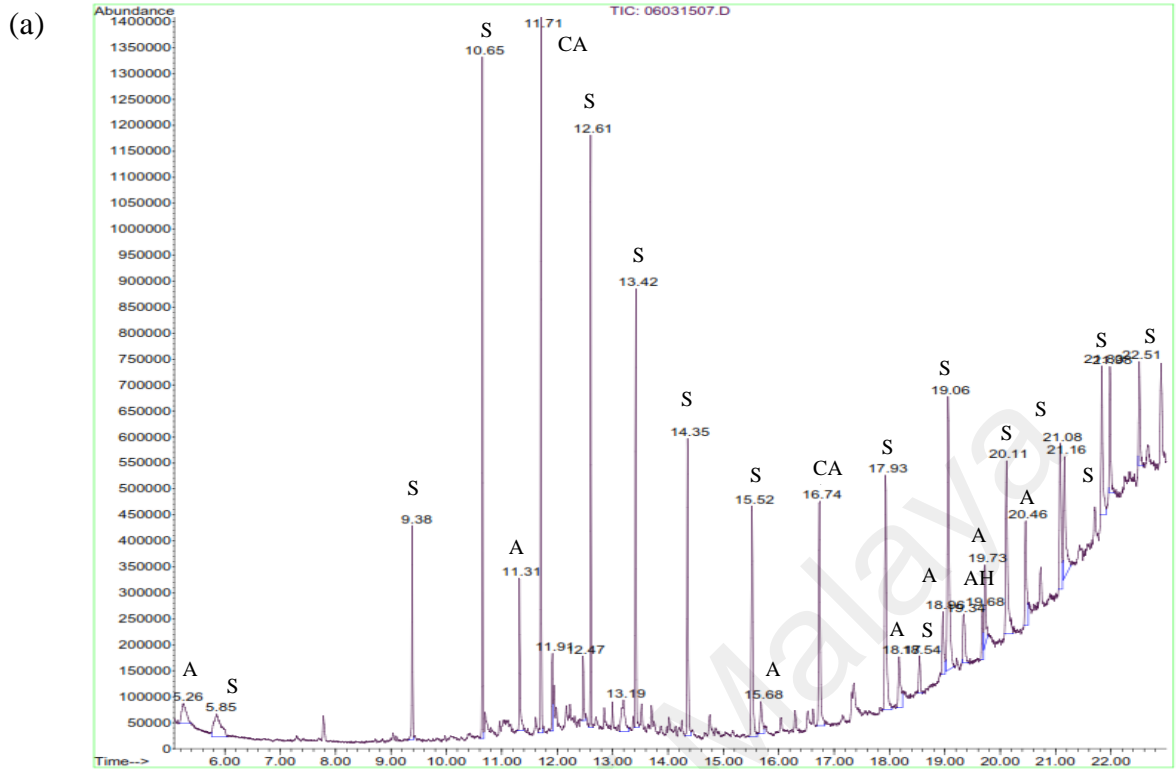
Figure 4.25: GC/MS Chromatogram for organic in Batik wastewater (a) before and (b) after Fenton Process (S=Siloxaaanes, A=Alkanes, AH=Aromatic hydrocarbon alkane, ES=Ester, CA=Carboxylic acid)

a) Raw Wastewater

b) Fenton Treated Wastewater
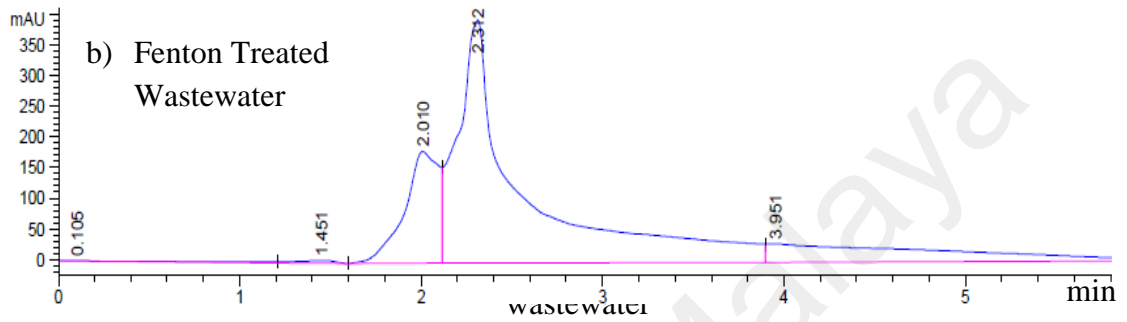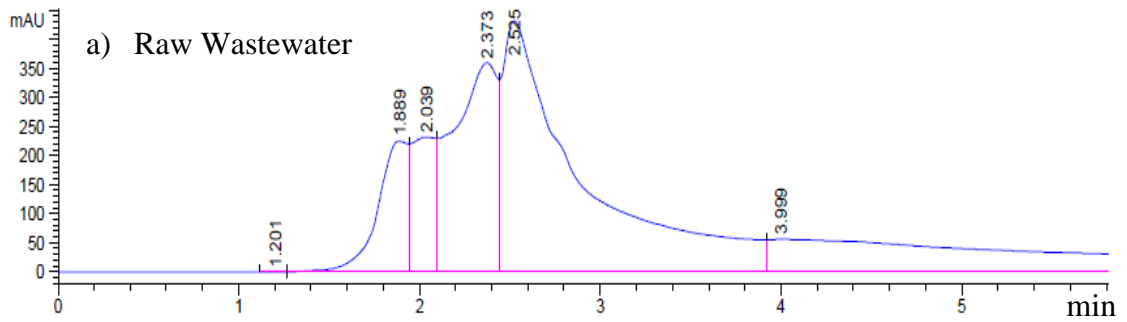
Table 4.13: Optimum value of the process parameters for constraint conditions and experimental values for different types of wastewater

Pollutants	Predicted (Removal %)			Experimental (Removal %)		
	COD	TOC	Color	COD	TOC	Color
Metal Finishing Industry	80.1	68.2	96.6	67.5	50.2	100
POME	80.1	68.2	96.6	98.9	72.5	99.4
Leachate	80.1	68.2	96.6	92.7	71.6	99.5

143

4.3   UV Integrated Fenton Oxidation for the Treatment of Batik Wastewater

4.3.1   Optimization of Treatment Process

The independent variables used in this experimental study were mass ratios of H_2O_2:COD and H_2O_2:Fe^{2+}, initial pH of the solution, retention time and UV- radiation intensity, that was coded as A, B, C, D and E respectively. In this work, the mass ratio was used as this the common practice by many researchers to analyze degradation efficiency (Benatti et al., 2006; Diya'uddeen Basheer Hasan et al., 2012). The range of these factors is shown in Table 4.14. The experimental design matrices and responses based on the experimental runs and the predicted color, COD and TOC removal efficiencies, as proposed by CCD are given in Table 4.15. The observed COD and TOC removal efficiencies varied between 57.6 - 84.3% and 43.8 - 71.6% respectively. The predicted values by the model matched the experimental results satisfactorily. On the other hand, the color removal percentages varied between 72.5– 99.6%.

Table 4.14: Experimental range and levels of the independent variables used in UV-Fenton process

Variable	Factor	Range and level				
		-2	-1	0	+1	+2
H_2O_2:COD	A	6.56	1	6.50	12	19.56
H_2O_2:Fe^{2+}	B	6.96	2	8.50	15	23.96
Initial pH	C	2.82	2	5.50	9	13.82
Retention time	D	11.40	30	60.00	90	131.40
UV (W)	E	10.00	15	35.00	75	60.00

Table 4.15: Experimental design matrix and responses based on the experimental runs values on Color, COD and TOC removals (%) proposed by CCD design

Run	Independent variable					Responses (%)		
	A	B	C	D	E	Experimental		
						COD	TOC	Color
1	12.0	2.0	9.0	90	55	72.8	63.1	98.8
2	1.0	15.0	2.0	90	15	67.7	5.9	92.3
3	1.0	15.0	9.0	90	55	65.6	53.3	86.3
4	12.0	2.0	9.0	30	15	78.2	71.3	99.1
5	12.0	2.0	2.0	90	15	80.2	70.0	89.6
6	12.0	15.0	2.0	30	15	63.5	50.5	91.6
7	12.0	15.0	2.0	90	55	65.3	54.7	73.6
8	6.5	8.5	5.5	60	35	79.9	60.7	98.4
9	6.5	8.5	5.5	60	35	80.5	59.7	97.9
10	6.5	8.5	5.5	60	35	82.1	60.2	99.2
11	1.0	2.0	2.0	90	55	62.2	56.5	87.6
12	12.0	15.0	9.0	90	15	62.3	49.9	95.3
13	1.0	2.0	9.0	30	55	62.5	53.4	88.6
14	1.0	15.0	2.0	30	55	65.6	51.2	87.3
15	1.0	15.0	9.0	30	15	61.3	50.1	85.6
16	1.0	2.0	2.0	30	15	69.6	55.8	89.4
17	12.0	2.0	2.0	30	55	75.2	65.3	98.7
18	6.5	8.5	5.5	60	35	81.9	61.5	98.5
19	1.0	2.0	9.0	90	15	66.1	50.2	88.5
20	12.0	15.0	9.0	30	55	58.3	45.6	91.8
21	12.0	2.0	9.0	30	55	75.3	66.3	98.3
22	6.5	8.5	5.5	60	35	83.1	62.6	98.6
23	6.5	8.5	5.5	60	35	82.6	59.6	97.9
24	1.0	15.0	9.0	90	15	66.3	51.1	88.2
25	1.0	2.0	2.0	90	15	68.5	55.5	88.7
26	1.0	2.0	9.0	90	55	62.3	51.5	89.3
27	1.0	2.0	2.0	30	55	66.6	54.1	85.5
28	1.0	15.0	9.0	30	55	61.9	48.6	84.3
29	12.0	15.0	9.0	30	15	61.4	48.9	92.4
30	1.0	15.0	2.0	30	15	66.2	51.8	88.5
31	12.0	15.0	9.0	90	55	58.3	44.1	93.4
32	1.0	2.0	9.0	30	15	64.4	53.2	84.9
33	1.0	15.0	2.0	90	55	64.5	56.5	90.2
34	12.0	2.0	2.0	90	55	76.6	71.6	88.5
35	12.0	15.0	2.0	90	15	62.3	53.5	72.5
36	12	15	2	30	55	62.3	48.4	90.4
37	6.5	8.5	5.5	60	35	79.5	60	99.3
38	12	2	2	30	15	79.2	70.3	94.6
39	6.5	8.5	5.5	60	35	83.2	59.1	98.8
40	12	2	9	90	15	78.3	66.1	99.6

Table 4.16: Continued

Run	Independent variable					Responses (%)		
	A	B	C	D	E	Experimental		
						COD	TOC	Color
41	6.6	8.5	5.5	60	35	71.1	53.5	90.4
42	6.5	8.5	5.5	131	35	66.1	50.9	98.2
43	6.5	8.5	5.5	60	35	82.6	58.4	98.6
44	19.6	8.5	5.5	60	35	78.2	66.3	96.3
45	6.5	23.9	5.5	60	35	57.6	44.2	94.3
46	6.5	8.5	5.5	60	35	84.3	59.0	98.5
47	6.5	8.5	13.8	60	35	58.2	57.9	94.7
48	6.5	8.5	5.5	60	35	83.4	60.7	98.6
49	6.5	6.9	5.5	60	35	79.3	66.9	92.5
50	6.5	8.5	5.5	11	35	58.5	43.8	96.2
51	6.5	8.5	5.5	60	65	64.1	50.6	97.9
52	6.5	8.5	5.5	60	10	67.4	53.8	97.6
53	6.5	8.5	2.8	60	35	60.0	62.8	78.3

4.3.2 Statistical Analysis

Based on the experimental design presented in Table 4.16, a second-order polynomial response equation was used to demonstrate the empirical interaction between the dependent and independent variables. Table 4.17 shows all the three the quadratic equations derived for COD, TOC and color removal efficiencies. It was proven from the equations that all the five operating parameters investigated had positive effects on the degradation and mineralization efficiencies. Positive interactions between the mass ratio of H_2O_2:COD and initial pH, the mass ratio of H_2O_2:Fe^{2+} and retention time, the mass ratio of H_2O_2:Fe^{2+} and UV radiation intensity, initial pH and retention time were observed. For color removal, the interaction between the mass ratio of H_2O_2:COD and UV, the mass ratio of H_2O_2:Fe^{2+} and initial pH were also important. ANOVA was applied to evaluate the adequacy of the model. ANOVA results are illustrated in Table 4.18. The model's F-values of 60.72, 70.53, and 7.40 for the removal percentages of COD, TOC and color removal respectively indicated that the three models were

significant for the degradation of Batik wastewater. There was only a 0.01 % chance that the 'model F value' could occur due to noise. Besides, $P < 0.05$ indicated that model terms were significant at 95 % confidence level or more. It should be noted that P value less than 0.0001 for all the models indicated that the models were highly significant to describe decolorization, degradation and mineralization. The factors that had relatively less effect on COD and TOC removals were retention time (0.0335) and UV radiation (0.0047). Values greater than 0.1000 indicated that the model terms were not significant. Retention time and UV-radiation intensity were the insignificant variables for decolorization.In addition, light intensity was insignificant, as irradiation did not contribute much to decolorization.

The 'lack-of-fit F- value' of 0.1494 and 0.3447 for COD and TOC removals implies that these models are not significant relative to pure error. The non-significant lack-of-fit confirmed the good predictability of the models. There are only 14.94% and 34.47% chances that the 'lack-of-fit F- value' for both models could occur due to noise. The R^2 value of the response variables followed the order of R^2 (TOC) > R^2 (COD) > and R^2 (color). However, not much difference in the R^2 value for both COD and TOC removal efficiencies. The TOC and COD removal efficiencies denoted that established model, showing satisfactory quadratic fit, could represent 97.9% and 97.6% of the total variation. However, the model in terms of color removal could explain only around 83.1 % of the total variation. The adjusted determination coefficients (R^2 adj) showed that 97 % and 96 % of the variabilities were observed. The adequate precision ratios of 30.17, 22.39 and 10.15 derived for TOC, COD and color removal percentages indicated an adequate signal for all response variables. A ratio greater than 4 is desirable as this indicates that the models can be used to navigate the design space.

Table 4.16: Experimental design matrix and responses based on the experimental runs values on Color, COD and TOC removals (%) proposed by CCD design

Responses (%)	Proposed quadratic model
COD removal	$43.8500 + 1.9000\ H_2O_2{:}COD + 0.7500\ H_2O_2{:}Fe^{2+} + 3.3500\ pH + 0.4800\ RT + 0.4600\ UV - 0.100\ H_2O_2{:}COD \times H_2O_2{:}Fe^{2+} + 0.0010\ H_2O_2{:}COD \times pH - 0.0004\ H_2O_2{:}COD \times RT - 0.0007\ H_2O_2{:}COD \times UV - 0.0050\ H_2O_2{:}Fe^{2+} \times pH + 0.0030\ H_2O_2{:}Fe^{2+} \times RT + 0.0050\ H_2O_2{:}Fe^{2+} \times UV + 0.0030\ pH \times RT - 0.0010\ pH \times UV - 0.0004\ RT \times UV - 0.0470\ (H_2O_2{:}COD)^2 - 0.0600\ (H_2O_2{:}Fe^{2+})^2 - 0.3400\ pH^2 - 0.0040\ RT^2 - 0.007\ UV^2$
TOC removal	$41.9100 + 1.8500\ H_2O_2{:}COD + 0.0900\ H_2O_2{:}Fe^{2+} + 0.3900\ pH + 0.31590\ RT + 0.22\ UV - 0.1200\ H_2O_2{:}COD \times H_2O_2{:}Fe^{2} - 0.0050\ H_2O_2{:}COD \times pH - 0.0010\ H_2O_2{:}COD \times RT - 0.0070\ H_2O_2{:}COD \times UV - 0.0090\ H_2O_2{:}Fe^{2+} \times pH + 0.0050\ H_2O_2{:}Fe^{2+} \times RT + 0.0003\ H_2O_2{:}Fe^{2+} \times UV - 0.01039\ pH \times RT - 0.0044\ pH \times UV + 0.0009\ RT \times UV - 0.0002\ (H_2O_2{:}COD)^2 - 0.0180\ (H_2O_2{:}Fe^{2+})^2 + 0.0060\ pH^2 - 0.0020\ RT^2 - 0.0030\ UV^2$
Color removal	$80.5950 + 1.39\ H_2O_2{:}COD + 0.9200\ H_2O_2{:}Fe^{2+} + 1.0700\ pH + 0.1000\ RT + 0.14\ UV - 0.0580\ H_2O_2{:}COD \times H_2O_2{:}Fe^{2+}\ 0.1300\ H_2O_2{:}COD \times pH - 0.0120\ H_2O_2{:}COD \times RT + 0.0020\ H_2O_2{:}COD \times UV + 0.0090\ H_2O_2{:}Fe^{2+} \times pH - 0.0020\ H_2O_2{:}Fe^{2+} \times RT - 0.0020\ H_2O_2{:}Fe^{2+} \times UV + 0.01708\ pH \times RT + 0.0011\ pH \times UV - 0.0003\ RT \times UV - 0.0500\ (H_2O_2{:}COD)^2 - 0.0350\ (H_2O_2{:}Fe^{2+})^2 - 0.2200\ pH^2 - 0.0009\ RT^2 - 0.002\ UV^2$

4.3.3 Effect of Operating Parameters on Color Reduction

High color removal efficiencies (80-90%) were obtained under all working conditions. It confirms the capability of Fenton to eliminate color-imparting chromophore groups such as azo group, nitro group, keto group, nitroso group, quinonoid group and ethylenic group from real wastewater, which contains various types of dyes and chemicals (Otterstätter, 1999). Figure 4.27 shows the effects of the mass ratio of $H_2O_2{:}Fe^{2+}$ and pH on wastewater color removal at a mass ratio of $H_2O_2{:}COD = 6.5$, the retention time of 60 minutes and UV intensity of 35W. Initial pH is responsible for controlling the stability of hydrogen peroxide and oxidation ability of $HO\bullet$ radical. Increase in the mass ratio of $H_2O_2{:}COD$ from 1-12 and initial pH of the solution from 2-9 increased the color removal efficiency. However, increasing the mass ratio of $H_2O_2{:}COD$ up to 19 and pH value above

12 at similar experimental conditions reduced the color removal (as shown in the Table 4.16). This confirms the scavenging effect caused by excess amount of excess amount of H_2O_2, which reduces the $HO\bullet$ radical available for the Fenton process. It is also important to optimize the use of H_2O_2 to reduce the operating cost.

Table 4.17: ANOVA results for the quadratic model of Batik wastewater treatment using UV integrated Fenton process

Res. (%)	Source	SS	DF	MS	F-ratio	P-value	P> F value
Color Removal	***Model***	1705.83	20	85.29	7.40	<0.0001	Sig.
	Residual	345.69	30	11.52	-	-	-
	Lack of fit	343.82	22	15.63	66.62	< 0.0001	Sig.
	Pure Error	1.88	8	0.23	-	-	-
	Cor Total	2158.73	52	-	-	-	-
	Adq. Prec. Ratio	10.15	-	-	-	-	-
	R^2	0.83149	-	-	-	-	-
	R^2 adj	0.71916	-	-	-	-	-
	Pred.	0.29974	-	-	-	-	-
COD Removal	***Model***	3778.99	20	188.95	60.72	< 0.0001	Sig.
	Residual	93.36	30	3.12			
	Lack of fit	79.25	22	3.60	2.04	0.1494	Not Sig.
	Pure Error	14.11	8	1.76	-	-	-
	Cor Total	3872.46	52	-	-	-	-
	Adq. Prec. Ratio	22.39	-	-	-	-	-
	R^2	0.97589	-	-	-	-	-
	R^2 adj	0.95982	-	-	-	-	-
	R^2 Pred	0.90263	-	-	-	-	-
TOC Removal	***Model***	2640.21	20	132.01	70.53	< 0.0001	Sig.
	Residual	56.15	30	1.87			
	Lack of fit	44.23	22	2.01	1.35	0.3447	Not Sig.
	Pure Error	11.92	8	1.49	-	-	-
	Cor Total	2702.54	52	-	-	-	-
	Adq. Prec. Ratio	30.17	-	-	-	-	-
	R^2	0.97917	-	-	-	-	-
	R^2 adj	0.96529	-	-	-	-	-
	R^2 Pred	0.92411	-	-	-	-	-

In addition, the results confirm that the UV integrated Fenton process is not favorable at very acidic condition ($<$ pH 3) for color removal while good removal was achieved at initial pH of around 5.5. The color removal may be resulted from the coagulation reaction at pH values of above 5. However, increasing the pH above 12 reduced the degradation efficiency. This is due to the decrease in the oxidation potential of the processes caused by the transformation of catalyst ferrous ions (Fe^{2+}) to ferric iron (Fe^{3+}). The experimental runs with medium acidic (pH 5.5) and alkaline conditions (pH 9) showed immediate coagulation after Fe^{2+} was added and decolorization occurred within 2 minutes after hydrogen peroxide was added to the wastewater. This clearly showed the two-step concept of the Fenton-based processes: oxidation and coagulation.

Retention time was observed to have an effect on decolorization of batik wastewater. As seen from the plot (Figure 4.28), color removal percentages increased with the mass ratio of H_2O_2: Fe^{2+} and retention time up to 12 and 30 minutes, respectively. However, a further increase in both values reduced the color removal. This may be due to the longer retention that could cause generation of toxic intermediates in the presence of excess amount of $HO\bullet$ radical. Therefore, it is necessary to optimize the retention time and Fenton reagents to avoid the formation of toxic by-products at the end of the reaction. In addition, it was also observed that decolorization increased with the mass ratio of H_2O_2:COD and UV radiation intensity. The optimal condition was at H_2O_2: COD=9.8 and UV intensity=35. Beyond this point, a reduction in the removal efficiency was observed and a further increase in the mass ratio resulted in scavenging effects caused by unreacted H_2O_2. The intermediates formed in this reaction also prevented penetration of light into wastewater. A similar trend was also observed for the effects of the mass ratio of H_2O_2:Fe^{2+} and UV intensity on the color removal percentage. As observed in the plot (Figure 4.27), there was an increase in the color removal percentage with increasing ratios of H_2O_2:Fe^{2+} and initial pH of the solution. The optimum color removal efficiency

(99.4%) was achieved at the mass ratio $H_2O_2:Fe^{2+}= 5$ and initial pH around 6.5. Increasing both ratios beyond the optimal region resulted in the decrease in color removal. This is due to the formation of free radicals and precipitation of ferric oxyhydroxides. Therefore, it could be concluded that the UV integrated Fenton system is pH sensitive and medium acidic or near-neutral pH condition is found to be the most effective for Batik wastewater based on the experimental studies.
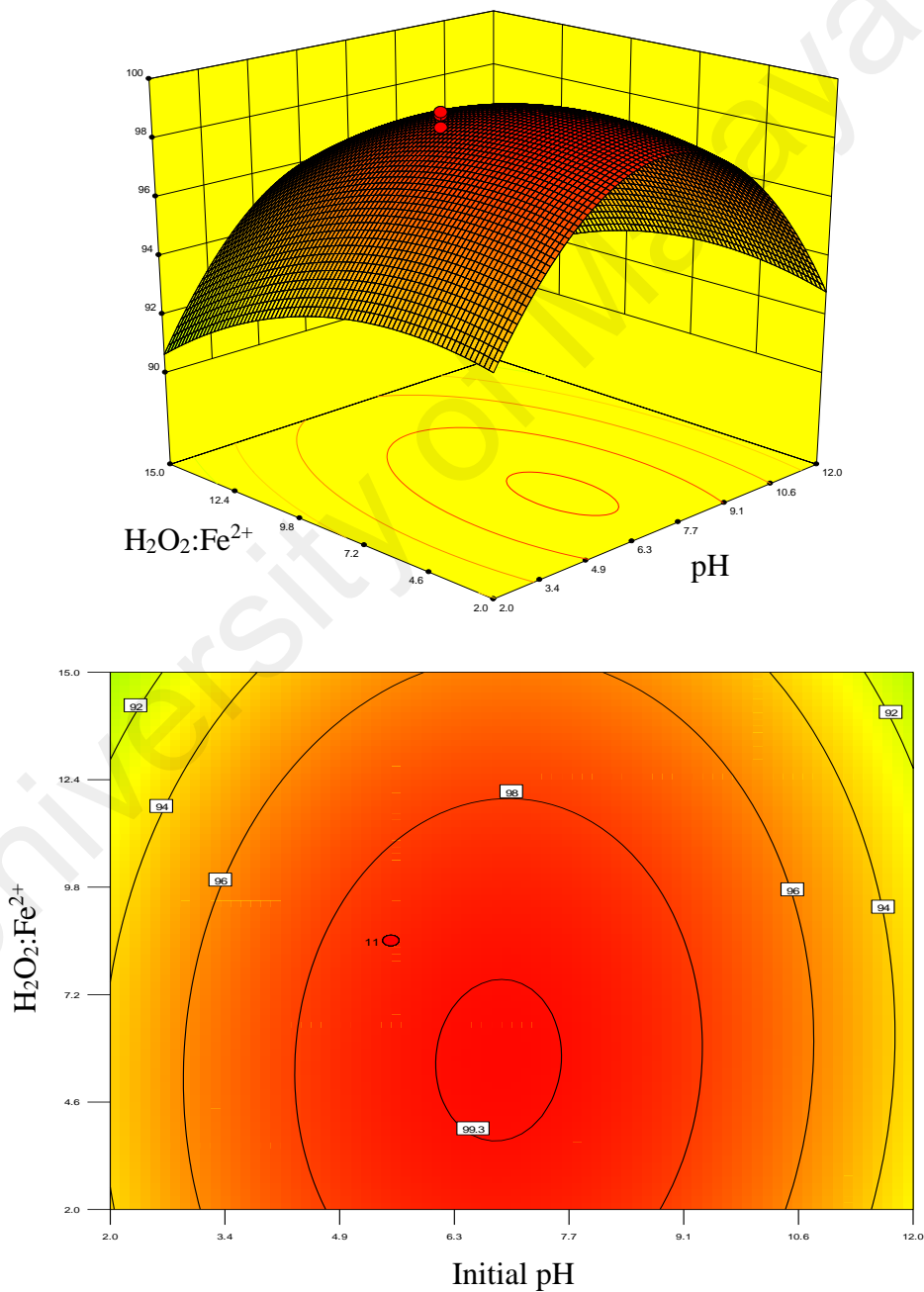
Figure 4.27: Effects of mass ratios of $H_2O_2:COD$ and retention time on Color removal of Batik Wastewater by UV integrated Fenton Process
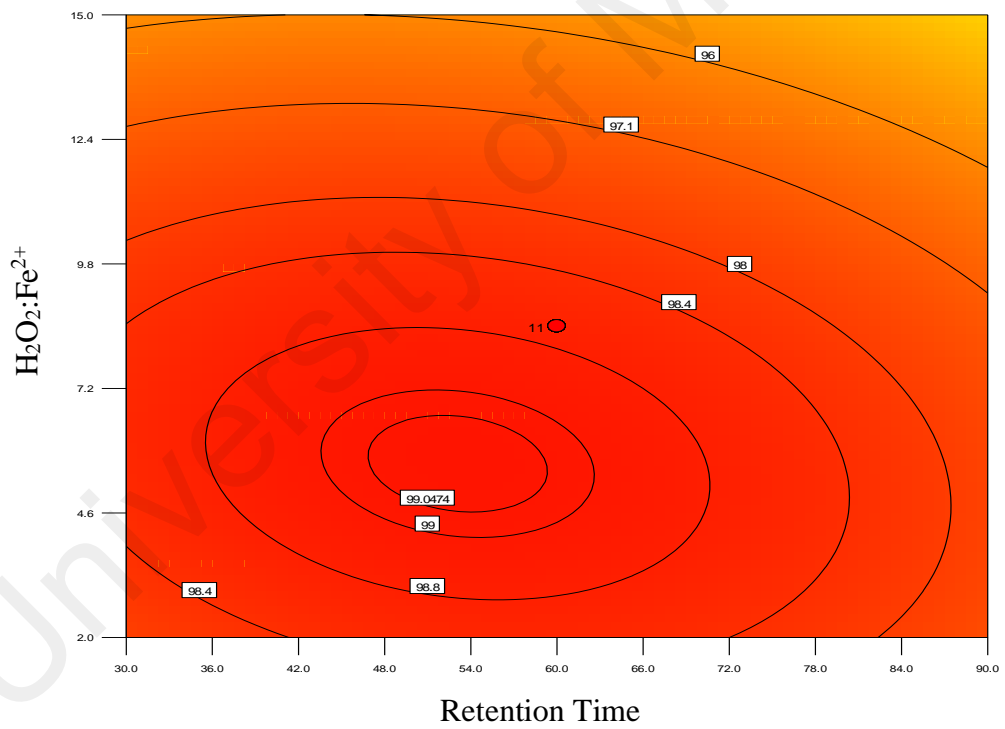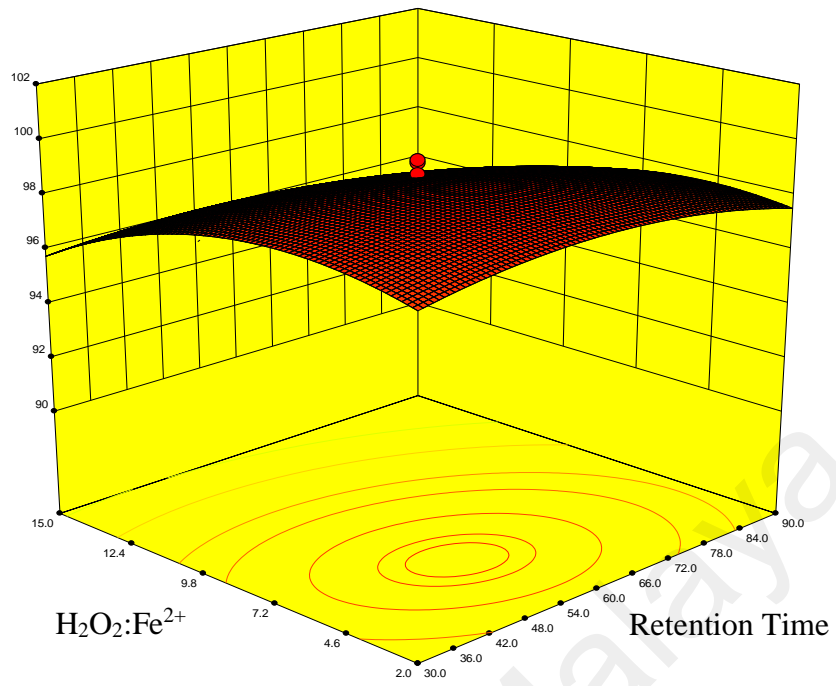
Figure 4.28: Effects of mass ratios of $H_2O_2:Fe^{2+}$ and pH on color removal of Batik wastewater by UV integrated Fenton Process

4.3.4 Effect of Operating Parameters on COD and TOC Removal Efficiencies

Since the removal percentage of COD and TOC follow the similar trend, the effects of the mass ratio of H_2O_2: COD and H_2O_2: Fe^{2+}, initial pH of the solution, retention time and UV intensity on COD and TOC removal efficiencies were discussed the following section.

4.3.4.1 Effects of Mass Ratio of H_2O_2:COD on COD and TOC Removals

Figure 4.29 (a and b) depicts the 2D plots of the effects of the mass ratio of H_2O_2:COD and H_2O_2:Fe^{2+} on COD and TOC removals from batik wastewater through the UV-integrated Fenton process. The plots showed that increase in the mass ratio of H_2O_2:COD from 1-12 increased the COD and TOC removals from 77.8% to 87.2 % and 58% to 80%, respectively. The increase in the mass ratio of H_2O_2:COD favored the simultaneous generation of more $HO\bullet$ radicals as a result of increased oxidation efficiency. On the other hand, increasing the ratio of H_2O_2:COD above 12 caused a drastic decrease in the COD and TOC removals. Lower COD and TOC reductions were observed as a consequence of radical scavenging reactions caused by excessive hydrogen peroxide in the system. Besides, excessive H_2O_2 in the treated wastewater also increases the COD value as 1 mg/l of H_2O_2 contributes to 27 mg/l of the COD.

The effect of mass ratios of H_2O_2:COD on COD removal and electrical energy per order is shown in Figure 4.30. When the mass ratio of H_2O_2:COD increased from 1 to 9, the electrical energy per order decreased from 1.76 to 1.2 kWh/m³order[1]. The electrical energy per order increased from 1.45 to 1.81 kWh/m³order[1] with further increase of the ratio from 12 to 19. The observed result clearly showed that optimum H_2O_2:COD was needed to produce sufficient $HO\bullet$ radical for efficient treatment.
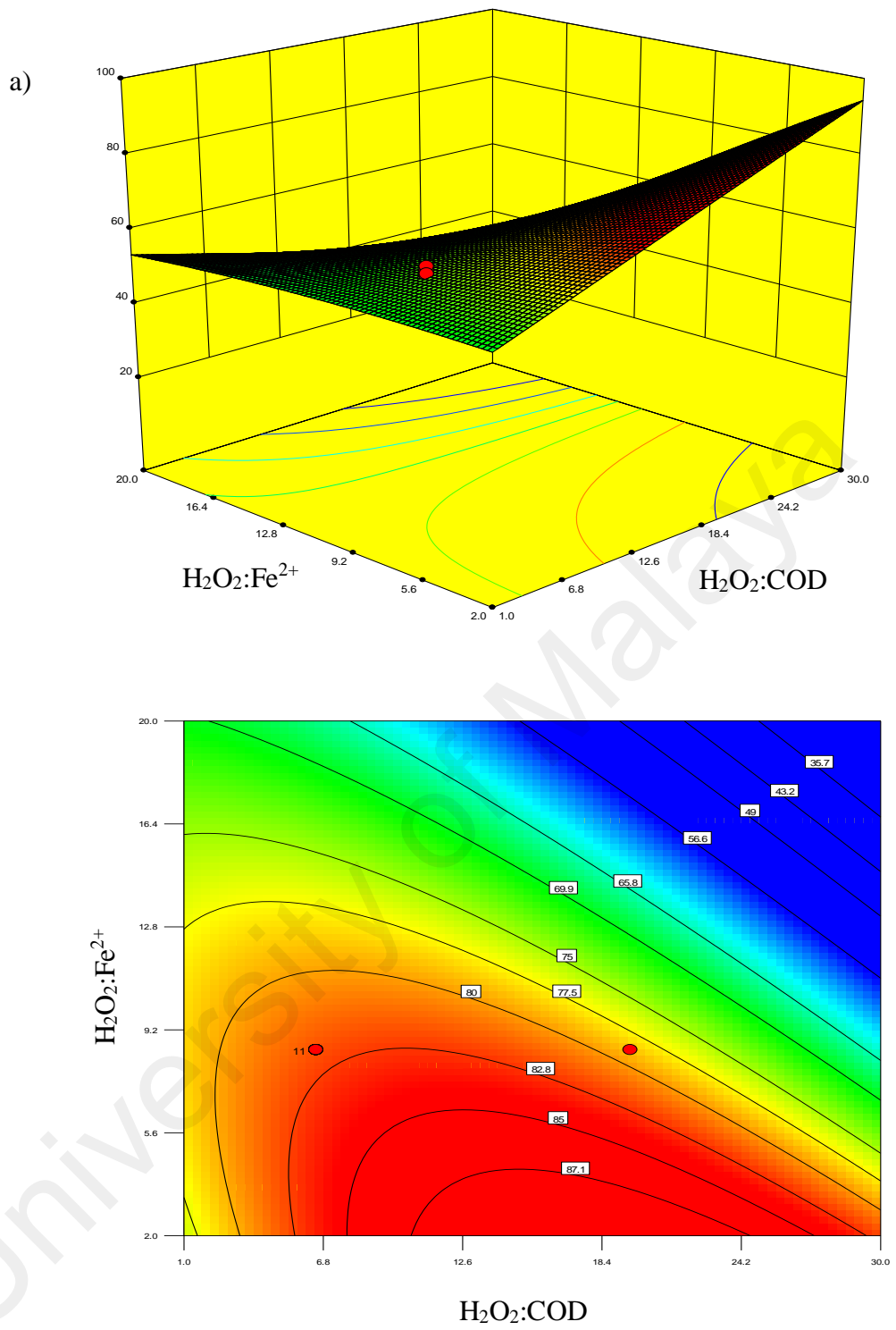
Figure 4.29: a) 2D contour of interaction between H_2O_2:COD and H_2O_2:Fe^{2+} on COD removal
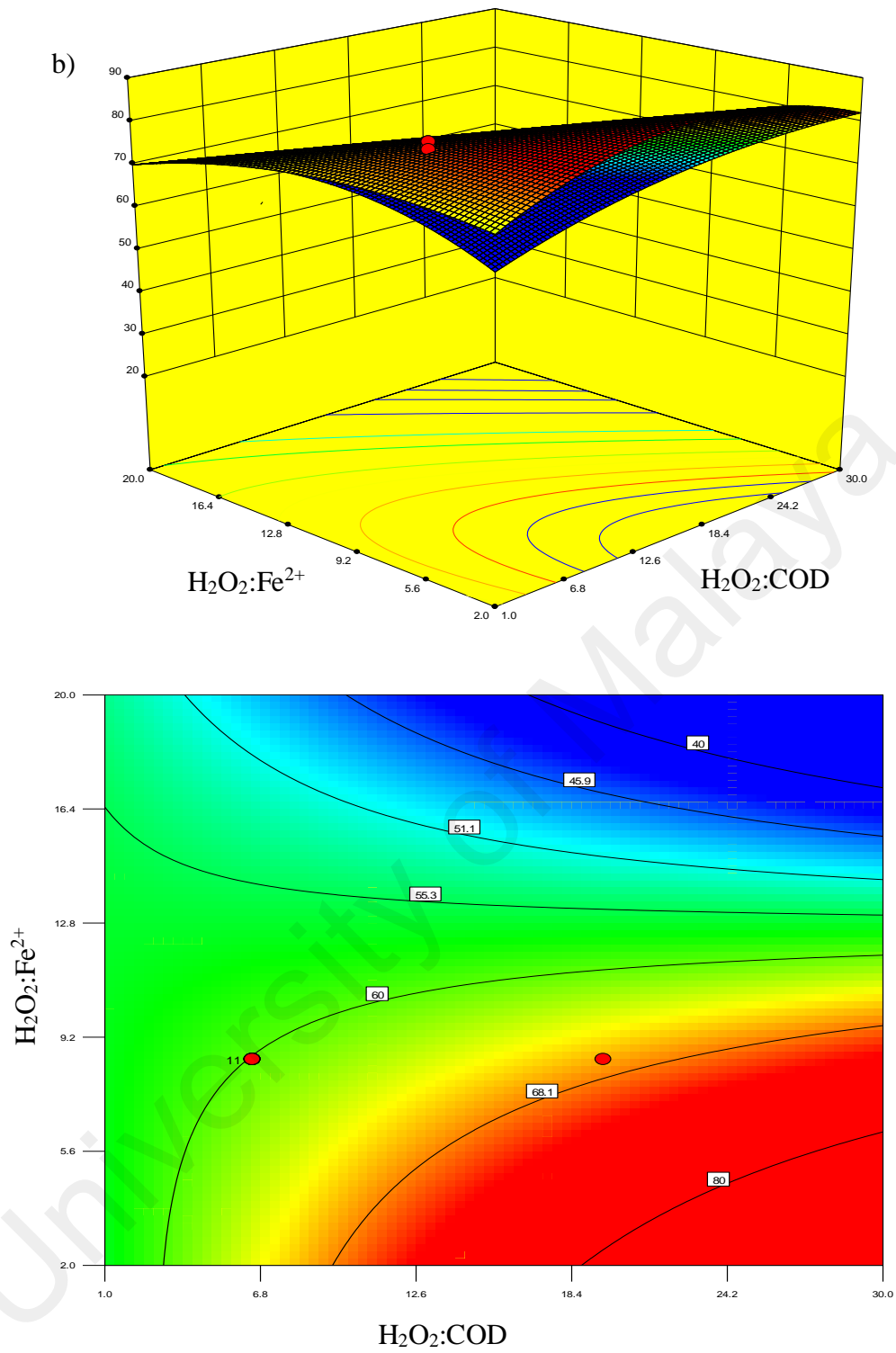
Figure 4.29: b) 2D contour of interaction between $H_2O_2:COD$ and $H_2O_2:Fe^{2+}$ on TOC removal
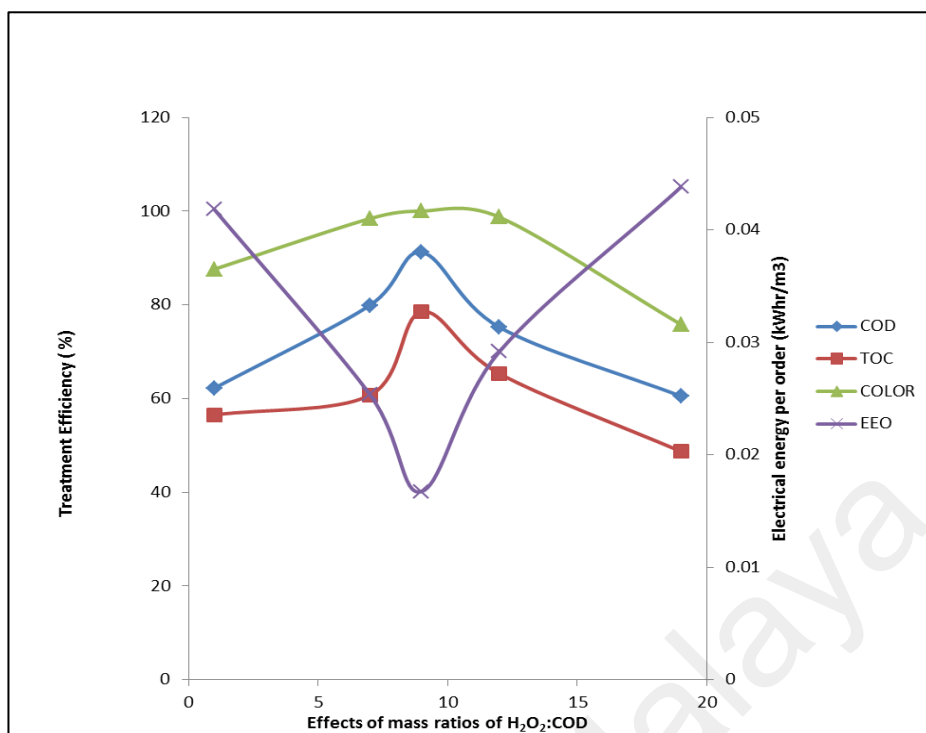
Figure 4.30: Effect of mass ratios of H_2O_2:COD on color, COD , TOC removals and electrical energy per order in UV/Fe^{2+}/H_2O_2

4.3.4.2 Effects of Mass Ratio of H_2O_2:Fe^{2+} on COD and TOC Removals

The ratio of H_2O_2:Fe^{2+} (wt/wt) was varied from 2- 15 and initial pH value of 5.5, the mass ratio of H_2O_2:COD =6.5 and reaction time of 60 min were used to investigate the effects of Fe^{2+} concentration on the COD removal efficiency. As observed in Figure 4.29, the COD removal efficiency significantly increased by decreasing the ratio of H_2O_2:Fe^{2+} and increasing the H_2O_2: COD ratio. The maximum COD removal was achieved at H_2O_2:Fe^{2+} = 2 and H_2O_2: COD = 12 and a reduction in the COD removal efficiency was observed when the ratio was increased to above 12. The COD removal efficiency decreased from 77 % to 75 % due to a limited number of iron salts to complete the oxidation reaction. Increase in the mass ratio of H_2O_2:Fe^{2+} decreased the amount of iron salts in the system (Fe^{2+}). Therefore, it contributes to an insufficient amount of catalyst for the oxidation process and thus decreased the removal efficiency. There is a direct relation between the H_2O_2:COD ratio and COD removal efficiency whilst an inverse trend were observed with

H_2O_2: Fe^{2+}. The improvement in the COD removal efficiency was observed with increment in the mass ratio of H_2O_2: COD as more oxidants (H_2O_2) available for the reaction that increased the efficiency of the Fenton process. Figure 4.29shows that the removal efficiency was the lowest in the range of 1-3 and increasing H_2O_2: COD up to 12 caused a significant improvement in the removal efficiency.

4.3.4.3 Effects of pH on COD and TOC Removals

In this study, the initial pH was varied from 2–9 to determine its effect on degradation efficiency. At a mass ratio of H_2O_2: Fe2+=4.8 , and initial pH approximately 5 the maximum COD removal efficiency (83.6 %) was achieved and it was found to decrease by increasing pH to above 6 as can be seen in Figure 4.31. Generally, at very low pH, iron is present in the form of ferric iron complex, which acts slowly with hydrogen peroxide to form $HO\bullet$ radical (M. Lucas et al., 2006). Most of the ferrous ions precipitate as $Fe(OH)_3$ and form amorphous oxyhydroxides ($Fe_2O_3\cdot nH_2O$) at higher pH (Ghiselli et al., 2004). The presence of iron precipitates does not only reduce the light absorption but increase the cost of post-treatment. The optimum pH value of the present research was found to be between 5- 6. It was observed from the experimental studies that at pH > 6, the coagulations process happened immediately after the addition of Fe^{2+}. However, it is not suitable to use higher pH since coagulation could hinder light penetration, which is an important requirement for degradation. Besides, wax could be efficiently removed at pH between 2 and 6 via the UV integrated Fenton system. The electrical energy per order also was studied at different initial pH of the wastewater. The analysis showed that pH around 5.5 was suitable to generate the maximum $HO\bullet$ radicals. It was observed from Figure 4.32 that the electrical energy per order decreased from 0.038 to 0.015 kWh/m^3 order[1] with increased effluent pH from 2 to 6. Hence, the electrical energy per order also

increased from 0.018 to 0.052 kWh/m^{3}order[1] by further increasing the initial effluent pH from 7 to 11.
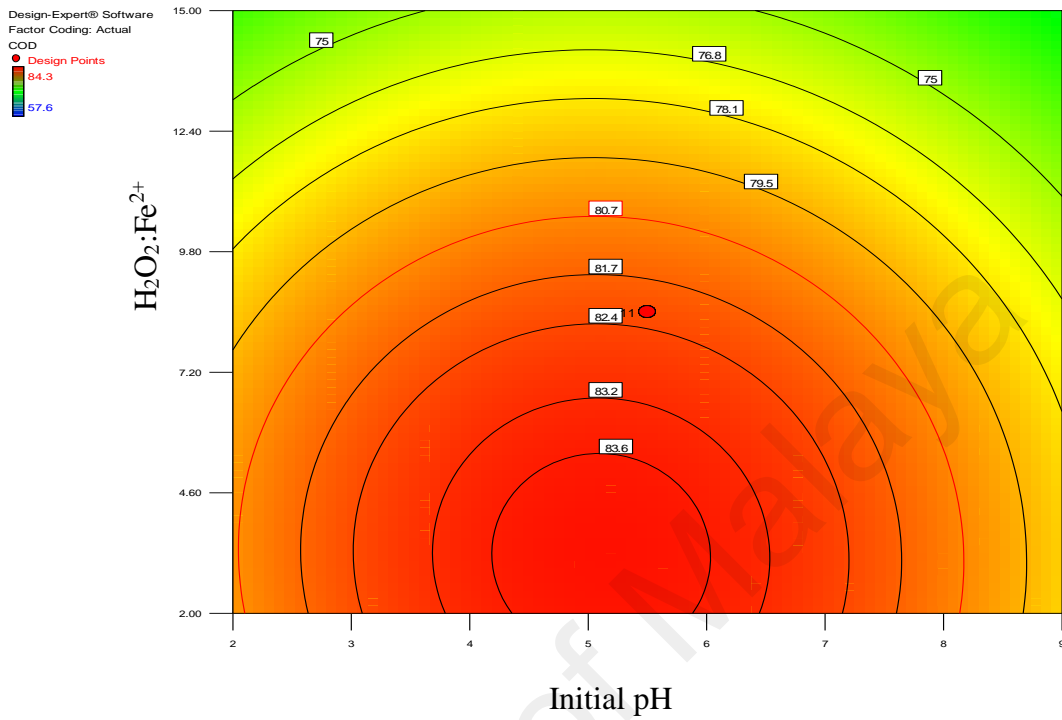
Figure 4. 31: 2D contours of interation between a) H$_2$O$_2$:COD and initial PH and b) H$_2$O$_2$:Fe^{2+} and initial pH on COD removal
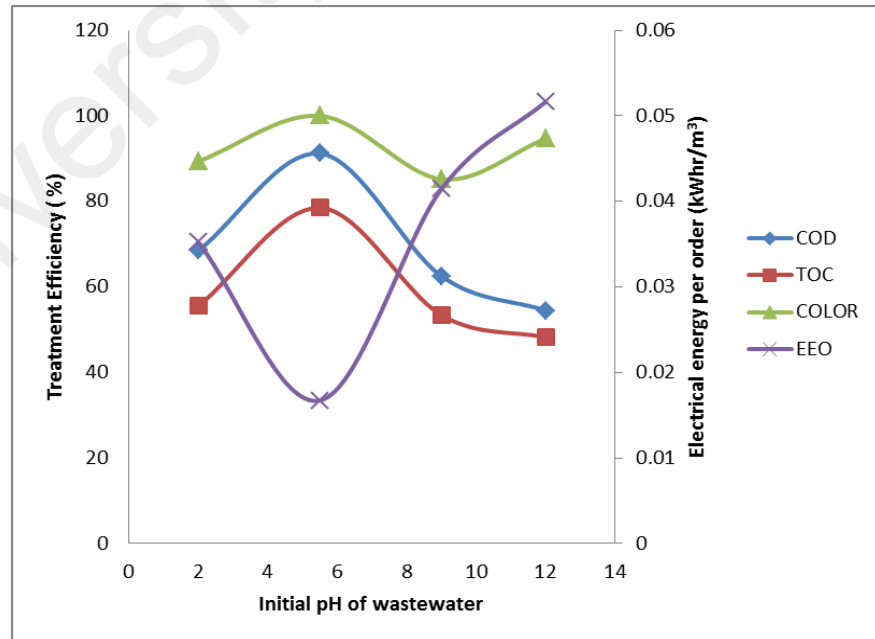
Figure 4.32: Effect of initial pH on color, COD , TOC removals and electrical energy per order in UV/Fe^{2+}/H$_2$O$_2$

4.3.4.4 Effects of UV Light Intensity on COD and TOC Removals

UV irradiation can significantly influence the direct formation of $HO\cdot$ and the photo-reduction rate of Fe^{3+} to Fe^{2+} (Papic et al., 2009). The reaction rate is directly proportional to the intensity of radiation, but the reaction rate reduced when the magnitude of intensity exceeded certain level. Use of radiation in AOPs helps increase the decolorization and mineralization efficiencies. The decolorization efficiency of the system also depends on both the reactivity and photosensitivity of the dye. UV radiation can be combined with H_2O_2 to enhance the photolysis process (Dükkancı et al., 2014).

The experimental results showed that light intensity had a significant effect on both the degradation and mineralization efficiencies. The COD removal efficiency drastically increased with light intensity up to 25W but a rapid reduction of efficiency was observed by increasing the intensity of light above 30W as can be seen in Figure 4.33. COD removal efficiency was observed to decrease from 84 to 75 % with an increase in the mass ratios of H_2O_2:Fe^{2+} above 4.8 and H_2O_2:COD above 9 and UV light intensity above 30W as can be seen in Figure 4.33. This is because an excess amount of Fenton reagents in the system generated toxic intermediates that hinder light penetration that eventually decreased the removal efficiency (Zapata et al., 2009). In addition, a higher amount of iron salts can form iron complexes that can increase the turbidity of wastewater (Yu et al., 2016). The quadratic model showed a negative interaction between UV and pH on degradation efficiency. This could be explained by the properties of wastewater that contained a higher amount of wax. At pH>6, coagulation process was found to be very prominent after the iron salts were added into the treatment system. It is well known that turbidity is one of the factors that affect the UV process so this might be the main reason for the negative relationship between these two variables. It should be noted that it is crucial to optimize the amount of Fenton reagents, especially in the UV-Fenton process,

to maximize the utilization of light intensity and improve the treatment efficiency. The effects of UV radiation on electrical energy per order are shown in Figure 4.34. Experiments were conducted by varying UV radiation from 10 to 80W. When the intensity of the UV radiation was increased from 10 to 20W, the electrical energy per order was found to decrease from 0.038 to 0.018 kWh/m^{3}order[1]. The electrical energy per order was observed to increase from 0.018 to 0.052 kWh/m^{3}order[1] by further increasing the initial UV radiation from 20 to 80W. The results showed that COD, TOC, color removal efficiencies and electrical energy per order changed significantly at higher UV dosages.
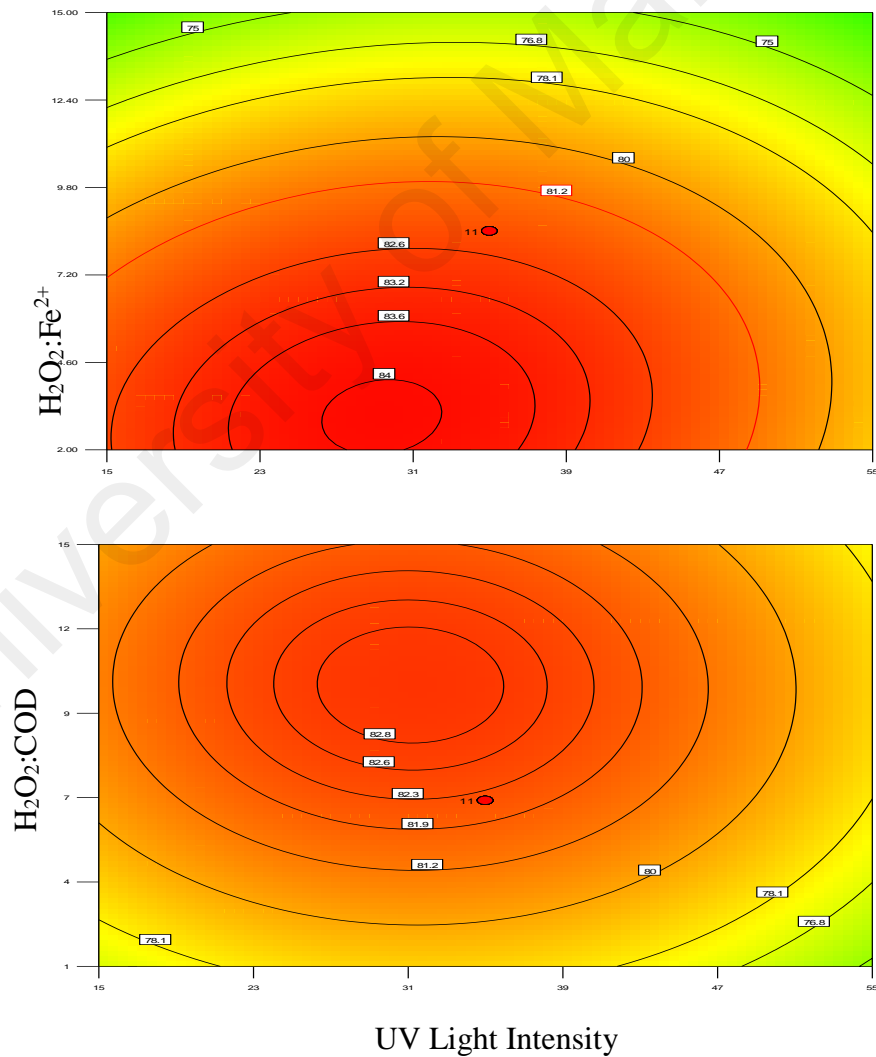
UV Light Intensity

Figure 4. 33: Effect of interaction between a) H_2O_2:COD and UV intensity b) H_2O_2:Fe^{2+} and UV light intensity on COD removal
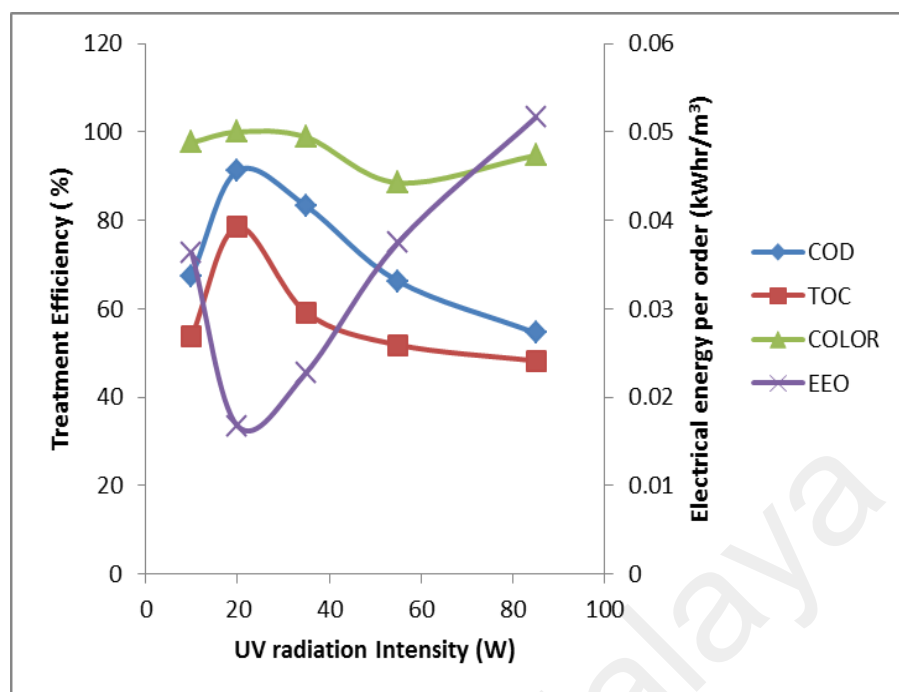
Figure 4.34: Effect of UV radiation Intensity on color, COD , TOC removals and electrical energy per order (EEO) in UV/Fe^{2+}/H$_2$O$_2$

4.3.5 Validation of the Experimental Models and Treatment of Other Type of Industrial Wastewaters

Table 4.18 shows the predicted optimum conditions and the maximum treatment efficiency (color, TOC and COD removal) by the model based on the experimental results obtained in this study. The average color removal, degradation and mineralization efficiencies obtained from three experiment replicates are presented in the Table. The model predicted 99.6 % of color, 85.4 % of COD and 71.1 % of TOC removals under the optimized working conditions. The experimentally obtained values for the UV integrated Fenton oxidation were compared with the value predicted by the model to confirm the validity of the optimization procedure under the established operating conditions.

The maximum color removal (99.9%), COD (91.2 %) and TOC (78.5 %) were obtained using the optimised operating conditions: pH=5.4, H$_2$O$_2$:COD= 8.9, H$_2$O$_2$:Fe^{2+}= 4.8,

RT= 50.7 min and UV =20W. It should be noted that 42.9 ml of H_2O_2 (stock solution of H_2O_2: 33.3mg/ml), 14.7 ml of Fe^{2+} (Stock solution of $Fe_2SO_4.7H_2O$: 100mg/l) and about 50 -100 ml NaOH and H_2SO_4 were required for pH adjustment and neutralization of the reaction for 100 ml of the real batik wastewater. It was clear that the optimum conditions for the experimental studies were identical to those predicted by the model. This implied that the strategy to optimize the operating conditions to obtain the maximum degradation and mineralization efficiency by RSM for the treatment of real wastewater was successful.

Further studies were conducted in order to determine if the model developed for the textile wastewater could be used for other types of wastewater. The validity of the RSM-predicted model for the optimum efficiency could be verified by applying the empirical model with varied initial COD values. The maximum COD removals of 98.0 %, 95.3% and 75.0% were achieved using the optimized conditions for palm oil mill effluents, leachate wastewater and wastewater from the metal finishing industry, respectively. In conclusion, the RSM model attained for the textile wastewater could be used to treat different types of wastewater.

4.3.6   Degradation Kinetics of Wastewater

The regression analyses based on zero-, first- and second-order reaction kinetics for COD removals from the wastewater was conducted and the results are shown in Figure 4.35 and Table 4.18. The first-order kinetic showed higher correlation (R^2= 0.9822) than the zero- (R^2=0.7902) and first-order (R^2=0.9409) kinetics in the case of the photo-Fenton oxidation reaction. Therefore, the first-order kinetic reaction was the best to describe the degradation of batik wastewater by the Photo-Fenton treatment system.
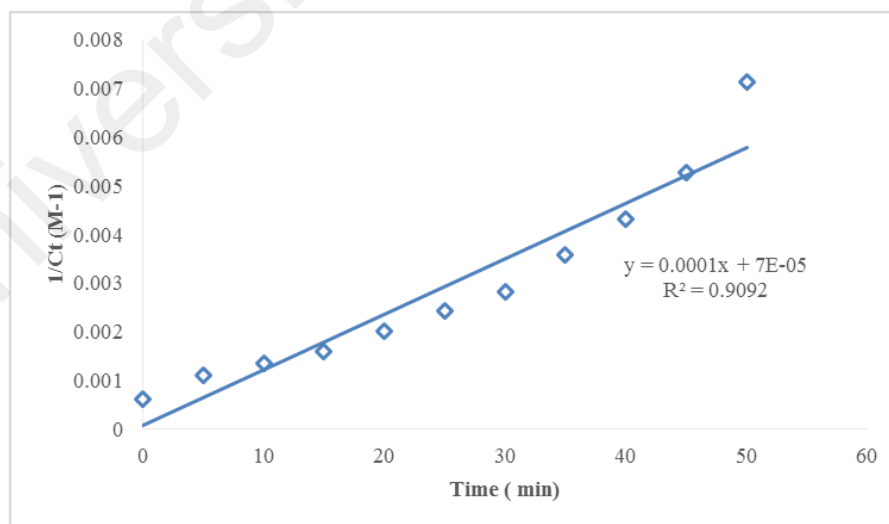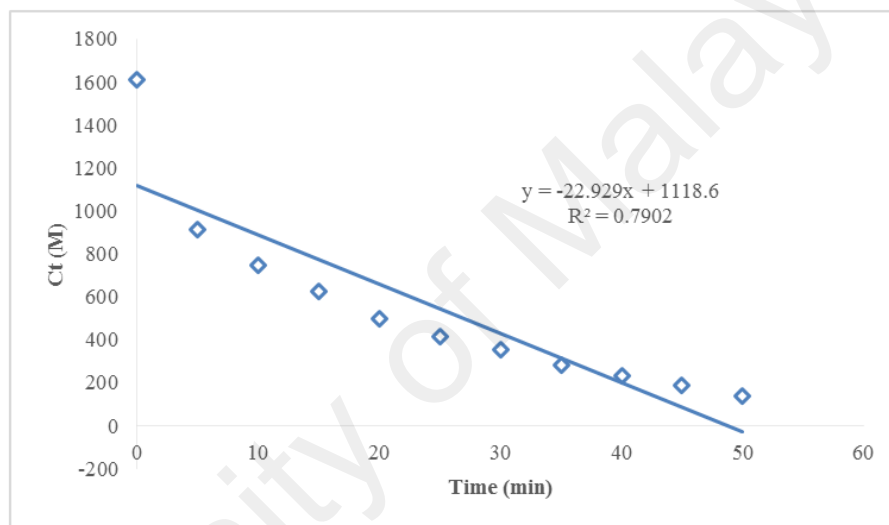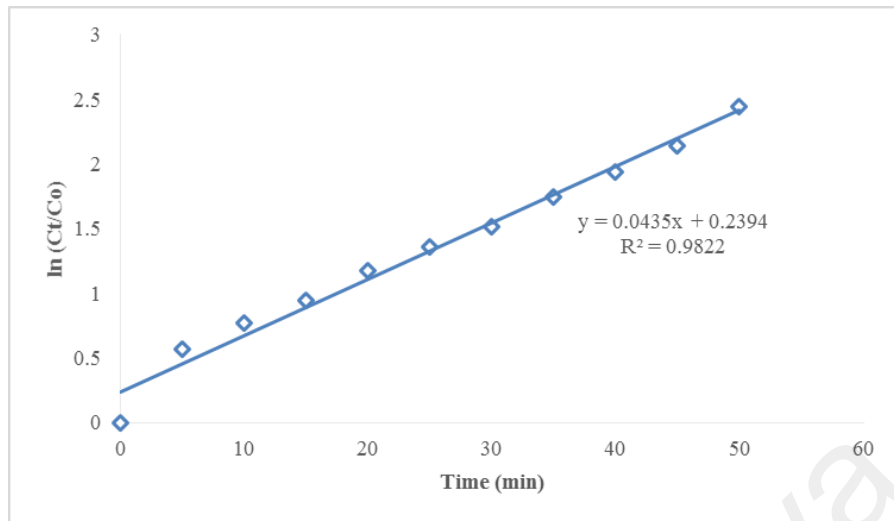
Figure 4.35: Zero, First and Second order reaction kinetics for the COD removal by UV integrated Fenton oxidation

Table 4. 18: Optimum reagent doses maximizing the percent of color, COD and TOC removal for UV-Fenton oxidation

Res.	COD (mg/l)	H_2O_2:COD	H_2O_2:Fe^{2+}	pH	RT (min)	UV (W)	H_2O_2 (ml)	Fe^{2+} (ml)	Pred. (%)	Exp. (%)
CR	1610	8.9	4.8	5.4	50.7	20	42.9	14.7	99.6	99.9
COD	1610	8.9	4.8	5.4	50.7	20	42.9	14.7	85.4	91.2
TOC	1610	8.9	4.8	5.4	50.7	20	42.9	14.7	71.1	78.5

*Res..= Response, CR= Color removal, Pred..= Predicted, Exp.= Experimental

Table 4. 19: The kinetics models and correlation coefficients for the degradation of batik wastewater by the UV integrated Fenton oxidation

Kinetics order	Expression	Regression coefficient	Kinetics Equation
Zero-order	$c_t = c_0 - -k_0\, t$	$R^2 = 0.7902$	y = -22.929x + 1118.6
First-order	$c_t = c_0 e^{-k1t}$	$R^2 = 0.9822$	y = 0.0435x + 0.2394
Second-order	$\frac{1}{c_t} = \frac{1}{c_0} + k_2\, t$	$R^2 = 0.9092$	y = 0.0001x + 7E-05

*Where C_t represents the COD of wastewater at any time (t), k_o, k_1 and k_2 represent the apparent kinetic rate constant of zero-, first- and second-order reaction kinetics, respectively and t is the reaction time.

4.3.7 Organic Contaminants Analyses of Treated Wastewater

The GC-MS results of the wastewater after the UV-Fenton oxidation process are presented in Figure 4.36. The chromatogram showed that most of the peak intensities after the UV integrated Fenton oxidation was lower than those after the Fenton process. The chromatogram showed that the UV-Fenton process more efficiently removed these inorganic compounds than the Fenton oxidation process. Besides, the hydrocarbons present may be caused by the application of wax on the cloth to fix dyes and create marbled look. Most of the peaks almost completely disappeared after the UV-Fenton process. It was concluded that the UV-Fenton process could oxidize high-molecular-weight substances into small organic compounds, which could then be readily detected by GC–MS. Besides, as can be seen in Figure 4.36 (b and c) FTIR and HPLC chromatographic analyses also confirmed the removal of organic compounds via UV-Fenton are more efficient compared to Fenton process. The FTIR, GC/MS and HPLC spectrums of real wastewater before treatment are given in the previous section (section 4.2).

a)

GC/MS Spectrum of Treated Sample
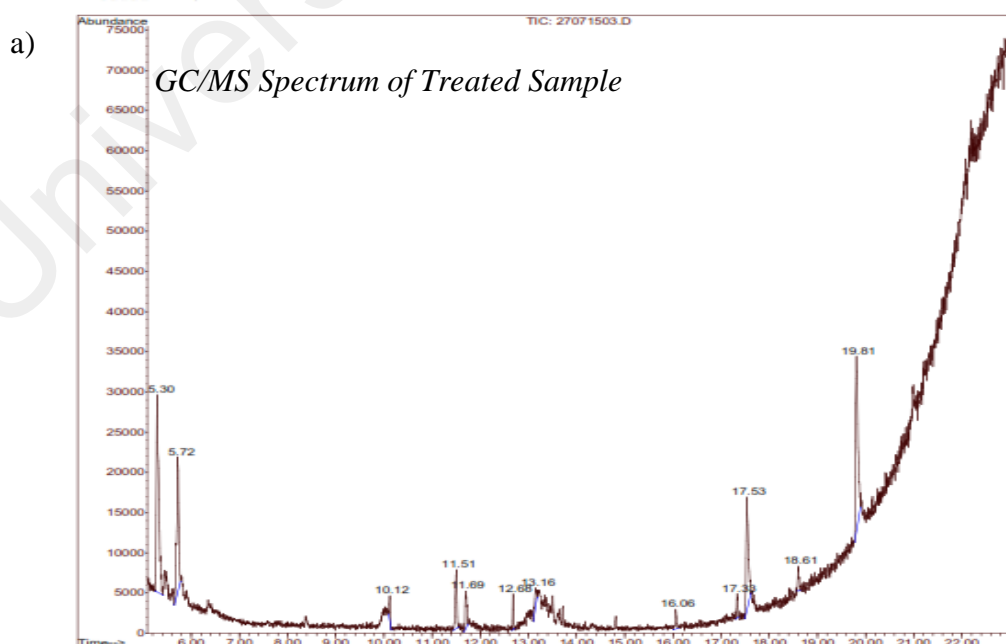
Figure 4.36: GC/MS, FTIR and HPLC spectrums of raw wastewater, after UV integrated Fenton process

164

b)

FTIR Spectrum

Raw Wastewater

After Treatment

c)

HPLC Spectrum of Treated Sample
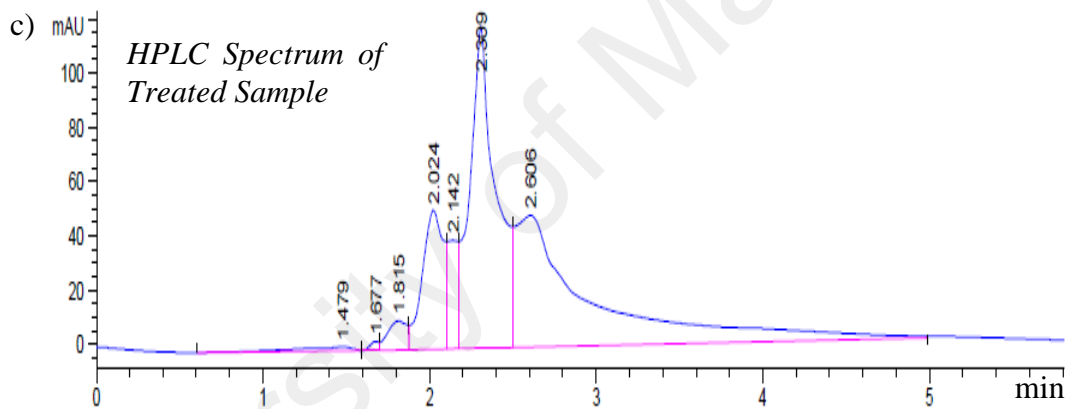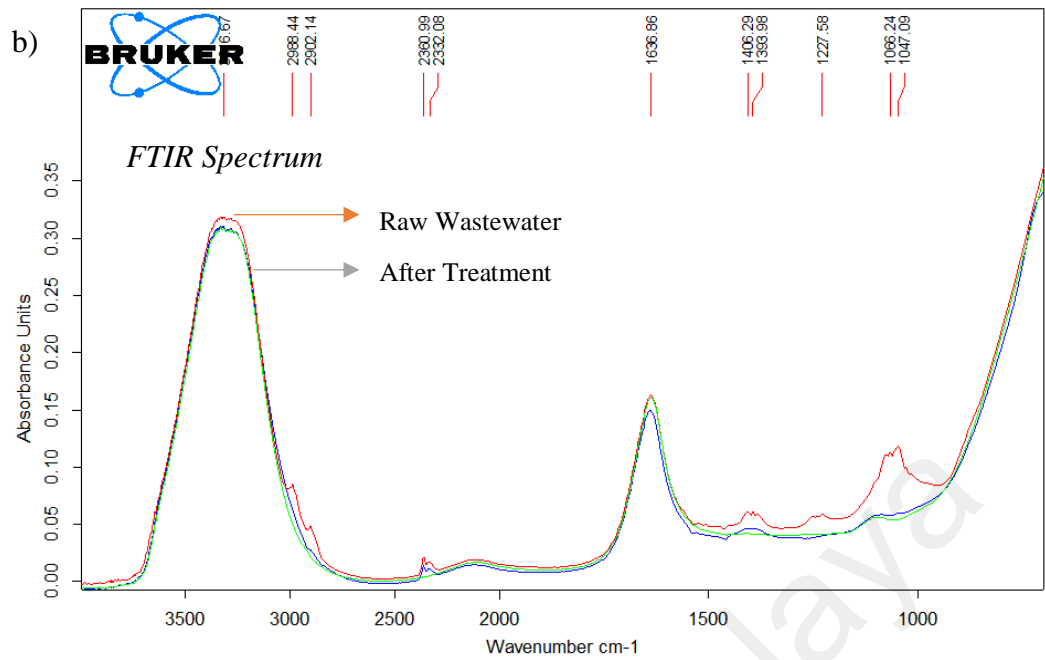
Figure 4.36: Continued

4.3.8   Sludge Characterization

UV integrated Fenton oxidation process produced sludge with a much smaller particle size that measured around 0.145 microns compared to the Fenton oxidation process (which is around 10.24- 50.78 microns) (Figure 4.37). This translated to about 99.7% reduction in the particle size of the sludge. The sludge content was found to reduce by about 20.0 % via the UV integrated Fenton oxidation process.

The concept of recycling/reusing treated water is an economical and green solution for textile industries (Hasan et al., 2011; Rashidi et al., 2012; Vergili et al., 2012). The integration of the Fenton oxidation process with membrane separation is a recommended option and this concept has been discussed in the unpublished work. Membrane separation offers a sustainable and cost effective solution to separate pollutants from wastewater. This hybrid method introduces the idea of zero waste discharge by completely recycling the treated effluent. The results obtained shows that less sludge production could reduce the cost of the treatment systems as the life expectancy of the membrane would increase as a result of less membrane fouling (Arnal et al., 2008; De Angelis et al., 2016; Rashidi et al., 2012). Besides, SEM-EDX analysis also shows the percentage of the oxygen was the most abundant element followed by sodium in the sludge generated by UV-Fenton which is in accordance with Fenton process. In addition, the sludge generation reduced up to 20% by UV integrated Fenton process.
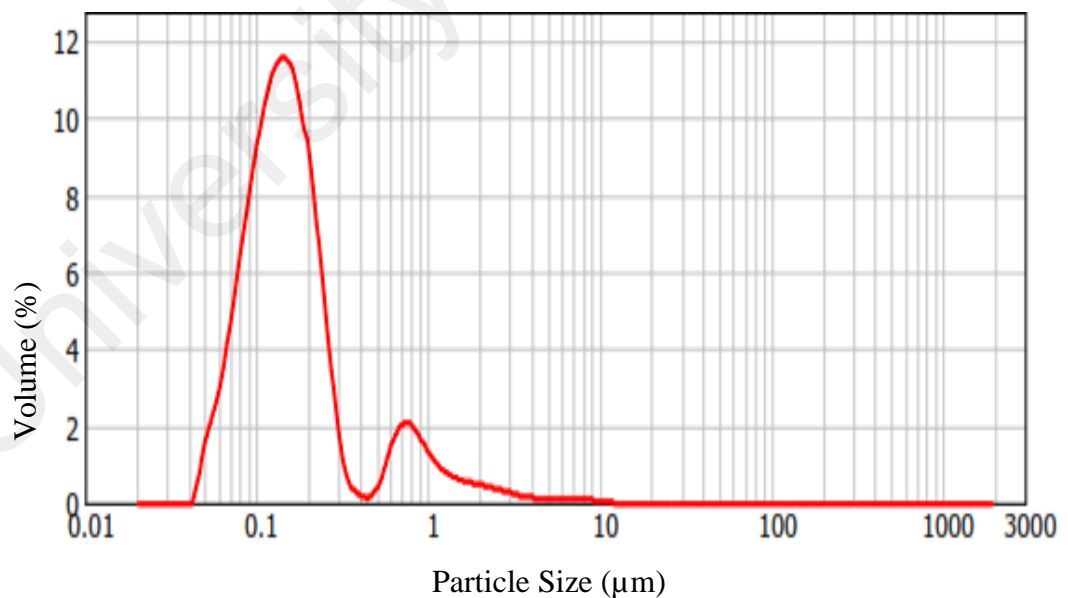
Figure 4.37: Particle size distribution of sludge generated in the UV integrated Fenton process

4.4 Comparison of UV, UV/H$_2$O$_2$, UV/Fe^{2+} and Fe^{2+} Coagulation Processes

In this study, photochemical and non-photochemical AOPs were conducted to further confirm the efficiency of UV-assisted processes. These processes include direct photolysis (UV), photolysis of hydrogen peroxide using UV light (UV/H$_2$O$_2$), UV assisted coagulation (UV/Fe^{2+}) and coagulation (Fe^{2+}). The experiments were conducted and results were compared with Fenton and UV integrated Fenton processes to treat the real textile wastewater.

4.4.1 Evaluation of UV and UV/H$_2$O$_2$ Processes

In initial stages of comparison, degradation efficiency of batik wastewater was evaluated through direct photolysis (UV alone) at 254 nm. The results show that the use of direct photolysis was not effective in the degradation of wastewater. Maximum of 10% degradation efficiency and 15% decolorization efficiency were obtained during 90 min of UV irradiation. With the increase in UV irradiation intensity from 10 to 40W, decolorization rate increased from 2 % to 10 % but increasing the UV intensity more than 40 W doesn't show any significant changes in the COD removal. The finding of this study is consistent with the previous study that UV radiation alone was not able to completely degrade organic pollutants that were present in the wastewater (Hu et al., 2011; C.-C. Lin et al.; Santos et al., 2015). The effectiveness of UV treatment is dependent on the COD values, suspended solids present in the wastewater, exposure time, and the doses of UV intensity (Oms-Oliu et al., 2010; Uslu et al., 2016). UV radiation is highly effective in destroying microorganism, does not produce any hazardous by-products that require post treatment, minimal reaction time and relatively small equipment and requires less space (Blatchley et al., 1996; Buthiyappan et al., 2015; Jaafarzadeh et al.). However, the primary challenges of using UV as a disinfectant are they require a high dosage of UV radiation for effective disinfection.

In general, the application of UV irradiation alone did not achieve significant results in the degradation of pollutant. To improve the process efficiency, UV integrated with the H_2O_2 process was studied. Photolysis of hydrogen peroxide using UV radiation (by photons of wavelengths <300 nm) generates powerful HO·) (De la Cruz et al., 2013). A total of 30 experiments were conducted to investigate the efficiency of H_2O_2/UV for the organic pollutant removal from raw textile wastewater (Table 4.20). Four operating parameters including the concentration of H_2O_2, intensity of light, retention time and initial pH were examined to find the optimal condition to achieve maximum treatment efficiency. Replicates were used to estimate the experimental error and accuracy of the model. Experiments were made in a random order to minimize the effects of variability in the observed responses due to extraneous factors.

2D contours as shown in Figure 4.38(a, b and c) were used to study the interaction of independent variables for the COD removal efficiency. As shown in Figure 4.40 (a) the COD removal efficiency increases with increase in H_2O_2 concentration. Maximum of 64% degradation efficiency was obtained at 3800 mg/L of H_2O_2. However, at concentrations higher than 3800 mg/L, a decrease in COD removal efficiency was observed. This is because, an excessive amount of H_2O_2 results in a competitive reaction, which reduce the degradation efficiency (Schrank et al., 2007; X.-R. Xu et al., 2009). Hydroxyl radicals are prone to recombine with each other and produce inhibitory effect on the rate of reaction (Hu et al., 2011; Santos et al., 2015). Beside H_2O_2 concentration, pH was also found to have a significant impact on the treatment efficiency of UV/H_2O_2 process. As shown in Figure 4.38 (a)), an increase in COD removal efficiency (62. 4 %) was obtained when pH was increased from 3 to 5. Nevertheless, a further increase in pH value resulted in a decrease in COD removal efficiency to 52.9 %.

Figure 4.38 (b) illustrates the combined effect of H_2O_2 concentration and UV intensity on COD removal efficiency. The COD removal efficiency was observed to increase with initial H_2O_2 concentration and UV intensity at fixed retention time of 60 minutes and initial pH of 5.5. However, the marginal benefit decreased with further increase in both H_2O_2 concentration and UV intensity. Besides, the results obtained indicate that, significant COD removal can be achieved by prolonging the treatment time to an hour and above compared to Fenton-based processes (Figure 4.38 (c)).

In summary, based on experimental results, a maximum of 68% COD, 50% TOC and 75% color removal efficiency were obtained within 80 min at optimum conditions of 3364 mg/l H_2O_2, pH 4 and 35 W UV intensity. Thus, the finding of the experimental study confirms that UV/H_2O_2 process required longer time, and higher amount of H_2O_2 to achieve the maximum COD removal efficiency in comparison with UV-integrated Fenton process.

Table 4.20: Observed percent of degradation, mineralization and decolorization efficiencies under different experimental conditions

Run	H_2O_2 (mg/l)	pH	Ret. Time (min)	UV Intensity (W)	COD (mg/l)	TOC (mg/l)	Color (ADMI)
1	4000	2.0	90	55	60.3	50.1	65.2
2	4000	9.0	90	15	55.2	40.1	60.3
3	100	9.0	90	55	35.2	15.1	68.1
4	100	9.0	30	15	42.4	30.3	65.3
5	4000	2.0	30	15	45.1	32.3	71.8
6	4000	9.0	30	55	50.3	41.5	76.2
7	100	2.0	90	15	51.2	35.0	79.0
8	2050	5.5	60	35	65.1	54.5	76.3
9	2050	5.5	60	35	63.3	46.1	77.1
10	100	2.0	30	55	49.2	37.6	66.3
11	2050	5.5	60	35	65.5	45	71.7
12	100	2.0	90	55	53.2	41.2	70.0
13	100	9.0	30	55	49.1	34.2	64.2
14	100	2.0	30	15	43.4	35.2	60.0
15	2050	5.5	60	35	65.1	55.5	72.3
16	4000	9.0	30	15	50.4	40.7	72.1
17	4000	2.0	90	15	63.2	52.5	71.2
18	4000	9.0	90	55	50.1	51.3	62.4
19	100	9.0	90	15	40.3	30.8	65.7
20	4000	2.0	30	55	49.2	35.2	73.2
21	2050	5.5	120	35	42.3	34.5	55.2
22	2050	5.5	60	75	25.2	15.3	71.5
23	2050	1.5	60	35	50.1	40.2	58.2
24	2050	5.5	60	35	59.1	49.0	56.2
25	5950	5.5	60	35	53.3	40.1	68.2
26	2050	12.5	60	35	45.2	32.0	50.5
27	2050	5.5	0	35	34.3	20.2	55.1
28	1850	5.5	60	35	42.1	30.5	60.0
29	2050	5.5	60	35	58.2	48.0	62.1
30	2050	5.5	60	5	25.3	10.3	65.0
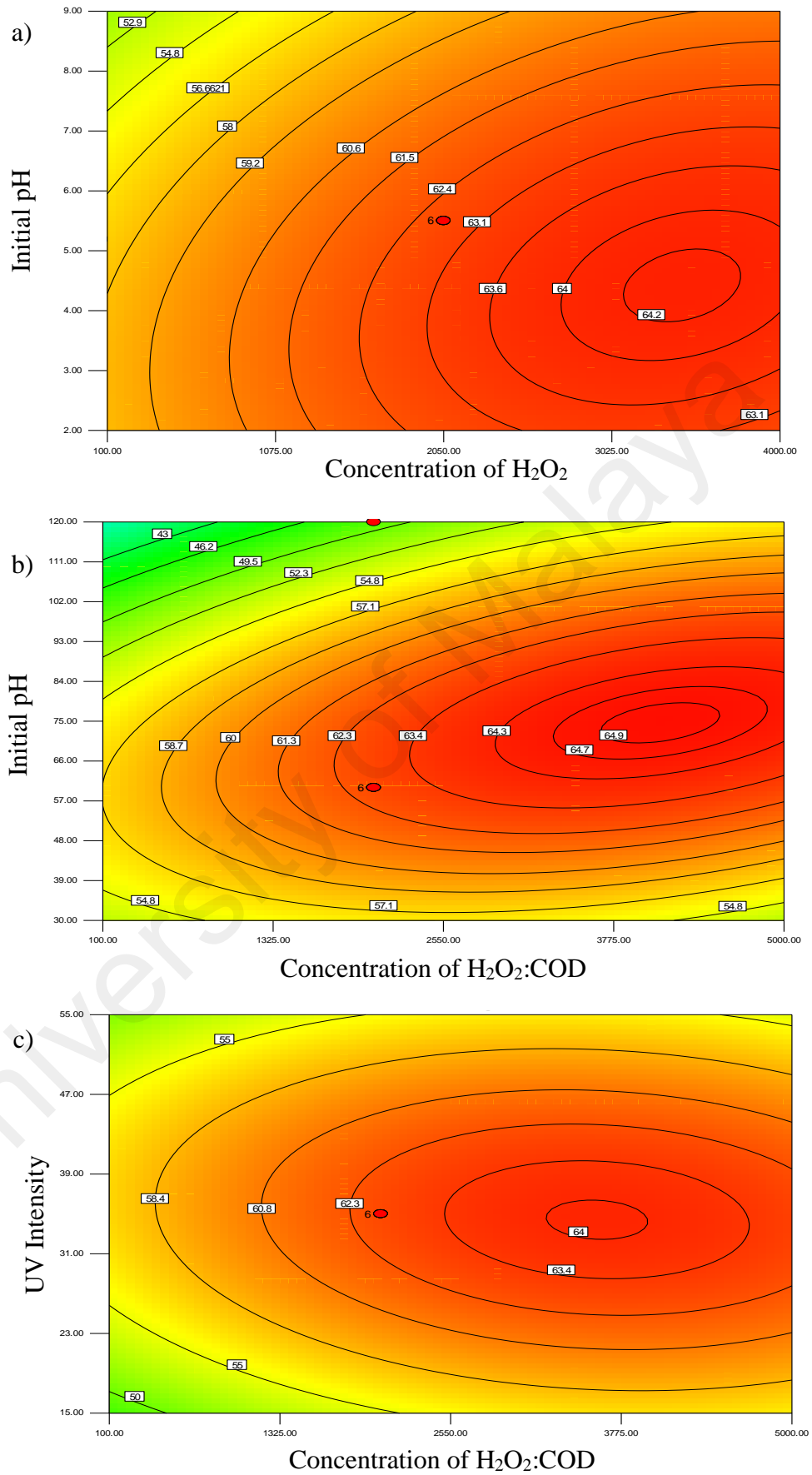
Figure 4.38: Interaction effects of different parameters on the percent COD removal

4.4.2 Treatment Efficiency of Fe^{2+} and UV-Fe^{2+} Coagulation Processes

Fenton process is a two-staged process, comprising of oxidation and coagulation processes. The contribution of oxidation stage to COD removal efficiency is already confirmed through the UV-H_2O_2 process. Nevertheless, the contribution of coagulation to COD removal efficiency is not elucidated yet. Therefore, Fe^{+2} and UV-Fe^{+2} processes were carried out to investigate the effect of coagulation on COD removal efficiency. Ferrous and Ferric ions were used as a source of coagulation. Initial pH, retention time and dosage of Fe^{2+} were selected as operating parameters selected for coagulation process.

A total 30 experimental runs were performed under different experimental conditions in accordance with the experimental runs proposed by the model used for ferrous sulfate (Fe^{2+}) coagulation. Fe^{2+} coagulation of the raw wastewater was examined at pH 2-9 at a coagulant dose of 0.5- 48.0 ml and retention time were varied between 30 to 90 minutes. COD removal efficiency was varied between 20- 45% for the investigated textile effluent. Fe^{2+} coagulation process exhibited a maximum removal efficiency of 43 % at pH 6.5, Fe^{2+}= 6.1 ml and retention time of 80 minutes. And relatively low COD removal (10-20%) rates were obtained at other investigated values. From experimental results, it was also observed that increase in Fe^{2+} dosage results in an increase in percent COD removal efficiency. However, beyond the optimum value resulted in the decrease in the percent of COD removal, because of the scavenging effects caused by excess amount of unreacted Fe^{2+}. As can be observed in plot, increases in the Fe^{2+} dosage from 6.5 ml to 16.5 ml, showed a remarkable decrease in the percent of COD removal efficiency. The COD removal efficiency was observed between 55.8% and 33.7%. Comparatively, low removal was obtained for varying Fe^{2+} doses between 0.5 and 4 ml, at pH 2.

Therefore, it can be concluded that Fe^{2+} coagulation process depends on pH and Fe^{2+} dosage. Optimization of these parameters is important to enhance the degradation efficiency (Figure 4.39). Higher coagulation efficiency (65.8%) is achieved at pH 6.5 may be because at this pH, wastewater has lower solubility and ionization rate. It should be noted that, higher decolorization efficiency (>60%) was also observed at pH 6.5. In addition to pH, reaction time was also observed to play a crucial role to enhance the efficiency of the coagulation process. Percent of COD removal efficiency increased with increase in the retention time as can be seen in Figure 4.39 (b). But beyond optimal value (> 75 minutes) decreases in the COD removal was observed because the remaining turbidity has decreased the coagulation efficiency.

Following Fe^{+2} coagulation experiments, UV/Fe^{+2} process was investigated to determine the effect of UV on Fe^{+2} coagulation. The COD removal was increased from 34-63% when 40W UV light was used at the pH value of 5.5. This value was significantly higher than that of Fe^{2+} coagulation process. Besides, it was also observed that minimal sludge was generated at optimized condition compared to Fe^{2+} coagulation. The negative effect of excess ferrous ions was also observed as reported in previous works (Ryu et al., 2009). Table 4.21 summarize the degradation efficiency and optimized conditions of both Fe^{2+} coagulation and UV- Fe^{2+} coagulation processes.

In summary, it can be concluded that Fe^{+2} and Fe^{2+}/UV processes are not as efficient as UV intergraded Fenton process. Fe^{2+} and Fe^{2+}/UV processes require excess amount of Fe^{2+} salt which eventually transformed into excessive iron sludge, thus requiring a post-treatment process. Further investigation regarding the characterization and the quality of the solids sludge is required that the two methods produced.

Table 4.21: Comparison of Fe^{2+} and UV-Fe^{2+} Coagulation processes

Processes	Fe^{2+} Coagulation	UV- Fe^{2+} Coagulation
Degradation Efficiency (%)		
i. Minimum COD removal	20	36
ii. Maximum COD removal	43	55
Fe^{2+} Consumption (mg)	123	100
Initial pH	6.5	5.5
Mixing Speed (rpm)	350	350
Retention Time	90	80
UV intensity (W)	N/A	40
Solid Generated (mg/l)	High	High
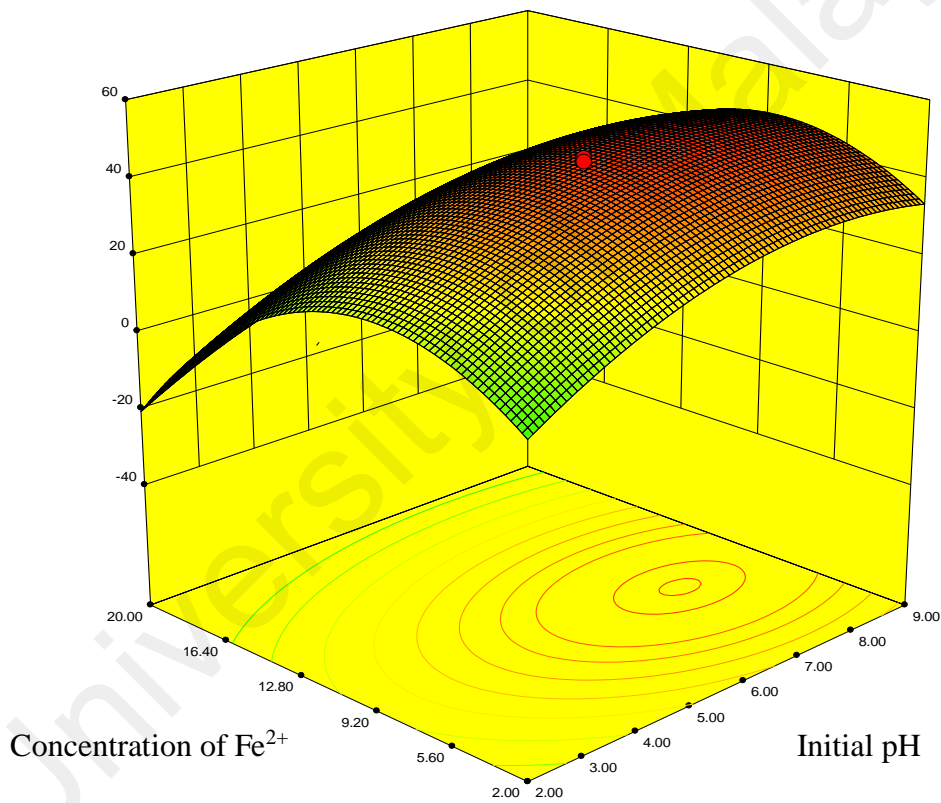
Figure 4.39: 3D contours represent the interaction effects of different parameters on COD removal:
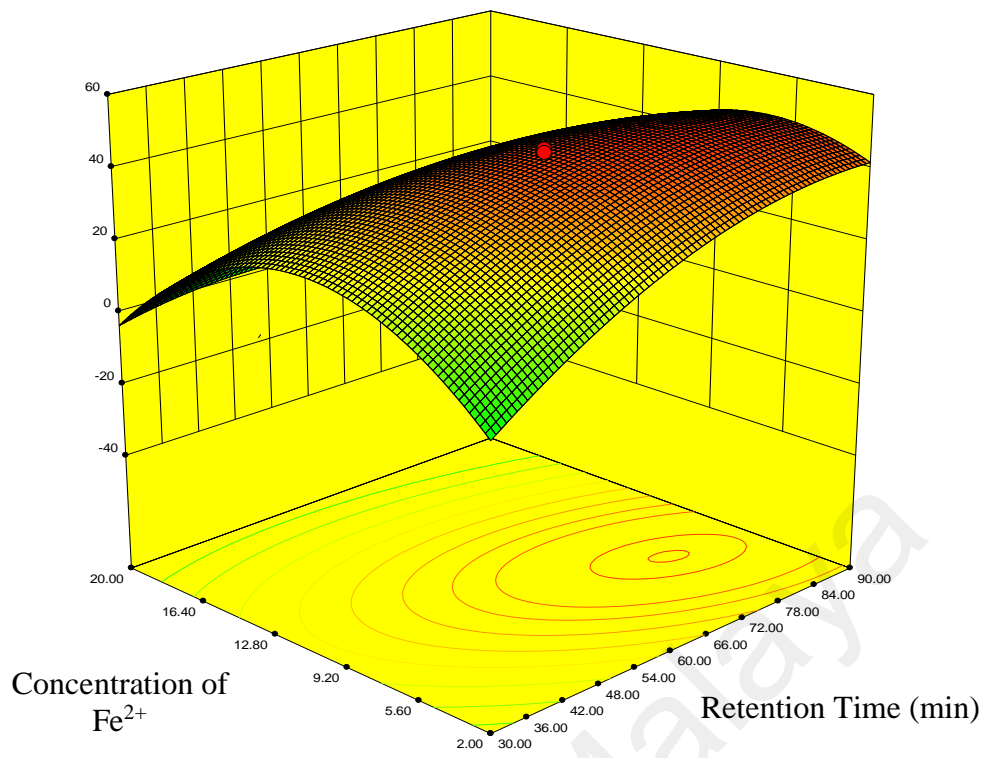
Figure 4.39: Continued

4.5 Comparison of Processes

In this study, all the photochemical and non-photochemical AOPs are compared in terms of COD removal, type of treatment, generation of sludge, pH condition, visual aesthetics of treated effluent, treatment complexity, and energy requirement as can be seen in Table 4.23.

As can be observed from Table 4.22, among the processes evaluated, direct photolysis (UV alone) is found to be less effective for the degradation of wastewater, resulting in a COD removal efficiency of 10% and color removal efficiency of 15% in 60 min. The highest COD removal was achieved in UV integrated Fenton oxidation (91 %), followed by Fenton (81 %), UV/H$_2$O$_2$ (68 %), UV assisted Fe^{2+} coagulation (55 %), Fe^{2+} coagulation (43 %) and direct photolysis (10 %). Figure 4.40 shows the treatment efficiency in terms of COD% removals and electrical energy per order (EE/O) after the application of UV, Fe^{2+} coagulation, Fe^{2+}/H$_2$O$_2$, UV/Fe^{2+} coagulation, UV/H$_2$O$_2$, UV/Fe$^{2+/}$H$_2$O$_2$.
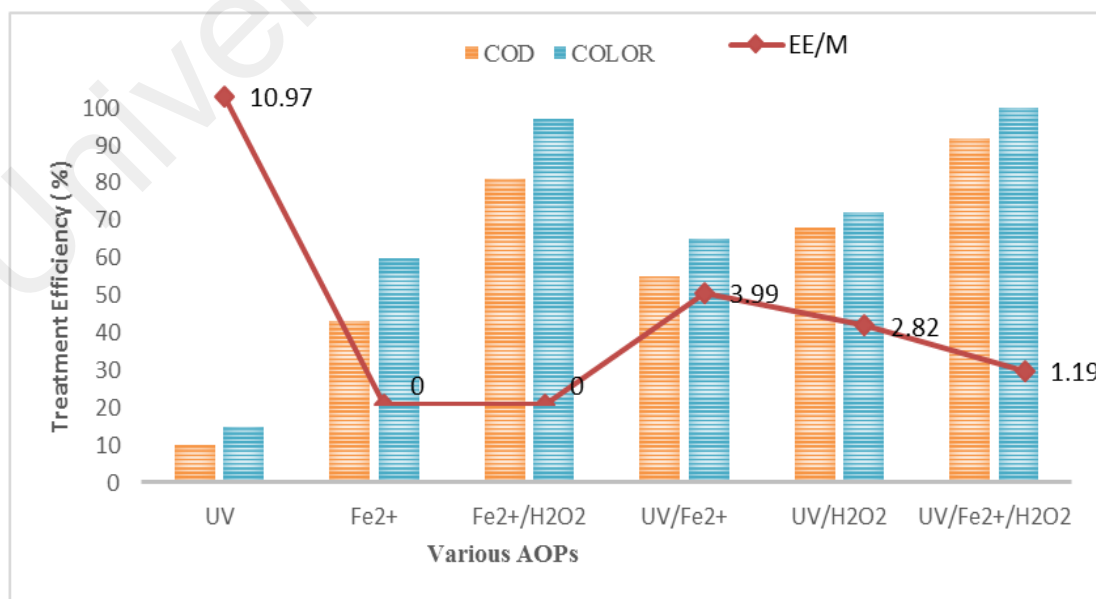
Figure 4.40: Fe^{2+}/H$_2$O$_2$, UV/Fe^{2+}, UV/H$_2$O$_2$, UV0/Fe^{2+}/H$_2$O$_2$ on color ad COD removal and electrical energy per order (EE/M)

The treatment efficiency of UV/H₂O₂ is better compared to direct photolysis due to the formation of more $HO\cdot$ by photolysis reaction of H₂O₂. Besides, although UV/H₂O₂ system has a neutralization step, no sludge was generated. Degradation accomplished with the UV/H₂O₂ treatment did not results in complete degradation of organic pollutants and may lead to the formation of intermediate recalcitrant compounds, which can increase the toxicity of the treated wastewater.

Fenton process enhances the biodegradability of refractory organic pollutants based on the generation of strong and relatively non-selective $HO\bullet$ radical. The $HO\bullet$ radical produced through the catalytic reaction of Fe^{2+} with hydrogen peroxide can be increased by the action of UV light.

Figure 4.40 shows that Fe^{2+}/H_2O_2 yielded higher COD and TOC removal efficiencies of 81.4% and 70.5 %, respectively, and almost complete color removal (97%). But in the UV integrated Fenton process, much higher treatment efficiencies were observed. The maximum color removal (99.9%), COD removal (92 %) and TOC removal (78.5 %) were obtained within irradiation time of 51 min and initial pH of 5.36. The UV integrated Fenton process exhibited higher degradation efficiency at short reaction time compared to the Fenton process due to continuous and more generation of reactive oxygen species, especially $HO\bullet$ radical. Besides, the Fenton process is also able to increase the rate of contaminants removal under UV irradiation by stimulating the photoreduction of Fe^{3+} to Fe^{2+}.

The need for acidification in the Fenton-based process is often considered as a major drawback. Although radical production is favored at the acidic condition, but the result obtained in this study shows that high COD and TOC removal efficiencies were achieved at pH close to 7. Besides, UV radiation also reduced the amount of sludge generated by 20% compared to Fenton process.

However, lower COD and TOC removal efficiencies were obtained with Fe^{2+} and UV/Fe^{2+} processes without the addition of H_2O_2, as seen in Figure 4.40. It is observed that coagulation with Fe^{2+} or with the presence of UV is able to remove organic pollutants from real wastewater although both processes are not efficient as Fenton and UV integrated Fenton processes.

4.5.1 Electrical Energy per Order Evaluation

Unlike Fenton and Fe^{+2} coagulation processes, UV photolysis, H_2O_2/UV, UV/Fe^{2+} coagulation and $Fe^{2+}/H_2O_2/UV$ are energy dissipative processes. In UV integrated-Fenton processes, 92% degradation efficiency was achieved at the minimum consumption of electrical energy per order (EE/O) of 1.19 kWhr/m^3. Among the processes investigated in this study, UV photolysis consumed a large amount of energy (10.97 kWhr/m^3), followed by UV-Fe^{2+} coagulation (4.00 kWhr/m^3). The addition of hydrogen peroxide into the UV treatment system increased the degradation efficiency and thus lowered the energy consumption (2.82 kWhr/m^3) compared to the UV treatment alone (Figure 4.40).

4.5.2 Economical Analysis

For economic evaluation, AOPs achieving more than 80% degradation efficiency were considered. In this study, Fenton and UV-Fenton processes were observed to show high degradation efficiencies. The comparison was made in terms of the cost of reagents and power consumption. For this purpose, the results obtained under optimized condition were considered and information regarding the cost of commercially grade chemicals and electricity was obtained. The electricity cost is 0.38 RM/kWh, hydrogen peroxide (30 %) price is 140 \$/ton and iron (II) sulfate heptahydrate price is 100 \$/ton (industrial price). Both processes were scaled up to 1m^3 batch process containing 1610g of COD value. The result as can be seen from Figure 4.41 shows that UV integrated Fenton process is cost

effective with highest degradation efficiency of 91%. In this study, UV integrated Fenton process costs $0.0016/g of COD in comparison with Fenton process which costs $0.0021. Since the COD of the wastewater is varying based on manufacturing processes, the scaled up study for 15,000 mg/l of COD (maximum COD values of textile industry wastewater as reported in the literature) was also conducted. The treatment cost of $0.024 and $0.032, was obtained to treat 15 g of COD using UV integrated Fenton process and Fenton process respectively. Accordingly, 24 % reduction in the cost was observed with UV integrated Fenton process. Furthermore, the amount of Fe^{2+} and H_2O_2 required in the Fenton process is very high (10 % more than UV integrated Fenton process) which led to the generation of large volume of sludge. Thus, it requires further treatment which adds up to the overall cost of the process.
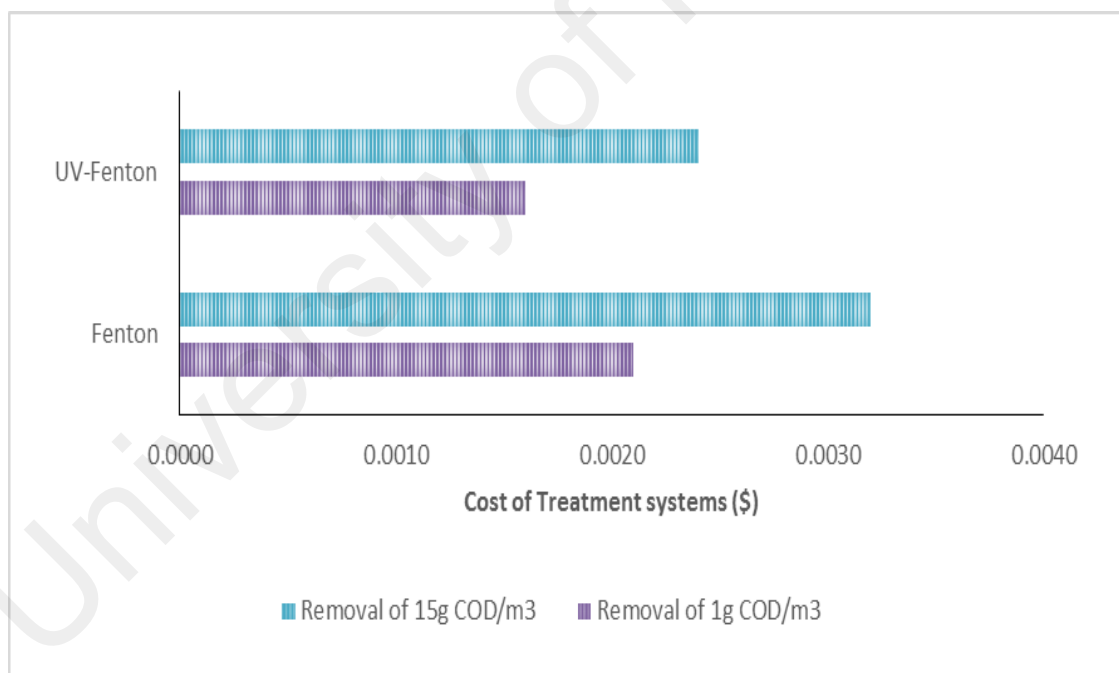
Figure 4.41: Comparison of chemical consumptions and estimated cost of Fenton and UV-Fenton process

Table 4.22: Comparison of processes

Factors	UV	Fe^{2+}	UV/Fe^{2+}	UV/H_2O_2	Fe^{2+}/H_2O_2	$UV/Fe^{2+}/H_2O_2$
Degradation Efficiency	10 %	43 %	55 %	68 %	81 %	91 %
Color removal	Low	Medium	Medium	Low	High	High
pH requirement	Acidic	Acidic	Alkaline	Acidic	Acidic to Neutral	Acidic to Neutral
Type of treatment	Physical & Chemical 0xidation	Physical	Physical & Chemical Oxidation	Physical & Chemical Oxidation	Physical & Chemical Oxidation	Physical & Chemical Oxidation
Sludge	No	Significant	Significant	No	Significant	Significant
Visual aesthetics of treated effluent	Clear	Yellowish	Yellowish	Clear	Yellowish	Yellowish
Treatment complexity	Low	Low	Moderate	Moderate	Moderate	Moderate
Chemical consumption	Low	Medium	Medium	High	High	High
Energy requirement	High	Low	High	High	Low	Medium

CHAPTER 5: CONCLUSION

5.1 Conclusion

In this study, the treatment efficiencies of the Fenton process and UV integrated Fenton oxidation hybrid process were evaluated using a laboratory sized experimental setup for batik industrial wastewater. The aim of the study is to develop a simple, stand-alone, small and highly efficient treatment system by integrating Fenton process with UV radiation for small-scale industries. Seven parameters were used to compare the effectiveness of these processes, namely: COD removal, TOC removal, decolorization efficiency, chemical consumption, pH condition, sludge formation, visual aesthetic of effluent, energy requirement and operational cost. Studies on the treatment efficiencies of direct photolysis, UV/H_2O_2, UV/Fe^{2+} coagulation and Fe^{2+} coagulation were also compared.

An RSM-CCD optimization tool was successfully used to determine the most significant operating parameters and optimum ratios of pollutant:oxidant:catalyst to increase the removal efficiencies, while reducing the operating cost directly. The experimental design developed using RSM-CCD was proven to be efficient in evaluating the critical effects of the selected operating parameters, the mass ratio of H_2O^2:COD and H_2O_2:Fe^{2+}, retention time, UV radiation intensity and initial pH of the wastewater. The GC/MS, FTIR and HPLC analyses of pre and post treated wastewater samples were used to evaluate the organic contaminant destruction based on the disappearance of functional groups. Since sludge formation is one of the biggest falling of the conventional Fenton process attention was given to the properties and volume of sludge generated in both the Fenton and UV integrated Fenton oxidation hybrid processes. This work also validated the application of the model developed for batik wastewater for other industrial

wastewater including palm oil mill effluent (POME), landfill leachate and metal finishing wastewater. The main conclusions derived from the study based on the defined objectives and related activities are as follows:

Objective 1

1. Among the processes evaluated, the highest COD removal was achieved for the UV integrated Fenton oxidation (91 %) process, followed by the Fenton process (81 %), the UV/H_2O_2 (68 %) process, the UV assisted Fe^{2+} coagulation (55 %) process, the Fe^{2+} coagulation (43 %) process and the direct photolysis (10 %) process.

2. This study clearly demonstrated that the UV integrated Fenton oxidation exhibited higher COD, TOC and color removal efficiencies compared to other investigated AOPs. The maximum color removal (99.9%), COD removal (91.2 %) and TOC removal (78.5 %) were achieved at the optimum operating condition (initial pH of the wastewater=5.36, mass ratios of H_2O_2:COD= 8.87 and H_2O_2:Fe^{2+}= 4.82, retention time= 50.7 min and UV radiation intensity =20W). The solution became colorless even more rapidly using the UV integrated Fenton oxidation process owing to the production of larger amounts of $HO\bullet$ radical. The Fenton process shows 99.6 %, 81.4 % and 70.5%, of color, COD and TOC removal efficiencies, respectively under the optimum conditions of H_2O_2:COD= 10.18, H_2O_2:Fe^{2+}= 4.74, initial pH=4.77 and retention time of 63.4 min.

3. A reduction in the Fenton reagent consumption (10 %), volume of sludge (20 %) and reaction time was observed in the UV integrated Fenton oxidation hybrid process in comparison with the Fenton process. The UV integrated Fenton oxidation process produced sludge with a much smaller particle size that measured around 0.145 microns compared to the Fenton oxidation process (1024 to 50.78 microns). This translated into about 99.7% reduction in the particle size of the sludge.

4. The instrumental analyses (FTIR, GC/MS, and HPLC) of the treated samples revealed that the UV integrated Fenton oxidation could oxidize high-molecular-weight substances into small organic compounds. The GC/MS analysis confirmed that the UV integrated Fenton oxidation successfully removed about 87% of siloxanes from batik wastewater. Additionally, the HPLC analysis showed that the treated effluent contained a small amount of carboxylic acids and sodium ions, which was in accordance with the GC/MS analysis.

5. The kinetic study showed that the UV integrated Fenton oxidation best fit the first-order kinetic reaction with higher reaction rate compared to the Fenton process.

6. The treatment efficiency of the H_2O_2/UV process was better compared to the UV process alone due to the formation of more $HO\bullet$ radicals by the photolysis reaction of H_2O_2. A considerable advantage of the UV/H_2O_2 was is that there was no sludge generated. However, the treatment efficiency of UV/H_2O_2 was not remarkable and it required a very long reaction time compared to the UV integrated Fenton oxidation process. In addition, the Fe^{2+} and UV/Fe^{2+} coagulation processes were not advantageous since they required a high concentration of Fe^{2+} and most importantly produced a large amount of sludge that requires post treatment.

Objective 2

1. Based on the economical analysis conducted, it was confirmed that the UV integrated Fenton oxidation process was the cheapest with the highest removal efficiency (91.2%) as it required only \$0.0016 to degrade 1g of COD compared to Fenton process which cost \$0.0021. Accordingly, compared to the Fenton oxidation process, a 24 % reduction in the cost was observed with the integrated UV Fenton oxidation process.

2. It was confirmed that the UV integrated Fenton oxidation process was highly effective for degradation of textile wastewater with the minimum electrical energy per order (EE/O) of 1.19 kWhr/m^3 compared to other photochemical AOPs.

3. The sludge characterization studies by SEM/EDX and PSD showed that the UV integrated Fenton oxidation process generated sludge with the suitable quality for disposal.

Objective 3

This study also confirmed that the COD, TOC and Color removal models developed for batik wastewater could be applied for wastewater from palm oil mills, leachate and metal finishing industry with various COD values that require smaller treatment systems. The results indicated that the models could be used to design and operate a mini treatment plant to treat any recalcitrant wastewater containing high TOC and COD.

5.2   Recommendation for Future Work

Although the scope of the current work is wide, the following aspects could be explored further to obtain more information and insight into hybrid Fenton systems.

1. Utilization of the UV integrated Fenton oxidation process as a pre-treatment to biological treatment.

2. Investigation of different types of lamps and photo-reactors with different configurations (annular reactors with coaxial or perpendicular lamp positions, an external lamp with reflectors, contact-free photo-reactors).

3. The $HO\bullet$ radical exposure distribution should be evaluated for each UV-based system.

4. A detailed study on the scavenging effect as it could adversely affect the treatment efficiency and cause the formation of by-products that could possibly increase the COD, TOC, total suspended solids (TSS) and toxicity value.

5. CFD models can be used to determine the performance of different UV-AOP systems. For scale-up, a proper and accurate kinetic model needs to be developed based on the types of pollutants as the reaction pathways solely depend on the parental compounds, intermediates and final products. The intermediates formed during the reaction should also be analyzed. It is important because they can increase the toxicity of the reaction solution sometimes.

6. High water consumption in industries causes excessive and irresponsible use of groundwater, so zero water discharge can contribute to the conservation and replenishment of groundwater resources. Since no effluent will be produced in the zero water discharge system, it will eliminate the cost required to process the discharge water after treatment. Since most of the UV-AOPs system managed to achieve higher COD and TOC value, it is suggested to look into the modification of the UV-based AOPs system by integrating the filtration system and designing a hybrid system which could recycle the water into the system.

5.3 Knowledge Contribution

Four high-impact publications have been generated from this work and two more publications are under review. The details are given in Appendix A. The following is the knowledge contribution from this work.

1. Development of a systematic methodology that can be used to set up a batch-scale UV integrated Fenton oxidation process using UV-C irradiation.

2. Development of a model that can be used to determine the effect various operating parameters on the treatment efficiency of a wide range of recalcitrant wastewater.

3. Kinetic information obtained from this study can be used as a foundation to develop a reliable kinetic model, which can be used to design Fenton reactors.

4. Methods to identify intermediate organic compounds were synthesized using FTIR, GC/MS and HPLC.

5. A simple procedure was developed to determine the treatment cost for the selected hybrid Fenton process based on the chemical and energy consumption.

REFERENCES

Ahmad, M. A., Herawan, S. G., & Yusof, A. A. (2014). Equilibrium, Kinetics, and Thermodynamics of Remazol Brilliant Blue R Dye Adsorption onto Activated Carbon Prepared from Pinang Frond. *ISRN Mechanical Engineering, 2014*, 7.

Akan, J. C., Abdulrahman, F. I., Ayodele, J. T., & Ogugbuaja, V. O. (2009). Impact of tannery and textile effluent on the chemical characteristics of Challawa River, Kano State, Nigeria. *Australian Journal of Basic and Applied Sciences, 3*(3), 1933-1947.

Al-Amrani, W. A., Lim, P.-E., Seng, C.-E., & Wan Ngah, W. S. (2014). Factors affecting bio-decolorization of azo dyes and COD removal in anoxic–aerobic REACT operated sequencing batch reactor. *Journal of the Taiwan Institute of Chemical Engineers, 45*(2), 609-616.

Al-Kdadi, A., Idris, A., Katayon, S., & Teong Guan, C. (2004). Treatment of Textile Wastewater by Advanced Oxidation Processes- A Review. *Global Nest: the Int.J., 6*, 222-230.

Alaton, I. A., & Teksoy, S. (2007). Acid dyebath effluent pretreatment using Fenton's reagent: Process optimization, reaction kinetics and effects on acute toxicity. *Dyes and Pigments, 73*(1), 31-39.

Aleboyeh, A., Moussa, Y., & Aleboyeh, H. (2005). The effect of operational parameters on UV/H2O2 decolorisation of Acid Blue 74. *Dyes and Pigments, 66*(2), 129-134.

Ali, H., & Muhammad, S. K. (2008). Biodecolorization of acid violet 19 by Alternaria solani. *African Journal of Biotechnology, 7*(6), 831-833.

Ali, M. E. M., Gad-Allah, T. A., & Badawy, M. I. (2013). Heterogeneous Fenton process using steel industry wastes for methyl orange degradation. *Applied Water Science, 3*(1), 263-270

Alinsafi, A., Khemis, M., Pons, M. N., Leclerc, J. P., Yaacoubi, A., Benhammou, A., & Nejmeddine, A. (2005). Electro-coagulation of reactive textile dyes and textile wastewater. *Chemical Engineering and Processing: Process Intensification, 44*(4), 461-470.

Alkan, U., Teksoy, A., Atesli, A., & Baskaya, H. S. (2007). Efficiency of the UV/H2O2 process for the disinfection of humic surface waters. *J Environ Sci Health A Tox Hazard Subst Environ Eng, 42*(4), 497-506.

Allègre, C., Moulin, P., Maisseu, M., & Charbit, F. (2006). Treatment and reuse of reactive dyeing effluents. *Journal of Membrane Science, 269*(1–2), 15-34.

Alvárez', P. M., Beltrán, F. J., Masa, F. J., & Pocostales, J. P. (2009). A comparison between catalytic ozonation and activated carbon adsorption/ozone-regeneration processes for wastewater treatment. *Applied Catalysis B: Environmental, 92*(3-4), 393-400.

Amaral, F. M., Kato, M. T., Florêncio, L., & Gavazza, S. (2014). Color, organic matter and sulfate removal from textile effluents by anaerobic and aerobic processes. *Bioresource Technology, 163*(0), 364-369.

Amat, A. M., Arques, A., Miranda, M. A., & Lopez, F. (2005). Use of ozone and/or UV in the treatment of effluents from board paper industry. *Chemosphere, 60*(8), 1111-1117.

Archina, B., Abdul Aziz, A. R., & Wan Mohd Ashri, W. D. (2015). Degradation performance and cost implication of UV-integrated advanced oxidation processes for wastewater treatments. *Reviews in Chemical Engineering, 31*(3), 263-302.

Arnal, J. M., León, M. C., Lora, J., Gozálvez, J. M., Santafé, A., Sanz, D., & Tena, J. (2008). Ultrafiltration as a pre-treatment of other membrane technologies in the reuse of textile wastewaters. *Desalination, 221*(1–3), 405-412.

Asghar, A., Abdul Raman, A. A., & Daud, W. M. A. W. (2014). A Comparison of Central Composite Design and Taguchi Method for Optimizing Fenton Process. *The Scientific World Journal, 2014*, 14.

Asghar, A., Abdul Raman, A. A., & Wan Daud, W. M. A. (2015). Advanced oxidation processes for in-situ production of hydrogen peroxide/hydroxyl radical for textile wastewater treatment: a review. *Journal of Cleaner Production, 87*, 826-838.

Audenaert, W. T. M., Vermeersch, Y., Van Hulle, S. W. H., Dejans, P., Dumoulin, A., & Nopens, I. (2011). Application of a mechanistic UV/hydrogen peroxide model at full-scale: Sensitivity analysis, calibration and performance evaluation. *Chemical Engineering Journal, 171*(1), 113-126.

Autin, O., Hart, J., Jarvis, P., MacAdam, J., Parsons, S. A., & Jefferson, B. (2012). Comparison of UV/H2O2 and UV/TiO2 for the degradation of metaldehyde: Kinetics and the impact of background organics. *Water Res, 46*(17), 5655-5662.

Ayodele, O. B., Lim, J. K., & Hameed, B. H. (2012). Pillared montmorillonite supported ferric oxalate as heterogeneous photo-Fenton catalyst for degradation of amoxicillin. *Applied Catalysis A: General, 413-414*, 301-309.

Azimi, Y., Allen, D. G., & Farnood, R. R. (2012). Kinetics of UV inactivation of wastewater bioflocs. *Water Res, 46*(12), 3827-3836.

Babuponnusami, A., & Muthukumar, K. (2012). Removal of phenol by heterogenous photo electro Fenton-like process using nano-zero valent iron. *Separation and Purification Technology, 98*(0), 130-135.

Babuponnusami, A., & Muthukumar, K. (2013). A review on Fenton and improvements to the Fenton process for wastewater treatment. *Journal of Environmental Chemical Engineering*.

Babuponnusami, A., & Muthukumar, K. (2014). A review on Fenton and improvements to the Fenton process for wastewater treatment. *Journal of Environmental Chemical Engineering, 2*(1), 557-572.

Bagal, M. V., & Gogate, P. R. (2014). Wastewater treatment using hybrid treatment schemes based on cavitation and Fenton chemistry: A review. *Ultrason Sonochem, 21*(1), 1-14.

Balcıoglu, I. A., Alaton, I. A., Otker, M., Bahar, R., Bakar, N., & Ikiz, M. (2003). Application of Advanced Oxidation Processes to Different Industrial Wastewaters. *Journal of Environmental Science and Health, Part A, 38*(8), 1587-1596.

Balcıoğlu, I. A., Alaton, I. A., Ötker, M., Bahar, R., Bakar, N., & Ikiz, M. (2003). Application of Advanced Oxidation Processes to Different Industrial Wastewaters. *Journal of Environmental Science and Health, Part A, 38*(8), 1587-1596.

Balcioglu, I. A., & Arslan, I. (1997). Treatment of Textile Waste Water by Heterogenous Photocatalytic Oxidation Processes. *Environmental Technology, 18*(10), 1053-1059.

Balcioglu, I. A., Arslan, I., & Sacan, M. T. (2001). Homogenous and heterogenous advanced oxidation of two commercial reactive dyes. *Environ Technol, 22*(7), 813-822.

Banat, F., Al-Asheh, S., Al-Rawashdeh, M. m., & Nusair, M. (2005). Photodegradation of methylene blue dye by the UV/H2O2 and UV/acetone oxidation processes. *Desalination, 181*(1-3), 225-232.

Bandala, E. R., Peláez, M. A., García-López, A. J., Salgado, M. d. J., & Moeller, G. (2008). Photocatalytic decolorisation of synthetic and real textile wastewater containing benzidine-based azo dyes. *Chemical Engineering and Processing: Process Intensification, 47*(2), 169-176.

Bauer.R, Waldner.G, Fallmann. H, Hager.S, Klare.M, Krutzler.T, . . . Maletzky.P. (1993). The photo-fenton reaction and the TiO2UV process for waste water treatment − novel developments.pdf. *Catalysis Today, 53*, 131-144.

Bautista, P., Mohedano, A. F., Gilarranz, M. A., Casas, J. A., & Rodriguez, J. J. (2007). Application of Fenton oxidation to cosmetic wastewaters treatment. *J Hazard Mater, 143*(1-2), 128-134.

Beltrán, F. J., Aguinaco, A., & García-Araya, J. F. (2012). Application of Ozone Involving Advanced Oxidation Processes to Remove Some Pharmaceutical Compounds from Urban Wastewaters. *Ozone: Science & Engineering, 34*(1), 3-15.

Benatti, C. T., Tavares, C. R., & Guedes, T. A. (2006). Optimization of Fenton's oxidation of chemical laboratory wastewaters using the response surface methodology. *J Environ Manage, 80*(1), 66-74.

Bezerra, M. A., Santelli, R. E., Oliveira, E. P., Villar, L. S., & Escaleira, L. A. (2008). Response surface methodology (RSM) as a tool for optimization in analytical chemistry. *Talanta, 76*(5), 965-977.

Bezerra, M. A., Santelli, R. E., Oliveira, E. P., Villar, L. S., & Escaleira, L. A. (2008). Response surface methodology (RSM) as a tool for optimization in analytical chemistry. *Talanta, 76*(5), 965-977.

Bielski, B. H. J., Cabelli, D. E., Arudi, R. L., & Ross, A. B. (1985). Reactivity of HO2/O−2 Radicals in Aqueous Solution. *Journal of Physical and Chemical Reference Data, 14*(4), 1041-1100.

Biń, A. K., & Sobera-Madej, S. (2012). Comparison of the Advanced Oxidation Processes (UV, UV/H2O2and O3) for the Removal of Antibiotic Substances during Wastewater Treatment. *Ozone: Science & Engineering, 34*(2), 136-139.

Bingöl, D., Hercan, M., Elevli, S., & Kılıç, E. (2012). Comparison of the results of response surface methodology and artificial neural network for the biosorption of lead using black cumin. *Bioresour Technol, 112*(0), 111-115.

Blanco, J., Torrades, F., De la Varga, M., & García-Montaño, J. (2012). Fenton and biological-Fenton coupled processes for textile wastewater treatment and reuse. *Desalination, 286*, 394-399.

Blatchley, E. R., Bastian, K. C., Duggirala, R. K., Alleman, J. E., Moore, M., & Schuerch, P. (1996). Ultraviolet Irradiation and Chlorination/Dechlorination for Municipal Wastewater Disinfection: Assessment of Performance Limitations. *Water Environment Research, 68*(2), 194-204.

Borba, F. H., Modenes, A. N., Espinoza-Quinones, F. R., Manenti, D. R., Bergamasco, R., & Mora, N. D. (2012). Toxicity assessment of tannery effluent treated by an optimized photo-Fenton process. *Environmental Technology*, 1-9.

Bouafia-Chergui, S., Oturan, N., Khalaf, H., & Oturan, M. A. (2010). Parametric study on the effect of the ratios [H2O2]/[Fe3 +] and [H2O2]/[substrate] on the photo-Fenton degradation of cationic azo dye basic blue 41. *J Environ Sci Health A Tox Hazard Subst Environ Eng, 45*(5), 622-629.

Bouasla, C., Samar, M. E. H., & Ismail, F. (2010). Degradation of methyl violet 6B dye by the Fenton process. *Desalination, 254*(1-3), 35-41.

Bustos, Y. A., Vaca, M., Lopez, R., & Torres, L. G. (2010). Disinfection of a wastewater flow treated by advanced primary treatment using O(3), UV and O(3)/UV combinations. *J Environ Sci Health A Tox Hazard Subst Environ Eng, 45*(13), 1715-1719.

Buthiyappan, A., Abdul Aziz, A. R., & Wan Daud, W. M. A. (2015). Degradation performance and cost implication of UV-integrated advanced oxidation processes for wastewater treatments. *Reviews in Chemical Engineering, 31*(3).

Buthiyappan, A., Abdul Aziz, A. R., & Wan Daud, W. M. A. (2016). Recent advances and prospects of catalytic advanced oxidation process in treating textile effluents. *Reviews in Chemical Engineering, 32*(1), 1-47.

Buthiyappan, A., Daud, W. M. A. W., & Abdul Raman, A. A. (2016). Development of Advanced Chemical Oxidation Wastewater Treatment System for the Batik Industry in Malaysia. *RSC Advances*.

Buxton, G. V., Greenstock, C. L., Helman, W. P., & Ross, A. B. (1988). Critical Review of rate constants for reactions of hydrated electrons, hydrogen atoms and hydroxyl radicals (·OH/·O− in Aqueous Solution. *Journal of Physical and Chemical Reference Data, 17*(2), 513-886.

Cañizares, P., Paz, R., Sáez, C., & Rodrigo, M. A. (2009). Costs of the electrochemical oxidation of wastewaters: A comparison with ozonation and Fenton oxidation processes. *J Environ Manage, 90*(1), 410-420.

Cardoso, N. F., Lima, E. C., Calvete, T., Pinto, I. S., Amavisca, C. V., Fernandes, T. H. M., . . . Alencar, W. S. (2011). Application of Aqai Stalks As Biosorbents for the Removal of the Dyes Reactive Black 5 and Reactive Orange 16 from Aqueous Solution. *Journal of Chemical & Engineering Data, 56*(5), 1857-1868. Cervantes, F. J., Pavlostathis, S. G., & van Haandel, A. C. (2006). *Advanced Biological Treatment Processes for Industrial Wastewaters: Principles and Applications*: IWA Publishing.

Chakma, S., & Moholkar, V. S. Mechanistic analysis of hybrid sono-photo-ferrioxalate system for decolorization of azo dye. *Journal of the Taiwan Institute of Chemical Engineers*.

Chang, M.-W., & Chern, J.-M. (2010). Decolorization of peach red azo dye, HF6 by Fenton reaction: Initial rate analysis. *Journal of the Taiwan Institute of Chemical Engineers, 41*(2), 221-228.

Chang, M.-W., Chung, C.-C., Chern, J.-M., & Chen, T.-S. (2010). Dye decomposition kinetics by UV/H2O2: Initial rate analysis by effective kinetic modelling methodology. *Chemical Engineering Science, 65*(1), 135-140.

Chelme-Ayala, P., El-Din, M. G., & Smith, D. W. (2010). Degradation of bromoxynil and trifluralin in natural water by direct photolysis and UV plus H(2)O(2) advanced oxidation process. *Water Res, 44*(7), 2221-2228.

Chen, J., & Zhu, L. (2007). Heterogeneous UV-Fenton catalytic degradation of dyestuff in water with hydroxyl-Fe pillared bentonite. *Catalysis Today, 126*(3-4), 463-470.

Chen, T. Y., Kao, C. M., Hong, A., Lin, C. E., & Liang, S. H. (2009). Application of ozone on the decolorization of reactive dyes — Orange-13 and Blue-19. *Desalination, 249*(3), 1238-1242.

Cheremisinoff, N. P. (2002). *Handbook of Water and Wastewater Treatment Technologies*: Butterworth-Heinemann.

Choi, J.-W., Song, H. K., Lee, W., Koo, K.-K., Han, C., & Na, B.-K. Reduction of COD and color of acid and reactive dyestuff wastewater using ozone. *Korean Journal of Chemical Engineering, 21*(2), 398-403.

Choudhury, A. K. R. (2006). *Textile Preparation and Dyeing*: Science Publishers.

Christie, R. (2014). *Color Chemistry*: Royal Society of Chemistry.

Colombo, R., Ferreira, T. C. R., Alves, S. A., Carneiro, R. L., & Lanza, M. R. V. (2013). Application of the response surface and desirability design to the Lambda-cyhalothrin degradation using photo-Fenton reaction. *J Environ Manage, 118*(0), 32-39.

Comninellis, C., Kapalka, A., Malato, S., Parsons, S. A., Poulios, I., & Mantzavinos, D. (2008). Advanced oxidation processes for water treatment: advances and trends for R&D. *Journal of Chemical Technology & Biotechnology, 83*(6), 769-776.

Cooper, C., & Burch, R. (1999). An investigation of catalytic ozonation for the oxidation of halocarbons in drinking water preparation1. *Water Res, 33*(18), 3695-3700.

Dantas, T. L. P., Mendonça, V. P., José, H. J., Rodrigues, A. E., & Moreira, R. F. P. M. (2006). Treatment of textile wastewater by heterogeneous Fenton process using a new composite Fe2O3/carbon. *Chemical Engineering Journal, 118*(1-2), 77-82.

De Angelis, L., & de Cortalezzi, M. M. F. (2016). Improved membrane flux recovery by Fenton-type reactions. *Journal of Membrane Science, 500*, 255-264.

De Jager, D., Sheldon, M. S., & Edwards, W. (2014). Color removal from textile wastewater using a pilot-scale dual-stage MBR and subsequent RO system. *Separation and Purification Technology, 135*(0), 135-144.

De la Cruz, N., Esquius, L., Grandjean, D., Magnet, A., Tungler, A., de Alencastro, L. F., & Pulgarín, C. (2013). Degradation of emergent contaminants by UV, UV/H2O2 and neutral photo-Fenton at pilot scale in a domestic wastewater treatment plant. *Water Research, 47*(15), 5836-5845.

Deng, Y., & Englehardt, J. D. (2006). Treatment of landfill leachate by the Fenton process. *Water Res, 40*(20), 3683-3694.

Dias, F. F., Oliveira, A. A. S., Arcanjo, A. P., Moura, F. C. C., & Pacheco, J. G. A. (2016). Residue-based iron catalyst for the degradation of textile dye via heterogeneous photo-Fenton. *Applied Catalysis B: Environmental, 186*, 136-142.

Ding, N., Neumann, N. F., Price, L. M., Braithwaite, S. L., Balachandran, A., Belosevic, M., & Gamal El-Din, M. (2014). Ozone inactivation of infectious prions in rendering plant and municipal wastewaters. *Sci Total Environ, 470-471*, 717-725.

Dopar, M., Kusic, H., & Koprivanac, N. (2011). Treatment of simulated industrial wastewater by photo-Fenton process. Part I: The optimization of process parameters using design of experiments (DOE). *Chemical Engineering Journal, 173*(2), 267-279.

Dükkancı, M., Vinatoru, M., & Mason, T. J. (2014). The sonochemical decolorisation of textile azo dye Orange II: Effects of Fenton type reagents and UV light. *Ultrason Sonochem, 21*(2), 846-853.

Duran, A., Monteagudo, J. M., Carnicer, A., & Ruiz-Murillo, M. (2011). Photo-Fenton mineralization of synthetic municipal wastewater effluent containing acetaminophen in a pilot plant. *Desalination, 270*(1-3), 124-129.

Economic, U. N. D. o., Affairs, S., & Development, U. N. C. o. S. (2007). *Industrial Development for the 21st Century: Sustainable Development Perspectives*: UN.

Elmorsi, T. M., Riyad, Y. M., Mohamed, Z. H., & Abd El Bary, H. M. (2010). Decolorization of Mordant red 73 azo dye in water using H2O2/UV and photo-Fenton treatment. *J Hazard Mater, 174*(1-3), 352-358.

Engin, A. B., Özdemir, Ö., Turan, M., & Turan, A. Z. (2008). Color removal from textile dyebath effluents in a zeolite fixed bed reactor: Determination of optimum process conditions using Taguchi method. *J Hazard Mater, 159*(2–3), 348-353. doi:http://dx.doi.org/10.1016/j.jhazmat.2008.02.065

Engineers, E. C. a. (2005). *Technology Of Synthetic Dyes, Pigments And Intermediates*. Delhi: Engineers India Research Institute.

Eren, Z. (2012). Ultrasound as a basic and auxiliary process for dye remediation: a review. *J Environ Manage, 104*, 127-141.

Ertugay, N., & Acar, F. N. (2013). Removal of COD and color from Direct Blue 71 azo dye wastewater by Fenton's oxidation: Kinetic study. *Arabian Journal of Chemistry*.

Fard Masoumi, H. R., Basri, M., Kassim, A., Kuang Abdullah, D., Abdollahi, Y., Abd Gani, S. S., & Rezaee, M. (2013). Statistical Optimization of Process Parameters for Lipase-Catalyzed Synthesis of Triethanolamine-Based Esterquats Using Response Surface Methodology in 2-Liter Bioreactor. *The Scientific World Journal, 2013*, 962083.

Faryal, R., & Hameed, A. (2005). Isolation and characterization of various fungal strains from textile effluent for their use in bioremediation. *Pakistan Journal of Botany, 37*(4), 1003-1008.

Feng, J., Hu, X., & Yue, P. L. (2006). Effect of initial solution pH on the degradation of Orange II using clay-based Fe nanocomposites as heterogeneous photo-Fenton catalyst. *Water Res, 40*(4), 641-646. doi:http://dx.doi.org/10.1016/j.watres.2005.12.021

Fenton, H. J. H. (1894). LXXIII. - Oxidation of tartaric acid in presence of iron. *Journal of the Chemical Society, Transactions, 65*, 899-910.

Gao, S., Zhao, Z., Xu, Y., Tian, J., Qi, H., Lin, W., & Cui, F. (2014). Oxidation of sulfamethoxazole (SMX) by chlorine, ozone and permanganate—A comparative study. *Journal of Hazardous Materials, 274*, 258-269.

Garrido-Ramírez, E. G., Theng, B. K. G., & Mora, M. L. (2010). Clays and oxide minerals as catalysts and nanocatalysts in Fenton-like reactions — A review. *Applied Clay Science, 47*(3-4), 182-192.

Gaya, U. I., & Abdullah, A. H. (2008). Heterogeneous photocatalytic degradation of organic contaminants over titanium dioxide: A review of fundamentals, progress and problems. *Journal of Photochemistry and Photobiology C: Photochemistry Reviews, 9*(1), 1-12.

Germirli Babuna, F., Orhon, D., Ubay Çokgör, E., Insel, G., & Yaprakli, B. (1998). Modelling of activated sludge for textile wastewaters. *Water Science and Technology, 38*(4–5), 9-17.

Ghaly, M. Y., Härtel, G., Mayer, R., & Haseneder, R. (2001). Photochemical oxidation of p-chlorophenol by UV/H2O2 and photo-Fenton process. A comparative study. *Waste Manag, 21*(1), 41-47.

Ghiselli, G., Jardim, W. F., Litter, M. I., & Mansilla, H. D. (2004). Destruction of EDTA using Fenton and photo-Fenton-like reactions under UV-A irradiation. *Journal of Photochemistry and Photobiology A: Chemistry, 167*(1), 59-67.

Ghodbane, H., & Hamdaoui, O. (2009). Intensification of sonochemical decolorization of anthraquinonic dye Acid Blue 25 using carbon tetrachloride. *Ultrasonics Sonochemistry, 16*(4), 455-461.

Ginni, G., Adishkumar, S., Rajesh Banu, J., & Yogalakshmi, N. (2014). Treatment of pulp and paper mill wastewater by solar photo-Fenton process. *Desalination and Water Treatment, 52*(13-15), 2457-2464.

Giroto, J. A., Teixeira, A. C. S. C., Nascimento, C. A. O., & Guardani, R. (2008). Photo-Fenton removal of water-soluble polymers. *Chemical Engineering and Processing: Process Intensification, 47*(12), 2361-2369.

Glaze, W. H. (2000). Water, 6. Treatment by Oxidation Processes *Ullmann's Encyclopedia of Industrial Chemistry*: Wiley-VCH Verlag GmbH & Co. KGaA.

Gogate, P. R. (2008). Treatment of wastewater streams containing phenolic compounds using hybrid techniques based on cavitation: A review of the current status and the way forward. *Ultrason Sonochem, 15*(1), 1-15.

Gogate, P. R., & Pandit, A. B. (2004a). A review of imperative technologies for wastewater treatment I: oxidation technologies at ambient conditions. *Advances in Environmental Research, 8*(3-4), 501-551.

Gogate, P. R., & Pandit, A. B. (2004b). A review of imperative technologies for wastewater treatment II: hybrid methods. *Advances in Environmental Research, 8*(3-4), 553-597.

Gomathi Devi, L., Girish Kumar, S., Mohan Reddy, K., & Munikrishnappa, C. (2009). Photo degradation of Methyl Orange an azo dye by Advanced Fenton Process using zero valent metallic iron: Influence of various reaction parameters and its degradation mechanism. *Journal of Hazardous Materials, 164*(2-3), 459-467.

Gong, J., Liu, Y., & Sun, X. (2008). O3 and UV/O3 oxidation of organic constituents of biotreated municipal wastewater. *Water Res, 42*(4-5), 1238-1244.

Grcic, I., Maljković, M., Papić, S., & Koprivanac, N. (2011). Low frequency US and UV-A assisted Fenton oxidation of simulated dyehouse wastewater. *Journal of Hazardous Materials, 197*, 272-284.

Gu, L., Nie, J.-Y., Zhu, N.-w., Wang, L., Yuan, H.-P., & Shou, Z. (2012). Enhanced Fenton's degradation of real naphthalene dye intermediate wastewater containing 6-nitro-1-diazo-2-naphthol-4-sulfonic acid: A pilot scale study. *Chemical Engineering Journal, 189–190*(0), 108-116.

Gulkaya, İ., Surucu, G. A., & Dilek, F. B. (2006). Importance of H2O2/Fe2+ ratio in Fenton's treatment of a carpet dyeing wastewater. *J Hazard Mater, 136*(3), 763-769.

Gunukula, R. V. B., & Tittlebaum, M. E. (2001). Industrial Wastewater Treatment by an Advanced Oxidation Process. *Journal of Environmental Science and Health, Part A, 36*(3), 307-320.

Haber, F., & Weiss, J. (1934). The Catalytic Decomposition of Hydrogen Peroxide by Iron Salts. *Proceedings of the Royal Society of London A: Mathematical, Physical and Engineering Sciences, 147*(861), 332-351.

Hammami, S., Oturan, M. A., Oturan, N., Bellakhal, N., & Dachraoui, M. (2012). Comparative mineralization of textile dye indigo by photo-Fenton process and anodic oxidation using boron-doped diamond anode. *Desalination and Water Treatment, 45*(1-3), 297-304.

Hartmann, M., Kullmann, S., & Keller, H. (2010). Wastewater treatment with heterogeneous Fenton-type catalysts based on porous materials. *Journal of Materials Chemistry, 20*(41), 9002-9017.

Hasan, D. u. B., Abdul Aziz, A. R., & Daud, W. M. A. W. (2012). Oxidative mineralisation of petroleum refinery effluent using Fenton-like process. *Chemical Engineering Research and Design, 90*(2), 298-307.

Hasan, D. u. B., Aziz, A. R. A., & Daud, W. M. A. W. (2011). Using D-optimal experimental design to optimise remazol black B mineralisation by Fenton-like peroxidation. *Environmental Technology, 33*(10), 1111-1121.

Hasan, D. u. B., Aziz, A. R. A., & Daud, W. M. A. W. (2012). Using D-optimal experimental design to optimise remazol black B mineralisation by Fenton-like peroxidation. *Environmental Technology, 33*(10), 1111-1121.

Hassan, S. S., Awwad, N. S., & Aboterika, A. H. (2009). Removal of synthetic reactive dyes from textile wastewater by Sorel's cement. *J Hazard Mater, 162*(2-3), 994-999.

Hey, G., Grabic, R., Ledin, A., la Cour Jansen, J., & Andersen, H. R. (2012). Oxidation of pharmaceuticals by chlorine dioxide in biologically treated wastewater. *Chemical Engineering Journal, 185-186*, 236-242. doi:10.1016/j.cej.2012.01.093

Hu, X., Wang, X., Ban, Y., & Ren, B. (2011). A comparative study of UV–Fenton, UV–H2O2 and Fenton reaction treatment of landfill leachate. *Environmental Technology, 32*(9), 945-951.

Ikehata, K., & El-Din, M. G. (2004). Degradation of Recalcitrant Surfactants in Wastewater by Ozonation and Advanced Oxidation Processes: A Review. *Ozone: Science & Engineering, 26*(4), 327-343.

Ingamells, W., Dyers, S. o., & Colorists. (1993). *Color for Textiles: A User's Handbook*: Society of Dyers and Colorists.

Inoue, M., Okada, F., Sakurai, A., & Sakakibara, M. (2006). A new development of dyestuffs degradation system using ultrasound. *Ultrasonics Sonochemistry, 13*(4), 313-320.

Iurascu, B., Siminiceanu, I., Vione, D., Vicente, M. A., & Gil, A. (2009). Phenol degradation in water through a heterogeneous photo-Fenton process catalyzed by Fe-treated laponite. *Water Res, 43*(5), 1313-1322.

Jaafarzadeh, N., Omidinasab, M., & Ghanbari, F. Combined electrocoagulation and UV-based sulfate radical oxidation processes for treatment of pulp and paper wastewater. *Process Safety and Environmental Protection*.

Jung, Y. J., Kim, W. G., Yoon, Y., Kang, J. W., Hong, Y. M., & Kim, H. W. (2012). Removal of amoxicillin by UV and UV/H2O2 processes. *Sci Total Environ, 420*, 160-167. doi:10.1016/j.scitotenv.2011.12.011

Jung, Y. S., Lim, W. T., Park, J. Y., & Kim, Y. H. (2009). Effect of pH on Fenton and Fenton-like oxidation. *Environmental Technology, 30*(2), 183-190.

Karthikeyan, S., Titus, A., Gnanamani, A., Mandal, A. B., & Sekaran, G. (2011). Treatment of textile wastewater by homogeneous and heterogeneous Fenton oxidation processes. *Desalination, 281*, 438-445.

Kavitha, V., & Palanivelu, K. (2004). The role of ferrous ion in Fenton and photo-Fenton processes for the degradation of phenol. *Chemosphere, 55*(9), 1235-1243.

Kim, J. S., Kim, H. Y., Won, C. H., & Kim, J. G. (2001). Treatment of leachate produced in stabilized landfills by coagulation and fenton oxidation process. *Journal of the Chinese Institute of Chemical Engineers, 32*(5), 425-429.

Kusic, H., Koprivanac, N., Bozic, A. L., & Selanec, I. (2006). Photo-assisted Fenton type processes for the degradation of phenol: a kinetic study. *J Hazard Mater, 136*(3), 632-644.

Kusic, H., Koprivanac, N., & Srsan, L. (2006). Azo dye degradation using Fenton type processes assisted by UV irradiation: A kinetic study. *Journal of Photochemistry and Photobiology A: Chemistry, 181*(2-3), 195-202.

Lahkimi, A., Oturan, M. A., Oturan, N., & Chaouch, M. (2006). Removal of textile dyes from water by the electro-Fenton process. *Environmental Chemistry Letters, 5*(1), 35-39.

Legube, B., Croue, J. P., Reckhow, D. A., Dore, V., Perry, R., & McLntyre, A. E. (1985). *in Proceedings of the International Conference on The Role of Ozone in Water and Wastewater Treatment* (Vol. null).

Leong, S. K., & Bashah, N. A. A. (2012). Kinetic Study on COD Removal of Palm Oil Refinery Effluent by UV-Fenton. *APCBEE Procedia, 3*, 6-10.

Leube, H. (2004). Textile Dyeing *Industrial Dyes* (pp. 339-425): Wiley-VCH Verlag GmbH & Co. KGaA.

Li, H., Pan, Y., Wang, Z., Chen, S., Guo, R., & Chen, J. (2015). An algal process treatment combined with the Fenton reaction for high concentrations of amoxicillin and cefradine. *RSC Advances, 5*(122), 100775-100782.

Li, W., Lu, S., Qiu, Z., & Lin, K. (2011). UV and VUV photolysis vs. UV/H2O2and VUV/H2O2treatment for removal of clofibric acid from aqueous solution. *Environmental Technology, 32*(10), 1063-1071.

Lide, D. R. (2004). *CRC Handbook of Chemistry and Physics, 85th Edition*: Taylor & Francis.

Lin, C.-C., Lin, H.-Y., & Hsu, L.-J. Degradation of ofloxacin using UV/H2O2 process in a large photoreactor. *Separation and Purification Technology*.

Lin, J.-j., Zhao, X.-s., Liu, D., Yu, Z.-g., Zhang, Y., & Xu, H. (2008). The decoloration and mineralization of azo dye C.I. Acid Red 14 by sonochemical process: Rate improvement via Fenton's reactions. *J Hazard Mater, 157*(2–3), 541-546.

Liu, P., Li, C., Kong, X., Lu, G., Xu, J., Ji, F., & Liang, X. (2013). Photocatalytic degradation of EDTA with UV/Cu(II)/H2O2process. *Desalination and Water Treatment, 51*(40-42), 7555-7561.

Liu, R., Chiu, H. M., Shiau, C.-S., Yeh, R. Y.-L., & Hung, Y.-T. (2007). Degradation and sludge production of textile dyes by Fenton and photo-Fenton processes. *Dyes and Pigments, 73*(1), 1-6.

Liu, S.-T., Huang, J., Ye, Y., Zhang, A.-B., Pan, L., & Chen, X.-G. (2013). Microwave enhanced Fenton process for the removal of methylene blue from aqueous solution. *Chemical Engineering Journal, 215–216*, 586-590.

Lodha, B., & Chaudhari, S. (2007). Optimization of Fenton-biological treatment scheme for the treatment of aqueous dye solutions. *J Hazard Mater, 148*(1–2), 459-466.

Loeb, B. L., Thompson, C. M., Drago, J., Takahara, H., & Baig, S. (2012). Worldwide Ozone Capacity for Treatment of Drinking Water and Wastewater: A Review. *Ozone: Science & Engineering, 34*(1), 64-77.

Lopez-Alvarez, B., Torres-Palma, R. A., Ferraro, F., & Penuela, G. (2012). Solar photo-Fenton treatment of carbofuran: Analysis of mineralization, toxicity, and organic by-products. *J Environ Sci Health A Tox Hazard Subst Environ Eng, 47*(13), 2141-2150.

Lopez, A., Pagano, M., Volpe, A., & Claudio Di Pinto, A. (2004). Fenton's pre-treatment of mature landfill leachate. *Chemosphere, 54*(7), 1005-1010.

Lucas, M., & Peres, J. (2006). Decolorization of the azo dye Reactive Black 5 by Fenton and photo-Fenton oxidation. *Dyes and Pigments, 71*(3), 236-244.

Lucas, M. S., Dias, A. A., Sampaio, A., Amaral, C., & Peres, J. A. (2007). Degradation of a textile reactive Azo dye by a combined chemical–biological process: Fenton's reagent-yeast. *Water Research, 41*(5), 1103-1109.

Lucas, M. S., & Peres, J. A. (2007). Degradation of Reactive Black 5 by Fenton/UV-C and ferrioxalate/H2O2/solar light processes. *Dyes and Pigments, 74*(3), 622-629.

Lucas, M. S., & Peres, J. A. (2009). Removal of COD from olive mill wastewater by Fenton's reagent: kinetic study. *J Hazard Mater, 168*(2-3), 1253-1259.

Mahamuni, N. N., & Adewuyi, Y. G. (2010). Advanced oxidation processes (AOPs) involving ultrasound for waste water treatment: a review with emphasis on cost estimation. *Ultrason Sonochem, 17*(6), 990-1003.

Malik, P. (2004). Kinetics of decolorisation of azo dyes in wastewater by UV/H2O2 process. *Separation and Purification Technology, 36*(3), 167-175.

Mantzavinos, D., & Psillakis, E. (2004). Enhancement of biodegradability of industrial wastewaters by chemical oxidation pre-treatment. *Journal of Chemical Technology and Biotechnology, 79*(5), 431-454.

Marcinowski, P. P., Bogacki, J. P., & Naumczyk, J. H. (2014). Cosmetic wastewater treatment using the Fenton, Photo-Fenton and H2O2/UV processes. *Journal of Environmental Science and Health, Part A, 49*(13), 1531-1541.

Martins, L. M., Silva, C. E. d., Moita Neto, J. M., Lima, Á. S., & Moreira, R. d. F. P. M. (2011). Aplicação de Fenton, foto-Fenton e UV/H2O2 no tratamento de efluente têxtil sintético contendo o corante Preto Biozol UC. *Engenharia Sanitaria e Ambiental, 16*, 261-270.

Matafonova, G., & Batoev, V. (2012). Recent progress on application of UV excilamps for degradation of organic pollutants and microbial inactivation. *Chemosphere, 89*(6), 637-647.

McMullan, G., Meehan, C., Conneely, A., Kirby, N., Robinson, T., Nigam, P., . . . Smyth, W. F. (2001). Microbial decolorisation and degradation of textile dyes. *Appl Microbiol Biotechnol, 56*(1-2), 81-87.

Meriç, S., Kaptan, D., & Ölmez, T. (2004). Color and COD removal from wastewater containing Reactive Black 5 using Fenton's oxidation process. *Chemosphere, 54*(3), 435-441.

Meric, S., Selcuk, H., & Belgiorno, V. (2005). Acute toxicity removal in textile finishing wastewater by Fenton's oxidation, ozone and coagulation-flocculation processes. *Water Res, 39*(6), 1147-1153.

Métivier-Pignon, H., Faur-Brasquet, C., Jaouen, P., & Le Cloirec, P. (2003). Coupling ultrafiltration with an activated carbon cloth for the treatment of highly colored wastewaters : A techno-economic study. *Environmental Technology, 24*(6), 735-743.

Módenes, A. N., Espinoza-Quiñones, F. R., Manenti, D. R., Borba, F. H., Palácio, S. M., & Colombo, A. (2012). Performance evaluation of a photo-Fenton process applied to pollutant removal from textile effluents in a batch system. *J Environ Manage, 104*(0), 1-8.

Modirshahla, N., Behnajady, M. A., & Ghanbary, F. (2007). Decolorization and mineralization of C.I. Acid Yellow 23 by Fenton and photo-Fenton processes. *Dyes and Pigments, 73*(3), 305-310.

Moyer, E., & Kostecki, P. T. (2004). *MTBE Remediation Handbook*: Springer US.

Muruganandham, M., & Swaminathan, M. (2006). Advanced oxidative decolorisation of Reactive Yellow 14 azo dye by UV/TiO2, UV/H2O2, UV/H2O2/Fe2+ processes—a comparative study. *Separation and Purification Technology, 48*(3), 297-303.

Nair, N. (2014, September 25). Designer's work lifts profile of traditional fabric. *The Star* http://m.thestar.com.my/

Navarro, R. R., Ichikawa, H., & Tatsumi, K. (2010). Ferrite formation from photo-Fenton treated wastewater. *Chemosphere, 80*(4), 404-409.

Neamtu, M., Yediler, A., Siminiceanu, I., & Kettrup, A. (2003). Oxidation of commercial reactive azo dye aqueous solutions by the photo-Fenton and Fenton-like processes. *Journal of Photochemistry and Photobiology A: Chemistry, 161*(1), 87-93.

Neyens, E., & Baeyens, J. (2003). A review of classic Fenton's peroxidation as an advanced oxidation technique. *Journal of Hazardous Materials, 98*(1-3), 33-50.

Nezamzadeh, E. A., & Amiri, M. (2013). CuO supported Clinoptilolite towards solar photocatalytic degradation of p-aminophenol. *Powder Technology, 235*, 279-288.

Nezamzadeh, E. A., & Banan, Z. (2013). Photodegradation of dimethyldisulfide by heterogeneous catalysis using nanoCdS and nanoCdO embedded on the zeolite A synthesized from waste porcelain. *Desalination and Water Treatment, 52*(16-18), 3328-3337.

Nezamzadeh, E. A., & Khodabakhshi-Chermahini, F. (2014). Incorporated ZnO onto nano clinoptilolite particles as the active centers in the photodegradation of phenylhydrazine. *Journal of Industrial and Engineering Chemistry, 20*(2), 695-704.

Nezamzadeh, E. A., & Shirvani, K. (2013). CdS Loaded an Iranian Clinoptilolite as a Heterogeneous Catalyst in Photodegradation of p-Aminophenol. *Journal of Chemistry, 2013*, 11.

Nitoi, I., Oncescu, T., & Oancea, P. (2013). Mechanism and kinetic study for the degradation of lindane by photo-Fenton process. *Journal of Industrial and Engineering Chemistry, 19*(1), 305-309.

Nordin, R., & Bakar, S. S. A. (2012). Malaysian batik industry: Protecting local batik design by Copyright and industrial design laws. *International Journal of Business and Society, 13*(2), 117 - 132.

Oms-Oliu, G., Aguiló-Aguayo, I., Martín-Belloso, O., & Soliva-Fortuny, R. (2010). Effects of pulsed light treatments on quality and antioxidant properties of fresh-cut mushrooms (Agaricus bisporus). *Postharvest Biology and Technology, 56*(3), 216-222.

Otterstätter, G. (1999). *Coloring of Food, Drugs, and Cosmetics*: Taylor & Francis.

Oturan, M. A., Bellakhal, N., Oturan, N., & Trabelsi-Souissi, S. (2011). Application of the photo-Fenton process to the mineralization of phthalic anhydride in aqueous medium. *Desalination and Water Treatment*, 210-215.

Pang, Y. L., Abdullah, A. Z., & Bhatia, S. (2011). Review on sonochemical methods in the presence of catalysts and chemical additives for treatment of organic pollutants in wastewater. *Desalination, 277*(1-3), 1-14.

Papadopoulos, A. E., Fatta, D., & Loizidou, M. (2007). Development and optimization of dark Fenton oxidation for the treatment of textile wastewaters with high organic load. *J Hazard Mater, 146*(3), 558-563.

Papic, S., Vujevic, D., Koprivanac, N., & Sinko, D. (2009). Decolorization and mineralization of commercial reactive dyes by using homogeneous and heterogeneous Fenton and UV/Fenton processes. *J Hazard Mater, 164*(2-3), 1137-1145.

Park, J. H., Cho, I. H., & Chang, S. W. (2006). Comparison of fenton and photo-fenton processes for livestock wastewater treatment. *J Environ Sci Health B, 41*(2), 109-120.

Patel, H., & Vashi, R. T. (2015). *Characterization and Treatment of Textile Wastewater*: Elsevier Science.

Pelosi, B. T., Lima, L. K. S., & Vieira, M. G. A. (2014). Removal of the synthetic dye Remazol Brilliant Blue R from textile industry wastewaters by biosorption on the macrophyte Salvinia natans. *Brazilian Journal of Chemical Engineering, 31*, 1035-1045.

Pera-Titus, M., García-Molina, V., Baños, M. A., Giménez, J., & Esplugas, S. (2004). Degradation of chlorophenols by means of advanced oxidation processes: a general review. *Applied Catalysis B: Environmental, 47*(4), 219-256.

Philippopoulos, C. J., & Poulopoulos, S. G. (2003). Photo-assisted oxidation of an oily wastewater using hydrogen peroxide. *J Hazard Mater, 98*(1-3), 201-210.

Pignatello, J. J., Oliveros, E., & MacKay, A. (2006). Advanced Oxidation Processes for Organic Contaminant Destruction Based on the Fenton Reaction and Related Chemistry. *Critical Reviews in Environmental Science and Technology, 36*(1), 1-84.

Prousek, J., Palacková, E., Priesolová, S., Marková, L., & Alevová, A. (2007). Fenton- and Fenton-Like AOPs for Wastewater Treatment: From Laboratory-To-Plant-Scale Application. *Separation Science and Technology, 42*(7), 1505-1520.

Punzi, M., Mattiasson, B., & Jonstrup, M. (2012). Treatment of synthetic textile wastewater by homogeneous and heterogeneous photo-Fenton oxidation. *Journal of Photochemistry and Photobiology A: Chemistry, 248*, 30-35.

Qiu, M., & Huang, C. (2010). A comparative study of degradation of the azo dye C.I. Acid Blue 9 by Fenton and photo-Fenton oxidation. *Desalination and Water Treatment, 24*(1-3), 273-277.

Qiu, M., & Huang, C. (2012). A comparative study of degradation of the azo dye C.I. Acid Blue 9 by Fenton and photo-Fenton oxidation. *Desalination and Water Treatment, 24*(1-3), 273-277.

Ramirez, J. H., Costa, C. A., Madeira, L. M., Mata, G., Vicente, M. A., Rojas-Cervantes, M. L., . . . Martín-Aranda, R. M. (2007). Fenton-like oxidation of Orange II solutions using heterogeneous catalysts based on saponite clay. *Applied Catalysis B: Environmental, 71*(1-2), 44-56.

Rashidi, H. R., Sulaiman, N. M. N., & Hashim, N. A. (2012). Batik Industry Synthetic Wastewater Treatment Using Nanofiltration Membrane. *Procedia Engineering, 44*, 2010-2012.

Rauf, M. A., & Ashraf, S. S. (2009). Radiation induced degradation of dyes—An overview. *Journal of Hazardous Materials, 166*(1), 6-16.

Reife, A., & Freeman, H. S. (1996). *Environmental Chemistry of Dyes and Pigments*: Wiley.

Rigg, T., Taylor, W., & Weiss, J. (1954). The rate constant of the reaction between hydrogen peroxide and ferrous ions. *The Journal of Chemical Physics, 22*(4), 575-577.

Rodrigues, C. S., Madeira, L. M., & Boaventura, R. A. (2009). Treatment of textile effluent by chemical (Fenton's Reagent) and biological (sequencing batch reactor) oxidation. *J Hazard Mater, 172*(2-3), 1551-1559.

Romero, V., Acevedo, S., Marco, P., Giménez, J., & Esplugas, S. (2016). Enhancement of Fenton and photo-Fenton processes at initial circumneutral pH for the degradation of the β-blocker metoprolol. *Water Res, 88*, 449-457.

Ryu, H. D., Cho, Y. O., & Lee, S. I. (2009). Effect of ferrous ion coagulation on biological ammonium nitrogen removal in treating coke wastewater. *Environmental Engineering Science, 26*(12), 1739-1746.

Sahoo, B. (1993). *Problems and Prospects of Textile Industry*: Mittal Publications.

Saldaña-Robles, A., Guerra-Sánchez, R., Maldonado-Rubio, M. I., & Peralta-Hernández, J. M. (2014). Optimization of the operating parameters using RSM for the Fenton oxidation process and adsorption on vegetal carbon of MO solutions. *Journal of Industrial and Engineering Chemistry, 20*(3), 848-857.

Samanta, C. (2008). Direct synthesis of hydrogen peroxide from hydrogen and oxygen: An overview of recent developments in the process. *Applied Catalysis A: General, 350*(2), 133-149.

Santos, L. V. d. S., Meireles, A. M., & Lange, L. C. (2015). Degradation of antibiotics norfloxacin by Fenton, UV and UV/H2O2. *J Environ Manage, 154*, 8-12.

Sarathy, S., & Mohseni, M. (2010). Effects of UV/H2O2 advanced oxidation on chemical characteristics and chlorine reactivity of surface water natural organic matter. *Water Res, 44*(14), 4087-4096.

Savin, I. I., & Butnaru, R. (2008). Wastewater characteristics in textile finishing mills. *Environmental Engineering and Management Journal, 7*(6), 859-864.

Schrank, S. G., Santos, J. N. R. d., Souza, D. S., & Souza, E. E. S. (2007). Decolorisation effects of Vat Green 01 textile dye and textile wastewater using H2O2/UV process. *Journal of Photochemistry and Photobiology A: Chemistry, 186*(2-3), 125-129.

Sharma, M. (2006). *Textile Industry of India and Pakistan*: APH Publishing Corporation.

Shemer, H., Kunukcu, Y. K., & Linden, K. G. (2006). Degradation of the pharmaceutical metronidazole via UV, Fenton and photo-Fenton processes. *Chemosphere, 63*(2), 269-276.

Shojaeimehr, T., Rahimpour, F., Khadivi, M. A., & Sadeghi, M. (2014). A modeling study by response surface methodology (RSM) and artificial neural network (ANN) on Cu2+ adsorption optimization using light expended clay aggregate (LECA). *Journal of Industrial and Engineering Chemistry, 20*(3), 870-880.

Shu, H. Y., & Chang, M. C. (2005a). Decolorization and mineralization of a phthalocyanine dye C.I. Direct Blue 199 using UV/H2O2 process. *J Hazard Mater, 125*(1-3), 96-101.

Shu, H. Y., & Chang, M. C. (2005b). Pilot scale annular plug flow photoreactor by UV/H2O2 for the decolorization of azo dye wastewater. *J Hazard Mater, 125*(1-3), 244-251.

Shu, H. Y., Fan, H. J., Chang, M. C., & Hsieh, W. P. (2006). Treatment of MSW landfill leachate by a thin gap annular UV/H2O2 photoreactor with multi-UV lamps. *J Hazard Mater, 129*(1-3), 73-79.

Silva, A. C., Pic, J. S., Sant'Anna, G. L., Jr., & Dezotti, M. (2009). Ozonation of azo dyes (Orange II and Acid Red 27) in saline media. *J Hazard Mater, 169*(1-3), 965-971.

Singh, S. K., & Tang, W. Z. (2013). Statistical analysis of optimum Fenton oxidation conditions for landfill leachate treatment. *Waste Manag, 33*(1), 81-88.

Smith, B. C. (2011). *Fundamentals of Fourier Transform Infrared Spectroscopy, Second Edition*: CRC Press.

Soares, P. A., Batalha, M., Souza, S. M. A. G. U., Boaventura, R. A. R., & Vilar, V. J. P. (2015). Enhancement of a solar photo-Fenton reaction with ferric-organic ligands for the treatment of acrylic-textile dyeing wastewater. *Journal of Environmental Management, 152*, 120-131.

Soon, A. N., & Hameed, B. H. (2011). Heterogeneous catalytic treatment of synthetic dyes in aqueous media using Fenton and photo-assisted Fenton process. *Desalination, 269*(1-3), 1-16.

Su, C.-C., Pukdee-Asa, M., Ratanatamskul, C., & Lu, M.-C. (2011a). Effect of operating parameters on decolorization and COD removal of three reactive dyes by Fenton's reagent using fluidized-bed reactor. *Desalination, 278*(1-3), 211-218. doi:10.1016/j.desal.2011.05.022

Su, C.-C., Pukdee-Asa, M., Ratanatamskul, C., & Lu, M.-C. (2011b). Effect of operating parameters on the decolorization and oxidation of textile wastewater by the fluidized-bed Fenton process. *Separation and Purification Technology, 83*(0), 100-105.

Tehrani-Bagha, A. R., Mahmoodi, N. M., & Menger, F. M. (2010). Degradation of a persistent organic dye from colored textile wastewater by ozonation. *Desalination, 260*(1-3), 34-38.

Tekin, H., Bilkay, O., Ataberk, S. S., Balta, T. H., Ceribasi, I. H., Sanin, F. D., . . . Yetis, U. (2006). Use of Fenton oxidation to improve the biodegradability of a pharmaceutical wastewater. *J Hazard Mater, 136*(2), 258-265.

Thiruvenkatachari, R., Ouk Kwon, T., & Shik Moon, I. (2006). Degradation of phthalic acids and benzoic acid from terephthalic acid wastewater by advanced oxidation processes. *J Environ Sci Health A Tox Hazard Subst Environ Eng, 41*(8), 1685-1697.

Ting, W. P., Lu, M. C., & Huang, Y. H. (2009). Kinetics of 2,6-dimethylaniline degradation by electro-Fenton process. *J Hazard Mater, 161*(2-3), 1484-1490.

Tokumura, M., Morito, R., & Kawase, Y. (2013). Photo-Fenton process for simultaneous colored wastewater treatment and electricity and hydrogen production. *Chemical Engineering Journal, 221*, 81-89.

Tony, M. A., Purcell, P. J., & Zhao, Y. (2012). Oil refinery wastewater treatment using physicochemical, Fenton and Photo-Fenton oxidation processes. *J Environ Sci Health A Tox Hazard Subst Environ Eng, 47*(3), 435-440.

Torrades, F., & García-Montaño, J. (2014). Using central composite experimental design to optimize the degradation of real dye wastewater by Fenton and photo-Fenton reactions. *Dyes and Pigments, 100*, 184-189.

203

Torrades, F., García-Montaño, J., Antonio García-Hortal, J., Domènech, X., & Peral, J. (2004). Decolorization and mineralization of commercial reactive dyes under solar light assisted photo-Fenton conditions. *Solar Energy, 77*(5), 573-581.

Tunay, O., Kabdasli, I., & Arslan-Alaton, I. (2010). *Chemical Oxidation Applications for Industrial Wastewaters*: IWA Publishing.

Turhan, K., Durukan, I., Ozturkcan, S. A., & Turgut, Z. (2012). Decolorization of textile basic dye in aqueous solution by ozone. *Dyes and Pigments, 92*(3), 897-901.

Uslu, G., Demirci, A., & Regan, J. M. (2016). Disinfection of synthetic and real municipal wastewater effluent by flow-through pulsed UV-light treatment system. *Journal of Water Process Engineering, 10*, 89-97.

Vankar, P. S. (2007). *Handbook On Natural Dyes For Industrial Applications*: NIIR Project Consultancy Services.

Vergili, I., Kaya, Y., Sen, U., Gönder, Z. B., & Aydiner, C. (2012). Techno-economic analysis of textile dye bath wastewater treatment by integrated membrane processes under the zero liquid discharge approach. *Resources, Conservation and Recycling, 58*, 25-35.

Vilar, V. J. P., Pinho, L. X., Pintor, A. M. A., & Boaventura, R. A. R. (2011). Treatment of textile wastewaters by solar-driven advanced oxidation processes. *Solar Energy, 85*(9), 1927-1934.

Vogna, D., Marotta, R., Napolitano, A., Andreozzi, R., & d'Ischia, M. (2004). Advanced oxidation of the pharmaceutical drug diclofenac with UV/H2O2 and ozone. *Water Res, 38*(2), 414-422.

Vujevic, D., Papic, S., Koprivanac, N., & Bozic, A. L. (2010). Decolorization and Mineralization of Reactive Dye by UV/Fenton Process. *Separation Science and Technology, 45*(11), 1637-1643.

Vujević, D., Papić, S., Koprivanac, N., & Božić, A. L. (2010). Decolorization and Mineralization of Reactive Dye by UV/Fenton Process. *Separation Science and Technology, 45*(11), 1637-1643.

Walling, C. (1975). Fenton's reagent revisited. *Accounts of Chemical Research, 8*(4), 125-131.

Walling, C., & Goosen, A. (1973). Mechanism of the ferric ion catalyzed decomposition of hydrogen peroxide. Effect of organic substrates. *J Am Chem Soc, 95*(9), 2987-2991.

Walling, C., & Kato, S. (1971). The oxidation of alcohols by Fenton's reagent. The effect of copper ion. *J Am Chem Soc, 93*(17), 4275-4281.

Wang, J. L., & Xu, L. J. (2012). Advanced Oxidation Processes for Wastewater Treatment: Formation of Hydroxyl Radical and Application. *Critical Reviews in Environmental Science and Technology, 42*(3), 251-325.

Wang, L. K., Hung, Y. T., Lo, H. H., & Yapijakis, C. (2004). *Handbook of Industrial and Hazardous Wastes Treatment*: CRC Press.

Wang, Y., Liu, H., Liu, G., Xie, Y., & Liu, X. (2015). Kinetics for diclofenac degradation by chlorine dioxide in aqueous media: Influences of natural organic matter additives. *Journal of the Taiwan Institute of Chemical Engineers, 56*, 131-137.

Wenhai, C., Tengfei, C., Erdeng, D., Deng, Y., Yingqing, G., & Naiyun, G. (2016). Increased formation of halomethanes during chlorination of chloramphenicol in drinking water by UV irradiation, persulfate oxidation, and combined UV/persulfate pre-treatments. *Ecotoxicology and Environmental Safety, 124*, 147-154.

Wu, C.-H., Kuo, C.-Y., & Chang, C.-L. (2008). Decolorization of C.I. Reactive Red 2 by catalytic ozonation processes. *J Hazard Mater, 153*(3), 1052-1058.

Wu, D., Chen, Y., Zhang, Z., Feng, Y., Liu, Y., Fan, J., & Zhang, Y. (2016). Enhanced oxidation of chloramphenicol by GLDA-driven pyrite induced heterogeneous Fenton-like reactions at alkaline condition. *Chemical Engineering Journal, 294*, 49-57.

Wu, D., Yang, Z., Wang, W., Tian, G., Xu, S., & Sims, A. (2012). Ozonation as an advanced oxidant in treatment of bamboo industry wastewater. *Chemosphere, 88*(9), 1108-1113.

Wu, J., Doan, H., & Upreti, S. (2008). Decolorization of aqueous textile reactive dye by ozone. *Chemical Engineering Journal, 142*(2), 156-160.

Xu, H., Xu, W., & Wang, J. (2011). Degradation kinetics of azo dye reactive Red SBE wastewater by complex ultraviolet and hydrogen peroxide process. *Environmental Progress & Sustainable Energy, 30*(2), 208-215.

Xu, X.-R., Li, X.-Y., Li, X.-Z., & Li, H.-B. (2009). Degradation of melatonin by UV, UV/H2O2, Fe2+/H2O2 and UV/Fe2+/H2O2 processes. *Separation and Purification Technology, 68*(2), 261-266.

Xu, X. R., Li, H. B., Wang, W. H., & Gu, J. D. (2004). Degradation of dyes in aqueous solutions by the Fenton process. *Chemosphere, 57*(7), 595-600.

Xu, Y., Lebrun, R. E., Gallo, P.-J., & Blond, P. (1999). Treatment of Textile Dye Plant Effluent by Nanofiltration Membrane. *Separation Science and Technology, 34*(13), 2501-2519.

Yeh, R. Y.-L., Hung, Y.-T., Liu, R. L.-H., Chiu, H.-M., & Thomas, A. (2002). Textile Wastewater Treatment With Activated Sludge And Powdered Activated Carbon. *International Journal of Environmental Studies, 59*(5), 607-622.

Yonar, T., Kestioglu, K., & Azbar, N. (2006). Treatability studies on domestic wastewater using UV/H2O2 process. *Applied Catalysis B: Environmental, 67*(3-4), 223-228.

Youssef, N. A., Shaban, S. A., Ibrahim, F. A., & Mahmoud, A. S. (2016). Degradation of methyl orange using Fenton catalytic reaction. *Egyptian Journal of Petroleum*.

Yu, W., Yang, J., Shi, Y., Song, J., Shi, Y., Xiao, J., . . . Hu, J. (2016). Roles of iron species and pH optimization on sewage sludge conditioning with Fenton's reagent and lime. *Water Research, 95*, 124-133.

Zaharia, C., & Suteu, D. (2012). Coal fly ash as adsorptive material for treatment of a real textile effluent: operating parameters and treatment efficiency. *Environ Sci Pollut Res Int*.

Zapata, A., Oller, I., Bizani, E., Sánchez-Pérez, J. A., Maldonado, M. I., & Malato, S. (2009). Evaluation of operational parameters involved in solar photo-Fenton degradation of a commercial pesticide mixture. *Catalysis Today, 144*(1-2), 94-99.

Zarora, C., Segura, C., Mansilla, H., Mondaca, M. A., & Gonzalez, P. (2010). Kinetic study of imidacloprid removal by advanced oxidation based on photo-Fenton process. *Environ Technol, 31*(13), 1411-1416.

Žgajnar Gotvajn, A., Zagorc-Končan, J., & Cotman, M. (2011). Fenton's oxidative treatment of municipal landfill leachate as an alternative to biological process. *Desalination, 275*(1-3), 269-275.

Zhang, A., Li, Y., Song, Y., Lv, J., & Yang, J. (2014). Characterization of pharmaceuticals and personal care products as N-nitrosodimethylamine precursors during disinfection processes using free chlorine and chlorine dioxide. *Journal of Hazardous Materials, 276*, 499-509.

Zhang, H., Fei, C., Zhang, D., & Tang, F. (2007). Degradation of 4-nitrophenol in aqueous medium by electro-Fenton method. *J Hazard Mater, 145*(1-2), 227-232.

Zhang, Y., & Pagilla, K. (2010). Treatment of malathion pesticide wastewater with nanofiltration and photo-Fenton oxidation. *Desalination, 263*(1-3), 36-44.

Zhao, G., Lu, X., Zhou, Y., & Gu, Q. (2013). Simultaneous humic acid removal and bromate control by O3 and UV/O3 processes. *Chemical Engineering Journal, 232*(0), 74-80.

Zoschke, K., Börnick, H., & Worch, E. (2014). Vacuum-UV radiation at 185 nm in water treatment – a review. *Water Res*.

Zuorro, A., Fidaleo, M., & Lavecchia, R. (2013). Response surface methodology (RSM) analysis of photodegradation of sulfonated diazo dye Reactive Green 19 by UV/H2O2 process. *J Environ Manage, 127*, 28-35.

Zuorro, A., & Lavecchia, R. (2013). Evaluation of UV/H2O2advanced oxidation process (AOP) for the degradation of diazo dye Reactive Green 19 in aqueous solution. *Desalination and Water Treatment*, 1-7.

APPENDIX

LIST OF PUBLICATIONS AND PAPERS PRESENTED

Patent

Buthiyappan, A., Abdul Aziz, A. R., & Wan Daud, W. M. A. Miniature integrated wastewater treatment based on advanced oxidation process, Patent Reference Number: UM.TNC2/UMCIC/603/1121 (*In Application Process*)

Publications

1. **Buthiyappan, A**., Abdul Aziz, A. R., & Wan Daud, W. M. A. (2015). Degradation performance and cost implication of UV-integrated advanced oxidation processes for wastewater treatments. Reviews in Chemical Engineering, 31(3). doi:10.1515/revce-2014-0039 *(ISI-Cited Publication, **Impact Factor:2.833**)*

2. **Buthiyappan, A**., Abdul Aziz, A. R., & Wan Daud, W. M. A. (2016). Recent advances and prospects of catalytic advanced oxidation process in treating textile effluents. Reviews in Chemical Engineering, *32*(1), 1-47. doi:10.1515/revce-2015-0034 *(ISI-Cited Publication, **Impact Factor:2.414**)*

3. **Buthiyappan, A**., Abdul Aziz, A. R., & Wan Daud, W. M. A. (2016). Development of Advanced Chemical Oxidation Wastewater Treatment System for the Batik Industry in Malaysia. RSC Advances. doi:10.1039/C5RA26775G *(ISI-Cited Publication **Impact Factor: 3.84**)*

4. **Buthiyappan, A**., Abdul Aziz, A. R., & Wan Daud, W. M. A. (2016). Parametric study and Process evaluation of Fenton oxidation for high strength textile wastewater treatment: Application of Sequential Response surface methodology and Adaptive Neuro-Fuzzy Inference System computing Technique. Chemical

Engineering Communication. *(Accepted; ISI-Cited Publication **Impact Factor: 1.104**)*

5. **Buthiyappan, A**., Abdul Aziz, A. R., & Wan Daud, W. M. A.. (2016). Parametric study and Process evaluation of Fenton oxidation for high strength textile wastewater treatment: Treatment Performance of UV, UV/H_2O_2, Fe^{2+} Coagulation, UV/Fe^{2+}, Fe^{2+}/H_2O_2 and UV/Fe^{2+}/H_2O_2 for the Degradation of Recalcitrant Contaminants in Actual Industry Effluent. Journal of Cleaner Production. *(Accepted; ISI-Cited Publication **Impact Factor: 4.959**)*

6. **Buthiyappan, A**., Raja Shazrin Shah Raja Ehsan Shah., Anam Asghar, Abdul Aziz, A. R., & Wan Daud, W. M. A., Shaliza Ibrahim , & F. Handan Tezel (2016). Textile Wastewater Treatment Efficiency by Fenton Oxidation with Integration of Membrane Separation System. Waste Management. *(Ready to be Submitted)*

7. **Buthiyappan, A**., Abdul Aziz, A. R., & Wan Daud, W. M. A., (2016). Photo Degradation and Detoxification of textile wastewater by Sono-Fenton and Sono-Fenton-like Processes: Comparison of Chemical Oxidants Chemical Engineering Journal. *(Ready to be Submitted)*

8. **Buthiyappan, A**., Abdul Aziz, A. R., & Wan Daud, W. M. A. (2016). Pesticide containing wastewater degradation with miniature ultrasound assisted Fenton oxidation treatment. *Separation and Purification Technology.* *(Ready to be Submitted)*

9. **Buthiyappan, A**., Abdul Aziz, A. R., & Wan Daud, W. M. A. (2016). Photo-Fenton degradation of a industrial effluent: Intensification with persulfate and the study of radicals. *RSC Advances*. *(Ready to be submitted)*

Conference Proceeding

Buthiyappan, A., Abdul Raman, A. A & Daud, W. M. A. W., 2013. Optimization of Reactive Dyes Degradation by Fenton Oxidation Using Response Surface Method. Proceedings of Hong Kong International Conference on Engineering and Applied Science, December 19-22, 2013. Hong Kong. (*Conference Paper*)

Book Chapter

Abdul Raman, A. A, Asghar, A, **Buthiyappan, A.**, & Wan Mohd Ashri Wan Daud., 'Chapter 16:Treatment of Recalcitrant Waste'. *Current Developments in Biotechnology and Bioengineering, Book 4: Biological Treatment of Industrial Effluents.*